UNIVERSITÀ DEGLI STUDI DI MILANO

UNIVERSITÀ DEGLI STUDI DI MILANO

PhD Course in Environmental Sciences

XXXI cycle

Characterization of *Hermetia illucens* (Diptera: Stratiomyidae) midgut

PhD Thesis of

Marco BONELLI

R11252

Scientific Tutor: Prof. **Morena CASARTELLI**

Academic Year: 2017/2018

INDEX

ABSTRACT

Introduction

The search for new protein sources for animal feed is a mandatory and actual issue, since the current population increase is leading to an increase in global demand for meat with a consequent higher request of protein for feed production. Another serious global problem is food waste, since it is estimated that about one third of the food produced globally is wasted. In this context, in addition to policies to reduce meat consumption and production of food waste, a possible perspective is to consider insects as feed, because they are good agents for organic waste bioconversion into high nutritional value proteins. One of the most promising species for this purpose is *Hermetia illucens* (Linnaeus, 1758) (Diptera: Stratiomyidae), due to the ability of the larvae to grow on a wide variety of organic substrates, their high efficiency in the bioconversion process and their high content of proteins with high nutritional value, and other macro- and micro-nutrients important for animal feed. Despite the great interest toward this species, the current literature mainly provides information on rearing methods for this insect, the use of larvae for waste treatment, their nutrient composition, and their suitability for feed production, while little is known on the biology of this insect. In particular, a deep understanding of the physiology of the midgut, which is the organ responsible for nutrient digestion and absorption, is essential to better comprehend the extraordinary dietary plasticity of the larva and to better exploit its bioconversion ability.

Chapter 1

In the first chapter, an in-depth morphofunctional characterization of the larval midgut of *H. illucens* is reported. Our results demonstrate that the larval midgut is composed of distinct anatomical regions with different luminal pH and specific morphofunctional features. The midgut epithelium is formed by different cell types that accomplish nutrient digestion and absorption, acidification of the lumen of the middle region, endocrine regulation, and growth of the epithelium. A detailed characterization of the activity of enzymes involved in nutrient digestion and their mRNA expression levels reveals that protein and carbohydrate digestion is associated to specific regions of this organ. Moreover, a significant lysozyme activity in the lumen of the anterior and middle regions of the midgut was detected. This enzyme, together with the strong acidic luminal pH of middle tract, may play an important role in killing pathogenic microorganisms ingested with the feeding substrate. The obtained data allow us to propose a detailed functional model of the larval midgut of *H. illucens* in which each region is characterized by peculiar features to accomplish specific functions.

Chapter 2

The second chapter reports the effects of feeding substrates with different nutritional composition on morphofunctional properties of the larval midgut. Our data show a diet-dependent adaptation process of this organ: differences in cell morphology, activity of digestive enzymes, and accumulation of long-term storage molecules were observed. These results demonstrated the existence of a diet-dependent adaptation process of the midgut. This plasticity may be responsible for the ability of *H. illucens* larvae to growth and develop on very different organic substrates.

Chapter 3

In the third chapters, the effect of diets with different nutrient content on the midgut microbiota of *H. illucens* larvae, and the impact of the insect feeding activity on the diet microbiota are investigated. In particular, using three feeding substrates with different protein/carbohydrates (P/C) ratio, we established that the diet impacts on the midgut microbiota, in particular a diet with very high P/C ratio do not seem to be optimal for *H. illucens* rearing, since it induces a dysbiosis. Moreover, the regionalization of this organ influences the microbiota: the bacterial community of the anterior midgut always shows higher diversity than the posterior, whereas bacterial load has an opposite trend, being maximal in the posterior region. We also demonstrated that *H. illucens* larvae do not affect the microbiota composition of the feeding substrate. The overall data indicate the importance of taking into account the presence of different midgut structural and functional domains, as well as the microbiota of the diet, in any further study that aims at clarifying microbiological aspects concerning *H. illucens* larval midgut.

Chapter 4

In the fourth chapter, the remodeling process of *H. illucens* larval midgut during metamorphosis, the morphological and functional properties of the adult midgut, and the feeding habits of the fly are investigated. Our results show that the larval midgut is removed during metamorphosis and a new pupal-adult epithelium is formed by proliferation and differentiation of intestinal stem cells. Moreover, at variance with majority of current literature, we demonstrated that the adult insect possesses a functional digestive system: mouthpart allows food ingestion, the bolus can transit along the gut, and the midgut epithelium is endowed with digestive capability. This new scenario, not only opens up the possibility to manipulate the feeding substrate of the adult insect to improve its performances in mass rearing procedures, but could also provide insights into the safety on the use of this insect for feed purposes.

INTRODUCTION

Over the coming decades, the world will have to deal with an increasing competition for limited natural resources. With a growing global population, estimated to reach about 8.5 billion in 2030 and almost 10 in 2050 (United Nations, 2017), and increasingly demanding consumers, the production of adequate amounts of proteins from livestock, poultry and fish represents a serious challenge for the future. It is estimated that the highest request in tons will be for pigs, poultry and fish (Alexandratos and Bruinsma, 2012; Waite et al., 2014). Moreover, the consequent increase in demand for feed for farmed animals raises environmental and economic issues. It is estimated that 70% of total agriculture land use is for livestock production and that about 35% of cereal production are fed to farm animals (Steinfield et al., 2006; Alexandratos and Bruinsma, 2012). By diverting such huge quantities of resources for animal feed, less is consequently available for humans. Furthermore, an important share of animal production cost is due to feed cost: the latter can reach up to 70% of the expenses (Verbeke et al., 2015; Chaalala et al., 2018). In addition to the increased demand, climate change will have an impact on the primary production systems like agriculture, livestock and fisheries (Roessig et al., 2004; Allison et al., 2009; Thornton et al., 2009, Rosenzweig et al., 2014; Escarcha et al., 2018). For these reasons, a transition is needed towards the best exploitation of the available renewable biological resources, and towards a more sustainable primary production and processing systems, to produce more food and other bio-based products in a more sustainable, efficient and integrated manner, with fewer inputs, costs and lower environmental impact.

Another serious concern is represented by food waste disposal: one third of the food produced globally is wasted, amounting to about 1.3 billion tons *per* year (Gustavsson et al., 2011). One mandatory policy to face this problem is to reduce organic waste during the cycles of production and consumption, and the processing, storage, recycling and disposal of waste, but the valorisation of this huge amount of organic material through its bioconversion into valuable biomass is an opportunity that must be considered.

In this context, insects emerge as a relevant issue since some species offer enormous opportunities for the bioconversion of organic waste into valuable protein for feed industry, in particular for monogastric feed. Insect-based feed products appear to be competitive on the market and insect meal has a nutrient composition comparable with fish- and soy-mail; in particular, Diptera present an amino acid profile similar to fish meal (St-Hilaire et al., 2007; Diener et al., 2009; Kroeckel et al., 2012; Van Huis, 2013; Van Huis et al., 2013; Barroso et al., 2014; Makkar et al., 2014; Oonincx et al., 2015; Magalhães et al., 2017). Moreover, insects can represent a more environment-friendly alternative to conventional feed ingredients, due to their considerably reduced water requirement and high feed conversion efficiency (Oonincx et al., 2010; Van Huis and Oonincx, 2017; Halloran

et al., 2018). However, careful attention must be paid to the choice of feed ingredients, because of animal welfare, possible diseases, and because, in animals raised for food production, their feed is a link of the human food chain. The first general objective of the food safety policy of the European Union (EU) is to ensure that food and animal feed are safe and nutritious (European Union, 2014). EU has a wide legislation on animal feed that applies to a wide range of animal feed businesses and activities (Regulations (EC) 999/2001, (EC) 178/2002, (EC) 1829/2003, (EC) 1831/2003, (EC) 882/2004, (EC) 183/2005, (EC) 152/2009, (EC) 767/2009). In particular, the Regulation (EC) 999/2001 prohibited the use of processed animal proteins (PAPs) in feed for farmed animals, and proteins derived from insect fell within this category, even though not explicitly mentioned. The feeding of non-ruminant PAPs to aquaculture animals was allowed by Regulation (EU) 56/2013. In 2015 the EFSA Scientific Committee published a Scientific Opinion on the risk profile related to production and consumption of insects as food and feed (EFSA Scientific Committee, 2015). This document mainly addressed the core issues of potential biological, chemical and environmental hazards associated with farmed insects used as food and feed considering the entire chain, from farming to the final product. The Scientific Committee concluded that the specific production methods, the substrate used to rear insects, the stage of harvest, the insect species and the methods used for further processing have an impact on the possible presence of biological and chemical contaminants in insect food and feed products. Moreover, it was stated that the adoption of existing waste management strategies should be applicable for managing waste from insect production. The document also emphasized some knowledge gaps, underlying the importance of further scientific research on this field. Finally, the Regulation (EU) 2017/893 explicitly admits the use of PAPs derived from insects for feeding aquaculture animals, establishing rearing, processing, storage, transport and use conditions. Moreover, this Regulation states that: "Processed animal protein derived from farmed insects, intended for the production of feed for farmed animals (…) may only be obtained from the following insect species: (i) Black Soldier Fly (*Hermetia illucens*) and Common Housefly (*Musca domestica*); (ii) Yellow Mealworm (*Tenebrio molitor*) and Lesser Mealworm (*Alphitobius diaperinus*); (iii) House cricket (*Acheta domesticus*), Banded cricket (*Gryllodes sigillatus*) and Field Cricket (*Gryllus assimilis*)". The production of PAPs derived from insects and of other insect derivatives destined for pet food falls within the competence of the Member States, as well as the use of live insects to feed non-ruminant animals. In Italy, on the 5th May 2017, the Health Ministry issued a circular that provides information on the regulatory framework currently applicable to the use of insects as feed, and states that the use of live insects as feed for pets and animals not raised for food production must be regarded as admissible.

Another important issue is the choice of substrates to feed insects destined for animal feed. The Annex III to the Regulation (EC) 767/2009 prohibits the use of faeces and separated digestive tract content as feed and the Regulation (EC) No 1069/2009 bans the use of manure or catering waste. Moreover, according to Regulation (EU) No 142/2011, unprocessed former foodstuffs containing meat or fish are currently not authorised as feed for farmed animals. It appears clear that the substrates to feed insects must be environmentally and economically sustainable, but any specific organic by-product or waste used for this purpose must satisfy the above-mentioned conditions, and be highly safe, considering the issues raised by the EFSA Scientific Opinion and the European legislation.

Among the six "permitted insect species" reported in the Regulation (EU) 2017/893, *Hermetia illucens* (Linnaeus, 1758) (Diptera: Stratiomyidae) is among the most promising insect species for waste bioconversion in order to obtain protein for feed production, as reported by European Food Safety Authority (EFSA Scientific Committee, 2015) and Food and Agriculture Organization of the United Nations (Van Huis et al., 2013).

H. illucens was first described by Linneaus as *Musca illucens* in 1758 in the first volume of the 10th edition of *Systema Naturae* (Fig. 1) and, belonging to the family Stratiomydae, is an orthorraphous Brachycera (Wiegmann et al., 2011).

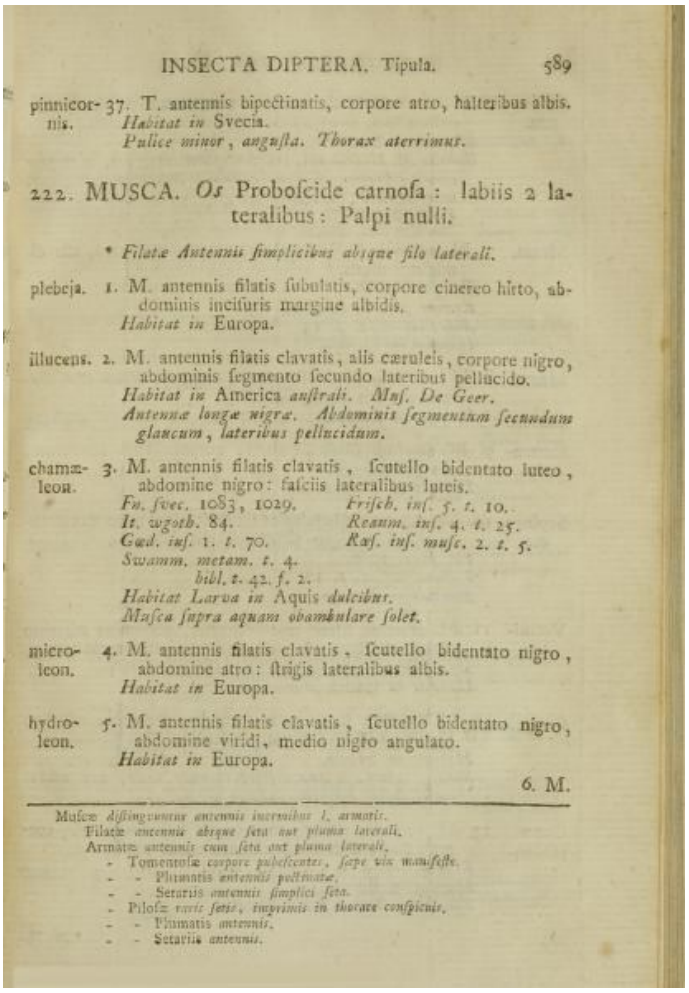

INSECTA DIPTERA. Tipula. 589

pinnicornis. 37. T. antennis bipectinatis, corpore atro, halteribus albis.
Habitat in Svecia.
Pulice minor, angusta. Thorax aterrimus.

222. MUSCA. *Os* Proboscide carnosa: labiis 2 lateralibus: Palpi nulli.

* *Filatæ Antennis simplicibus absque filo laterali.*

plebeja. 1. M. antennis filatis subulatis, corpore cinereo hirto, abdominis incisuris margine albidis.
Habitat in Europa.

illucens. 2. M. antennis filatis clavatis, alis cæruleis, corpore nigro, abdominis segmento secundo lateribus pellucido.
Habitat in America *australi. Mus. De Geer.*
Antennæ longæ nigræ. Abdominis segmentum secundum glaucum, lateribus pellucidum.

chamæleon. 3. M. antennis filatis clavatis, scutello bidentato luteo, abdomine nigro: fasciis lateralibus luteis.
Fn. suec. 1083, 1029. *Frisch. ins. 5. t. 10.*
It. wgoth. 84. *Reaum. ins. 4. t. 25.*
Gœd. ins. 1. t. 70. *Raj. ins. musc. 2. t. 5.*
Swamm. metam. t. 4.
bibl. t. 42. f. 2.
Habitat Larva in Aquis *dulcibus.*
Musca supra aquam obambulare solet.

microleon. 4. M. antennis filatis clavatis, scutello bidentato nigro, abdomine atro: strigis lateralibus albis.
Habitat in Europa.

hydroleon. 5. M. antennis filatis clavatis, scutello bidentato nigro, abdomine viridi, medio nigro angulato.
Habitat in Europa.

6. M.

Muscæ *distinguuntur antennis inermibus 1. armatis.*
Filatæ *antennis absque seta aut pluma laterali.*
Armatæ *antennis cum seta aut pluma laterali.*
- Tomentosæ *corpore pubescente, sæpe vix manifesto.*
- - Plumatis *antennis pectinatis.*
- - Setariis *antennis simplici seta.*
- Pilosæ *raris setis, imprimis in thorace conspicuis.*
- - Plumatis *antennis.*
- - Setariis *antennis.*

Figure 1. Original description of the species. The original description of the *Hermetia illucens* as *Musca illucens* given by Linnaeus in the 10th edition of *Systema Naturae*.

This fly is traditionally thought to be native of America (Rozkošný, 1983; Wang and Shelomi, 2017) however, recently, a possible Palearctic origin was advanced (Benelli et al., 2014) and now it is distributed worldwide in tropical and temperate regions. Adults (Fig. 2) range from 13 to 20 mm in length, a parameter that is affected by the larval diet (Tomberlin et al., 2002; Gobbi et al., 2013).

Figure 2. *H. illucens* adult. (photograph by Didier Descouens, distributed under CC BY-SA-4.0; illustration by United States government, distributed under CC0 1.0)

They have a "wasp-like" appearance and are black, with a pair of translucent white oblong "windows" on proximal abdominal tergites, a white "window" on proximal abdominal sternites, and white tarsi and basal halves of hind tibiae. The antennae, longer in female than males, consist of scape, pedicel and non-aristate flagellum with eight antennomeres (Pezzi et al., 2017). Head has three ocelli and a pair of large compound eyes, broadly separated in both sexes. The adult stage of *H. illucens* does not bite or sting and, according to the current literature but without any supporting experimental data, it does not need to eat or is even considered unable to eat, therefore it depends exclusively on reserves accumulated during the larval stage (Sheppard et al., 1994; Sheppard et al., 2002; Tomberlin and Sheppard, 2002; Tomberlin et al., 2002; Tomberlin et al., 2009; Gobbi et al., 2013; Wang and Shelomi, 2017). In nature, mating occurs in full sunlight, but it is possible to use specific lamps for mating in captivity (Oonincx et al., 2016). After mating, females lay eggs (Fig. 3), varying in number from 200 to 2000, in clusters (Booth and Sheppard, 1984; Tomberlin et al., 2002; Chaalala et al., 2018), near a food source for the larvae.

Figure 3. *H. illucens* eggs. (photograph by Daniele Bruno)

Eggs hatch in about 4 days (Booth and Sheppard, 1984). Larvae of this holometabolus insect are apodous, whitish in first instars and darker near pupation, distinctly segmented, and characteristically dorsoventrally flattened (Fig. 4). They have a very well developed mandibular-maxillary complex (Fig. 5) that allows them to grow on a wide variety of organic matters (Kim et al., 2010). There is no full agreement about the number of larval instars, but many authors indicate six (e.g., Kim et al., 2010; Barragan-Fonseca et al., 2017; Gligorescu et al., 2018). The duration of larval development, as well as the size and length reached by larvae, depends on alimentary and environmental conditions, however in optimal conditions they can develop in about 15 days and their fresh weight exceeds 200 mg (Gobbi et al., 2013, Harnden and Tomberlin, 2016; Spranghers et al., 2017). Prepupae migrate from moist substrate to a dry, suitable substrate for pupation (Diener et al., 2011; Spranghers et al., 2017). This instinct could be useful for large-scale rearing, to separate prepupae from substrate without the man's intervention (self-harvesting) (Sheppard et al., 1994; Diener et al., 2011). Pupae have dark brown, sclerotized cuticle (Fig. 4). The duration of the pupal stage is extremely variable according to environmental conditions (Furman et al., 1959).

Figure 4. *H. illucens* larvae and pupae. (photograph by Wikimedia Commons User MOs810, distributed under CC BY-SA-4.0)

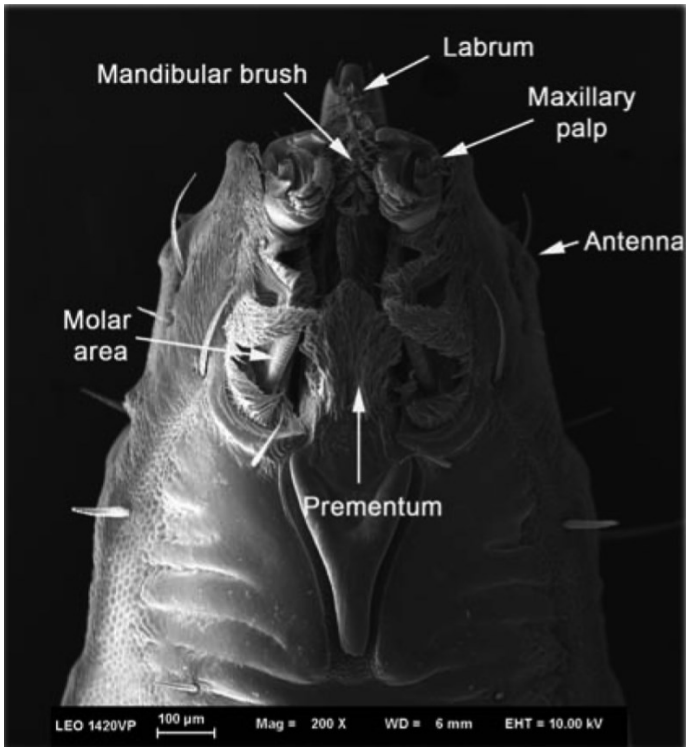

Figure 5. Dorsal view of the mouth part of *H. illucens* larva. (Kim et al., 2010)

The great potential of *H. illucens* larvae as feed ingredient is due to their ability to grow on a wide variety of organic substrates, their high efficiency in the bioconversion process and their high content of proteins with high nutritional value, and other macro- and micro-nutrients important for animal feed (Čičková et al., 2015; Nguyen et al., 2015). In addition, the larval survival rate does not significantly vary with diet, even if the feeding substrate impacts on the chemical composition of the insect (Makkar et al., 2014; Oonincx et al, 2015, Barragan-Fonseca et al., 2017; Jucker et al., 2017; Wang and Shelomi, 2017).

H. illucens larvae biomass could also be exploited for the isolation of bioactive compounds (e.g., antimicrobial peptides, chitosan and degrading enzymes) and biodiesel production (Müller *et al.*, 2017; Wang and Shelomi, 2017); finally, larvae can be used as agents for waste composting thus offsetting capital and environmental costs of nitrogen-fertilization in agriculture (Choi et al., 2009; Green and Popa, 2012; Lalander et al., 2015).

The interest towards *H. illucens* and its potential applications are demonstrated by the growing trend in published papers in the last years (Fig. 6).

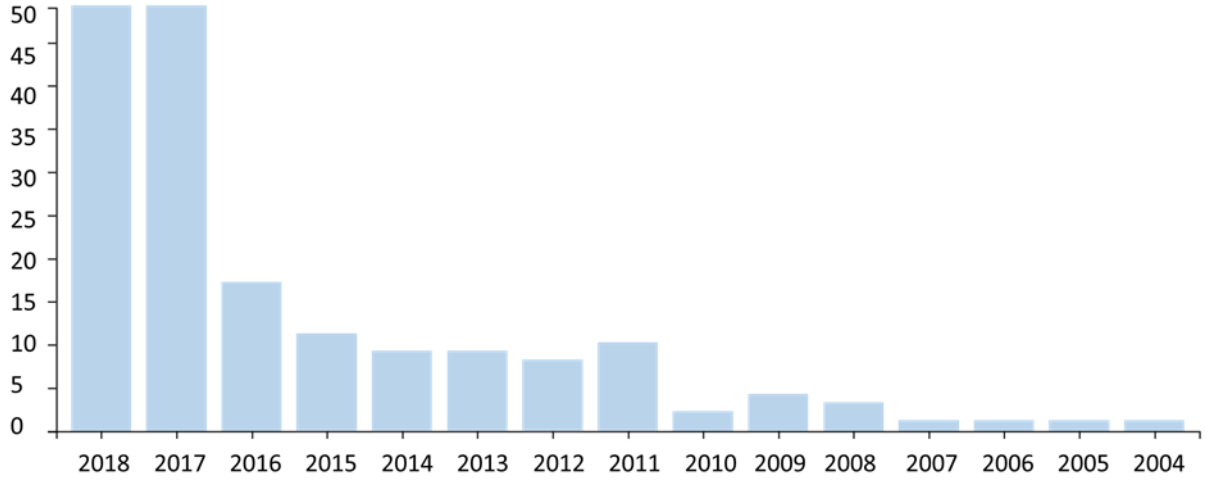

Figure 6. Number of papers on *H. illucens* in last 15 years. Records for papers with "*Hermetia illucens*" or "black soldier fly" in the title from Web of Science Core Collection database, accessed on 28th September 2018.

The total number of published papers in the current (2018) and last year (2017) already exceeds the total number of papers published in the previous 13 years (from 2004 to 2016). The interest is also demonstrated by the great attention paid to this species in Conferences: at the 2nd International Conference "Insects to Feed the World" (IFW 2018) held in May 2018 at Wuhan (China) about 40% of the abstracts were on *H. illucens*, and in the XI European Congress of Entomology (Naples, 2-6 July 2018) a session was dedicated to edible insect in which different oral and poster presentations dealt with this insect.

Most of information available in literature is on *H. illucens* rearing methods, its use for waste treatment, the nutritional composition of larvae and their suitability for feed production, but many

aspects of the biology of this insect, and in particular of its physiology are still uninvestigated. Indeed, despite the digestive system represents a fundamental interface between the insect and the external environment and is responsible for food ingestion, digestion of macromolecules and nutrient absorption, and therefore is directly involved in bioconversion processes, its functional properties has been neglected so far. In particular, a deep understanding of the physiology of the midgut, which is the central portion of the gut and the main site of digestive enzyme production, nutrient digestion and absorption, is fundamental, to understand the extraordinary feeding plasticity of *H. illucens* larvae and to exploit at best this ability.

Aims of the work

The overall objective of my PhD project is to shed light on the biology of *H. illucens* midgut. To characterize this organ a multidisciplinary approach was used and the results have been collected in four manuscripts presented in the next chapters.

Firstly, a morphofunctional characterization of the larval midgut of *H. illucens* was performed, with an in-depth description of the morphological, ultrastructural and functional properties of the different regions in which this organ can be subdivided.

Moreover, considering that *H. illucens* larvae are able to grow and develop on a wide variety of waste substrates but little information is available on diet-related adaptation of the midgut, we compared larvae reared on a vegetable mix diet, a substrate that simulates an organic waste not containing material of animal origin, with larvae reared on standard diet for Diptera. In particular, changes in the duration of larval developmental, in the morphological features of the midgut epithelium, in the activity of digestive enzymes and in the accumulation of long-term storage molecules inside the midgut cells were evaluated.

We also examined the effect of diets with different nutrient content on the midgut microbiota of *H. illucens* larvae, and the impact of the insect feeding activity on the diet microbiota. This last aspect is interesting since it has been stated that *H. illucens* larvae feeding activity can potentially reduce the bacterial load of the diet (Erickson et al., 2004; Liu et al., 2008; Lalander et al., 2015).

Finally, a structural and functional characterization of the midgut of *H. illucens* during larva-pupa and pupa-adult transition was performed to investigate the remodeling process of this organ during metamorphosis. Moreover, we monitored the feeding habits of the fly, and investigated the morphology and functionality of the midgut of the adult insect, and its ability to exploit the ingested nutrients by means of vital stains and measurements of digestive enzyme activity. Investigations on the feeding habits of the adult are particularly important to ensure the safety of the rearing procedures and to improve the performances of the fly.

REFERENCES

Alexandratos, N., Bruinsma, J. (2012). World agriculture towards 2030/2050: the 2012 revision. Food and Agriculture Organization of the United Nations, Rome.

Allison, E. H., Perry, A. L., Badjeck, M. C., Adger, W. N., Brown, K., Conway, D., Halls, A. S., Pilling, G. M., Reynolds, J. D., Andrew, N. L., Dulvy, N. K. (2009). Vulnerability of national economies to the impacts of climate change on fisheries. Fish and fisheries, 10, 173-196.

Barragan-Fonseca, K., Dicke, M., Van Loon, J. (2017). Nutritional value of the black soldier fly (*Hermetia illucens* L.) and its suitability as animal feed – a review. Journal of Insects as Food and Feed, 3, 105-120.

Barroso, F. G., Haro, C. D., Sánchez-Muros, M., Venegas, E., Martínez-Sánchez, A., Pérez-Bañón, C. (2014). The potential of various insect species for use as food for fish. Aquaculture, 422-423, 193-201.

Benelli, G., Canale, A., Raspi, A., Fornaciari, G. (2014). The death scenario of an Italian Renaissance princess can shed light on a zoological dilemma: did the black soldier fly reach Europe with Columbus? Journal of Archaeological Science, 49, 203-205.

Booth, D. C., Sheppard, C. (1984). Oviposition of the black soldier fly, *Hermetia illucens* (Diptera: Stratiomyidae): eggs, masses, timing, and site characteristics. Environmental Entomology, 13, 421-423.

Chaalala, S., Leplat, A., Makkar, H. (2018). Importance of insects for use as animal feed in low-income countries. In: Edible insects in sustainable food systems, 303-319. Springer, Cham.

Choi, Y. C., Choi, J. Y., Kim, J. G., Kim, M. S., Kim, W. T., Park, K. H., Bae, S. W., Jeong, G. S. (2009). Potential usage of food waste as a natural fertilizer after digestion by *Hermetia illucens* (Diptera: Stratiomyidae). International Journal of Industrial Entomology, 19, 171-174.

Čičková, H., Newton, G. L., Lacy, R. C., & Kozánek, M. (2015). The use of fly larvae for organic waste treatment. Waste Management, 35, 68-80.

Diener, S., Solano, N. M. S., Gutiérrez, F. R., Zurbrügg, C., Tockner, K. (2011). Biological treatment of municipal organic waste using black soldier fly larvae. Waste and Biomass Valorization, 2, 357-363.

Diener, S., Zurbrügg, C., Tockner, K. (2009). Conversion of organic material by black soldier fly larvae: establishing optimal feeding rates. Waste Management & Research, 27, 603-610.

EFSA Scientific Committee (2015). Risk profile related to production and consumption of insects as food and feed. EFSA Journal, 13, 4257.

Erickson, M. C., Islam, M., Sheppard, C., Liao, J., Doyle, M. P. (2004). Reduction of *Escherichia coli* O157: H7 and *Salmonella enterica* serovar enteritidis in chicken manure by larvae of the black soldier fly. Journal of Food Protection, 67, 685-690.

Escarcha, J., Lassa, J., & Zander, K. (2018). Livestock under climate change: a systematic review of impacts and adaptation. Climate, 6, 54.

European Union (2014). Food safety – Ensuring a high level of protection of human health and consumers interests. Publications Office of the European Union, Luxembourg.

Furman, D. P., Young, R. D., Catts, P. E. (1959). *Hermetia illucens* (Linnaeus) as a factor in the natural control of *Musca domestica* Linnaeus. Journal of Economic Entomology, 52, 917-921.

Gligorescu, A., Toft, S., Hauggaard-Nielsen, H., Axelsen, J. A., Nielsen, S. A. (2018). Development, metabolism and nutrient composition of black soldier fly larvae (*Hermetia illucens*;

Diptera: Stratiomyidae) in relation to temperature and diet. Journal of Insects as Food and Feed, 4, 123-133.

Gobbi, P., Martinez-Sanchez, A., Rojo, S., 2013. The effects of larval diet on adult life-history traits of the black soldier fly, *Hermetia illucens* (Diptera: Stratiomyidae). European Journal of Entomology, 110, 461-468.

Green, T. R., Popa, R. (2012). Enhanced ammonia content in compost leachate processed by black soldier fly larvae. Applied biochemistry and biotechnology, 166, 1381-1387.

Gustavsson J., Cederberg C., Sonesson U., Van Otterdijk R., Meybeck A. (2011). Global food losses and food waste: extent, causes and prevention. Food and Agriculture Organization of the United Nations, Rome.

Halloran, A., Hansen, H. H., Jensen, L. S., Bruun, S. (2018). Comparing environmental impacts from insects for feed and food as an alternative to animal production. In: Edible Insects in Sustainable Food Systems, 163-180. Springer, Cham.

Harnden, L. M., Tomberlin, J. K. (2016). Effects of temperature and diet on black soldier fly, *Hermetia illucens* (L.) (Diptera: Stratiomyidae), development. Forensic Science International, 266, 109-116.

Jucker, C., Erba, D., Leonardi, M. G., Lupi, D., Savoldelli, S. (2017). Assessment of vegetable and fruit substrates as potential rearing media for *Hermetia illucens* (Diptera: Stratiomyidae) larvae. Environmental Entomology, 46, 1415-1423.

Kim, W., Bae, S., Park, H., Park, K., Lee, S., Choi, Y., Han, S., Koh, Y. (2010). The larval age and mouth morphology of the black soldier fly, *Hermetia illucens* (Diptera: Stratiomyidae). International Journal of Industrial Entomology, 21, 185-187.

Kroeckel, S., Harjes, A., Roth, I., Katz, H., Wuertz, S., Susenbeth, A., Schulz, C. (2012). When a turbot catches a fly: Evaluation of a pre-pupae meal of the black soldier fly (*Hermetia illucens*) as fish meal substitute – Growth performance and chitin degradation in juvenile turbot (*Psetta maxima*). Aquaculture, 364-365, 345-352.

Lalander, C. H., Fidjeland, J., Diener, S., Eriksson, S., Vinnerås, B. (2015). High waste-to-biomass conversion and efficient *Salmonella* spp. reduction using black soldier fly for waste recycling. Agronomy for Sustainable Development, 35, 261-271.

Liu, Q., Tomberlin, J. K., Brady, J. A., Sanford, M. R., Yu, Z. (2008). Black soldier fly (Diptera: Stratiomyidae) larvae reduce *Escherichia coli* in dairy manure. Environmental Entomology, 37, 1525-1530.

Magalhães, R., Sánchez-López, A., Leal, R. S., Martínez-Llorens, S., Oliva-Teles, A., Peres, H. (2017). Black soldier fly (*Hermetia illucens*) pre-pupae meal as a fish meal replacement in diets for European seabass (*Dicentrarchus labrax*). Aquaculture, 476, 79-85.

Makkar, H. P., Tran, G., Heuzé, V., Ankers, P. (2014). State-of-the-art on use of insects as animal feed. Animal Feed Science and Technology, 197, 1-33.

Müller, A., Wolf, D., Gutzeit, H. O. (2017). The black soldier fly, *Hermetia illucens* – a promising source for sustainable production of proteins, lipids and bioactive substances. Zeitschrift für Naturforschung C, 72, 351-363.

Nguyen, T. T., Tomberlin, J. K., & Vanlaerhoven, S. (2015). Ability of Black Soldier Fly (Diptera: Stratiomyidae) Larvae to Recycle Food Waste. Environmental Entomology, 44, 406-410.

Oonincx, D. G. A. B., Volk, N., Diehl, J. J. E., Van Loon, J. J. A., Belušič, G. (2016). Photoreceptor spectral sensitivity of the compound eyes of black soldier fly (*Hermetia illucens*) informing the

design of LED-based illumination to enhance indoor reproduction. Journal of Insect Physiology, 95, 133-139

Oonincx, D. G., Van Broekhoven, S., Van Huis, A., Van Loon, J. J. (2015). Feed conversion, survival and development, and composition of four insect species on diets composed of food by-products. Plos One, 10.

Oonincx, D. G., Van Itterbeeck, J., Heetkamp, M. J., Van den Brand, H., Van Loon, J. J., Van Huis, A. (2010). An exploration on greenhouse gas and ammonia production by insect species suitable for animal or human consumption. PLoS ONE, 5.

Pezzi, M., Leis, M., Chicca, M., Falabella, P., Salvia, R., Scala, A., Whitmore, D. (2017). Morphology of the antenna of *Hermetia illucens* (Diptera: Stratiomyidae): an ultrastructural investigation. Journal of medical entomology, 54, 925-933.

Roessig, J. M., Woodley, C. M., Cech, J. J., Hansen, L. J. (2004). Effects of global climate change on marine and estuarine fishes and fisheries. Reviews in Fish Biology and Fisheries, 14, 251-275.

Rosenzweig, C., Elliott, J., Deryng, D., Ruane, A. C., Müller, C., Arneth, A., Boote, K. J., Folberth, C., Glotter, M., Khabarov, N., Neumann, K., Piontek, F., Pugh, T. A. M., Schmid, E., Stehfest, E., Yang, H., Jones, J W. (2014). Assessing agricultural risks of climate change in the 21st century in a global gridded crop model intercomparison. Proceedings of the National Academy of Sciences, 111, 3268-3273.

Rozkošný, R. (1983). A biosystematic study of the European Stratiomyidae (Diptera) Vol. 2 Clitellariinae Hermetiinae Pachygasterinae Bibliography. Dr W. Junk publishers, The Hague.

Sheppard, D. C., Newton, G. L., Thompson, S. A., Savage, S. (1994). A value-added manure management-system using the black soldier fly. Bioresource Technology, 50, 275-279.

Sheppard, D. C., Tomberlin, J. K., Joyce, J. A., Kiser, B. C., Sumner, S. M. (2002). Rearing methods for the black soldier fly (Diptera: Stratiomyidae). Journal of Medical Entomology, 39, 695-698.

Spranghers, T., Ottoboni, M., Klootwijk, C., Ovyn, A., Deboosere, S., De Meulenaer, B., Michiels, J., Eeckhout, M., De Clercq, P., De Smet, S. (2017). Nutritional composition of black soldier fly (*Hermetia illucens*) prepupae reared on different organic waste substrates. Journal of the Science of Food and Agriculture, 97, 2594-2600.

Steinfeld, H., Gerber, P., Wassenaar, T. D., Castel, V., Rosales, M., Rosales, M., de Haan, C. (2006). Livestock's long shadow: environmental issues and options. Food and Agriculture Organization of the United Nations, Rome.

St-Hilaire, S., Sheppard, C., Tomberlin, J. K., Irving, S., Newton, L., Mcguire, M. A., Mosley, E. E., Hardy, R. W., Sealey, W. (2007). Fly prepupae as a feedstuff for rainbow trout, *Oncorhynchus mykiss*. Journal of the World Aquaculture Society, 38, 59-67.

Thornton, P. K., Van De Steeg, J., Notenbaert, A., Herrero, M. (2009). The impacts of climate change on livestock and livestock systems in developing countries: A review of what we know and what we need to know. Agricultural Systems, 101, 113-127.

Tomberlin, J. K., Adler, P. H., Myers, H. M. (2009). Development of the black soldier fly (Diptera: Stratiomyidae) in relation to temperature. Environmental Entomology, 38, 930-934.

Tomberlin, J. K., Sheppard, D. C. (2002). Factors influencing mating and oviposition of black soldier flies (Diptera: Stratiomyidae) in a colony. Journal of Entomological Science, 37, 345-352.

Tomberlin, J. K., Sheppard, D. C., Joyce, J. A. (2002). Selected life-history traits of black soldier flies (Diptera: Stratiomyidae) reared on three artificial diets. Annals of the Entomological Society of America, 95, 379-386.

United Nations (2017). World population prospects: the 2017 revision, key findings and advance tables. United Nations Department of Economic and Social Affairs/Population Division.

Van Huis, A., Oonincx, D. G. (2017). The environmental sustainability of insects as food and feed. A review. Agronomy for Sustainable Development, 37.

Van Huis, A., Van Itterbeeck, J., Klunder, H., Mertens. E., Halloran, A., Muir, G., Vantomme, P. (2013). Edible insects - Future prospects for food and feed security. Food and Agriculture Organization of the United Nations, Rome.

Van Huis. A. (2013). Potential of insects as food and feed in assuring food security. Annual Review of Entomology, 58, 563-583.

Verbeke, W., Spranghers, T., De Clercq, P., De Smet, S., Sas, B., Eeckhout, M. (2015). Insects in animal feed: acceptance and its determinants among farmers, agriculture sector stakeholders and citizens. Animal Feed Science and Technology, 204, 72-87.

Waite, R., Beveridge, M., Brummett, R., Castine, S., Chaiyawannakarn, N., Kaushik, S., Mungkung, R., Nawapakpilai, S., Phillips, M. (2014). Improving productivity and environmental performance of aquaculture. World Resources Institute, Washington DC.

Wang, Y., Shelomi, M. (2017). Review of black soldier fly (*Hermetia illucens*) as animal feed and human food. Foods, 6, 91.

Wiegmann, B. M., Trautwein, M. D., Winkler, I. S., Barr, N. B., Kim, J. W., Lambkin, C., Bertone, M. A, Cassel, B. K., Bayless, K. M., Heimberg, A. M., Wheeler, B. M., Kevin J. Peterson, K. J., Pape, T., Sinclair, B. J., Skevington, J. H., Blagoderov, V., Caravas, J., Kutty, S. N., Schmidt-Ott, U., Kampmeier, G. E., Thompson, F. C., Grimaldi, D. A., Beckenbach, A. T., Courtney, G. W., Friedrich, M., Meier, R., Yates, D. K. (2011). Episodic radiations in the fly tree of life. Proceedings of the National Academy of Sciences, 108, 5690-5695.

CHAPTER 1

Structural and functional characterization of *Hermetia illucens* larval midgut

Structural and functional characterization of *Hermetia illucens* larval midgut

Marco Bonelli[1,*], Daniele Bruno[2,*], Silvia Caccia[3], Giovanna Sgambetterra[1], Silvia Cappellozza[4], Costanza Jucker[5], Gianluca Tettamanti[2], Morena Casartelli[1]

[1]Department of Biosciences, University of Milan, Milano, Italy

[2]Department of Biotechnology and Life Sciences, University of Insubria, Varese, Italy

[3]Department of Agricultural Sciences, University of Napoli, Napoli, Italy

[4]CREA Department of Agriculture and Environment (CREA-AA), Sericulture Laboratory of Padova, Padova, Italy

[5]Department of Food, Environmental and Nutritional Science, University of Milan, Milano, Italy

*These authors contributed equally to the work

Corresponding authors:

Morena Casartelli, morena.casartelli@unimi.it

Gianluca Tettamanti, gianluca.tettamanti@uninsubria.it

submitted to *Frontiers in Physiology* in September 2018

under review, minor revision required

ABSTRACT

The use of insects as a primary agent for organic waste reduction and bioconversion into usable
The larvae of *Hermetia illucens* are among the most promising agents for the bioconversion of low quality biomass, such as organic waste, into sustainable and nutritionally valuable proteins for the production of animal feed. Despite the great interest toward this insect, the current literature provides information limited to the optimization of rearing methods for *H. illucens* larvae, with particular focus on their efficiency in transforming different types of waste and their nutritional composition in terms of suitability for feed production. Surprisingly, *H. illucens* biology is a neglected aspect and a deep understanding of the morphofunctional properties of the larval midgut, the key organ that determines the extraordinary dietary plasticity this insect, is completely overlooked. The present study aims at filling this gap of knowledge.

Our results demonstrate that the larval midgut is composed of distinct anatomical regions with different luminal pH and specific morphofunctional features. The midgut epithelium is formed by different cell types that accomplish nutrient digestion and absorption, acidification of the lumen of the middle region, endocrine regulation, and growth of the epithelium. A detailed characterization of the activity of enzymes involved in nutrient digestion and their mRNA expression levels reveals that protein and carbohydrate digestion is associated to specific regions of this organ. Moreover, a significant lysozyme activity in the lumen of the anterior and middle regions of the midgut was detected. This enzyme, together with the strong acidic luminal pH of middle tract, may play an important role in killing pathogenic microorganisms ingested with the feeding substrate.

The collected evidence led us to propose a detailed functional model of the larval midgut of *H. illucens* in which each region is characterized by peculiar features to accomplish specific functions. This platform of knowledge sets the stage for the development of rearing protocols to optimize the bioconversion ability of this insect and its biotechnological applications.

INTRODUCTION

Hermetia illucens (Linnaeus, 1758) (Diptera: Stratiomyidae), the black soldier fly (BSF), is a common and widespread fly in tropical and temperate regions. The insect is traditionally supposed to be of American origin (Rozkošný, 1983; Wang and Shelomi, 2017) although this hypothesis was recently questioned, advancing a possible Palearctic origin (Benelli et al., 2014). Adults do not bite or sting, and are not described as vector of any specific diseases (Wang and Shelomi, 2017). In contrast with adults, which do not need to feed according to several reports (Sheppard et al., 1994; Sheppard et al., 2002; Tomberlin and Sheppard, 2002; Tomberlin et al., 2002; 2009), the

larvae of this holometabolous insect are voracious and grow on a wide variety of organic matters (Nguyen et al., 2015; Wang and Shelomi, 2017) thanks to a well-developed mandibular-maxillary complex (Kim et al., 2010).

From the pioneering study dated back to the end of the seventies of the last century (Newton et al., 1977), a growing body of evidence indicates that *H. illucens* larvae are among the most promising agents for the bioconversion of low quality biomass (e.g., organic waste and byproducts of the agri-food transformation chain) into sustainable and nutritionally valuable proteins and lipids for the production of animal feed (Van Huis, 2013; Van Huis et al., 2013; Barragan-Fonseca et al., 2017; Wang and Shelomi, 2017). Moreover, *H. illucens* larvae are considered a potential source of bioactive substances, such as antimicrobial peptides (AMPs), a wide group of small cationic molecules that are currently studied as a possible alternative to conventional antibiotics and food or feed preservatives (Buchon et al., 2014). The production of a wide array of AMPs by *H. illucens* could be related to the alimentary habits of the larvae that feed on a variety of decomposing organic substrates, typically rich in microorganisms (Müller et al., 2017; Vogel et al., 2018). Furthermore, the ability of the larvae to grow on almost all organic matter makes this insect a potential source of enzymes able to degrade complex substrates that can have important industrial applications. For example, a cellulase has been characterized from *H. illucens* gut microbiota (Lee et al., 2014) and a recent review reported that BSF larvae represent a source of cellulose-, chitin-, and lignin-degrading enzymes (Müller et al., 2017). The interest in *H. illucens* as bioconverter and ingredient for animal feed or source of bioactive molecules is also demonstrated by the increasing number of newly founded companies that deal with BSF mass rearing (https://ilkkataponen.com/entomology-company-database/).

In the last decade, despite the increasing number of papers that demonstrate the broad range of applications that can derive from the exploitation of BSF larvae, little information on the biology of this insect has been obtained. This lack of knowledge may strongly hamper the exploitation of *H. illucens* as a source of nutrients, and bioactive molecules as well as any other possible future biotechnological development. Among the subjects that need deep consideration there are the characterization of the immune system, the description of the gut microbiota and its relationship with the rearing substrates, the fine definition of the critical requirements for insect development, and the characterization of the morphology and physiology of the larval midgut, which has a primary role in food digestion and nutrient absorption. The latter topic, which is essential to better comprehend the extraordinary dietary plasticity of the larva and optimize the exploitation of its bioconversion capability, is the object of this study.

Although the general properties of the larval midgut of non-hematophagous Diptera belonging to the taxon of Brachycera have been already defined (Terra et al., 1996; Nation, 2008), an exhaustive and comprehensive morphofunctional characterization of this organ, with particular attention to the role and the properties of its different districts, has never been performed. Basically, the information regarding the larval midgut of Brachycera species is limited to *Musca domestica* Linnaeus, 1758 and *Drosophila* spp. In the larval midgut of *Drosophila* spp. at least three regions are distinguishable from a morphological and physiological point of view (Dimltriadis and Kastritsis, 1984; McNulty et al., 2001; Dubreuil, 2004; Shanbhag and Tripathi, 2009). Ultrastructural features of midgut cells and the mechanisms of acid and base transport across the midgut epithelium responsible for the pH values recorded in the lumen have been studied (Shanbhag and Tripathi, 2009). The anterior region is characterized by a neutral-slightly alkaline luminal pH, as well as the first part of the posterior region, while the second part of the posterior region is strongly alkaline and the middle midgut is highly acidic (Shanbhag and Tripathi, 2009). A body of evidence indicates that copper cells, a peculiar cell type that is present in the first part of the middle midgut, are involved in the acidification of the lumen of this region (Dubreuil et al., 1998; McNulty et al., 2001; Dubreuil, 2004; Shanbhag and Tripathi, 2009). These cells, described for the first time by Strasburger (1932), are also known as cuprophilic or oxyntic cells.

In the larval midgut of *M. domestica* three regions can be also recognised, with a slightly acidic pH in the lumen of the anterior and posterior midgut and a strongly acidic pH in the middle region (Terra et al., 1988: Lemos and Terra, 1991a). At variance with *Drosophila* spp., in *M. domestica* a functional characterization of the larval midgut, especially regarding the digestive properties associated to the midgut regions, has been accomplished (Espinoza-Fuentes and Terra, 1987; Espinoza-Fuentes et al., 1987; Terra et al., 1988; Lemos and Terra, 1991b; Lemos et al., 1993; Jordão et al., 1996; Pimentel et al., 2018).

Morphofunctional studies on *H. illucens* larval midgut have never been performed. Only few data about the biochemical properties of digestive enzymes are present in the literature. Kim and coworkers (Kim et al., 2011a) investigated the enzymes released by salivary glands and gut. The authors evidenced that clarified gut homogenates have high amylase, lipase, and protease activities, but they did not explore if these activities are associated to a specific region of the organ. Moreover, a qualitative and quantitative comparison of the digestive enzymatic activity from *M. domestica* and *H. illucens* larvae evidenced that the latter possess more digestive enzymes with higher levels of activity (Kim et al., 2011a), a finding that supports the extraordinary digestive capability of *H. illucens*. Finally, two serine proteases were cloned and characterized (Kim et al., 2011b; Park et al., 2012).

The present work aims to provide an in-depth description of the morphological, ultrastructural, and functional properties of the midgut epithelium of *H. illucens* larvae, focusing the attention on the peculiar characteristics of each region in which this tract can be subdivided. In particular, we defined: (i) the morphology and ultrastructural features of the cells that form the midgut epithelium; (ii) the value of the luminal pH in the different midgut regions with particular attention to the district where a strongly acidic pH is present; iii) the enzymes that are involved in carbohydrate and protein digestion and the midgut region where they hydrolyze the substrates; and (iv) the expression levels of genes encoding for proteolytic enzymes in each midgut region. These data allowed us to propose a functional model of the larval midgut of *H. illucens* that clearly shows the peculiar features and functions of each midgut region.

MATERIALS AND METHODS

Insect rearing

H. illucens larvae used in this study were obtained from two colonies, one established in 2014 at the University of Milan (Milano, Italy) and one in 2015 at the University of Insubria (Varese, Italy) starting from larvae purchased from a local dealer (Redbug, Milano, Italy).

BSF adults were kept at 27 ± 0.5 °C, under a 12:12 h light:dark photoperiod, 70 ± 5% relative humidity with water supply and egg traps to promote oviposition. Eggs were collected in a Petri dish (9 × 1.5 cm), maintained at 27 ± 0.5 °C until hatching, and then subjected to a weaning procedure as described in Pimentel et al. (2017). Lots of 300 larvae were grown on Standard diet for Diptera (Hogsette, 1992), composed by 50% wheat bran, 30% corn meal, and 20% alfalfa meal mixed in the ratio 1:1 dry matter:water. The larvae were maintained at 27.0 ± 0.5 °C, 70 ± 5% relative humidity, in the dark. The feeding substrate was added with fresh diet every two days. All experiments were performed on actively feeding last instar larvae weighing between 180 and 230 mg. For the expression analysis of phospho-Histone 3, midgut samples collected from larvae molting from third to fourth instar were used.

Isolation of midgut epithelium and midgut juice

Larvae were anesthetized on ice with CO_2. The gut was isolated in Phosphate Buffered Saline (PBS, 137 mM NaCl, 2.7 mM KCl, 8.1 mM Na_2HPO_4, 1.76 mM KH_2PO_4, pH 7.4) at 4 °C. The midgut, with the enclosed intestinal content, was isolated and subdivided into five regions: anterior midgut, middle midgut 1 and 2, posterior midgut 1 and 2 (see Figure 1 and section "General organization of the larval midgut and pH of the midgut lumen" in Results).

After isolation, the midgut regions used for morphological analyses were fixed as described in the section below, whereas for immunohistochemical analyses the midgut regions were immediately frozen in liquid nitrogen and kept in liquid nitrogen until use.

For the rest of the analyses, the midgut epithelium was separated from the gut content as follows. The peritrophic matrix of each midgut region, with the enclosed intestinal content, was isolated, lightly blotted on filter paper and placed into microcentrifuge tubes. Samples were then centrifuged at 15000 × g for 10 min at 4 °C. Supernatant, i.e., the midgut juice, was collected and used fresh for pH determination, or stored at -80 °C for the enzymatic assays. The midgut epithelium was lightly blotted on filter paper, placed into cryovials and weighed. Tissues were stored in liquid nitrogen for aminopeptidase N assay, Western blot, and molecular analyses. For the determination of digestive enzyme activity and measurement of the luminal pH only anterior midgut, middle midgut 2 (for simplicity named middle midgut), and posterior midgut 2 (for simplicity named posterior midgut) were used, to avoid contaminations of midgut content between tracts.

Light and transmission electron microscopy

After isolation, midgut samples were fixed in 4% glutaraldehyde in 0.1 M Na-cacodylate buffer, pH 7.4, overnight at 4 °C. After postfixation in 2% osmium tetroxide for 2 h at room temperature, specimens were dehydrated in ascending ethanol series and embedded in Epon/Araldite 812 mixture resin. Sections were obtained with a Leica Reichert Ultracut S (Leica, Nussolch, Germany). Semi-thin sections were stained with crystal violet and basic fuchsin and then observed with an Eclipse Ni-U microscope (Nikon, Tokyo, Japan) equipped with a TrueChrome II S digital camera (Tucsen Photonics, Fazhou, China). Thin sections were stained with lead citrate and uranyl acetate and then observed with a JEM-1010 transmission electron microscope (Jeol, Tokyo, Japan) equipped with a Morada digital camera (Olympus, Münster, Germany).

Immunohistochemistry

After isolation, midguts were fixed in 4% paraformaldehyde in PBS overnight at 4 °C. Specimens were then dehydrated in ascending ethanol series and embedded in paraffin. Sections (7-µm-thick), obtained with microtome Jung Multicut 2045, were deparaffinized, rehydrated, and pre-incubated for 30 min with PBS containing 2% bovine serum albumin (BSA) before incubation with anti-H^+

V-ATPase, subunit V1, antibody (Ab 353-2, dilution 1:10000 in 2% PBS/BSA), for 1 h at room temperature. After washing with PBS, sections were incubated for 1 h at room temperature with an anti-guinea pig Cy2-conjugated secondary antibody (dilution 1:200 in 2% PBS/BSA, Jackson ImmunoResearch, Pennsylvania, USA). After washes with PBS, sections were incubated with DAPI (100 ng/ml in PBS) for nuclear staining and then washed. Slides were mounted in Citifluor (Citifluor Ltd, London, UK) with coverslips and analyzed with a Nikon Eclipse Ni microscope equipped with TrueChrome II S digital camera. The primary antibody was omitted in controls.

Western blot analysis

Tissues were homogenized with T10 basic ULTRA-TURRAX (IKA, Staufen, Germany) in RIPA buffer (150 mM NaCl, 2% NP-40, 0.5% sodium deoxycholate, 0.1% sodium dodecyl sulfate (SDS), and 50 mM Tris, pH 8.0) (1 ml/0.14 g of tissue), added with protease inhibitor cocktail (final concentrations: 1 mM AEBSF, 800 nM Aprotinin, 50 µM Bestatin, 15 µM E-64, 20 µM Leupeptin, 10 µM Pepstatin A) and phosphatase inhibitors (final concentrations: 1 mM sodium orthovanadate and 5 mM sodium fluoride) (Thermo Fisher Scientific, Massachusetts, USA). The homogenate was centrifugated at 15000 × g for 15 min at 4 °C and the pellet discarded. Bradford assay (Bradford, 1976) was used to determinate the protein concentration of the supernatant. Clarified homogenates were denaturated at 98 °C in 4× gel loading buffer for 5 min and loaded on 8% or 12% Tris-glycine acrylamide gel for SDS-PAGE analysis (60 µg protein/lane). Proteins were then transferred to a 0.45 µm nitrocellulose membrane (GE Healthcare Life Sciences, Little Chalfont, UK). The membranes were blocked with 5% milk in Tris-Buffered Saline (TBS) (50 mM Tris-HCl, 150 mM NaCl, pH 7.5) for 2 h at room temperature, and subsequently incubated for 1 h at room temperature with the following antibodies: anti-phospho-Histone 3 (Merck-Millipore, Massachusetts, USA), diluted 1:1000 in TBS added with 2% milk, anti-H^+ V-ATPase, diluted 1:10000 in TBS added with 5% milk, or anti-GAPDH (Proteintech, Illinois, USA), diluted 1:2500 in TBS added with 5% milk. After three washes with TBS added with 0.1% Tween 20, antigens of H3P and GAPDH were detected with an anti-rabbit (dilution 1:7500 in TBS added with 5% milk; Jackson ImmunoResearch Laboratories), and antigen of H^+ V-ATPase with an anti-guinea pig (dilution 1:10000 in TBS added with 5% milk, Jackson ImmunoResearch Laboratories) HRP-conjugated secondary antibody. After three washes with TBS added with 0.1% Tween 20, immunoreactivity was detected by SuperSignal chemiluminescence substrate (Thermo Fisher Scientific).

RNA extraction and qRT-PCR

Total RNA was extracted from 15-40 mg of frozen tissue by using TRIzol reagent (Thermo Fisher Scientific), according to manufacturer's instructions. DNA contamination was removed by using

TURBO DNA-free Kit (Thermo Fisher Scientific), then the purity of RNA was assessed by quantification and the integrity of RNA was tested by electrophoresis on 1% agarose gel. RNA was retrotranscribed with M-MLV reverse transcriptase (Thermo Fisher Scientific). qRT-PCR was performed with iTaq Universal SYBR Green Supermix (Biorad, California, USA) using a 96-well CFX Connect Real-Time PCR Detection System (Biorad). To calculate the relative expression of genes of interest, the $2^{-\Delta\Delta Ct}$ method was used, with *HiRPL5* (*Hermetia illucens* Ribosomal Protein L5) as a housekeeping gene. The primers used for *HiTrypsin* (accession number HQ424575) were: F: ATCAAGGTCTCCCAGGTC and R: GGCAAGAGCAATAAGTTGGAT; for *HiChymotrypsin* (accession number HQ424574) were: F: AGAATGGAGGAAAGTTGGAGA and R: CAATCGGTGTAAGCAGAGACA. The primers used for *Hi RPL5* (F: AGTCAGTCTTTCCCTCACGA and R: GCGTCAACTCGGATGCTA) were designed on conserved regions of *RPL5* in other insect species and the sequence was checked by sequencing the PCR product.

Determination of midgut juice pH

The pH of the midgut juice isolated from midgut samples as described above was measured by universal indicator strips with a resolution of 0.5 pH unit (Hydrion Brilliant pH Dip Sticks, Sigma-Aldrich, Milano, Italy). Samples of midgut juice of the different regions were extracted from at least 15 larvae and the experiment was repeated on 14 independent batches of larvae.

Functional characterization of copper cells

Last instar larvae were transferred to Standard diet prepared with a water solution containing 4 mM $CuCl_2$ and allowed to feed for 6, 12, 24, and 48 h. Control larvae were fed on diet prepared with water without $CuCl_2$. At the indicated time points, 15 larvae were collected, anesthetized on ice with CO_2 and dissected. The whole gut was removed and placed in ice-cold PBS. The midgut was divided into five regions as described above and fixed overnight at 4 °C in 3.7% formaldehyde in PBS. Tissue samples were then rinsed in PBS and mounted on microscope slides with mounting medium (2:1 glycerol:PBS). Copper-dependent fluorescence was observed with Olympus BX50 fluorescence microscope at 365 nm excitation wavelength, analyzing the emitted fluorescence between 585 and 620 nm.

At the same time points (6, 12, 24 and 48 h), midgut juice from 15 larvae was collected from both control and copper-feed larvae, and the luminal pH of anterior, middle, and posterior midgut region was measured as indicated above.

Enzymatic assays on midgut juice

Frozen samples of midgut juice were thawed at 4 °C and protein concentration was determined by the method of Bradford (1976), using BSA as standard. Assays were performed under conditions in which product formation was linearly associated with enzyme concentration.

Total proteolytic activity

The total proteolytic activity in midgut juice samples was assayed with azocasein (Sigma-Aldrich), measuring its degradation by release of azo chromophore (Charney and Tomarelli, 1947; Vinokurov et al., 2006; Caccia et al., 2014). Different volumes of midgut juice were diluted to 100 µl with Universal Buffer (UB), which has a constant ionic strength at different pH values (Coch Frugoni, 1957); the pH used for the assays is indicated in the captions to figures and in Results. Then, diluted samples were incubated for 30 min at 45 °C with 200 µl of 1% (w/v) azocasein solution dissolved in UB. The reaction was terminated by adding 300 µl of 12% (w/v) trichloroacetic acid (TCA) at 4°C, then the mixture was maintained for 30 min on ice to favor undigested substrate precipitation, and it was clarified by centrifugation at 15000 × g for 10 min at 4 °C. An equal volume of 500 mM NaOH was added to the supernatant and absorbance was measured at 440 nm with a spectrophotometer (Pharmacia Biotech Ultrospec 3000 UV-Visible, Biochrom Ltd. Cambridge, England). One unit (U) of total proteolytic activity was defined as the amount of enzyme that causes an increase in absorbance by 0.1 unit per min per mg of proteins. Controls were run on midgut juice samples heated to 100 °C for 5 minutes to denature proteolytic enzymes (three replicates for each region of the midgut). The mean absorbance of controls (2.6 ± 0.5 U) was identical for the different midgut regions (unpaired *t*-test) and was subtracted from the total proteolytic activity that was measured in each experiment. The total proteolytic activity in midgut juice samples from the posterior midgut was assayed at different temperatures ranging from 10 °C to 70 °C.

For inhibition assays of total proteolytic activity, midgut juice from posterior region of the midgut was diluted 1:10 in UB at pH 8.5 and preincubated with 5 mM phenylmethanesulfonyl fluoride (PMSF, Sigma-Aldrich) or 0.1 mM E-64 (Sigma-Aldrich) for 15 min at 25 °C. Inhibitor was omitted in controls. Total proteolytic activity in the absence and in the presence of inhibitors was measured as described above. Preliminary experiments were performed to verify the dose-dependent effect of the inhibitors on proteolytic activity, and the concentrations that guaranteed maximum inhibition were used.

Chymotrypsin- and trypsin-like proteolytic activity

Chymotrypsin- and trypsin-like proteolytic activity in midgut juice samples was assayed with N-succinyl-ALA-ALA-PRO-PHE-p-nitroanilide (SAAPPpNA, Sigma-Aldrich) and Na-Benzoyl-

D,L-arginine 4-nitroanilide hydrochloride (BApNA, Sigma-Aldrich), respectively, measuring their degradation by release of p-nitroaniline (pNA) (Hosseininaveh et al., 2007). Different volumes of midgut juice were diluted to 300 µl with UB at pH 8.5. The diluted samples were then incubated with 300 µl of 10 mM SAAPPpNA solution dissolved in UB or with the same volume of 10 mM BApNA solution in UB obtained from a stock solution of 100 mM BApNA in dimethyl sulfoxide for 10 min at 45 °C. The reaction was terminated by addition of 600 µl of ice-cold 12% TCA and after 5 min at 25 °C the absorbance was measured at 405 nm. One unit (U) of proteolytic activity was defined as the amount of enzyme that causes an increase in absorbance by 0.1 unit per min per mg of proteins.

Controls were run on midgut juice samples heated to 100 °C for 5 minutes to denature proteolytic enzymes (three replicates for each region of the midgut). The mean absorbance of controls (8.3 ± 1.4 U and 3.0 ± 0.4 U for chymotrypsin- and trypsin-like proteolytic activity, respectively) was identical for the different midgut regions (unpaired *t*-test) and was subtracted from the activity measured in each experiment.

Trypsin-like activity in midgut juice samples from the posterior region was assayed at different temperatures, ranging from 10 °C to 70 °C, at pH 8.5 to identify the optimum temperature, and at different pH values, ranging from 3.0 to 10.5, at 45 °C to identify the optimum pH.

α-amylase activity

α-amylase activity in midgut juice samples was assayed using starch as substrate, measuring the amount of maltose released (Bernfeld, 1955). A standard curve was determined through linear regression of the maltose absorbance at 540 nm. Different volumes of midgut juice were diluted to 595 µl in Amylase buffer (AB) (20 mM NaH_2PO_4, 6.7 mM NaCl, pH 6.9). Then, the diluted samples were incubated with 90 µl of 1% (w/v) soluble starch solution in AB. Controls without midgut juice sample and controls without substrate were performed for each experiment. All samples were incubated for 30 min at 45 °C, and, after the addition of 115 µl of Color Reagent Solution (CRS) (1 M sodium potassium tartrate, 48 mM 3,5-dinitrosalicylic acid, 0.4 M NaOH), heated at 100 °C for 15 min and then cooled in ice to 25 °C, mixed by inversion, and their absorbance was measured at 540 nm. Considering the standard curve and the absorbance in control samples, the production of maltose from enzymatic hydrolysis of starch was calculated. One unit of α-amylase activity (U) was defined as the amount of enzyme necessary to produce 1 mg of maltose per min per mg of proteins. Midgut juice samples heated to 100 °C for 5 minutes to denature amylolytic enzymes showed no α-amylase activity. α-amylase activity in midgut juice samples from the anterior region was assayed at different pH values ranging from 3.0 to 10.5 to identify the optimum pH.

Lysozyme activity

Lysozyme activity in midgut juice samples was assayed with *Micrococcus lysodeikticus* lyophilized cells (Sigma-Aldrich), measuring the rate of lysis of bacterial cells. Different volumes of midgut juice were diluted to 20 µl with 66 mM potassium phosphate buffer, pH 6.2. Then, the diluted samples were incubated with 980 µl of a suspension of 0.02 % (w/v) *Micrococcus lysodeikticus* lyophilized cells in the same buffer. The mixture was subjected to continuous absorbance reading at 450 nm at 45 °C. One unit/ml (U/ml) of lysozyme activity was defined as the amount of enzyme that causes a decrease in absorbance by 1 unit per min per ml of midgut juice sample.

Aminopeptidase N activity in midgut homogenates

The activity of aminopeptidase N (APN) was assayed using L-leucine p-nitroanilide (Sigma-Aldrich) as substrate (Franzetti et al., 2015) and measuring its degradation by release of p-nitroaniline (pNA). After thawing, midgut samples were homogenized with a microtube pestle in 50 mM Tris-HCl, pH 7.5 (1 ml/100 mg tissue). Different volumes of homogenate were diluted to 800 µl with the same buffer and then 200 µl of 20 mM L-leucine p-nitroanilide were added. The diluted samples were subjected to continuous absorbance reading at 410 nm at 45 °C. One unit/mg (U/mg) of APN activity was defined as the amount of enzyme that releases 1 µmol of pNA per min per mg of proteins.

Statistical analyses

Statistical analyses were performed with R-statistical software (ver. 3.3.2). The following analyses were performed: one-way analysis of variance (ANOVA) followed by Tukey's test, paired and unpaired *t*-tests. Statistical differences between groups were considered significant at p-value ≤ 0.05. The statistical analysis performed for each experiment and the *p*-values are reported in the captions to figures.

RESULTS

General organization of the larval midgut and pH of the midgut lumen

Three regions were clearly recognizable in the alimentary canal isolated from *H. illucens* larvae, i.e., the foregut, the midgut, and the hindgut (Figure 1A).

This organization of the gut into three regions of different embryonic origin characterizes all insects (Nation, 2008) and allows the sequential function of the gut, i.e., food ingestion, digestion and absorption of nutrients, and elimination of frass. At variance with other Brachycera (Terra et al., 1988; Dubreuil, 2004), the larval gut of *H. illucens* did not present gastric caeca (Figure 1A). The midgut, involved in the production and secretion of digestive enzymes, and the absorption of

nutrients represented the intermediate and the longest part of the digestive system (Figure 1B). In non-hematophagous brachycerous larvae examined so far, the midgut is at least subdivided into three distinct regions: anterior, middle and posterior, with the middle segment characterized by a strongly acidic pH of the lumen content (Terra et al., 1988; Lemos and Terra, 1991a; Shanbhag and Tripathi, 2009). Gross morphology and pH values of midgut juice isolated from different midgut districts revealed distinct regions also in the midgut of *H. illucens* larvae. The anterior midgut (AMG) (Figure 1C), with an acidic lumen content (Table 1) was formed by a deeply infolded layer, the middle region was characterized by a narrow and short tract (middle midgut 1, MMG1) that continued in a segment characterized by a larger diameter (middle midgut 2, MMG2) and absence of infolding (Figure 1D). The middle region, as reported for other non-hematophagous brachycerous larvae, was strongly acidic (Table 1). The posterior midgut, downstream of a constriction at the end of the middle tract and characterized by an alkaline luminal pH (Table 1), was the longest region and showed a short first tract (posterior midgut 1, PMG1) followed by a second one darker in color (posterior midgut 2, PMG2) (Figure 1E).

Midgut region	Mean ± SEM (n)
Anterior	5.9 ± 0.1 (14)[a]
Middle	2.1 ± 0.1 (14)[b]
Posterior	8.3 ± 0.2 (14)[c]

Table 1. pH values in the lumen of the midgut regions of *H. illucens* larvae. Different letters indicate statistically significant differences between groups (mean ± SEM, number of replicates in parenthesis. ANOVA test followed by Tukey's test. ANOVA p-value<0.001, Tukey's test p-values: Middle *vs* Anterior p<0.001, Posterior *vs* Anterior p<0.001, Posterior *vs* Middle p<0.001).

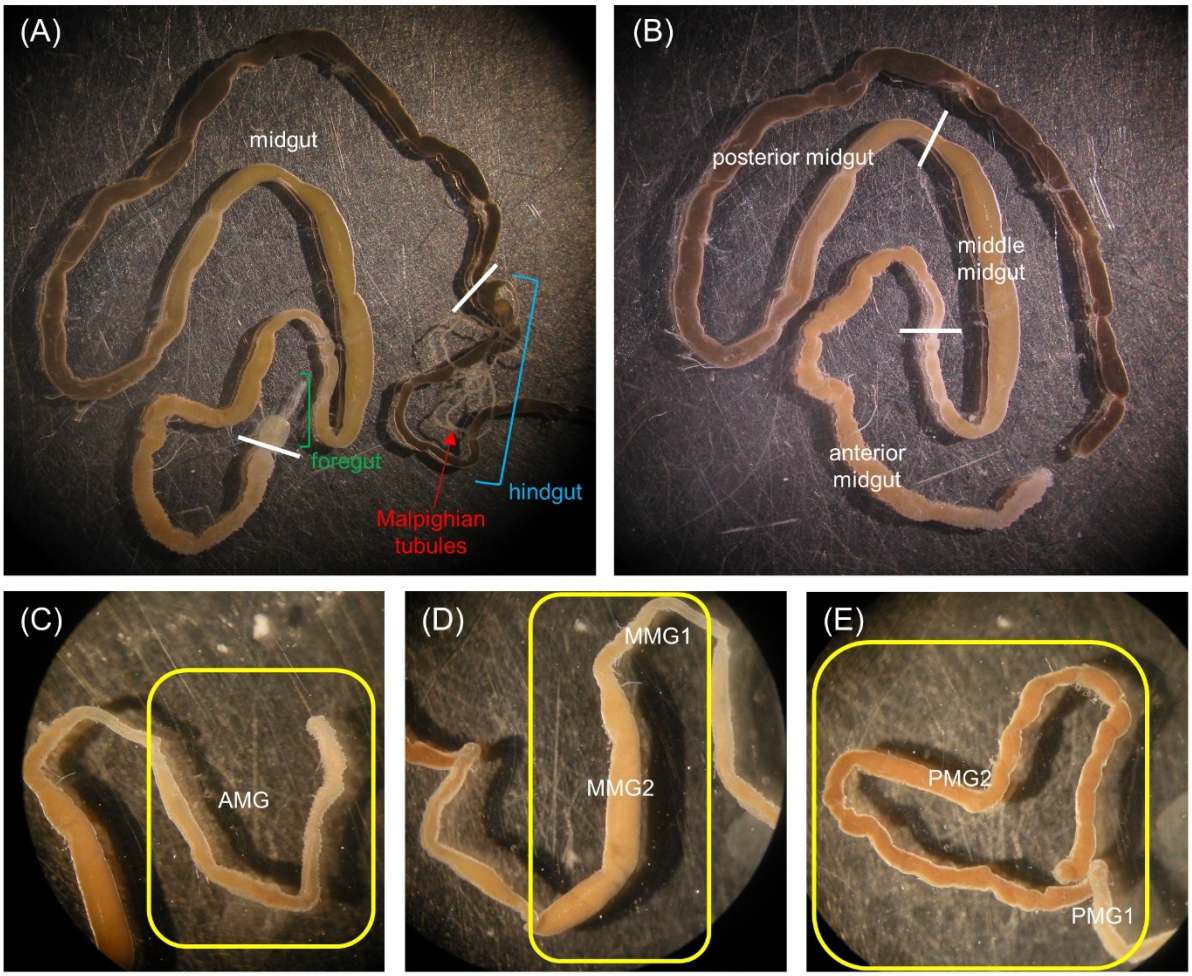

Figure 1. **Anatomy of the alimentary canal of *H. illucens* larvae and definition of the midgut regions.** The short foregut is followed by a very long midgut; the beginning of the hindgut is identifiable by the insertion of Malpighian tubules, structures involved in excretion (A). The midgut can be subdivided into three main regions: anterior, middle, and posterior (B). In (C), (D), and (E) details of each midgut region are reported. Anterior midgut (C); middle midgut (D) in which a first narrow and short tract (MMG1) is followed by a segment with a larger diameter (MMG2); posterior midgut (E) in which two tracts are recognizable, a first short part (PMG1) and a second tract darker in color (PMG2).

Morphological characterization of the midgut epithelium and regional differentiation

A detailed morphological characterization of the midgut epithelium was performed for all the five regions described above (see "General organization of the larval midgut and pH of the midgut lumen" and Figure 1). Three main cell types were found along the whole length of the midgut, i.e., columnar, endocrine, and stem cells. Columnar cells were the most representative cell type of the epithelium and were characterized by the presence of microvilli on the apical membrane and basal infolding (Figure 2A). The endocrine cells were localized in the basal region of the epithelium and presented electron-dense granules in the cytoplasm (Figure 2B). Finally, stem cells were randomly distributed at the base of the epithelium (Figure 2C). These cells were able to proliferate during larva-larva molt (Figure 2D), as confirmed by Western blot analysis of phospho-Histone 3: a 17-kDa band revealed a significant presence of this mitotic marker during the molting phase, which was absent in the intermolt period (last instar larvae actively feeding) (Figures 2E, S1).

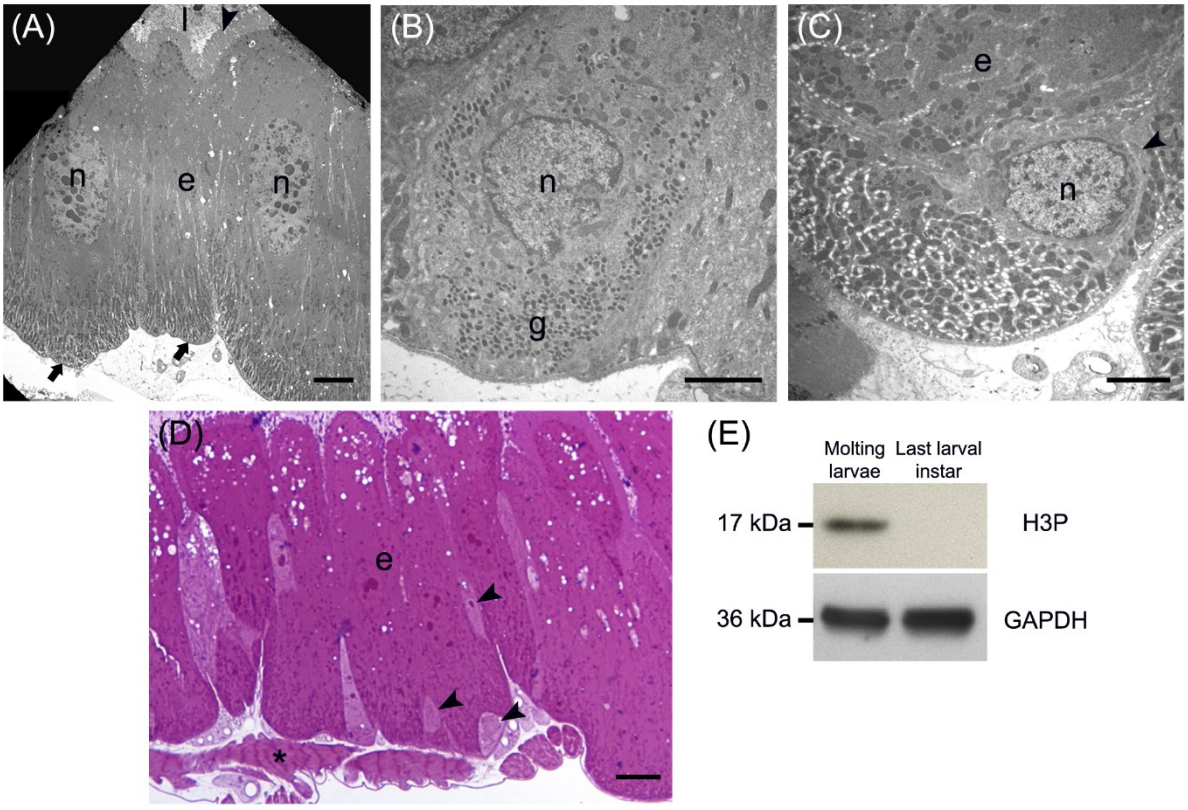

Figure 2. **Main cell types present in the larval midgut epithelium**. (A): columnar cells display a developed basal infolding (arrows) and long microvilli (arrowhead). (B): endocrine cells with electron-dense granules (g) inside the cytoplasm. (C): stem cell (arrowhead) located at the base of the midgut epithelium. (D): the amount of stem cells (arrowheads) increases during larva-larva molt. (E): Western blot analysis of phospho-Histone 3 (H3P). e: epithelium; l: lumen; asterisk: muscle cells; n: nucleus. Bars: 5 µm (A), 2 µm (B, C), 10 µm (D).

Besides the three cell types described above, every midgut district presented typical features, indicating a marked regional differentiation of this organ. The AMG showed a thick epithelium (Figure 3A) formed by columnar cells with a developed basal infolding (Figure 3B). These cells were characterized by abundant rough endoplasmic reticulum (RER) (Figure 3C), and numerous electron-dense granules and mitochondria were present in the apical region under the microvilli (Figure 3D).

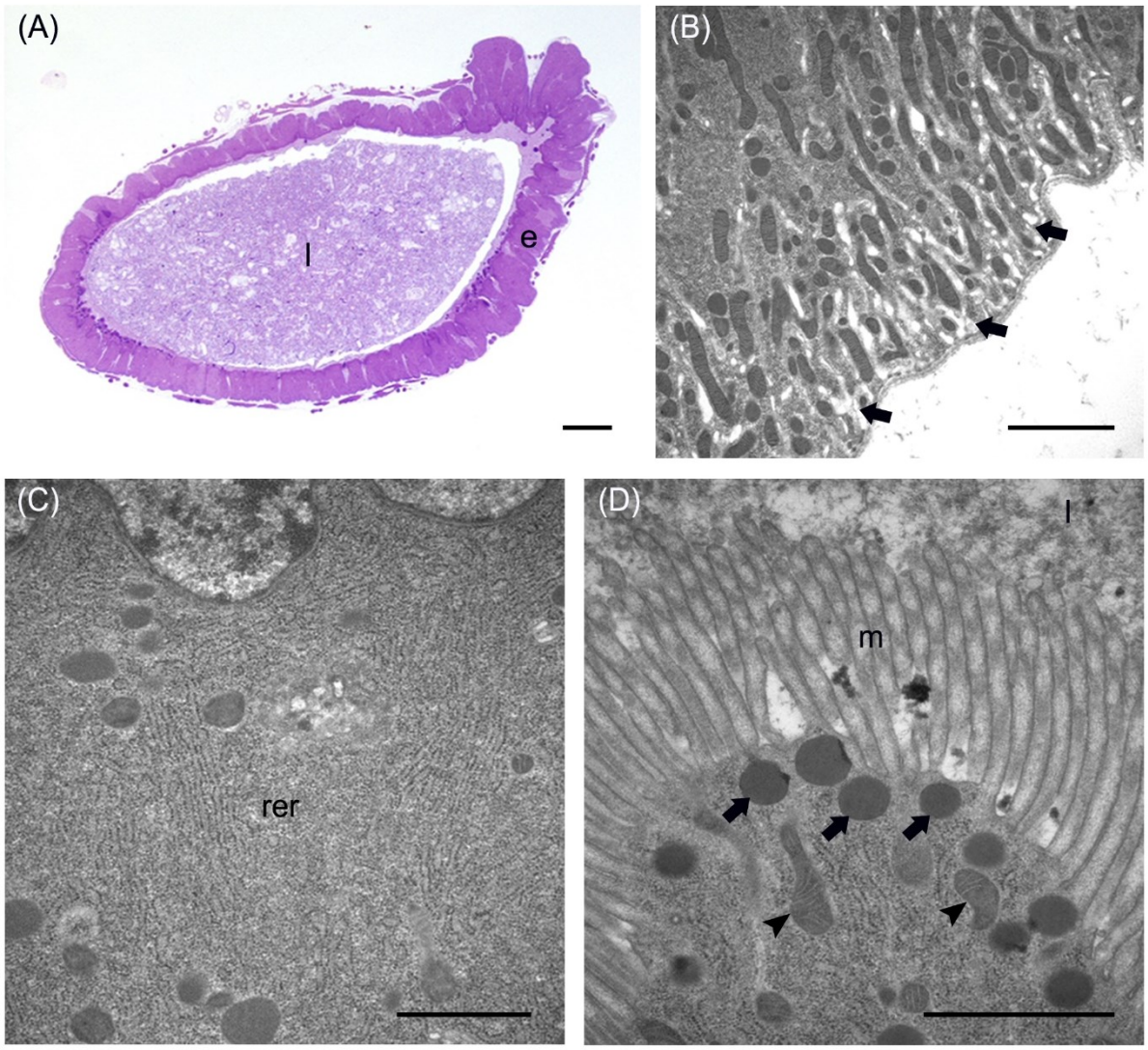

Figure 3. **Morphological organization of the anterior midgut.** (A): cross-section of anterior midgut. (B): wide basal infolding (arrows) in columnar cells. (C): rough endoplasmic reticulum (rer) in the cytoplasm of columnar cells. (D): electron-dense vesicles (arrows) in the apical part of columnar cells, under the microvilli (m). e: epithelium; l: lumen; arrowheads: mitochondria. Bars: 100 µm (A), 2 µm (B), 1 µm (C, D).

The epithelium of MMG1 contained specialized cells, i.e., copper cells, characterized by a cup shape (Figure 4A), a big central nucleus (Figure 4B) and long microvilli (Figure 4B). A peculiar trait of these cells was the presence of several and elongated mitochondria inside each microvillus (Figures 4C, D). On the apical membrane of the cells portasome-like particles could be observed (Figure 4E). The presence of H^+ V-ATPase, previously shown to be associated to portasomes (Shanbhag and Tripathi, 2009; Zhuang et al., 1999), was investigated by immunohistochemistry and Western blot analysis. Western blot revealed seven bands with molecular mass of 13-kDa, 14-kDa, 27-kDa, 34-kDa, 55-kDa, 56-kDa, and 67-kDa, corresponding to most of the subunits of the cytoplasmic V_1 complex of H^+ V-ATPase (Figure 4F). Immunostaining confirmed the presence of H^+ V-ATPase only in MMG1, specifically associated to the apical membrane of copper cells (Figures 4G-K).

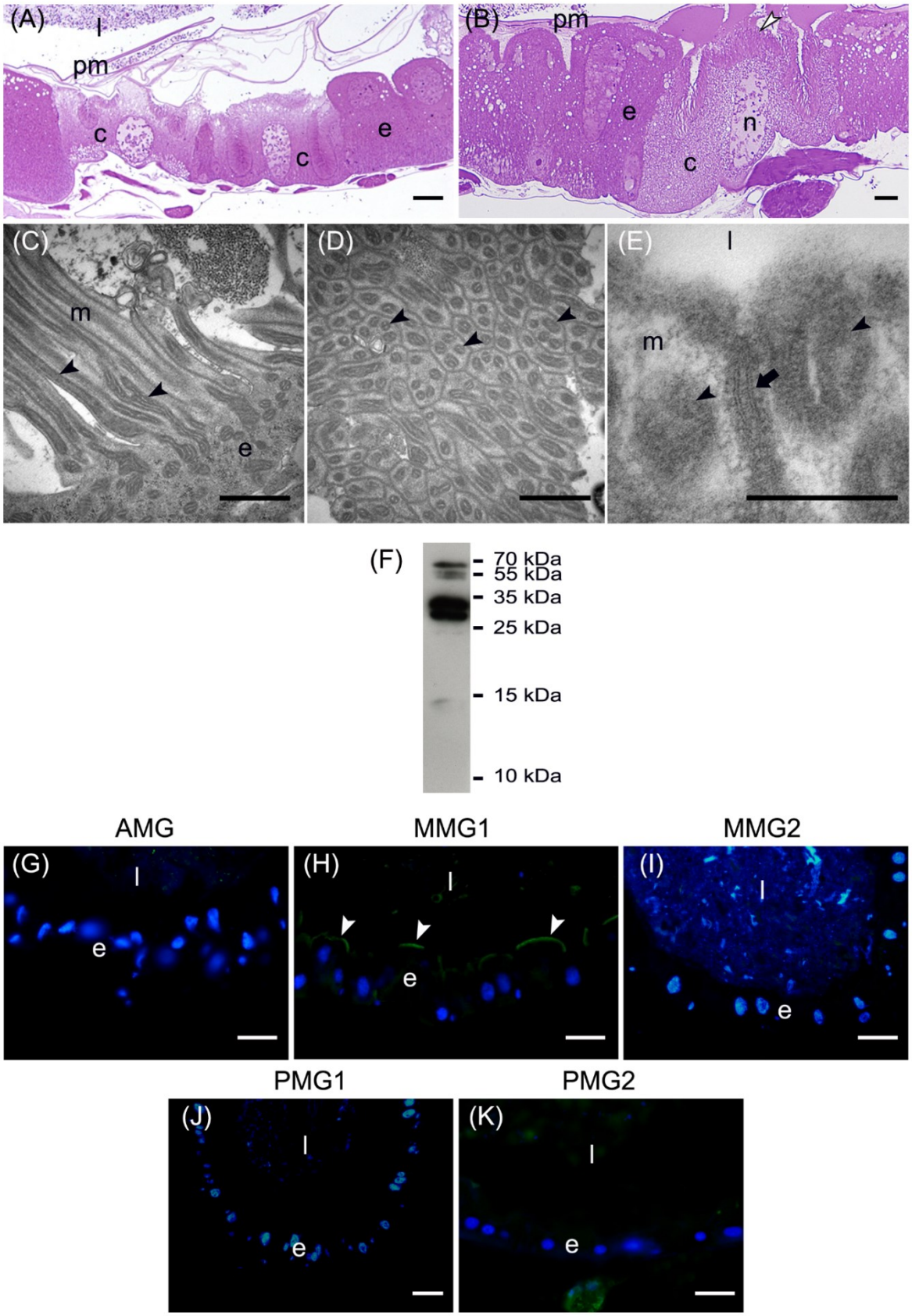

Figure 4. **Morphological organization of MMG1**. (A, B): cuprophilic cells (c) characterized by the long microvilli (open arrowheads). (C, D): Elongated mitochondria (arrowheads) are visible in longitudinal (C) and cross (D) section of microvilli (m). (E): Portasome-like structure (arrow) in the apical surface of microvilli. Mitochondria (arrowheads) are visible. (F): Western blot analysis of H^+ V-ATPase. (G-K): H^+

V-ATPase immunolocalization (white arrowheads) in the different midgut regions. e: epithelium; l: lumen; n: nucleus; pm: peritrophic matrix. Bars: 20 µm (A, G-K), 10 µm (B), 1 µm (C, D), 200 nm (E).

The ability of these cells to acidify the middle midgut lumen, thanks to the secretion of proton into the lumen *via* H^+ V-ATPase, was evaluated. In copper-fed larvae of *Drosophila melanogaster* Meigen, 1830, copper cells have been shown to acquire an orange fluorescence signal due to the formation of a copper ions-metallothionein complex and, in turn, the acid-secreting activity of these cells is reduced (McNulty et al., 2001). To verify whether copper cells in *H. illucens* midgut showed similar features, larvae fed on diet containing cupric chloride for different time points (6, 14, 24 and 48 h) were examined. MMG1, the region containing copper cells, from control larvae reared without $CuCl_2$ in the diet did not exhibit orange fluorescence when examined under UV excitation for all the time points considered (Figure 5A and data not shown). Conversely, the same midgut tract of larvae fed on copper-containing diet showed a fluorescence signal starting from 14 h that increased significantly over time (Figures 5B-E). Midgut cells of the other regions showed an orange fluorescence only in larvae fed on copper-containing diet for 48 h (data not shown). We also examined the relationship between copper-dependent fluorescence and midgut lumen pH. Midgut juice samples from anterior, middle, and posterior region of the midgut were extracted from larvae fed for 24 h on copper-containing diet and control diet, and the pH was measured using universal indicator strips. As indicated in Figure 5F, copper feeding reduced larval midgut acidification in the middle midgut, whereas no variation was recorded in the anterior and posterior midgut.

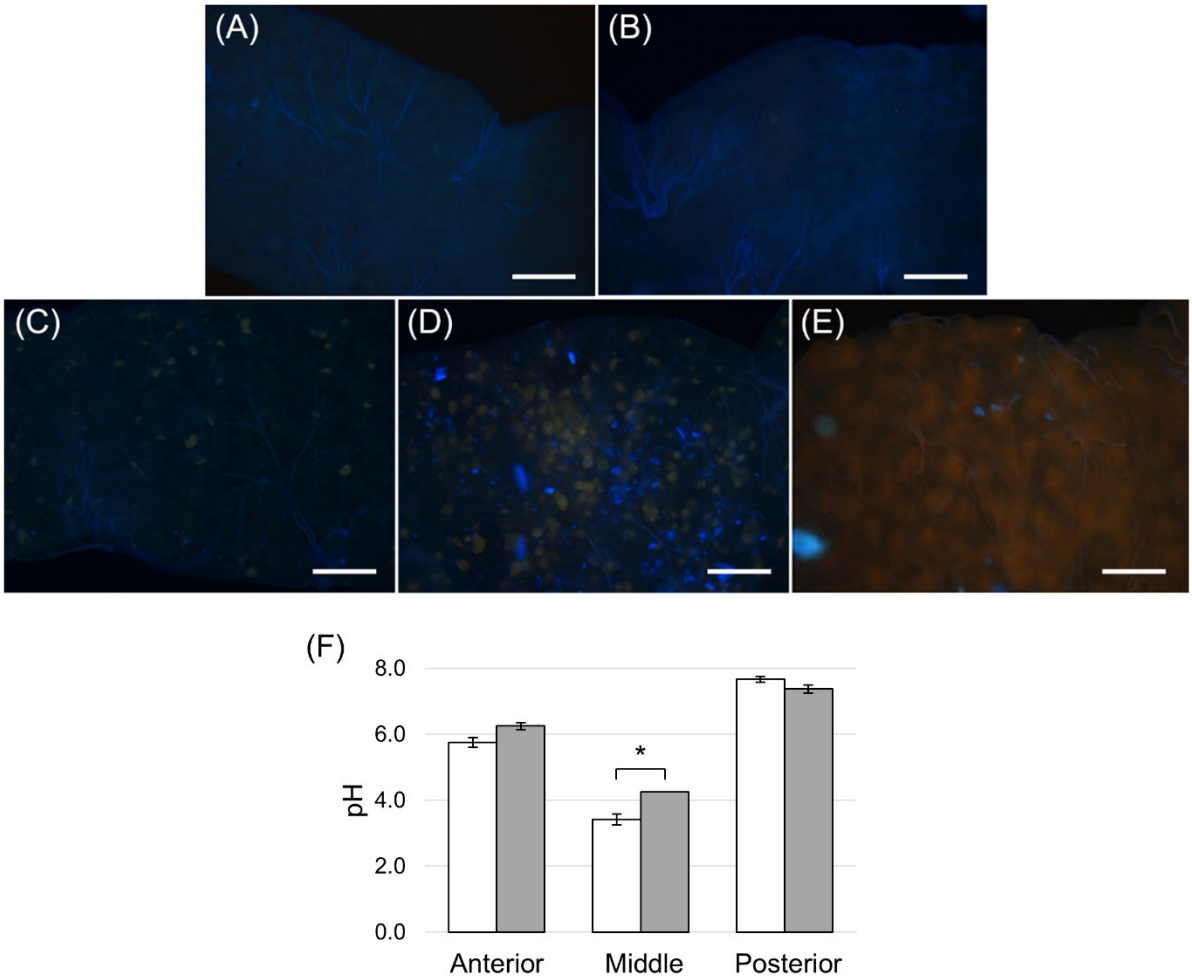

Figure 5. Copper feeding experiments. (A): dissected midgut from control larvae reared on standard diet without $CuCl_2$ for 24 h. (B, C, D, E): dissected midgut from larvae reared on standard diet added with $CuCl_2$ for 6, 14, 24 and 48 h, respectively. (F): pH measurement of midgut juice samples from anterior, middle and posterior region of midgut isolated from larvae fed for 24 h on control (white bar chart) and copper-containing diet (grey bar chart). The values are reported as mean ± SEM of at least 3 experiments. Only in the middle midgut a significant difference between groups was observed (unpaired *t*-test: $*p<0.01$). Bars: 100 µm (A-E).

MMG2 showed a wide lumen surrounded by a thin epithelium (Figure 6A) formed by large flat cells with a big elongated nucleus (Figure 6B) and a very short brush border (Figure 6C).

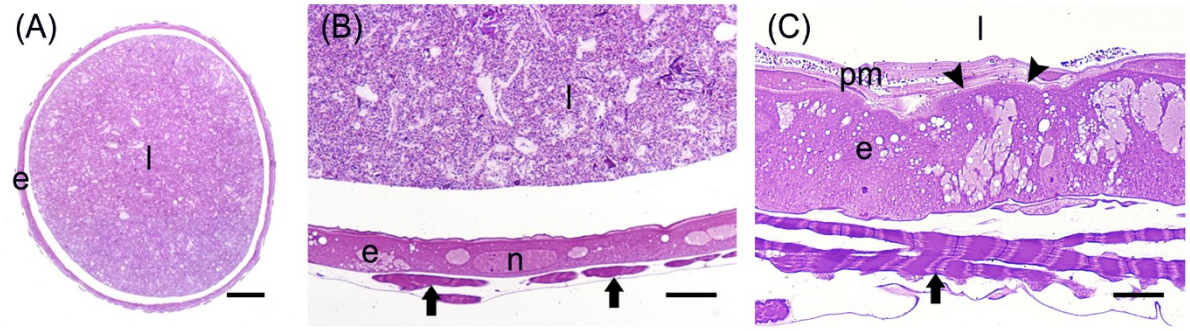

Figure 6. Morphological organization of MMG2. (A): cross-section of MMG2. (B, C): Details of the large flat cells that forms the thin epithelium in this midgut region. The short brush border (arrowheads) is visible in (C). e: epithelium; l: lumen; arrows: muscle cells; n: nucleus; pm: peritrophic matrix. Bars: 200 µm (A), 20 µm (B), 10 nm (C).

The posterior midgut displayed peculiar morphological features. In this region, the epithelium was thick (Figure 7A) with a well-developed brush border (Figure 7B). In particular, columnar cells in PMG1 differed from those of PMG2 for the numerous electron-dense granules localized under the microvilli (Figure 7B). Similarly to the anterior midgut, abundant RER (Figure 7C) was observed. Columnar cells of PMG2 showed very long microvilli (Figure 7D).

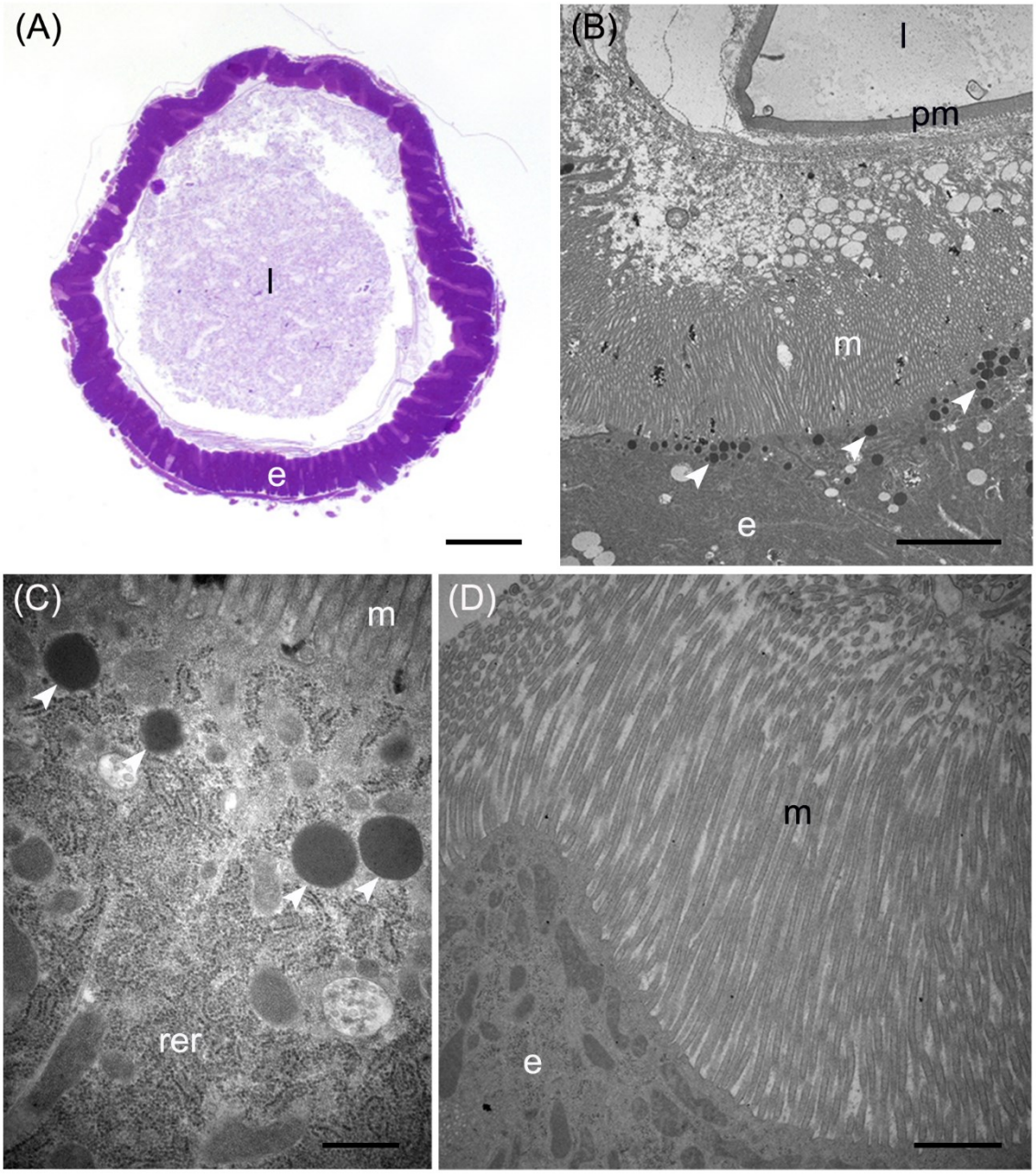

Figure 7. Morphological organization of the posterior midgut (PMG1 and PMG2). (A): cross-section of PMG1. (B, C): rough endoplasmic reticulum (rer), microvilli (m), and electron-dense vesicles (arrowheads) in the apical part of columnar cells in PMG1. (D): brush border of the epithelial cells in PMG2. e: epithelium; l: lumen; pm: peritrophic matrix. Bars: 100 µm (A), 5 µm (B), 500 nm (C), 1 µm (D).

Distribution of digestive enzymes in the midgut

A previous study indicated that salivary glands of *H. illucens* larvae are a minor source of digestive enzymes and that digestion is mainly accomplished by the midgut (Kim et al., 2011a). To evaluate whether the morphological differences observed in the different midgut regions, as well as the deep variation in the luminal pH along this organ, corresponded to a functional regionalization, we examined the activity of enzymes involved in protein and carbohydrate digestion in each midgut region.

We first measured the total proteolytic activity in the midgut juice isolated from the anterior, middle and posterior region using azocasein as substrate at pH values as close as possible to those present in the lumen of each region. As reported in Figure 8A, the posterior tract showed the highest activity that was more than forty- and twenty-fold higher than in the anterior and middle region, respectively. Since the posterior midgut may have a major role in protein digestion, a detailed characterization of the total proteolytic activity in this region was performed. First, we evaluated the dependence of the total proteolytic activity on temperature (Figure 8B). The highest activity was recorded at 45 °C, while beyond this temperature the residual activity declined, reaching approximately 10% at 10 and 70 °C. Since the lumen of the posterior midgut had an alkaline pH (Table 1), we evaluated if the total proteolytic activity measured in this region could be ascribed to serine proteases, the major family of endopeptidases that shows a significant activity at alkaline pH values (Terra and Ferreira, 1994; 2005). When the proteolytic activity was measured at acidic pH (pH 5.0), a highly significant decrease of the enzymatic activity (approximately 13-fold reduction) was observed compared to that recorded at pH 8.5 (Figure 8C). Moreover, PMSF, a rather specific, competitive, and irreversible inhibitor of serine proteases, caused a significant reduction of the total proteolytic activity compared to controls, with a percent of inhibition of 56.5 ± 1.4% (Figure 8D). On the contrary, no inhibition was observed with E-64, an irreversible inhibitor of a wide range of cysteine proteases (Figure 8D).

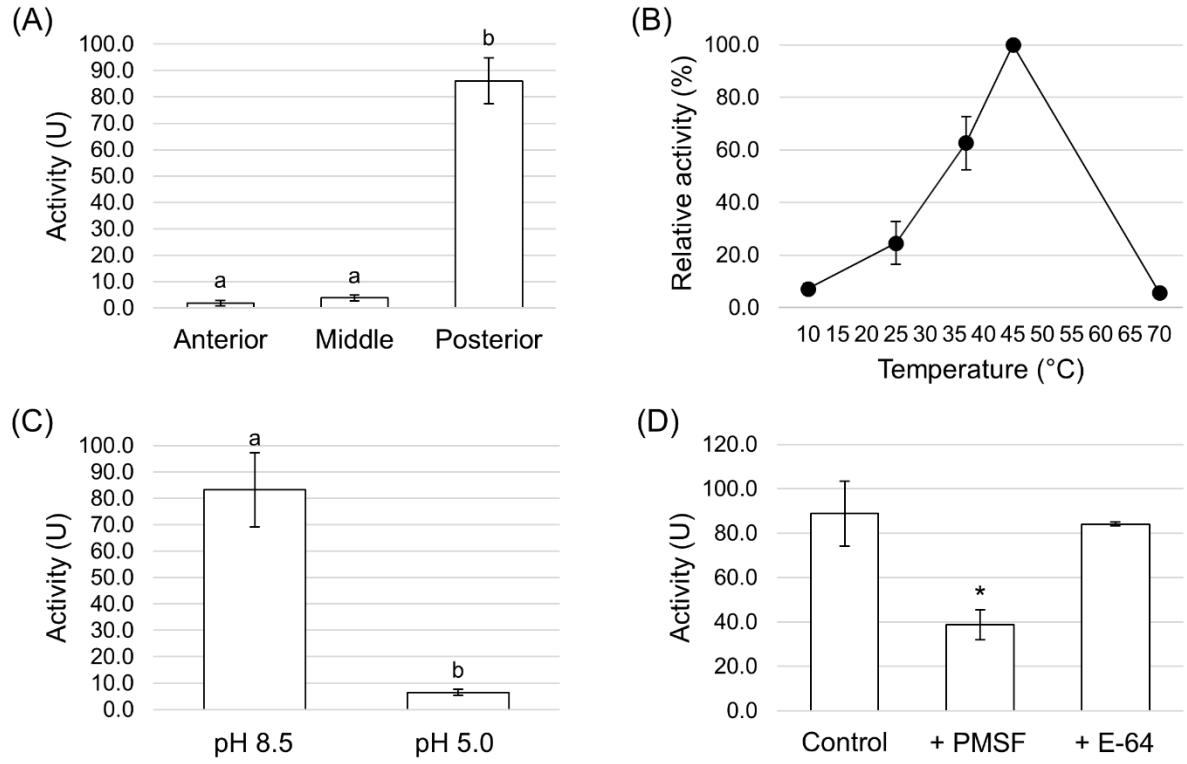

Figure 8. Total proteolytic activity in the different midgut regions. (A): total proteolytic activity in midgut juice extracted from anterior, middle and posterior midgut. For each tract the enzymatic assay was performed at pH as close as possible to that of the lumen (pH 6.0 for the anterior midgut, pH 5.0 for the middle midgut and pH 8.5 for posterior). The values are reported as mean ± SEM of at least 3 experiments. Different letters denote significant differences (ANOVA test followed by Tukey's test. ANOVA p-value<0.001, Tukey's test p-values: Middle *vs* Anterior p=0.975, Posterior *vs* Anterior p<0.001, Posterior *vs* Middle p<0.001). (B): dependence of total proteolytic activity on temperature in midgut juice from the posterior region of the midgut performed at pH 8.5. Relative activity values (%) are reported as mean ± SEM of at least 3 experiments and are expressed as percentage of the highest activity over the temperature range examined. (C): total proteolytic activity in midgut juice from the posterior midgut measured at pH 8.5 and 5.0. The values are reported as mean ± SEM of 3 experiments. Different letters denote significant differences (paired t-test: p-value<0.05). (D): total proteolytic activity in midgut juice from the posterior midgut measured at pH 8.5 in the absence (control) and in the presence of serine- (PMSF) and cysteine- (E-64) protease inhibitors. The values are reported as mean ± SEM of 5 experiments. A significant difference between groups was observed between the activity measure in the presence of PMSF *vs* control (paired t-test: *p-value<0.01).

Trypsin- and chymotrypsin-like enzymes are the major serine proteases involved in protein digestion in most insects (Terra and Ferreira, 1994; 2005). To verify the involvement of these enzymes in digestion processes, we first measured mRNA levels of two isoforms of these enzymes (Kim et al., 2011b) in the different midgut districts by qRT-PCR. Both genes were highly expressed in the posterior midgut, with mRNA levels significantly higher in PMG1 than PMG2 for *HiTrypsin* (Figures 9A, B).

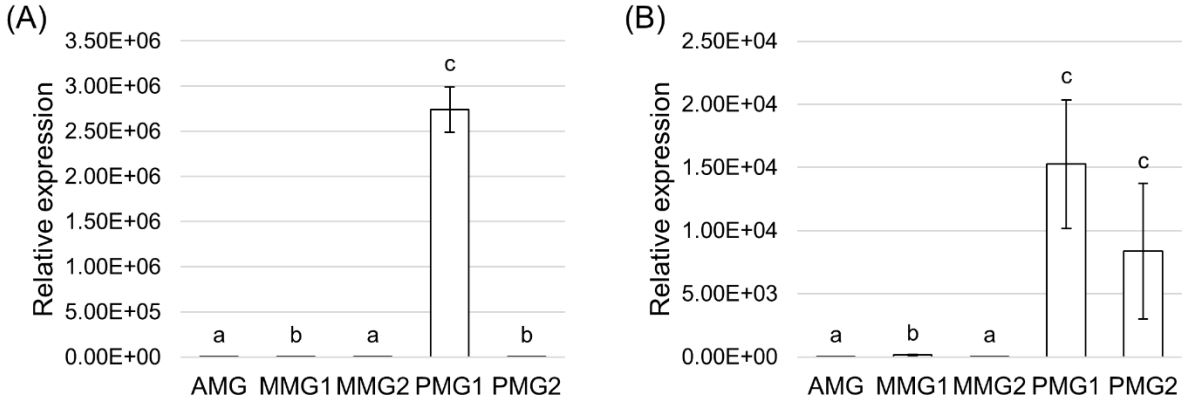

Figure 9. Expression profile of serine proteases. (A, B): qRT-PCR analysis of *HiTrypsin* (A) and *HiChymotrypsin* (B) in the different midgut regions. The values are reported as relative expression mean ± SEM of 3 experiments. Different letters denote significant differences: *HiTrypsin* (ANOVA test followed by Tukey's test. ANOVA *p*-value<0.001, Tukey's test *p*-values: AMG *vs* MMG1 $p<0.001$, AMG *vs* MMG2 $p=0.107$, AMG *vs* PMG1 $p<0.001$, AMG *vs* PMG2 $p<0.001$, MMG1 *vs* MMG2 $p<0.05$, MMG1 *vs* PMG1 $p<0.001$, MMG1 *vs* PMG2 $p=0.328$, MMG2 *vs* PMG1 $p<0.001$, MMG2 *vs* PMG2 $p<0.001$, PMG1 *vs* PMG2 $p<0.001$); *HiChymotrypsin* (ANOVA test followed by Tukey's test. ANOVA *p*-value<0.001, Tukey's test *p*-values: AMG *vs* MMG1 $p<0.01$, AMG *vs* MMG2 $p=0.237$, AMG *vs* PMG1 $p<0.001$, AMG *vs* PMG2 $p<0.001$, MMG1 *vs* MMG2 $p<0.001$, MMG1 *vs* PMG1 $p<0.01$, MMG1 *vs* PMG2 $p<0.01$, MMG2 *vs* PMG1 $p<0.001$, MMG2 *vs* PMG2 $p<0.001$, PMG1 *vs* PMG2 $p<0.790$).

By using specific substrates, we measured the tryptic and chymotryptic activity in the different midgut regions. Figure 10A reports trypsin-like activity in the midgut juice from anterior, middle and posterior region of the midgut using BApNA as substrate. No activity was recorded in the anterior and middle region, while a significant trypsin-like activity was present in the posterior region. To better characterize the tryptic activity, we evaluated its dependence on temperature and pH. The optimal temperature, as for the total proteolytic activity (Figure 8B), was 45 °C (Figure 10B). The evaluation of pH effect on trypsin activity using buffers at different pH, at temperature of 45 °C, evidenced that the highest BApNA hydrolysis occurred at pH values from 7.0 to 10.5, with an optimum at pH 8.5, and decreased significantly at acidic pH (Figure 10C). We also measured the activity of chymotrypsin-like proteases in the midgut juice extracted from the three regions of the midgut using SAAPPpNA as substrate (Figure 10D).

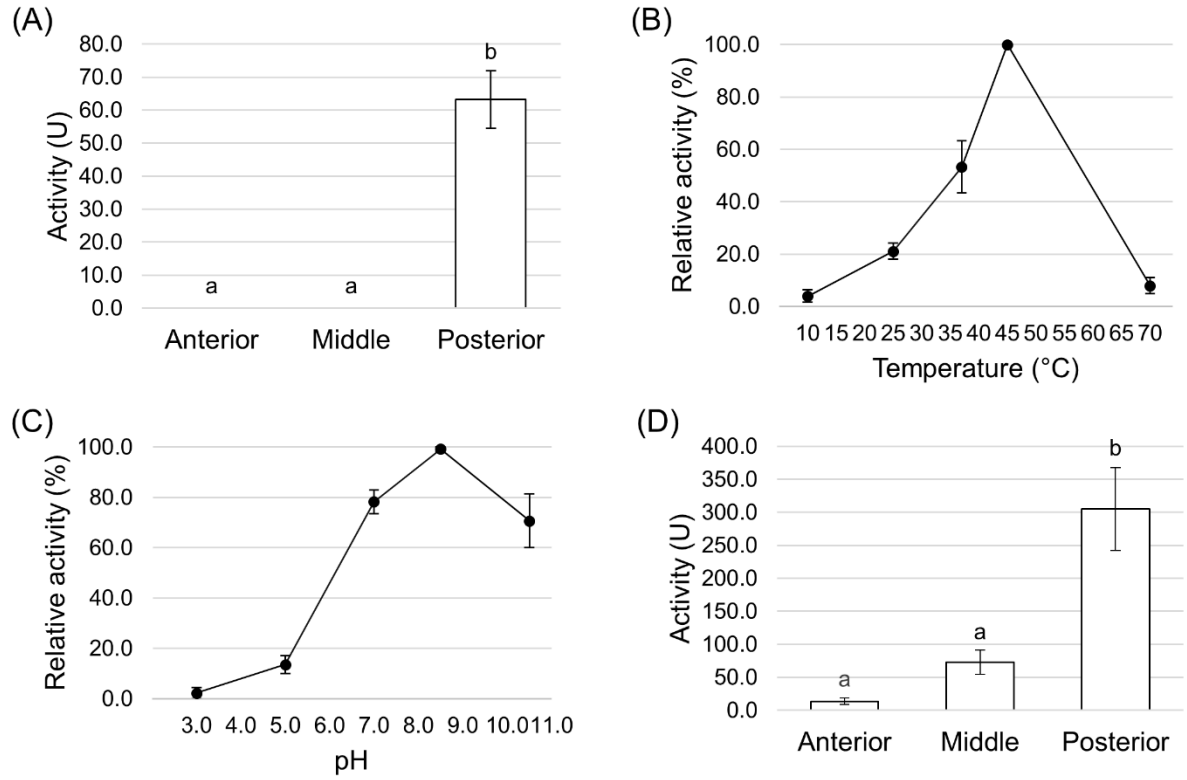

Figure 10. Trypsin and chymotrypsin activity in the different midgut regions. (A): trypsin activity in midgut juice extracted from anterior, middle and posterior midgut. For each tract the enzymatic assay was performed at pH 8.5. The values are reported as mean ± SEM of 3 experiments. Different letters denote significant differences (ANOVA test followed by Tukey's test. ANOVA p-value<0.001, Tukey's test p-values: Middle *vs* Anterior p=1.000, Posterior *vs* Anterior p<0.001, Posterior *vs* Middle p<0.001). (B): dependence of trypsin activity on temperature in midgut juice from the posterior region of the midgut performed at pH 8.5. Relative activity values (%) are reported as mean ± SEM of at least 3 experiments and are expressed as percentage of the highest activity over the temperature range examined. (C): dependence of trypsin activity on pH in midgut juice from the posterior region of the midgut performed at 45 °C. Relative activity values (%) are reported as mean ± SEM of at least 3 experiments and are expressed as percentage of the highest activity over the pH range examined. (D): chymotrypsin activity in midgut juice extracted from anterior, middle and posterior midgut. For each tract the enzymatic assay was performed at pH 8.5. The values are reported as mean ± SEM of at least 3 experiments. Different letters denote significant differences (ANOVA test followed by Tukey's test. ANOVA p-value<0.05, Tukey's test p-values: Middle *vs* Anterior p=0.845, Posterior *vs* Anterior p<0.05, Posterior *vs* Middle p=0.061).

The highest activity was recorded in the lumen content of the posterior midgut, confirming that this district is the main site where protein digestion by endopeptidases belonging to serine proteases family occurs.

To define whether the posterior midgut was also responsible for the final phase of protein digestion in which single amino acids are produced, we measured the activity of aminopeptidase N (APN), one of the abundant exopeptidase families present in the midgut brush border of insect larvae (Terra and Ferreira, 1994). APN activity was recorded only in tissue homogenates prepared from the posterior midgut (Figure 11).

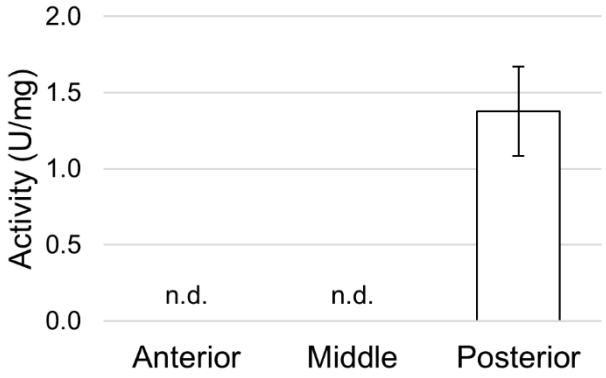

Figure 11. Aminopeptidase N activity in the different midgut regions using L-leucine p-nitroanilide as substrate. The values are reported as mean ± SEM of at least 3 experiments. In the anterior and middle midgut no activity was detectable (n.d.).

α-amylase activity in midgut juice samples from anterior, middle and posterior regions of the midgut was also determined. The highest activity was recorded in the anterior midgut, although a significant digestion of starch occurred also in the posterior region; conversely, no activity was present in the middle midgut (Figure 12A). Since in *H. illucens* larvae the pH of the lumen in the three midgut region was rather different (Table 1), to assess how this chemical parameter influenced α-amylase activity, a detailed evaluation of pH dependence in the anterior midgut was performed. High activity was recorded at pH values ranging from 5.0 to 8.0, with a maximum between pH 6.0 and 7.0. At pH values lower than 5.0 and higher than 8.0 α-amylase activity significantly decreased and dropped to zero at pH 3.0 and 10.0 (Figure 12B). Therefore, the luminal pH value of the anterior and posterior midgut (Table 1), the regions where hydrolysis of internal α-1,4-glycosidic bonds of polysaccharides (i.e., starch and glycogen) occurs (Figure 12A), fits with the optimum pH range of α-amylase activity (Figure 12B).

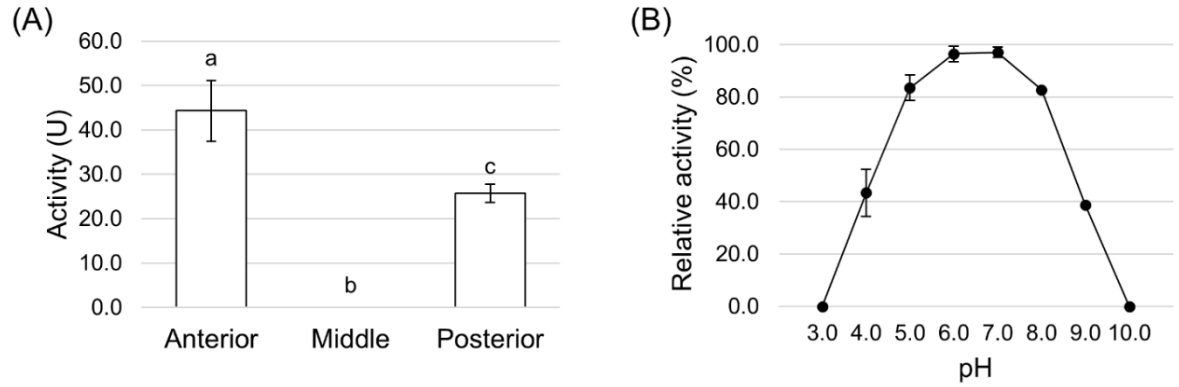

Figure 12. α-amylase activity in the different midgut regions. (A): α-amylases activity in midgut juice extracted from anterior, middle and posterior midgut. The values are reported as mean ± SEM of at least 3 experiments. Different letters denote significant differences (ANOVA test followed by Tukey's test. ANOVA p-value<0.001, Tukey's test p-values: Middle *vs* Anterior p<0.001, Posterior *vs* Anterior p<0.05, Posterior *vs* Middle p<0.05). (B): dependence of α-amylases activity on pH in midgut juice from the anterior region of the midgut. Relative activity values (%) are reported as mean ± SEM of at least 3 experiments and are expressed as percentage of the highest activity over the pH range examined.

Finally, since the midgut can be involved in the enzymatic clearance of ingested microorganisms (Lemos and Terra, 1991a; Lemos et al., 1993; Terra and Ferreira, 1994; Padilha et al., 2009), we measured the activity of lysozyme, which catalyzes the hydrolysis of 1,4-β-glyosidic bonds between N-acetylmuramic acid and N-acetyl-D- glucosamine residues in the peptidoglycan of the cell wall of many bacteria, thus compromising the integrity of the structure and causing the lysis of the cell. Lysozyme activity was measured in midgut juice samples extracted from anterior, middle, and posterior region of the midgut. The highest activity was present in the middle midgut, whereas the other two regions showed significantly lower activities, especially the posterior (Figure 13).

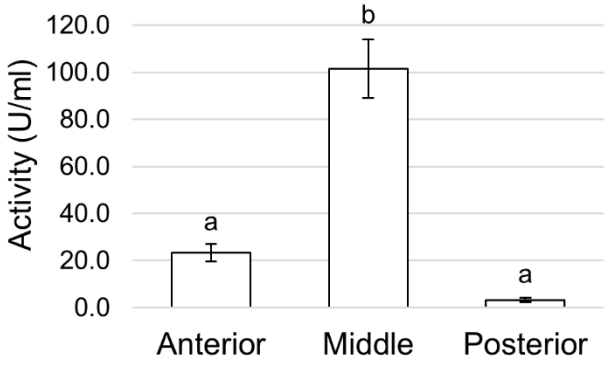

Figure 13. Lysozyme activity assayed in the different midgut regions measuring the rate of lysis of *Micrococcus lysodeikticus*. The values are reported as mean ± SEM of at least 3 experiments. Different letters denote significant differences (ANOVA test followed by Tukey's test. ANOVA p-value<0.001, Tukey's test p-values: Middle *vs* Anterior p<0.001, Posterior *vs* Anterior p=0.394, Posterior *vs* Middle p<0.001).

DISCUSSION

The great interest towards *H. illucens* larvae for their ability to bioconvert low quality substrates into valuable biomass (Barragan-Fonseca et al., 2017; Müller et al., 2017; Wang and Shelomi, 2017) is not supported by a knowledge of the physiology of this insect, in particular of the functional properties of the midgut, which is involved in nutrient digestion and absorption. This lack of information can negatively affect the exploitation of the bioconversion ability of *H. illucens* since the dietary plasticity of the larvae and the efficiency of bioconversion strictly depend on the physiological properties of this organ. In this work we fill this gap of knowledge performing an in depth morphofunctional characterization of the larval midgut.

Our results indicate that the midgut of *H. illucens* larvae shows a marked regionalization and each region possesses peculiar morphological and functional features (Figure 14).

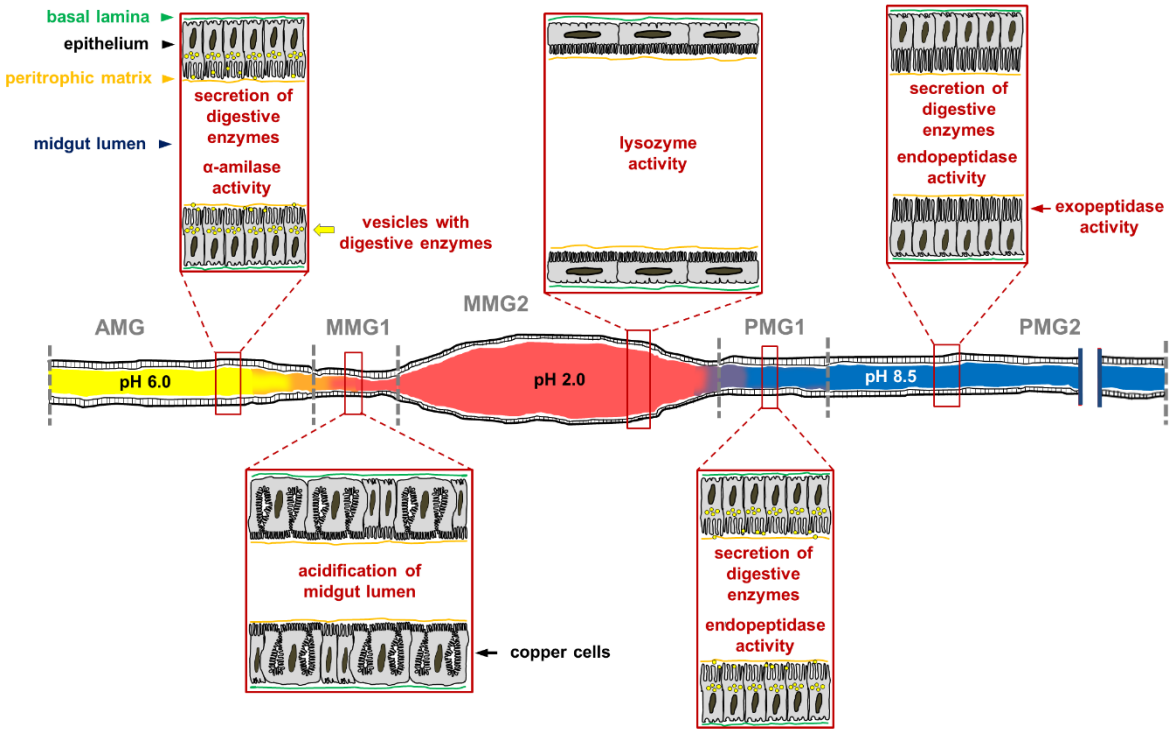

Figure 14. Schematic representation of H. illucens larval midgut in which the main morphofunctional features of each region of the organ are reported. AMG: anterior midgut, MMG1: first tract of the middle midgut, MMG2: second tract of the middle midgut, PMG1: first tract of the posterior midgut, PMG2: second tract of the posterior midgut.

A key parameter that confirms midgut regionalization is the pH of the lumen. In fact, the three main regions of the midgut present very different pH values, being acidic, strongly acidic and alkaline in the anterior, middle and posterior midgut, respectively. Although the pH values of the two first regions are similar to those measured in other Brachycera larvae (Terra et al., 1988; Shanbhag and Tripathi, 2009), the alkaline pH in the posterior midgut is not a common feature: in fact, although in *D. melanogaster* the pH of the lumen in this region is higher than 10 (Shanbhag

and Tripathi, 2009), in *M. domestica* a slightly acidic pH (pH 6.8) was measured (Terra et al., 1988). It has to be highlighted that luminal pH plays a crucial role in the functional properties of the midgut since it influences digestive enzyme activity, solubility of nutrients, neutralization of toxic ingested compounds, and gut microbiota (Appel, 1994; Nation, 2008).

Our data show that the epithelium of the anterior midgut of *H. illucens* larvae is characterized by the presence of columnar cells that possess structural and ultrastructural properties typical of secretory cells and are likely responsible for the production and secretion of amylases and lysozyme, whose activity has been recorded in the lumen of this region. Therefore, ingested polysaccharides begin to be degraded in the anterior midgut by soluble amylases that show the highest activity in this tract. In other brachycerous larvae, such as *M. domestica*, amylase expression (Pimentel et al., 2018) and activity (Espinosa-Fuentes and Terra, 1987) have been recorded especially in the posterior midgut, as well as the majority of digestive enzymes (Espinosa-Fuentes and Terra, 1987). It is difficult to explain the different localization of carbohydrate digestion in the two species on the base of their alimentary habits because both insect larvae are saprophagous and feed on very similar substrates, thus a possible explanation may reside in the phylogenetic distance between the two species (Wiegmann et al., 2011).

The first part of the middle midgut (MMG1) is characterized by the presence of copper cells. ATP produced by the elongated mitochondria inside microvilli is readily available to be used by H^+ V-ATPase localized in the apical membrane of these cells. By Western blot analysis multiple bands that correspond to the different subunits of the V1 complex were revealed. In particular, the 67- and 56-kDa bands correspond to the A and the B subunit, respectively, that are responsible for the binding of ATP (Novak et al., 1992; Wieczorek et al., 1999). The remaining bands correspond to other V1 subunits, as E (27-kDa) (Gräf et al., 1994a), F (14-kDa), G (13-kDa) (Gräf et al., 1994b; 1996; Lepier et al., 1996), H (55-kDa), and D (32-kDa) (Merzendorfer et al., 2000). Our data and evidence reported in the literature for other brachycerous larvae (Terra and Ferreira, 1994; Dubreuil et al., 1998; Dubreuil, 2004) indicate that copper cells, thanks to their ability to secrete H^+, are responsible for the acidification of middle midgut lumen. In fact, as demonstrated in *D. melanogaster* larvae (McNulty et al., 2001), when this ability is impaired by copper ingestion and the metal selectively accumulates in these cells, the pH value in the middle midgut increases. As previously suggested, the orange fluorescence signal is probably due to the formation of a complex between copper ions and a protein belonging to the metallothionein family (McNulty et al., 2001). It has been demonstrated that two metallothionein genes are constitutively expressed in the middle midgut of *D. melanogaster* larvae and adult, whereas are inducible in other regions of the gut (Durliat et al., 1995). A similar pattern can also occur in *H. illucens* larvae, since the fluorescence

signal appears more rapidly in copper cells (starting from 14 h of feeding on copper-containing diet) than in cells of other midgut regions, where the signal is visible only after 48 h. The physiological meaning and the relationship between florescence due the formation of the complex copper- metallothionein and acid secretion are not clear. Different hypotheses have been made (McNulty et al., 2001), but we can exclude that the reduction of middle midgut acidification by copper is due to nonspecific and detrimental effect of the metal on midgut cells, since the anterior and the posterior regions maintained their ability to regulate their own lumen pH. Another key factor essential for the acidification of the lumen of the middle midgut may be carbonic anhydrase, since this enzyme generates H^+ ions that are transported into the lumen (Shanbhag and Tripathi, 2008; 2009).

The epithelium present in the second part of the middle midgut (MMG2) shows a peculiar morphology since it is formed by large, flat cells. This region does not appear to be involved in digestive processes. Neither carbohydrate nor significant protein digestion takes place in this region, but only lysozyme activity has been recorded. The high activity of this enzyme in the middle midgut, together with the strong acidic luminal pH, suggests an important role of this region in killing pathogens ingested with the feeding substrate, as proposed for other brachycerous larvae (Lemos and Terra, 1991a; Lemos et al., 1993; Padilha et al., 2009). Recently, lysozyme and extreme pH values in the middle midgut of *H. illucens* larvae were indicated among the possible agents responsible for shaping the microbiota composition of the midgut and the microbial density along the different regions of this organ (Bruno et al., 2019).

Our data indicate that the posterior midgut plays a fundamental role in protein digestion. In this region, endo- and exo-peptidases accomplish the hydrolysis of peptide bonds that leads to the production of free amino acids. Columnar cells are the main cell type present in the posterior region, but they show different morphological features in the first and in the second part of this district that confer different functional properties to these two tracts. Columnar cells present in the first part of the posterior midgut (PMG1) are likely characterized by secretory activity. This evidence is supported by qRT-PCR data that demonstrate a primary involvement of PMG1 in the production of serine proteases, i.e., trypsin and chymotrypsin. These two enzymes are responsible for the initial phase of protein digestion that occurs in the posterior midgut. Moreover, since the assay conditions for the measurement of trypsin and chymotrypsin activity are the same and both specific chromogenic substrates release p-nitroaniline after the hydrolysis, it is possible to compare the relative activity of the two enzymes. Considering their activity in the posterior region of the midgut, chymotrypsin-like enzymes appear to be the major serine proteases responsible for the initial phase of protein digestion. In the second part of the posterior midgut (PMG2), columnar

cells have microvilli that are longer than in other regions while morphological traits ascribable to a secretory activity are less evident, supporting a main role of this tract in nutrient absorption. Moreover, APN activity is recorded only in the posterior region, confirming that this district plays a fundamental role in protein digestion from the initial to the final phases of the process, the latter producing single amino acids that, in turn, can be absorbed. *H. illucens* larvae are able to grow on a great variety of organic matter (Nguyen et al., 2015; Barragan-Fonseca et al., 2017; Wang and Shelomi, 2017), including vegetal materials (Jucker et al., 2017), a substrate rich in tannins and other secondary metabolites which bind to proteins at low pH values affecting the efficiency of digestion (Felton et al., 1989; 1991; Apple, 1994). Considering this evidence, the digestion of protein in the posterior midgut, a region with an alkaline pH of lumen, could ensure the best exploitation of these important nutrients. Moreover, the involvement of endopeptidases belonging to serine proteases, which have an optimum pH value in the alkaline range, fits with the pH values recorded in this region of the midgut. Apparently, endopeptidases able to work at acidic or very acidic pH, such as cysteine and aspartic proteases, whose involvement in protein digestion has been demonstrated in other insects including brachycerous larvae (Espinosa-Fuentes and Terra, 1987; Lemos and Terra, 1991a; 1991b; Terra and Ferreira, 1994; Padilha et al., 2009), play a marginal role in *H. illucens* larvae, since the total proteolytic activity measured in the anterior and middle regions of the midgut is negligible compared to posterior midgut. In this region serine proteases are active and therefore represent the major enzymes responsible for the initial phase of protein digestion.

We have also unraveled the influence of temperature on proteolytic activity in the midgut of BSF larvae. In accordance with previous findings (Kim et al., 2011a) we observed an optimum temperature around 45 °C. This result is not surprising if we consider that BSF larvae exhibit a very peculiar tendency to aggregate into the feeding substrate forming clusters in which the temperature increases due to the larval overcrowding and the heat generated by their movement (Parra Paz et al., 2015). In our rearing conditions (environmental temperature of 27.0 ± 0.5 °C), a temperature higher than 40 °C was recorded within the clusters, therefore proteolytic enzymes can work at their optimum temperature. This feature can strongly contribute to the efficiency of BSF larvae in the bioconversion of feeding substrates.

In conclusion, our work represents the first comprehensive description of the morphofunctional features of *H. illucens* larval midgut and sheds light on the unexpected complexity of this organ. Moreover, it also represents a useful platform of knowledge for the best exploitation of this insect in bioconversion processes.

AUTHOR CONTRIBUTIONS STATEMENT

MC, GT and SCaccia designed research; MB, DB and GS performed research; MB, DB, MC, GT SCappellozza, and CJ analyzed data; MC, SCaccia, and GT wrote the paper.

ACKNOWLEDGMENTS

This work was supported by Fondazione Cariplo (grant n° 2014-0550). The authors are grateful to Prof. Helmut Wieczorek (University of Osnabrück, Germany) for providing anti-H^+ V-ATPase antibody and to Prof. Alida Amadeo for providing anti-guinea pig Cy2-conjugated secondary antibody. The authors are also grateful to Prof. Franco Faoro and Prof. Matteo Montagna for helpful technical support. MB is a Ph.D. student of the "Environmental Sciences" course at Università degli Studi di Milano. DB is a Ph.D. student of the "Biotechnologies, Biosciences and Surgical Technologies" course at Università degli Studi dell'Insubria.

REFERENCES

Appel, H. M. (1994). "The chewing herbivore gut lumen: physicochemical conditions and their impact on plant nutrients, allelochemicals, and insect pathogens" in Insect-Plant Interactions, ed. E. A. Bernays. (Boca Raton, FL: CRC Press), vol. V, 209-223.

Barragan-Fonseca, K. B., Dicke, M., Van Loon, J. J. A. (2017). Nutritional value of the black soldier fly (*Hermetia illucens* L.) and its suitability as animal feed-A review. J. Insect Food Feed 3, 105-120. doi: 10.3390/foods6100091

Benelli, G., Canale, A., Raspi, A., Fornaciari, G. (2014). The death scenario of an Italian Renaissance princess can shed light on a zoological dilemma: did the black soldier fly reach Europe with Columbus? J. Archaeol. Sci. 49, 203-205. doi: 10.1016/j.jas.2014.05.015

Bernfeld, P. (1955) Amylase α and β. Methods Enzymol. 1, 149-158. doi: 10.1016/0076-6879(55)01021-5

Bradford, M. (1976). A rapid and sensitive method for the quantitation of microgram quantities of protein utilizing the principle of protein-dye binding. Anal. Biochem. 72, 248-254. doi: 10.1006/abio.1976.9999

Bruno, D., Bonelli, M., De Filippis, F., Di Lelio, I., Tettamanti, G., Casartelli, M., Ercolini, D., Caccia, S. (2019). The intestinal microbiota of *Hermetia illucens* larvae is affected by diet and shows a diverse composition in the different midgut regions. Appl. Environ. Microb. 85, e01864-18. doi: 10.1128/AEM.01864-18

Buchon, N., Silverman, N., Cherry, S. (2014). Immunity in *Drosophila melanogaster*-from microbial recognition to whole-organism physiology. Nat. Rev. Immunol. 14, 796-810. doi: 10.1038/nri3763

Caccia, S., Chakroun, M., Vinokurov, K., Ferré, J. (2014). Proteolytic processing of *Bacillus thuringiensis* Vip3A proteins by two Spodoptera species. J. Insect. Physiol. 67, 76-84. doi: 10.1016/j.jinsphys.2014.06.008

Charney, J., and Tomarelli, R. M. (1947) A colorimetric method for the determination of the proteolytic activity of duodenal juice. J. Biol. Chem. 171, 501-505.

Coch Frugoni, J. A. (1957) Tampone universale di Britton e Robinson a forza ionica costante. Gazz. Chim. Ital. 87, 403-407.

Dimltriadis, V. K., and Kastritsis, C. D. (1984). Ultrastructural analysis of the midgut of *Drosophila auraria* larvae, morphological observations and their physiological implications. Can. J. Zool. 62, 659-669. doi: 10.1139/z84-097

Dubreuil, R. R. (2004). Copper cells and stomach acid secretion in the *Drosophila* midgut. Int. J. Biochem. Cell. Biol. 36, 742-752. doi: 10.1016/j.biocel.2003.07.004

Dubreuil, R. R., Frankel, J., Wang, P., Howrylak, J., Kappil, M., and Grushko, T. A. (1998). Mutations of *α* spectrin and *labial* block cuprophilic cell differentiation and acid secretion in the middle midgut of *Drosophila* larvae. Dev. Biol. 194, 1-11. doi:10.1006/dbio.1997.8821

Durliat, M., Benneton, F., Boissonneau, E., Andre, M., Wegnez, M. (1995). Expression of metallothionein genes during the post-embryonic development of *Drosophila melanogaster*. Biometals. 8, 339-351 doi: 10.1007/BF00141608

Espinoza-Fuentes, F. P., and Terra, W. R. (1987). Physiological adaptations for digesting bacteria. Water fluxes and distribution of digestive enzymes in *Musca domestica* larval midgut. Insect Biochem. 17, 809-817. doi: 10.1016/0020-1790(87)90015-1

Espinoza-Fuentes, F. P., Ribeiro, A. F., Terra, W. R. (1987). Microvillar and secreted digestive enzymes from *Musca domestica* larvae. Subcellular fractionation of midgut cells with electron microscopy monitoring. Insect Biochem. 17, 819-827. doi: 10.1016/0020-1790(87)90016-3

Felton, G., Donato, K., Del Vecchio R. J., Duffey, S. S. (1989). Activation of plant foliar oxidases by insect feeding reduces nutritive quality of foliage for noctuid herbivores. J. Chem. Ecol. 15, 2667-2694. doi: 10.1007/BF01014725

Felton, G., and Duffey, S. S. (1991). Reassessment of the role of gut alkalinity and detergency in insect herbivory. J. Chem. Ecol. 17, 1821-1836. doi: 10.1007/BF00993731

Franzetti, E., Romanelli, D., Caccia, S., Cappellozza, S., Congiu, T., Rajagopalan, M., et al. (2015). The midgut of the silkmoth *Bombyx mori* is able to recycle molecules derived from degeneration of the larval midgut epithelium. Cell Tissue Res. 361, 509-528. doi:10.1007/s00441-014-2081-8

Gräf, R., Harvey, W. R., Wieczorek, H. (1994a). Cloning, sequencing and expression of cDNA encoding an insect V-ATPase subunit E. Biochim. Biophys. Acta 1190, 193-196. doi: 10.1016/0005-2736(94)90053-1

Gräf, R., Lepier, A., Harvey, W. R., Wieczorek, H. (1994b). A Novel 14-kDa V-ATPase subunit in the tobacco hornworm midgut. J. Biol. Chem. 269, 3767-3774.

Gräf, R., Harvey, W. R., Wieczorek, H. (1996). Purification and properties of a cytosolic V1-ATPase. J. Biol. Chem. 271, 20908-20913. doi: 10.1074/jbc.271.34.20908

Hogsette, J. A. (1992). New diets for production of house-flies and stable flies (Diptera, Muscidae) in the laboratory. J. Econ. Entom. 85, 2291-2294.

Hosseininaveh, V., Bandani, A., Azmayeshfard, P., Hosseinkhani, S., Kazzazi, M. (2007). Digestive proteolytic and amylolytic activities in *Trogoderma granarium* Everts (Dermestidae: Coleoptera). J. Stored Prod. Res. 43, 515-522. doi: 10.1016/j.jspr.2007.02.003

Jordão, B. P., Terra, W. R., Ribeiro, A. F., Lehane, M. J., Ferreira, C. (1996). Trypsin secretion in *Musca domestica* larval midguts: a biochemical and immunocytochemical study. Insect Biochem. Mol. Biol. 26, 337-346. doi: 0.1016/0965-1748(95)00084-4

Jucker, C., Erba, D., Leonardi, M. G., Lupi, D., Savoldelli, S. (2017). Assessment of vegetable and fruit substrates as potential rearing media for *Hermetia illucens* (Diptera: Stratiomyidae) larvae. Environ. Entomol. 46, 1415-1423. doi: 10.1093/ee/nvx154

Kim, W., Bae, S., Kim, A., Park, K., Lee, S., Choi, Y., et al. (2011b). Characterization of the molecular features and expression patterns of two serine proteases in *Hermetia illucens* (Diptera: Stratiomyidae) larvae. BMB reports 44, 387-392. doi: 10.5483/BMBRep.2011.44.6.387

Kim, W., Bae, S., Park, K., Lee, S., Choi, Y., Han, S., et al. (2011a). Biochemical characterization of digestive enzymes in the black soldier fly, *Hermetia illucens* (Diptera: Stratiomyidae). J. Asia Pac. Entomol. 14, 11-14. doi: 10.1016/j.aspen.2010.11.003

Kim, W., Bae, S., Park, H., Park, K., Lee, S., Choi, Y., et al. (2010). The larval age and mouth morphology of the black soldier fly, *Hermetia illucens* (Diptera: Stratiomyidae). Int. J. Indust. Entomol. 21, 185-187.

Lee, C. M., Lee, Y. S., Seo, S. H., Yoon, S. H., Kim, S. J., Hahn, B. S., et al. (2014). Screening and characterization of a novel cellulase gene from the gut microflora of *Hermetia illucens* using metagenomics library. J. Microbiol. Biotechnol. 24, 1196-1206, doi: 10.4014/jmb.1405.05001

Lemos, F. J., and Terra, W. R. (1991a). Digestion of bacteria and the role of midgut lysozyme in some insect larvae. Comp. Biochem. Physiol. 100, 265-268. doi: 10.1016/0305-0491(91)90372

Lemos, F. J., and Terra, W. R. (1991b). Properties and intracellular distribution of cathepsin D-like proteinase active at the acid region of *Musca domestica* midgut. Insect Biochem. 21, 457-465. doi: 10.1016/0020-1790(91)90098-Y

Lemos, F. J., Ribeiro, A. F., Terra, W. R. (1993). A bacteria-digesting midgut-lysozyme from *Musca domestica* (Diptera) larvae. Purification, properties and secretory mechanism. Insect Biochem. Mol. Biol. 23, 533-541. doi: 10.1016/0965-1748(93)90062-W

Lepier, A., Gräf, R., Azuma, M., Merzendorfer, H., Harvey, W. R., Wieczorek, H. (1996). The peripheral complex of the tobacco hornworm V-ATPase contains a novel 13-kDa subunit G. J. Biol. Chem. 271, 8502-8508. doi: 10.1074/jbc.271.14.8502

McNulty, M., Puljung, M., Jefford, G., Dubreuil, R. R. (2001). Evidence that a copper-metallothionein complex is responsible for fluorescence in acid-secreting cells of the *Drosophila* stomach. Cell Tissue Res. 304, 383-389. doi:10.1007/s004410100371

Merzendorfer, H., Reineke, S., Zhao, X., Jacobmeier, B., Harvey, W R., Wieczorek, H. (2000). The multigene family of the tobacco hornworm V-ATPase: novel subunits a, C, D, H, and putative isoforms. Biochim. Biophys. Acta 1467, 369-379. doi: 10.1016/S0005-2736(00)00233-9

Müller, A., Wolf, D., Gutzeit, H. O. (2017). The black soldier fly, *Hermetia illucens* - a promising source for sustainable production of proteins, lipids and bioactive substances. Z. Naturforsch. C 72, 351-363. doi: 10.1515/znc-2017-0030

Nation J. L. (2008). Insect Physiology and Biochemistry. Boca Raton, FL: CRC Press.

Newton, G. L., Booram, C. V., Barker, R. W., Hale, O. M. (1977). Dried *Hermetia illucens* larvae meal as a supplement for swine. J. Anim. Sci. 44, 395-400. doi: 10.2527/jas1977.443395x

Nguyen, T. T. X., Tomberlin, J. K., Vanlaerhoven, S., (2013). Influence of resources on *Hermetia illucens* (Diptera: Stratiomyidae) larval development. J. Med. Entomol. 50, 898-906. doi: 10.1603/ME12260

Novak, F. J. S., Gräf, R., Waring, R. B., Wolfersberger, M. G., Wieczorek, H., Harvey, W. R. (1992). Primary structure of V-ATPase subunit B from *Manduca sexta* midgut. Biochim. Biophys. Acta 1132, 67-71. doi: 10.1016/0167-4781(92)90053-3

Padilha, M. H. P., Pimentel, A. C., Ribeiro, A. F., Terra, W.R. (2009). Sequence and function of lysosomal and digestive cathepsine D-like proteinases of *Musca domestica* midgut. Insect Biochem. Mol. Biol. 39, 782-791. doi: 10.1016/j.ibmb.2009.09.003

Park, K. H., Choi, Y. C., Nam, S. H., Kim, W. T., Kim, A. Y., Kim, S. Y. (2012). Recombinant expression and enzyme activity of chymotrypsin-like protease from Black Soldier Fly, *Hermetia illucens* (Diptera: Stratiomyidae). Int. J. Indust. Entomol. 25, 181-185. doi: 10.7852/ijie.2012.25.2.181

Parra Paz, A. S., Carrejo, N. S., Gomez Rodriguez, C. H. (2015). Effects of larval density and feeding rates on the bioconversion of vegetable waste using black soldier fly larvae *Hermetia illucens* (L.), (Diptera: Stratiomyidae). Waste Biomass Valor. 6, 1059-1065. doi: 10.1007/s12649-015-9418-8

Pimentel, A. C., Montali, A., Bruno, D., Tettamanti, G. (2017). Metabolic adjustment of the larval fat body in *Hermetia illucens* to dietary conditions. J. Asia Pac. Entomol. 20, 1307-1313. doi: 10.1016/j.aspen.2017.09.017

Pimentel, A. C., Barroso, I. G., Ferreira, J. M., Dias, R. O., Ferreira, C., Terra, W. R. (2018). Molecular machinery of starch digestion and glucose absorption along the midgut of *Musca domestica*. J. Insect Physiol. 109, 11-20. doi: 10.1016/j.jinsphys.2018.05.009

Rozkošný, R. (1983). A biosystematic study of the European Stratiomyidae (Diptera) Vol. 2 Clitellariinae Hermetiinae Pachygasterinae Bibliography. The Hague: Dr W. Junk publishers.

Shanbhag, S., and Tripathi, S. (2008). Segmental bidirectional transport of H^+ in the adult Drosophila midgut. Comp. Biochem. Physiol. 150A, A11.29, S138

Shanbhag, S., and Tripathi, S. (2009). Epithelial ultrastructure and cellular mechanisms of acid and base transport in the *Drosophila midgut*. J. Exp. Biol. 212, 1731-1744. doi: 10.1242/jeb.029306.

Sheppard, D. C., Newton, G. L., Thompson, S. A., Savage, S. (1994). A value-added manure management-system using the Black Soldier Fly. Bioresour. Technol. 50, 275-279. doi: 10.1016/0960-8524(94)90102-3

Sheppard, D. C., Tomberlin, J. K., Joyce, J. A., Kiser, B. C., Sumner, S. M. (2002). Rearing methods for the black soldier fly (Diptera: Stratiomyidae). J. Med. Entomol. 39, 695-698. doi: 10.1603/0022-2585-39.4.695

Strasburger, M. (1932). Bau, Funktion und Variabilität des Darmtractus von *Drosophila melanogaster* Meigen. Z. Wiss. Zool. 140, 539-649.

Terra, W.R., and Ferreira, C. (1994). Insect digestive enzymes: properties, compartmentalization and function. Comp. Biochem. Physiol., 109B: 1-62. doi: 10.1016/0305-0491(94)90141-4

Terra, W. R., Ferreira C., Baker J. E. (1996). "Compartmentalization of digestion" in Biology of the Insect Midgut, eds. M. J. Lehane, and P. F. Billingsley (Dordrecht: Springer), 206-235.

Terra, W. R., Espinoza-Fuentes, F. P., Ribeiro, A. F., Ferreira, C. (1988). The larval midgut of the housefly (*Musca domestica*): ultrastructure, fluid fluxes and ion secretion in relation to the organization of digestion. J. Insect Physiol. 34, 463-472. doi: 10.1016/0022-1910(88)90187-4

Terra, W. R., and Ferreira, C. (2005). "Biochemistry of digestion", in: Comprehensive Molecular Insect Science, eds. L. I. Gilbert, K. Iatrou, S. Gill (Oxford: Elsevier Ltd) 171-224.

Tomberlin, J. K., Adler, P. H., Myers, H. M. (2009). Development of the black soldier fly (Diptera: Stratiomyidae) in relation to temperature. Environ. Entomol. 38, 930-934. doi: 10.1603/022.038.0347

Tomberlin, J. K., and Sheppard, D. C. (2002). Factors influencing mating and oviposition of black soldier flies (Diptera: stratiomyidae) in a colony. J. Entomol. Sci. 37, 345-352. doi: 10.18474/0749-8004-37.4.345

Tomberlin, J. K., Sheppard, D. C., Joyce, J. A. (2002). Selected life-history traits of black soldier flies (Diptera: Stratiomyidae) reared on three artificial diets. Ann. Entomol. Soc. Am. 95, 379-386. doi: 10.1603/0013-8746(2002)095[0379:SLHTOB]2.0.CO;2

Van Huis, A. (2013). Potential of insects as food and feed in assuring food security. Annu. Rev. Entomol. 58, 563-583. doi:10.1146/annurev-ento-120811-153704

Van Huis, A., Van Itterbeeck, J., Klunder, H., Mertens, E., Halloran, A., Muir, G., et al. (2013). Edible insects: future prospects for food and feed security. FAO Forestry Paper 171

Vinokurov, K. S., Elpidina, E. N., Oppert, B., Prabhakar, S., Zhuzhikov, D. P., Dunaevsky, Y. E., et al. (2006). Diversity of digestive proteinases in *Tenebrio molitor* (Coleoptera: Tenebrionidae) larvae. Comp. Biochem. Physiol. B, Biochem. Mol. Biol. 145, 126-137. doi: 10.1016/j.cbpb.2006.05.005

Vogel, H., Müller, A., Heckel, D.G., Gutzeit, H., and Vilcinskas, A. (2018). Nutritional immunology: diversification and diet-dependent expression of antimicrobial peptides in the black soldier fly *Hermetia illucens*. Dev. Comp. Immunol. 78, 141-148. doi: 10.1016/j.dci.2017.09.008

Wang, Y.S., and Shelomi, M. (2017). Review of Black Soldier Fly (*Hermetia illucens*) as animal feed and human food. Foods 6, 91. doi: 10.3390/foods6100091

Wieczorek, H., Brown, D., Grinstein, S., Ehrenfeld, J., Harvey, W. R. (1999). Animal plasma membrane energization by proton-motive V-ATPases. BioEssays 21, 637-648. doi: 10.1002/(SICI)1521-1878(199908)21:8<637::AID-BIES3>3.0.CO;2-W

Wiegmann, B. M., Trautwein, M. D., Winkler, I. S., Barr, N. B., Kim J-W., Lambkin, C., et al. (2011). Episodic radiations in the fly tree of life. PNAS 18, 5690-5695. doi: 10.1073/pnas.1012675108

Zhuang, Z., Linser, P. J., Harvey, W. R. (1999). Antibody to H^+ V-ATPase subunit E colocalizes with portasomes in alkaline larval midgut of freshwater mosquito (*Aedes aegypti*). J. Exp. Biol. 202, 2449-2460.

SUPPLEMENTARY MATERIAL

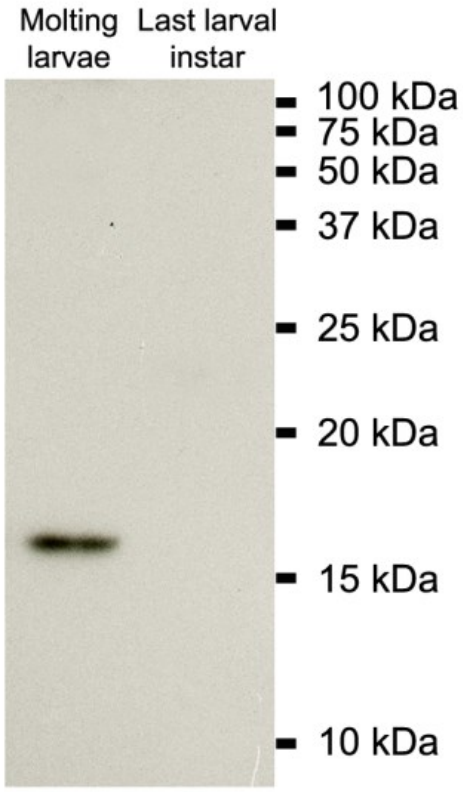

Figure S1. Western blot analysis: full lane of phospho-Histone 3.

CHAPTER 2

The feeding substrate affects morphological and functional features of the *Hermetia illucens* larval midgut

The feeding substrate affects morphological and functional features of the *Hermetia illucens* larval midgut

Marco Bonelli[a,*], Daniele Bruno[b,*], Novella Gianfranceschi[a], Daniela Lupi[c], Morena Casartelli[a], Gianluca Tettamanti[b]

[a]Department of Biosciences, University of Milan, Milano, Italy

[b]Department of Biotechnology and Life Sciences, University of Insubria, Varese, Italy

[c]Department of Food, Environmental and Nutritional Sciences, University of Milan, Milano, Italy

*These authors contributed equally

Corresponding authors:

Morena Casartelli, morena.casartelli@unimi.it

Gianluca Tettamanti, gianluca.tettamanti@uninsubria.it

ABSTRACT

The use of insects as a primary agent for organic waste reduction and bioconversion into usable protein products, as insect protein for animal feed to complement traditional plant sources, could contribute to solve problems related to the management of organic waste and, at the same time, free up land to grow crops for direct consumption by the human population. In this setting, the larvae of black soldier fly (BSF), *Hermetia illucens* (Diptera, Stratiomyidae), emerge as a relevant issue since they can convert low quality biomass as food waste, organic residues, and byproducts of the agri-food transformation chain into nutritionally valuable proteins.

Among the most promising substrates for rearing *H. illucens* larvae, fruit and vegetable waste provided in large amounts by large-scale retail trade and wholesale markets, poses limited chemical and microbiological risks compared to other waste substrates, and fulfils the requirements of the European Commission Regulation N°2017/893 on the use of insects for aquaculture.

In this study we investigated the impact of two feeding substrates with different nutritional composition (i.e. a diet composed of vegetables and fruits and a standard diet for Diptera), on the morphology and physiology of the *H. illucens* larval midgut. Our data show a diet-dependent adaptation process of this organ: in particular, differences in the morphology, activity of digestive enzymes, and accumulation of long-term storage molecules were observed. The diet-dependent plasticity of the midgut, the organ involved in the digestion and absorption of nutrients, may be responsible for the ability of BSF larvae to growth and develop on such different substrates.

INTRODUCTION

With an increasing world population estimated to reach nearly 10 billion in 2050 (United Nations, 2017), it is mandatory to face the crucial problem of feeding the planet, limiting food waste and the unsustainable exploitation and exhaustion of natural resources, such as land and water. The population growth, together with rising per capita demand for meat in developing countries (FAO, 2017), will lead to an increase in the global demand for food of animal origin in the next decades, in particular for pigs, poultry and fish (Alexandratos and Bruinsma, 2012; Waite et al., 2014). Moreover, the consequent need to increase the production of traditional feedstuff (e.g., soy, fishmeal) raises serious concerns in terms of land and water use, overfishing, diversion of resources from direct human food production (Steinfield et al., 2006; Alexandratos and Bruinsma, 2012; Mekonnen and Hoeksta, 2012; Cashion et al., 2017), and economic costs (Verbeke et al., 2015; Chaalala et al., 2018).

Another serious global problem is food loss and waste, since one third of the food produced globally is lost or wasted throughout the entire supply chain (Gustavsson et al., 2011). In addition to policies to reduce the consumption of food of animal origin and the production of food waste, a promising perspective is to consider insects for the bioconversion of organic waste into proteins for sustainable and large-scale feed production: insect-based feeds are comparable in terms of nutritional value with fishmeal and soy-based feed formulae and can represent a more environmentally friendly alternative to conventional feedstuff (St-Hilaire et al., 2007; Diener et al., 2009; Oonincx et al., 2010; Kroeckel et al., 2012; Van Huis et al., 2013; Van Huis, 2013; Barroso et al., 2014; Makkar et al., 2014; Oonincx et al., 2015; Magalhães et al., 2017; Van Huis and Oonincx, 2017; Halloran et al., 2018).

In this context, the black soldier fly (BSF), *Hermetia illucens* (Linnaeus, 1758) (Diptera: Stratiomydidae) emerges as a relevant issue since the larvae of this insect are able to grow on a wide variety of organic matter (Nguyen et al., 2015; Barragan-Fonseca et al., 2017; Wang and Shelomi, 2017), and the meal prepared from BSF larvae is suitable for partially replace traditional feedstuff for livestock and aquaculture (Barragan-Fonseca et al., 2017). In fact, *H. illucens* larvae contain high protein levels with a good quality amino acidic profile, and other macro- and micro-nutrients useful for animal feed (Spranghers et al., 2017). However, it must be taken into consideration that the feeding substrate strongly affects *H. illucens* larval growth, and protein, fat and fatty acid content in larvae and prepupae (Barragan-Fonseca et al., 2017; Wang and Shelomi, 2017). Even considering only organic matters of vegetal origin, nutrient composition of larvae and prepupae and performance indicators, such as duration of the larval development, and larval and pupal weights, vary significantly (Jucker et al., 2017). Nonetheless, *H. illucens* larvae show high survival rate on very different substrates, unlike other insects used for feedstuff production (Oonincx et al., 2015; Van der Fels-Klerx et al., 2016). However, the choice of the insect feeding substrates must consider not only their impact on larval composition and insect development, but also criteria regarding food security and economic and environmental sustainability. In recent years, many low-cost substrates such as manure, kitchen waste, municipal organic waste, and fruit and vegetable waste have been proposed (Nguyen et al., 2015; Barragan-Fonseca et al., 2017; Wang and Shelomi, 2017). However, in the European Union, it is not allowed to rear insects destined for animal feed on feces, manure, catering waste, and other organic matter containing products of animal origin (Regulation (EC) 767/2009; Regulation (EC) 1069/2009; Regulation (EU) 142/2011). Former foodstuffs not containing meat and fish, such as production surplus or misshapen products, are instead among the main substrates currently used in the European insect production (EFSA Scientific Committee, 2015). The share of non-animal origin matter of the

global food waste is about 86% and three quarters of this percentage are represented by roots, tubers, fruit, and vegetables waste (World Resource Institute, 2011). For this reason, fruit and vegetable waste, provided in large amounts by large-scale retail trade and wholesale markets, could represent a suitable feeding substrate to rear *H. illucens* larvae. However, although information on performances and nutritional composition of larvae and prepupae of *H. illucens* reared on fruit and vegetable waste is available (Jucker et al., 2017; Spranghers et al., 2017), it is essential to establish if and how a feeding substrate with a particularly low protein carbohydrate ratio, such as fruit and vegetable, determines morphofunctional adaptations in the midgut, the organ involved in digestion and nutrient absorption. These adaptations could be necessary to better exploit an unbalanced supply of nutrients, but have a metabolic cost for the insect and negatively affect development and nutrient composition of the larvae.

A deep morphofunctional characterization of *H. illucens* midgut has been already performed by Bonelli et al. (submitted), on larvae reared on Standard Diet (SD) for Diptera (Hogsette, 1992), and it has been demonstrated that this organ presents a marked regionalization, and the different midgut regions shows peculiar features and functions. In the present work, we investigated with a multidisciplinary approach a broad spectrum of morphofunctional properties of the BSF larval midgut reared on two different feeding substrates: Standard Diet (SD) for Diptera, used as control, and a Vegetable Mix Diet (VMD), composed of different vegetables and fruits, mimicking fruit and vegetable waste. Differences in larval growth rate, activity of digestive enzymes, morphological features of midgut cells, and long-term storage molecules in the midgut tissue were evaluated in relation to the provided diet. Our results indicate that *H. illucens* larval development, as well as morphofunctional features of the midgut, are strongly influenced by the nutritional composition of the diet.

MATERIALS AND METHODS

Insect rearing

Hermetia illucens larvae used in this work derived from a colony established in 2015 at University of Insubria (Varese, Italy).

Two specific substrates, with different nutrient composition, were used to rear the larvae: i) Standard Diet (SD) for Diptera (Hogsette, 1992), composed by 50% of wheat bran, 30% of corn meal and 20% of alfalfa meal, mixed in the ratio 1:1 dry matter/water ; ii) Vegetable Mix Diet (VMD), composed by seven vegetables (apple, banana, pear, broccoli, zucchini, potato and carrot) in equal quantity and appropriately minced. The VMD was realized miming the fruit and vegetable waste, but choosing ingredients available all year round, in order to standardize the experimental

conditions. The rearing methods of the larvae on both diets were described in Pimentel et al. (2017). The larvae were maintained at 27.0 ± 0.5 °C, 70 ± 5% relative humidity, in the dark. For all the experiments larvae at last instar were used.

Determination of nutrient content of the diets

Three samples of fresh VMD were lyophilized with freeze-dryer (Martin Christ GmbH, Alpha 2-4 LD plus) under 12-15 mbar at -80 °C and then analyzed for the determination of nutrient content. Samples of SD powder were analyzed as they were. Samples were analyzed at the Department of Agronomy, Food, Natural Resources, Animals and Environment, University of Padua, Agripolis, Legnaro PD, Italy.

Measurement of larval growth rate

Batches of 300 larvae were placed in plastic containers and random samples of 30 individuals were weighed every two days starting from the fourth day after hatching. For each experimental diet, the sampling and the annotation of the larval weight were made in triplicate. Before weighing, the larvae were washed in tap water to remove diet matter from the body and then wiped dry. The weight was recorded until 25% of insects reached pupal stage.

Midgut juice extraction and midgut epithelium isolation

Larvae were anesthetized on ice with CO_2. The gut was isolated in Phosphate Buffer Solution (PBS) (137 mM NaCl, 2.7 mM KCl, 8.1 mM Na_2HPO_4, 1.76 mM KH_2PO_4, pH 7.4) at 4 °C. The regions of the midgut were collected depending on the analysis performed, according to Bonelli et al. (submitted). For all the experiments, except for the detection of ferric iron, the midgut was subdivided into three regions, i.e. anterior, middle, and posterior.

The peritrophic matrix from each midgut region, with the enclosed intestinal content, was isolated from the epithelium, centrifuged at 15000 × g for 10 min at 4 °C to remove the insoluble material, and supernatant (midgut juice) was collected. The midgut juice from 15 larvae was used as fresh sample for the luminal pH measurement, or stored at -80 °C for the enzymatic assays. The epithelium of the posterior region of the midgut, deprived of the peritrophic matrix, was placed into cryovials, each containing the midgut epithelium collected from 15 larvae, and stored in liquid nitrogen for aminopeptidase N activity assay.

Luminal pH measurement

The pH of the midgut juice extracted from anterior, middle and posterior regions of the midgut was measured using universal indicator strips with a resolution of 0.5 pH unit (Hydrion Brilliant pH Dip Sticks, Sigma-Aldrich, Italy). The experiment was repeated on six independent samples for each diet.

Morphological analysis of the larval midgut

The larval midgut was processed for morphological analysis as described in Bonelli et al. (submitted). Briefly, after fixation in glutaraldehyde 4% in 0.1 M Na-cacodylate buffer, the specimens were dehydrated in ethanol ascending series and then embedded in epoxy resin (Epon/Araldite 812 mixture). 0.6-µm-thick sections were obtained with a Leica Reichert Ultracut S (Leica, Germany), stained with crystal violet and basic fuchsin, and then observed under Eclipse Ni-U microscope (Nikon, Japan) equipped with the digital camera TrueChrome II S (Tucsen photonics Co. Ltd, China).

Histochemical analysis of the larval midgut

For the detection of glycogen, the isolated midgut, with the enclosed intestinal content, was subdivided in the three regions as described above and immediately fixed in 4% paraformaldehyde in distilled water for 2 h at room temperature and then overnight at 4 °C. After dehydration in ascending ethanol series, the specimens were embedded in paraffin (Franzetti et al., 2015), and 7-µm-thick sections were obtained using microtome Jung Multicut 2045 (Leica). After deparaffinization, the sections were stained with periodic acid-Schiff kit (PAS) (Bio-Optica, Italy) according to the manufacturer's instructions to detect the glycogen deposits in the midgut tissues, and then analyzed under Eclipse Ni-U microscope equipped with digital camera.

For the detection of ferric iron, whole mount staining of the midgut was performed. After isolation, the tissue was fixed in 4% paraformaldehyde in distilled water for 20 minutes, and then stained with Perls' stain kit (Bio-optica) according to the manufacturer's instructions. Each region of the midgut was analyzed under NSZ-606 Zoom Stereo Microscope (Xiamen Phio Scientific Instruments Co. Ltd, China) equipped with TrueChrome II S digital camera.

Total proteolytic activity assay

Total proteolytic activity in midgut juice samples was assayed with azocasein (Sigma-Aldrich), measuring its degradation by release of azo chromophore (Charney and Tomarelli, 1947), as reported by Bonelli et al. (submitted). Assays were performed with Universal Buffer (UB), a buffer with constant ionic strength at different pH values (Coch Frugoni, 1957). The pH used for the assays is indicated in the captions to figures and in the Results section. One unit (U) of total proteolytic activity with azocasein was defined as the amount of enzyme that causes an increase in absorbance by 0.1 unit per min per mg of proteins.

Chymotrypsin- and trypsin-like proteolytic activity assay

Chymotrypsin- and trypsin-like proteolytic activity in midgut juice samples were assayed with N-succinyl-ALA-ALA-PRO-PHE-p-nitroanilide (SAAPPpNA, Sigma-Aldrich) and Na-Benzoyl-D,L-arginine 4-nitroanilide hydrochloride (BApNA, Sigma-Aldrich), respectively, measuring

their degradation by release of p-nitroaniline (pNA) (Bonelli et al., submitted). These assays were performed on midgut juice samples obtained from the posterior region, using UB at pH 8.5. One unit (U) of chymotrypsin- and trypsin-like proteolytic activity was defined as the amount of enzyme that causes an increase in absorbance by 0.1 unit per min per mg of proteins.

Aminopeptidase N activity assay

The activity of aminopeptidase N (APN) was assayed using L-leucine p-nitroanilide as substrate, measuring its degradation by release of p-nitroaniline (pNA), as reported by Bonelli et al. (submitted). Assays were performed on the homogenate of posterior midgut epithelium in50 mM Tris-HCl, pH 7.5. One unit/mg (U/mg) of APN activity was defined as the amount of enzyme that releases 1 µmol of pNA per min per mg of proteins.

α-amylase activity assay

α-amylase activity in midgut juice samples was assayed with starch as substrate, measuring its hydrolysis by the amount of maltose released (Bernfeld, 1955) as reported by Bonelli et al. (submitted). These assays were performed in amylase buffer (20 mM NaH_2PO_4, 6.7 mM NaCl, pH 6.9). One unit of α-amylase activity (U) was defined as the amount of enzyme necessary to produce 1 mg of maltose per min per mg of proteins.

Lysozyme activity assay

Lysozyme activity in midgut juice samples was assayed with *Micrococcus lysodeikticus* lyophilized cells, measuring the rate of lysis of these cells as reported by Bonelli et al. (submitted). These assays were performed on midgut juice samples extracted from the middle region of the midgut, in 66 mM potassium phosphate buffer, pH 6.2. Even though the luminal pH of the middle region is very acidic (Bonelli et al., submitted), it was not possible to measure lysozyme activity at pH values lower than 6.2 since in those conditions the enzyme is unable to lyse *Micrococcus lysodeikticus*, the substrate used in the classic method for lysozyme activity assay (Gagliardi et al., 1986; Pitotti et al., 1991). One unit/mL (U/mL) of lysozyme activity was defined as the amount of enzyme that causes a decrease in absorbance by 1 unit per min per mL of midgut juice sample.

Statistical analyses

Statistical analyses were performed with R-statistical software (ver. 3.3.2). The following analyses were performed: paired and unpaired t-tests. Statistical differences between groups were considered significant at p-value ≤ 0.05. The statistical analysis performed for each experiment and the p-values are reported in the captions to figures.

RESULTS

Larval growth rate

The larvae reared on both experimental diets (SD and VMD) were weighted every two days to evaluate differences in the length of the larval period and the maximum weight reached. The curves reported in Figure 1 show that the larvae reared on SD reached the maximum weight more rapidly than those grown on VMD (16 days vs 22 days, respectively). The diet affected not only the length of the larval period, but also the maximum weight reached before pupation. In fact, larvae reared on VMD reached a maximum mean weight 10.5 ± 0.6% (mean ± SEM) less than larvae reared on SD.

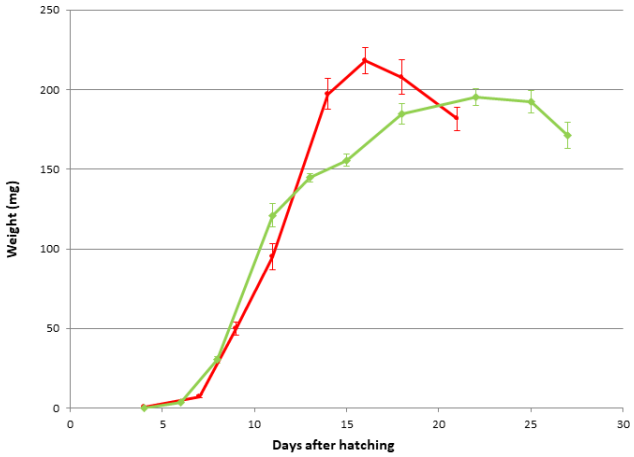

Figure 1. Larval grow rate. Larvae reared on SD are indicated in red while larvae grown on VMD are in green.

Nutrient content of the diets

For the evaluation of the nutritional content, VMD samples were weighted before and after the lyophilization process to calculate the water loss. Moreover, the amount of water lost during the analyses was considered. The nutrient content of the two diets is reported in Table 1.

	Standard diet[a]	Vegetable mix diet[b]
Ash	2.3 %	0.5 %
Protein	6.4 %	1.2 %
Lipid	1.2 %	0.1 %
Fiber	6.7 %	0.5 %
Hemicellulose	9.9 %	0.4 %
Cellulose	4.4 %	0.5 %
Lignin	1.7 %	0.1 %
Starch	8.6 %	1.3 %
Glucose and fructose	1.5 %	1.5 %
Iron	119.0 mg/kg	3.1 mg/kg

[a] 55% water
[b] 88% water

Table 1. Nutritional composition of the two experimental diets. The values of the fresh diets are reported.

Measurement of the midgut lumen pH

To evaluate if the feeding substrate could affect the pH of the midgut lumen, this parameter was measured in the three midgut regions of larvae reared on SD and VMD. As reported in Table 2, no significant differences were found between the pH values recorded in each midgut region of larvae reared on the two diets. The pH values are in agreement with those already reported (Bonelli et al., submitted), being acidic in the anterior midgut, strongly acidic in the middle, and alkaline in the posterior.

	SD	VMD
Anterior midgut	5.8 ± 0.1 (6)	6.0 ± 0.1 (6)
Middle midgut	2.4 ± 0.2 (6)	1.8 ± 0.2 (7)
Posterior midgut	8.3 ± 0.4 (6)	8.8 ± 0.1 (7)

Table 2. pH values in the lumen of *H. illucens* midgut regions. Mean ± SEM, number of replicates in parenthesis. No statistically significant differences were recorded among diet groups for each midgut region (unpaired t-test).

Morphological analysis of the larval midgut

The midgut of larvae reared on both diets was analyzed by optical and electron microscopy to evaluate if the feeding substrate could affect the morphology of the cells. The diet administered to the larva did not seem to cause substantial differences in the anterior midgut (Fig. 2A, B): in both cases columnar cells showed a big central nucleus, basal infoldings, and a well-developed brush border. Moreover, a large amount of dark vesicles, probably containing digestive enzymes, was clearly visible under the microvilli.

The middle midgut of *H. illucens* larvae is characterized by a first district with an epithelium in which copper cells are present and a second one characterized by a thin epithelium formed by large flat cells (Bonelli et al., submitted). All these cells showed the same characteristics, regardless of the feeding substrate: copper cells displayed the typical cup shape whit a big central nucleus and developed microvilli (Fig. 2C, D), while large flat cells presented an elongated nucleus and very short microvilli (Fig. 2E, F).

The most consistent change in the morphology of the epithelium was observed in the posterior midgut (Fig. 2G, H). In fact, the brush border of columnar cells showed a different length depending on the diet. In particular, columnar cells of larvae reared on VMD were characterized by microvilli that were longer than those of larvae reared on SD.

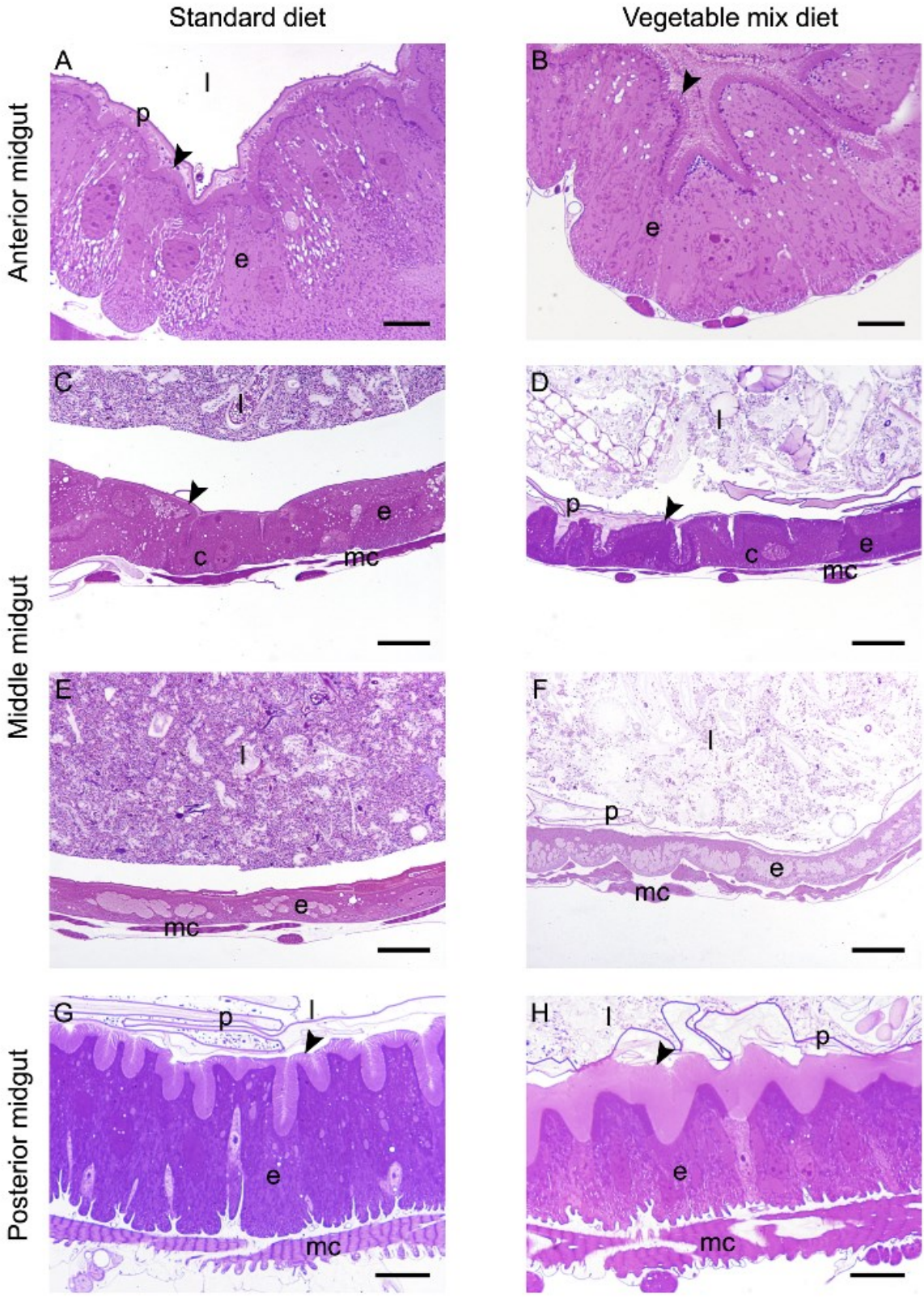

Figure 2. Morphological comparison of midgut from larvae reared on SD and VMD. (A, B): cross-section of the anterior midgut. (C-F): copper (C, D) and large flat cells (E, F) in the middle midgut of larvae. (G, H): cross-section of the posterior midgut. Larvae grown on VMD (H) show microvilli (arrow) that are longer than those of larvae reared on SD (G). c: copper cells; e: epithelium; l: lumen; mc: muscle cells; p: peritrophic matrix. Bars: 10 µm (A, B), 20 µm (C-H).

Histochemical characterization of the larval midgut

Detection of glycogen – PAS staining

The comparison of glycogen deposits in the midgut of larvae reared on the two diets evidenced a major difference in the anterior midgut. In fact, glycogen accumulation was more consistent in larvae reared on SD than on VMD (Fig. 3A, B). Moreover, the deposits in this region of the midgut were not localized in a specific area of the cell, but were sparse into the cytoplasm. In the middle and posterior midgut, the glycogen deposits showed almost the same presence in larvae grown on both diets (Fig. 3C-F), although their distribution differed in the two midgut regions. In fact, glycogen deposits were sparse in the cytoplasm in the middle midgut (Fig. 3C, D), while in the posterior midgut they were present in the apical region of columnar cells (Fig. 3E, F)

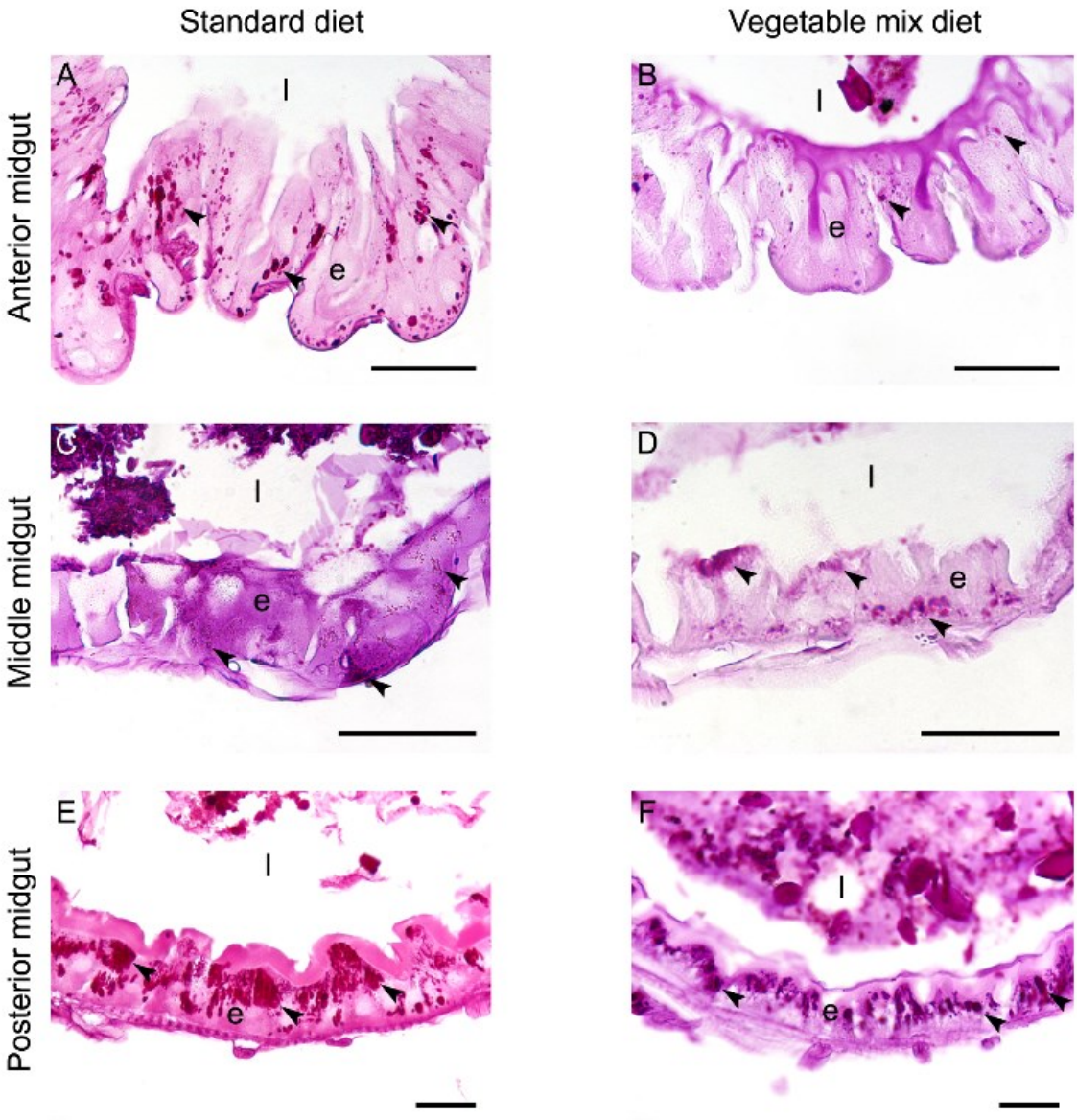

Figure 3. Comparison of glycogen accumulation in the three midgut regions of larvae reared on SD and VMD - PAS staining. (A, B): anterior midgut of larvae reared on SD (A) shows a higher accumulation of glycogen (arrowheads) than VMD (B). (C-F): middle (C, D) and posterior (E, F) midgut

of larvae reared on the two diets do not show significant differences in glycogen accumulation. e: epithelium; l: lumen. Bars 50 µm (A, B, E, F), 20 µm (C, D).

Detection of ferric iron - Perls' method

Ferric iron showed a broader distribution in the whole midgut of larvae grown on SD compared to VMD (Fig. 4). The presence of this compound in the first part of the posterior midgut (Fig. 4C, D) in larvae reared on the two diets could be attributed to iron cells, a peculiar cell type that has been identified in the midgut epithelium of other insects (Metha et al., 2009). Apart from this characteristic localization of ferric iron (Fig. 4C, D), in the anterior (Fig. 4A, B) and in the second part of the posterior region (Fig. 4E, F), the presence of ferric iron in larvae reared on SD was higher than in VMD (Fig. 4A, E). Regardless of the feeding substrate, the middle midgut did not show any staining (data not shown)

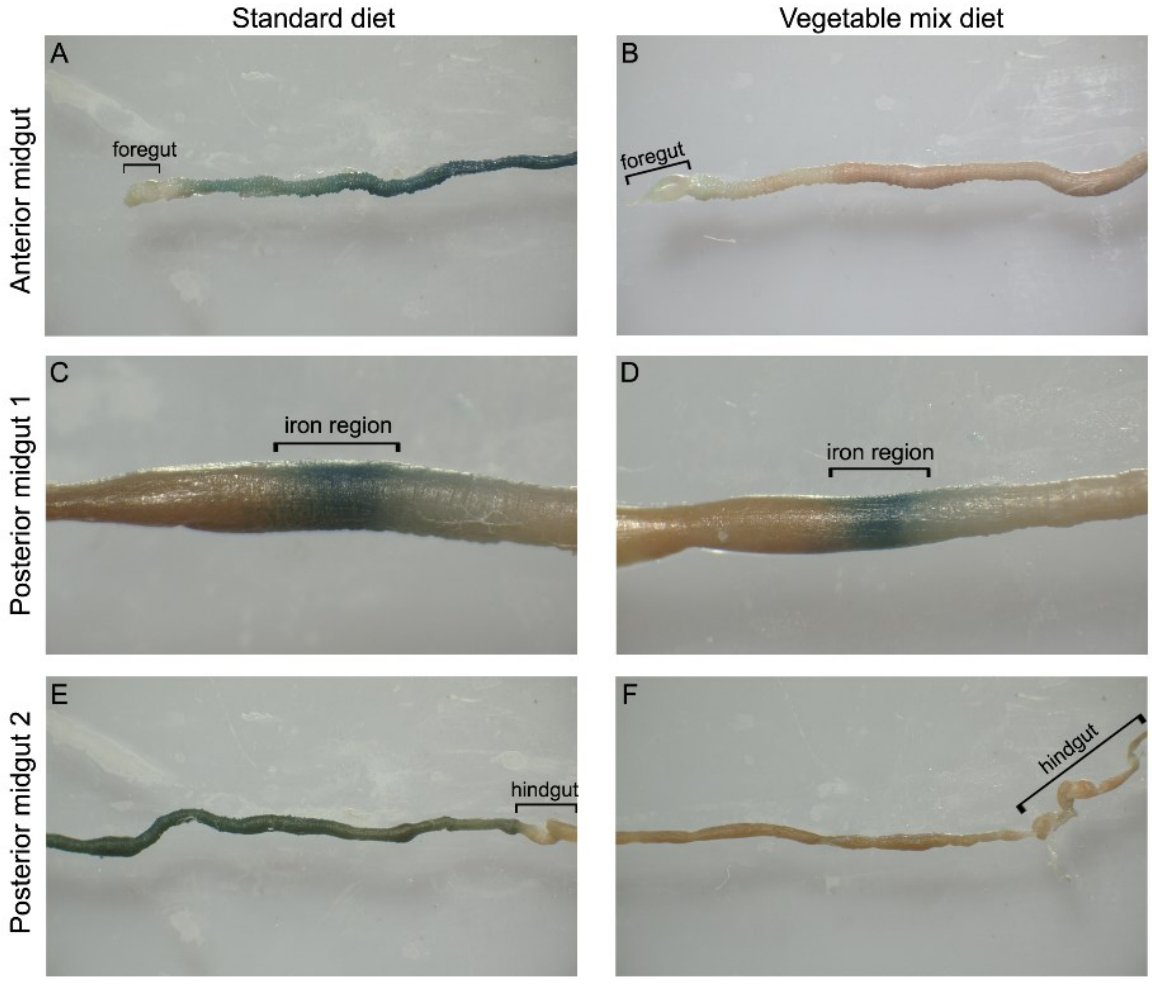

Figure 4. Comparison of iron accumulation between the three midgut regions of larvae reared on SD and VMD - Perls' method. (A, B): a higher iron accumulation in the anterior midgut of larvae reared on SD (A) compared to VMD (B) can be observed. (C, D): iron region of the first part of the posterior midgut of larvae reared on the two diets. (E, F): a higher accumulation of iron in the posterior midgut of larvae grown on SD than VMD is visible.

Enzymatic assays

To assess if *H. illucens* larvae can modulate the digestive efficiency in response to the nutrient composition of the feeding substrate, the activity of enzymes involved in protein and carbohydrate digestion was measured in larvae reared on both diets.

The total proteolytic activity was assayed on midgut juice samples using azocasein as substrate, at a pH as close as possible to the luminal pH of the investigated region (pH 6.0 for the anterior midgut, pH 5.0 for the middle midgut and pH 8.5 for posterior). As reported in figure 5, for all midgut regions we observed a significantly higher proteolytic activity in larvae reared on VMD, a feeding substrate with a lower protein content compared to SD (Table 1). For both diets, the highest proteolytic activity was measured in the posterior region.

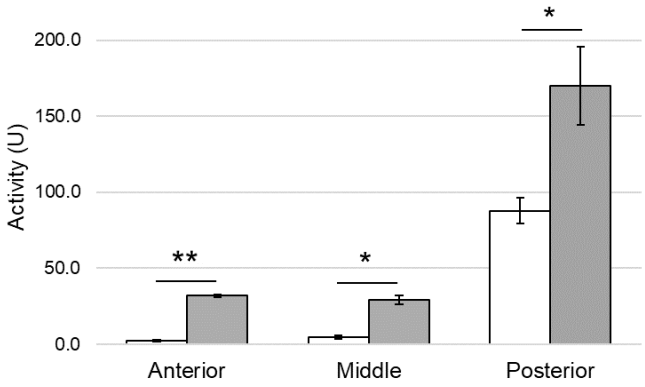

Figure 5. Total proteolytic activity in midgut juice extracted from anterior, middle, and posterior midgut of larvae reared on SD and VMD. For each tract the enzymatic assay was performed at pH as close as possible to that of the lumen (pH 6.0 for the anterior midgut, pH 5.0 for the middle midgut and pH 8.5 for posterior). The values are reported as mean ± SEM of at least 3 experiments. Asterisks indicate statistically significant differences between diet groups (unpaired t-test: *p-value < 0.05, **p-value < 0.001).

Previous data obtained on larvae reared on SD indicated that protein digestion essentially occurred in this tract and the enzymes involved in the initial phase of digestion of these macromolecules were mostly serine proteases (Bonelli et al., submitted). To establish if the increase in proteolytic activity observed in this region in larvae reared on VMD was due to a major activity of serine proteases, we evaluated the activity at acidic pH. When the proteolytic activity was measured at acidic pH (pH 5.0), a significant decrease of the enzymatic activity (five-fold reduction) was observed compared to that recorded at pH 8.5 (total proteolytic activity at pH 8.5: 169.7 ± 25.7 U, at pH 5.0: 34.1 ± 5.3 U, mean ± SEM of 4 experiments, paired *t*-test: *p*-value < 0.01). This result suggests that the increase in total proteolytic activity in the posterior region in larvae reared on VMD could be mainly due to serine proteases.

The two best studied serine proteases involved in protein digestion in insects are trypsin- and chymotrypsin-like proteases (Terra and Ferreira, 1994; Terra *et al.*, 1996). Their activity was measured in midgut juice samples from the posterior midgut using the specific substrates BApNA

and SAAPPpNA, respectively. As shown in figure 6, there was no significant difference in trypsin-like activity among larvae reared on the two diets (Fig. 6A), while chymotrypsin-like activity was significantly higher in larvae reared on VMD (Fig. 6B), more than double of that measured in larvae reared on SD.

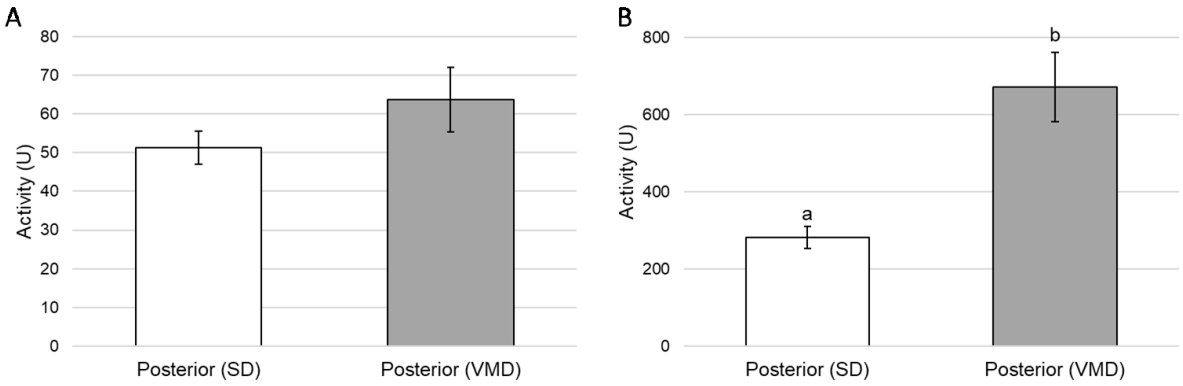

Figure 6. Trypsin- and chymotrypsin-like activity in midgut juice extracted from posterior midgut of larvae reared on SD and VMD. The values are reported as mean ± SEM of at least 3 experiments. For trypsin-like activity (A) no statistically significant difference among diet groups was recorded (unpaired t-test). For chymotrypsin-like activity (B) different letters indicate statistically significant difference among diet groups (unpaired t-test: p-value < 0.01).

In addition to the evaluation of the activity of enzymes present in the midgut lumen and involved in the initial phase of protein digestion, the activity of enzymes responsible for the final phase of digestion able to the release of single amino acids from small peptides was measured. In particular, we assayed the activity of APN, an exopeptidase that is anchored to the midgut brush border membrane (Terra and Ferreira, 1994). These assays were performed on the homogenate of posterior midgut epithelium. As shown in figure 7, APN activity was significantly higher in larvae reared on VMD, reaching values that were six-fold higher than those measured in larvae reared on SD.

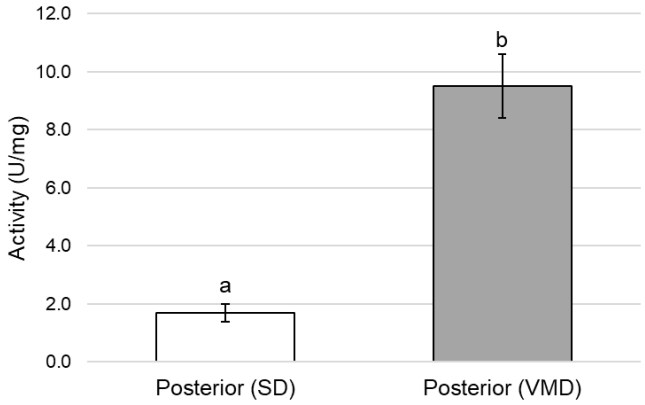

Figure 7. Aminopeptidase N activity in the posterior midgut of larvae reared on SD and VMD. The values are reported as mean ± SEM of at least 3 experiments. Different letters indicate statistically significant difference among diet groups (unpaired t-test: p-value < 0.01).

To examine carbohydrate digestion, we compared the activity of α-amylase (Terra and Ferreira, 1994; Terra *et al.*, 1996) in larvae reared on the two diets. As reported in figure 8 no significant difference in α-amylase activity was observed in the anterior and middle regions, while in the posterior region the activity was significantly lower in larvae reared on VMD, with a sixty-fold reduction compared to than that measured in larvae reared on SD.

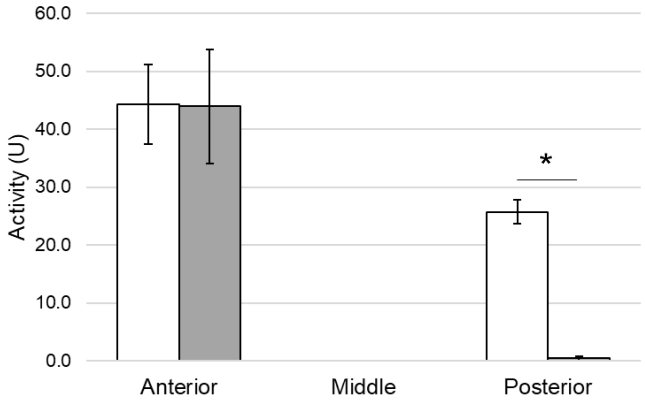

Figure 8. α-amylase activity in midgut juice extracted from anterior, middle, and posterior midgut of larvae reared on SD and VMD. The values are reported as mean ± SEM of at least 3 experiments. Asterisks indicate statistically significant differences between diet groups (unpaired t-test: *p-value < 0.001).

Finally, the activity of lysozyme, an enzyme responsible for the degradation of peptidoglycan present in the cell wall of many bacteria, was measured in the middle midgut (Fig. 9).

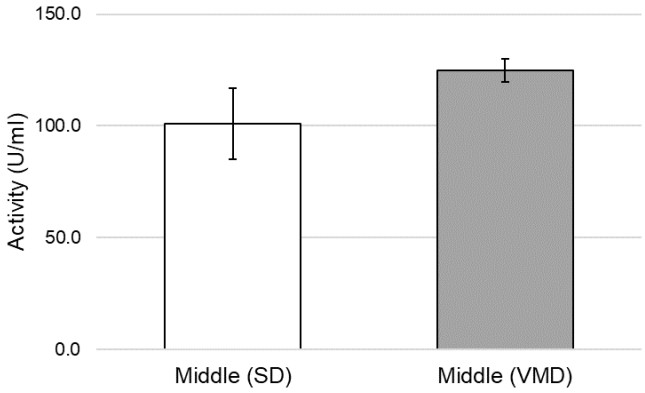

Figure 9. Lysozyme activity in midgut juice extracted from middle midgut of larvae reared on SD and VMD. The values are reported as mean ± SEM of at least 3 experiments. No statistically significant difference among diet groups was recorded (unpaired t-test).

We focused the attention on this tract since it has been suggested that lysozyme, together with the low pH value of the lumen of this region, is responsible for killing pathogens ingested with the diet in brachycerous larvae (Espinoza-Fuentes and Terra, 1987; Terra and Ferreira, 1994; Bonelli et al., submitted; Bruno et al., 2019). No significant difference was observed between larvae reared on the two diets.

DISCUSSION

The larvae of the black soldier fly are suitable for the bioconversion process (Rehman et al., 2017a; Wang et al., 2017; Xiao et al., 2018), since they are able to grow and convert a wide variety of different waste material, such as agro-industrial by-products, kitchen waste, fruit and vegetable waste, and manure into nutritionally valuable protein (Meneguz et al., 2018; Nguyen et al., 2013; Rehman et al., 2017b; Salomone et al., 2017). In particular, the bioconversion of fruit and vegetable waste into protein useful for production of feedstuffs (Magalhães et al., 2017; Newton et al., 1977; Schiavone et al., 2017) is a promising approach since in the EU insects destined for animal feed cannot be reared on organic matter containing products of animal origin (European Commission Regulations N°767/2009, 1069/2009 and 142/2011) and recently the European Commission Regulation N°2017/893 has partially uplifted the feed ban rules regarding the use of processed animal proteins from BSF and other six insect species for aquaculture. Regarding *H. illucens*, no information is available in literature about the morphofunctional modification of the midgut when the larvae are reared on substrates with different nutrient content. In the present work, we evaluated growth performances, activity of digestive enzymes, morphological features of midgut epithelium and long-term storage molecules changes in this tissue in larvae reared on vegetable mix diet (VMD) and standard diet (SD) for Diptera (Hogsette, 1992) to understand if the extraordinary feeding plasticity of BSF larvae corresponds to adaptations of the larval midgut, the organ directly involved in the bioconversion process.

It is known that several factors, such as temperature, humidity, density of insects in the rearing substrates influence the development of BSF larvae (Barragan-Fonseca et al., 2018; Harnden and Tomberlin, 2016; Holmes et al., 2012). For this reason, the larvae used in this study were kept at the same temperature, humidity and density conditions, to avoid bias due to these parameters and evaluate the impact only of the rearing substrates. Diet composition seems to be the major factor that influences larval performances, and the time required to complete the larval development decrease with the increase of diet quality. In particular, larvae show a high development rate on substrates with appropriate nutritional values such as standard diet, on which after 18 days 25% of insects are pupae, while poor performances were described on substrates such as fish meal, on which 36 days are necessary to have 25% of larvae to reach pupal stage (Bruno et al., 2019). Our data demonstrated that VMD is suitable for rearing *H. illucens* larvae although a lower developmental rate was observed compared to control diet. The nutritional composition of the two diets is very different in terms of protein, starch, and lipids, and larvae reared on VMD reached the pupal stage approximately one week later than larvae reared on control diet. Moreover, maximum weight reached before pupation by larvae reared on fruit and vegetable is about 10%

lower than that those reared on SD. These differences are probably caused by the lower nutritional content of a diet only composed by fruits and vegetables (Table 1).

Conversely, different growth pattern of BSF larvae reared on the two diets corresponds to different enzymatic expression and activity in the larval midgut. No information is available about the regulation of digestive enzymes in response to different nutritional composition of the diet, in particular in relation to different protein and carbohydrate content and their ratio, probably because of the very recent interest in insect farming. In fact, these issues have been deeply investigated in other arthropod species with consolidate economic interest such as shrimps (Brito et al., 2000; Muhlia-Almazán et al., 2003; Tantikitti et al., 2016; Shao et al., 2017). Our work represents the first attempt to shed light on relation between digestive enzyme activity and diet nutritional content in insects. Larvae of *H. illucens* reared on VMD show an increased activity of enzymes involved in both first and final phase of protein digestion, with higher total luminal proteolytic activity in all three midgut regions and higher APN activity in the homogenate of posterior midgut epithelium, respectively. Regarding carbohydrate digestion, α-amylase activity does not differ between diets in the anterior midgut, while it is strongly increased in the posterior midgut of larvae reared on SD. We hypothesize that these changes are an adaptation to better exploit a diet with a non-optimal nutritional content: in the presence of a low-protein diet, as for VMD, an increase in proteolytic activity is observed, while when larvae are reared on SD, which has a protein content 6-fold higher than VMD, the protein demand is satisfied without any need to increase protease activity, and the larvae invest on amylolytic enzymes to better exploit the carbohydrate content in the feeding substrate.

We also analyzed lysozyme activity, an enzyme involved in enzymatic killing of bacteria and fungi ingested with the diet. No difference in lysozyme activity was observed among larvae reared on the two substrates. The expression of these enzymes was recently analyzed in *H. illucens* larval gut by Vogel et al. (2018). The authors reported that only some lysozyme coding genes are upregulated in diets with a high bacterial load. Moreover, an overall similar microbiota composition in the midgut of *H. illucens* larvae reared on SD and VMD has been described and the two diets do not induce gut dysbiosis (Bruno et al., 2019). Therefore, it is reasonable that no significant variation in lysozyme activity was recorded in larvae fed on the two diets.

We demonstrated that the nutrient composition of the feeding substrate not only influences the length of larval development and activity of digestive enzymes, but also induces morphological modifications in midgut cells. Many studies demonstrated that diets induce ultrastructural changes in midgut cells of many insects. The modifications regard fluctuations in the number and structure of lysosomes (Sutherland et al., 2002), proliferation of both smooth and rough endoplasmic

reticulum (Houk and Vardy, 1982), and the increase of the basal labyrinth surface (Rudin and Hecker, 1979). Moreover, in other insects changes in structures associated to the midgut take place, for example the strong rearrangement of the perimicrovillar membrane forming a sort of peritrophic matrix after blood feeding in Hemiptera (Billingsley and Downe, 1983). The diet can also alter the structure of microvilli: in *Drosophila melanogaster* Meigen, 1830 (Diptera: Drosophilidae) variations in the shape and length of microvilli were observed, an effect similar to that caused by starvation (Li et al., 2009). Also in *H. illucens* larvae we observed changes in the morphology of midgut cells, and in particular in the length of microvilli. This modification is restricted to the posterior midgut, the region mainly involved in nutrient absorption (Bonelli et al., submitted). The higher length of microvilli in larvae reared on VMD probably responds to the need of a higher absorbing surface and represents an adaptation to the low nutritional content of VMD in terms of proteins.

Midgut cells of *H. illucens* larvae also showed differences in glycogen accumulation. Glycogen reserves are useful to sustain the insect during metamorphosis (Franzetti et al., 2015), a process that in *H. illucens* needs about twelve days to occur. During this period, indeed, glycogen deposits are mobilised and progressively reduced (Bruno et al., submitted). Our data demonstrate that larvae reared on VMD show lower accumulation of this long-term storage molecule than larvae reared on control diet, especially in the anterior midgut. The higher presence of glycogen reserves in larvae reared on the control diet could be related to the higher presence of carbohydrate level in SD than VMD (Table 1). Regardless of the feeding substrate, we observed that glycogen accumulation occurs differentially in the three midgut regions. In particular, the anterior and the posterior midgut are mainly involved in glycogen storage, indicating that the cells in the midgut epithelium accomplish different metabolic functions (Turunen and Crailsheim, 1996).

We also evaluated the accumulation of microelements in midgut cells of larvae grown on the two diets. In particular, our attention focused on iron. Several studies demonstrated that this element is fundamental for the development of Diptera (Law, 2002; Missirlis et al., 2007) due to its role as a cofactor for different enzymes involved in crucial physiological functions. Among these there are those responsible for respiration (Warburg, 1925) and synthesis of DNA (Clark, 1994), ecdysone (Chavez et al., 2000; Warren et al., 2002), and lipids (Navarro et al., 2010).

Ferritin is the major protein responsible for iron storage in insects (Pham and Winzerling, 2010), and is constitutively expressed in a peculiar cell type, called iron cells (Mandilaras et al., 2013). In *D. melanogaster* larvae these cells are located between the middle and posterior midgut, in a tract called iron region (Filshie et al., 1971). However, in this insect, the expression of this protein is inducible in other midgut cells. In fact, it has been demonstrated that when the iron content in

the diet is high, ferritin encoding genes are also expressed in the anterior and posterior midgut cells, allowing iron accumulation also in these regions (Poulson and Bowen, 1952; Mandilaras et al., 2013). Our data on *H. illucens* show a similar situation. The region in which iron cells are present has a location comparable to that observed in *D. melanogaster*: in these cells the iron accumulation occurs regardless the diet. By contrast, iron is accumulated also in anterior and posterior midgut region only in larvae reared on SD, substrate characterized by a high iron content. In conclusion, our work represents the first attempt to clarify how different feeding substrates with different nutrient composition affect the morphology and some physiological parameters of *H. illucens* larval midgut. Our results demonstrate that the extraordinary feeding plasticity of this insect is correlated with the plasticity of this organ, which is responsible for digestion and nutrient absorption. Although vegetal materials are suitable to rear *H. illucens* larvae (Jucker et al., 2017), more in depth studies are necessary to optimize their bioconversion, opening up interesting application perspectives.

AKNOWLEDGEMENTS

This work was supported by Fondazione Cariplo (grant n° 2014-0550). MB is a Ph.D. student of the "Environmental Sciences" course at Università degli Studi di Milano. DB is a Ph.D. student of the "Biotechnologies, Biosciences and Surgical Technologies" course at Università degli Studi dell'Insubria.

REFERENCES

Alexandratos, N., Bruinsma, J. (2012). World agriculture towards 2030/2050: the 2012 revision. Food and Agriculture Organization of the United Nations, Rome.

Barragan-Fonseca, K., Dicke, M., Van Loon, J. (2017). Nutritional value of the black soldier fly (*Hermetia illucens* L.) and its suitability as animal feed – a review. Journal of Insects as Food and Feed, 3, 105-120.

Barragan-Fonseca, K. B., Dicke, M., Van Loon, J. J. A. (2018). Influence of larval density and dietary nutrient concentration on performance, body protein, and fat contents of black soldier fly larvae (*Hermetia illucens*). Entomologia Experimentalis et Applicata, 166, 761-770.

Barroso, F. G., Haro, C. D., Sánchez-Muros, M., Venegas, E., Martínez-Sánchez, A., Pérez-Bañón, C. (2014). The potential of various insect species for use as food for fish. Aquaculture, 422-423, 193-201.

Bernfeld, P., 1955. Amylase α and β. Methods in Enzymology, 1, 149-158.

Billingsley, P. F., Downe, A. E. R. (1983). Ultrastructure changes in posterior midgut cells associated with blood feeding in adult female *Rhodnius prolixus* Stal (Hemiptera: Reduviidae). Canadian Journal of Zoology, 61, 2574-2586.

Bonelli, M., Bruno, D., Caccia, S., Sgambetterra, G., Cappellozza, S., Jucker, C., Tettamanti, G., Casartelli, M. (submitted). Structural and functional characterization of *Hermetia illucens* larval midgut.

Brito, R., Chimal, M. E., Gaxiola, G., Rosas, C. (2000). Growth, metabolic rate, and digestive enzyme activity in the white shrimp *Litopenaeus setiferus* early post larvae fed different diets. Journal of Experimental Marine Biology and Ecology, 255, 21-36.

Bruno, D., Bonelli, M., Cadamuro, A. G., Reguzzoni, M., Grimaldi, A., Casartelli, M., Tettamanti, G. (submitted). The digestive system of the adult *Hermetia illucens* (Diptera: Stratiomyidae): morphological features and functional properties.

Bruno, D., Bonelli, M., De Filippis, F., Di Lelio, I., Tettamanti, G., Casartelli, M., Ercolini, D., Caccia, S. (2019). The intestinal microbiota of *Hermetia illucens* larvae is affected by diet and shows a diverse composition in the different midgut regions. Applied and Environmental Microbiology, 85, e01864-18.

Cashion, T., Manach, F. L., Zeller, D., Pauly, D. (2017). Most fish destined for fishmeal production are food-grade fish. Fish and Fisheries, 18, 837-844.

Chaalala, S., Leplat, A., Makkar, H. (2018). Importance of insects for use as animal feed in low-income countries. In: Edible insects in sustainable food systems, 303-319. Springer, Cham.

Charney, J., Tomarelli, R. M. (1947). A colorimetric method for the determination of the proteolytic activity of duodenal juice. Journal of Biological Chemistry, 171:501-5.

Chávez, V. M., Marqués, G., Delbecque, J. P., Kobayashi, K., Hollingsworth, M., Burr, J., Natzle, J. E., O'Connor, M. B. (2000). The *Drosophila* disembodies gene controls late embryonic morphogenesis and codes for a cytochrome P450 enzyme that regulates embryonic ecdysone levels. Development, 127, 4115-4126.

Clark, D. V. (1994). Molecular and genetic analyses of *Drosophila* Prat, which encodes the first enzyme of de novo purine biosynthesis. Genetics, 136, 547-557.

Coch Frugoni, J. A. (1957) Tampone universale di Britton e Robinson a forza ionica costante. Gazzetta Chimica Italiana, 87, 403-407.

Diener, S., Zurbrügg, C., Tockner, K. (2009). Conversion of organic material by black soldier fly larvae: establishing optimal feeding rates. Waste Management & Research, 27, 603-610.

EFSA Scientific Committee (2015). Risk profile related to production and consumption of insects as food and feed. EFSA Journal, 13, 4257.

Espinoza-Fuentes, F. P., Terra, W. R. (1987). Physiological adaptations for digesting bacteria. Water fluxes and distribution of digestive enzymes in *Musca domestica* larval midgut. Insect Biochemistry, 17, 809-817.

FAO (2017). The future of food and agriculture - Trends and challenges. Rome.

Franzetti, E., Romanelli, D., Caccia, S., Cappellozza, S., Congiu, T., Rajagopalan, M., Grimaldi, A., de Eguileor, M., Casartelli, M., Tettamanti, G. (2015). The midgut of the silkmoth *Bombyx mori* is able to recycle molecules derived from degeneration of the larval midgut epithelium. Cell and Tissue Research, 361, 509-528.

Gagliardi, R., Cescut, A., Gamboz, C., Rugolo, F. (1986). Studi sulla lisi batterica da lisozima. Bollettino dell'Istituto Sieroterapico Milanese, 65, 112-117.

Gustavsson J., Cederberg C., Sonesson U., Van Otterdijk R., Meybeck A. (2011). Global food losses and food waste: extent, causes and prevention. Food and Agriculture Organization of the United Nations, Rome.

Halloran, A., Hansen, H. H., Jensen, L. S., Bruun, S. (2018). Comparing environmental impacts from insects for feed and food as an alternative to animal production. In: Edible Insects in Sustainable Food Systems, 163-180. Springer, Cham.

Harnden, L. M., Tomberlin, J. K. (2016). Effects of temperature and diet on black soldier fly, *Hermetia illucens* (L.) (Diptera: Stratiomyidae), development. Forensic Science International, 266, 109-116.

Hogsette, J. A. (1992). New diets for production of house flies and stable flies (Diptera: Muscidae) in the laboratory. Journal of Economic Entomology, 85, 2291-2294.

Holmes, L. A., Vanlaerhoven, S. L., Tomberlin, J. K. (2012). Relative humidity effects on the life history of *Hermetia illucens* (Diptera: Stratiomyidae). Environmental Entomology, 41, 971-978.

Houk, E. J., Hardy, J. J. (1982). Midgut cellular responses to bloodmeal digestion in the mosquito, *Culex tarsalis* Coquillett (Diptera: Culicidae). International Journal of Insect Morphology and Embryology, 11, 109-119.

Jucker, C., Erba, D., Leonardi, M. G., Lupi, D., Savoldelli, S. (2017). Assessment of vegetable and fruit substrates as potential rearing media for *Hermetia illucens* (Diptera: Stratiomyidae) larvae. Environmental Entomology, 46, 1415-1423.

Kroeckel, S., Harjes, A., Roth, I., Katz, H., Wuertz, S., Susenbeth, A., Schulz, C. (2012). When a turbot catches a fly: Evaluation of a pre-pupae meal of the black soldier fly (*Hermetia illucens*) as fish meal substitute - Growth performance and chitin degradation in juvenile turbot (*Psetta maxima*). Aquaculture, 364-365, 345-352.

Law, J. H. (2002). Insects, oxygen, and iron. Biochemical and Biophysical Research Communication, 292, 1191-1195.

Li, H M., Sun, L., Mittapalli, O., Muir, W. M., Xie, J., Wu, J., Schemerhorn, B. J., Sun, W., Pittendrigh, B. R., Murdock, L. L. (2009). Transcriptional signatures in response to wheat germ agglutinin and starvation in *Drosophila melanogaster* larval midgut. Insect Molecular Biology, 18, 21-31.

Magalhães, R., Sánchez-López, A., Leal, R. S., Martínez-Llorens, S., Oliva-Teles, A., Peres, H. (2017). Black soldier fly (*Hermetia illucens*) pre-pupae meal as a fish meal replacement in diets for European seabass (*Dicentrarchus labrax*). Aquaculture, 476, 79-85.

Makkar, H. P., Tran, G., Heuzé, V., Ankers, P. (2014). State-of-the-art on use of insects as animal feed. Animal Feed Science and Technology, 197, 1-33.

Mandilaras, K., Pathmanathan, T., Missirlis, F. (2013). Iron Absorption in *Drosophila melanogaster*. Nutrients, 5, 1622-1647.

Mehta, A., Deshpande, A., Bettedi, L., Missirlis, F. (2009). Ferritin accumulation under iron scarcity in *Drosophila* iron cells. Biochimie, 91, 1331-1334.

Mekonnen, M. M., Hoekstra, A. Y. (2012). A global assessment of the water footprint of farm animal products. Ecosystems, 15, 401-415.

Meneguz, M., Schiavone, A., Gai, F., Dama, A., Lussiana, C., Renna, M., Gasco, L. (2018). Effect of rearing substrate on growth performance, waste reduction efficiency and chemical composition of black soldier fly (*Hermetia illucens*) larvae. Journal of the Science of Food and Agriculture.

Missirlis, F., Kosmidis, S., Brody, T., Mavrakis, M., Holmberg, S., Odenwald, W. F., Skoulakis, E. M., Rouault, T. A. (2007). Homeostatic mechanisms for iron storage revealed by genetic manipulations and live imaging of *Drosophila* ferritin. Genetics, 177, 89-100.

Muhlia-Almazán, A., García-Carreño, F. L., Sánchez-Paz, J. A., Yepiz-Plascencia, G., Peregrino-Uriarte, A. B. (2003). Effects of dietary protein on the activity and mRNA level of trypsin in the midgut gland of the white shrimp *Penaeus vannamei*. Comparative Biochemistry and Physiology Part B: Biochemistry and Molecular Biology, 135, 373-383.

Navarro, J. A., Ohmann, E., Sanchez, D., Botella, J. A., Liebisch, G., Moltó, M. D., Ganfornina, M. D., Schmitz, G., Schneuwly, S. (2010). Altered lipid metabolism in a *Drosophila* model of Friedreich's ataxia. Human Molecular Genetics, 19, 2828-2840.

Newton, G. L., Booram, C. V., Barker, R. W., Hale, O. M. (1977). Dried *Hermetia Illucens* larvae meal as a supplement for swine. Journal of Animal Science, 44, 395-400.

Nguyen, T. T., Tomberlin, J. K., Vanlaerhoven, S. (2013). Influence of resources on *Hermetia illucens* (Diptera: Stratiomyidae) larval development. Journal of Medical Entomology, 50, 898-906.

Nguyen, T. T., Tomberlin, J. K., Vanlaerhoven, S. (2015). Ability of black soldier fly (Diptera: Stratiomyidae) larvae to recycle food waste. Environmental Entomology, 44, 406-410.

Oonincx, D. G., Van Broekhoven, S., Van Huis, A., Van Loon, J. J. (2015). Feed conversion, survival and development, and composition of four insect species on diets composed of food by-products. Plos One, 10.

Oonincx, D. G., Van Itterbeeck, J., Heetkamp, M. J., Van den Brand, H., Van Loon, J. J., Van Huis, A. (2010). An exploration on greenhouse gas and ammonia production by insect species suitable for animal or human consumption. PLoS ONE, 5.

Pham, D. Q., Winzerling, J. J. (2010). Insect ferritins: typical or atypical? Biochimica Et Biophysica Acta (BBA) - General Subjects, 1800, 824-833.

Pimentel, A. C., Montali, A., Bruno, D., Tettamanti, G. (2017). Metabolic adjustment of the larval fat body in *Hermetia illucens* to dietary conditions. Journal of Asia-Pacific Entomology, 20, 1307-1313.

Pitotti, A., Bo, A. D., Boschelle, O. (1991). Assay of lysozyme by its lytic action on *Leuconostoc oenos*: a suitable substrate at acidic pH. Journal of Food Biochemistry, 15, 393-403.

Poulson, D. F., Bowen, V. T. (1952). Organization and function of the inorganic constituents of nuclei. Experimental Cell Research (s1ry), 2, 161-179.

Rehman, K. U., Cai, M., Xiao, X., Zheng, L., Wang, H., Soomro, A. A., Zhou, Y., Li, W., Yu, Z., Zhang, J. (2017a). Cellulose decomposition and larval biomass production from the co-digestion of dairy manure and chicken manure by mini-livestock (*Hermetia illucens* L.). Journal of Environmental Management, 196, 458-465.

Rehman, K. U., Rehman, A., Cai, M., Zheng, L., Xiao, X., Somroo, A. A., Wang, H., Li, W., Yu, Z., Zhang, J. (2017b). Conversion of mixtures of dairy manure and soybean curd residue by black soldier fly larvae (*Hermetia illucens* L.). Journal of Cleaner Production, 154, 366-373.

Rudin, W., Hecker, H. (1979). Functional morphology of the midgut of *Aedes aegypti* L. (Insecta, Diptera) during blood digestion. Cell and Tissue Research, 200, 193-203.

Salomone, R., Saija, G., Mondello, G., Giannetto, A., Fasulo, S., Savastano, D. (2017). Environmental impact of food waste bioconversion by insects: Application of Life Cycle Assessment to process using *Hermetia illucens*. Journal of Cleaner Production, 140, 890-905.

Schiavone, A., Marco, M. D., Martínez, S., Dabbou, S., Renna, M., Madrid, J., Hernandez, F., Rotolo, L., Costa, P., Gai, F., Gasco, L. (2017). Nutritional value of a partially defatted and a highly defatted black soldier fly larvae (*Hermetia illucens* L.) meal for broiler chickens: Apparent nutrient digestibility, apparent metabolizable energy and apparent ileal amino acid digestibility. Journal of Animal Science and Biotechnology, 8.

Shao, J., Liu, M., Wang, B., Jiang, K., Wang, M., Wang, L. (2017). Evaluation of biofloc meal as an ingredient in diets for white shrimp *Litopenaeus vannamei* under practical conditions: Effect on growth performance, digestive enzymes and TOR signaling pathway. Aquaculture, 479, 516-521.

Spranghers, T., Ottoboni, M., Klootwijk, C., Ovyn, A., Deboosere, S., De Meulenaer, B., Michiels, J., Eeckhout, M., De Clercq, P., De Smet, S. (2017). Nutritional composition of black soldier fly (*Hermetia illucens*) prepupae reared on different organic waste substrates. Journal of the Science of Food and Agriculture, 97, 2594-2600.

St-Hilaire, S., Sheppard, C., Tomberlin, J. K., Irving, S., Newton, L., Mcguire, M. A., Mosley, E. E., Hardy, R. W., Sealey, W. (2007). Fly prepupae as a feedstuff for rainbow trout, *Oncorhynchus mykiss*. Journal of the World Aquaculture Society, 38, 59-67.

Steinfeld, H., Gerber, P., Wassenaar, T. D., Castel, V., Rosales, M., Rosales, M., de Haan, C. (2006). Livestock's long shadow: environmental issues and options. Food and Agriculture Organization of the United Nations, Rome.

Sutherland, P. W., Burgess, E. P. J., Philip, B. A., McManus, M. T., Watson, L., Christeller, J. T. (2002). Ultrastructure changes of the midgut of the black field cricket (*Teleogryllus commodus*) following ingestion of potato protease inhibitor II. Journal of Insect Physiology, 48, 327-336.

Tantikitti, C., Chookird, D., Phongdara, A. (2016). Effects of fishmeal quality on growth performance, protein digestibility and trypsin gene expression in pacific white shrimp (*Litopenaeus vannamei*). Songklanakarin Journal of Science and Technology, 38, 73-82.

Terra, W. R., Ferreira, C. (1994). Insect digestive enzymes: properties, compartmentalization and function. Comparative Biochemistry & Physiology, 109B: 1-62.

Terra, W. R., Ferreira, C., Jordao, B. P., Dillon, R. J. (1996). Digestive enzymes. In: Biology of the insect midgut, 153-194. Springer, Dordrecht.

Turunen, S., Crailsheim, K. (1996). Lipid and sugar absorption. In: Biology of the insect midgut, 293-320. Springer, Dordrecht.

United Nations (2017). World population prospects: the 2017 revision, key findings and advance tables. United Nations Department of Economic and Social Affairs/Population Division.

Van der Fels-Klerx, H. J., Camenzuli, L., Van der Lee, M. K., Oonincx, D. G. (2016). Uptake of cadmium, lead and arsenic by *Tenebrio molitor* and *Hermetia illucens* from contaminated substrates. Plos One, 11.

Van Huis. A. (2013). Potential of insects as food and feed in assuring food security. Annual Review of Entomology, 58, 563-583.

Van Huis, A., Oonincx, D. G. (2017). The environmental sustainability of insects as food and feed. A review. Agronomy for Sustainable Development, 37.

Van Huis, A., Van Itterbeeck, J., Klunder, H., Mertens. E., Halloran, A., Muir, G., Vantomme, P. (2013). Edible insects - Future prospects for food and feed security. Food and Agriculture Organization of the United Nations, Rome.

Verbeke, W., Spranghers, T., De Clercq, P., De Smet, S., Sas, B., Eeckhout, M. (2015). Insects in animal feed: acceptance and its determinants among farmers, agriculture sector stakeholders and citizens. Animal Feed Science and Technology, 204, 72-87.

Vogel, H., Müller, A., Heckel, D. G., Gutzeit, H., Vilcinskas, A. (2018). Nutritional immunology: Diversification and diet-dependent expression of antimicrobial peptides in the black soldier fly *Hermetia illucens*. Developmental & Comparative Immunology, 78, 141-148.

Waite, R., Beveridge, M., Brummett, R., Castine, S., Chaiyawannakarn, N., Kaushik, S., Mungkung, R., Nawapakpilai, S., Phillips, M. (2014). Improving productivity and environmental performance of aquaculture. World Resources Institute, Washington DC.

Wang, H., Rehman, K. U., Liu, X., Yang, Q., Zheng, L., Li, W., Cai, M., Li, Q., Zhang, J., Yu, Z. (2017). Insect biorefinery: A green approach for conversion of crop residues into biodiesel and protein. Biotechnology for Biofuels, 10: 304.

Wang, Y., Shelomi, M. (2017). Review of black soldier fly (*Hermetia illucens*) as animal feed and human food. Foods, 6(10), 91.

Warburg, O. (1925). Iron, the oxygen-carrier of respiration-ferment. Science, 61, 575-582.

Warren, J. T., Petryk, A., Marques, G., Jarcho, M., Parvy, J., Dauphin-Villemant, C., O'Connor, M. B., Gilbert, L. I. (2002). Molecular and biochemical characterization of two P450 enzymes in the ecdysteroidogenic pathway of *Drosophila melanogaster*. Proceedings of the National Academy of Sciences, 99, 11043-11048.

World Resource Institute (2011). WRI report based on FAO. Global food losses and food waste-extent, causes and prevention. World Resources Institute, Washington DC.

Xiao, X., Mazza, L., Yu, Y., Cai, M., Zheng, L., Tomberlin, J. K., Yu, J., Van Huis, A., Yu, Z., Fasulo, S., Zhang, J. (2018). Efficient co-conversion process of chicken manure into protein feed and organic fertilizer by *Hermetia illucens* L. (Diptera: Stratiomyidae) larvae and functional bacteria. Journal of Environmental Management, 217, 668-676.

CHAPTER 3

The intestinal microbiota of *Hermetia illucens* larvae is affected by diet and shows a diverse composition in the different midgut regions

The intestinal microbiota of *Hermetia illucens* larvae is affected by diet and shows a diverse composition in the different midgut regions

Daniele Bruno[a,*], Marco Bonelli[b,*], Francesca De Filippis[c,d], Ilaria Di Lelio[c], Gianluca Tettamanti[a], Morena Casartelli[b], Danilo Ercolini[c,d], Silvia Caccia[c,d]

[a]Department of Biotechnology and Life Sciences, University of Insubria, Varese, Italy

[b]Department of Biosciences, University of Milan, Milano, Italy

[c]Department of Agricultural Sciences, University of Naples "Federico II", Portici (NA), Italy

[d]Task Force on Microbiome Studies, University of Naples "Federico II", Napoli, Italy

*These authors contributed equally

Corresponding author:

Silvia Caccia, silvia.caccia@unina.it

Published on *Applied and Environmental Microbiology* 85(2):e01864-18 in January 2019

doi:10.1128/AEM.01864-18

ABSTRACT

The larva of the black soldier fly (*Hermetia illucens*) has emerged as an efficient system for the bioconversion of organic waste. Although many research efforts are devoted to the optimization of rearing conditions to increase the yield of the bioconversion process, microbiological aspects related to this insect are still neglected. Here we describe the microbiota of the midgut of *H. illucens* larvae showing the effect of different diets and midgut regions in shaping microbial load and diversity. The bacterial communities residing in the three parts of the midgut, characterized by remarkable changes in luminal pH values, differed in terms of bacterial numbers and microbiota composition. The microbiota of the anterior part of the midgut showed the highest diversity that gradually decreased along the midgut, whereas bacterial load had an opposite trend, being maximal in the posterior region. The results also showed that the influence of the microbial content of ingested food was limited to the anterior part of the midgut and that the feeding activity of *H. illucens* larvae did not affect significantly the microbiota of the substrate. Moreover, a high protein content compared to other macronutrients in the feeding substrate seems to favor midgut dysbiosis. The overall data indicate the importance of taking into account the presence of different midgut structural and functional domains, as well as substrate microbiota, in any further study that aims at clarifying microbiological aspects concerning *H. illucens* larval midgut.

IMPORTANCE

The demand for food of animal origin is expected to increase by 2050. Since traditional protein sources for monogastric diets are failing to meet the increasing demand for additional feed production, there is an urgent need to find alternative protein sources. The larvae of *Hermetia illucens* emerge as efficient converters of low quality biomass into nutritionally valuable proteins. Many studies have been performed to optimize *H. illucens* mass rearing on a number of organic substrates and to maximize quantitatively and qualitatively the biomass yield. On the contrary, although insect microbiota can be fundamental for bioconversion processes and its characterization is mandatory also for safety aspects, this topic is largely overlooked. Here we provide an in depth study of the microbiota of *H. illucens* larval midgut taking into account pivotal aspects such as the midgut spatial and functional regionalization as well as microbiota and nutrient composition of the feeding substrate.

INTRODUCTION

The black soldier fly (BSF), *Hermetia illucens* (Diptera: Stratiomyidae), is a true fly that occurs worldwide in tropical and temperate regions. Adults of this insect have never attracted interest because they do not approach humans, do not bite and are not known to vector pathogens. On the contrary, BSF larvae have been object of intense research efforts because of their remarkable utility for humans that take advantage of their feeding regime of generalist detritivore (Wang and Shelomi, 2017). In particular, BSF larvae are largely used in forensic entomology to estimate human postmortem interval (Lord et al., 1994; Turchetto et al., 2001) but the major promising potential of the voracious BSF larvae is their use as efficient bioconverters (Cicková et al., 2015; Makkar et al., 2014; Müller et al., 2017). Indeed, BSF larvae can be reared in mass cultures on a very wide variety of organic waste (e.g. crop and food processing residues, food waste, manure and feces) leading to the conversion of low quality material into valuable biomass. The latter is exploitable for the isolation of bioactive compounds (e.g. antimicrobial peptides, chitosan and degrading enzymes), biodiesel production, and as feed or feed ingredients (mainly for their content of high-quality proteins and lipids) for poultry, aquaculture, and livestock (Müller et al., 2017; Wang and Shelomi, 2017). The production of BSF larvae is technically simple, cost-effective and environmentally sustainable. However, the rate of waste recycling and the final value of the biomass obtained depend on the rearing strategy, in terms of feeding substrate composition, feed consumption rate, and environmental parameters (i.e. temperature, humidity and photoperiod) (Wang and Shelomi, 2017). For this reason, many research efforts now focus on the characterization of nutrient and micronutrient content of BSF larvae in response to different rearing conditions and substrates, in order to optimize biomass yield and quality (Cammack and Tomberlin, 2017; Harden and Tomberlin, 2016; Jucker et al., 2017; Ma et al., 2018; Müller et al., 2017; Wang and Shelomi, 2017).

Safety aspects concerning the microbiological load of intermediate and final products of bioconversion processes are also crucial, especially when BSF is exploited for feed applications. In principle, this issue can be approached by classical food microbiology methods to establish whether a product meets the recommendations imposed by current hygiene criteria. On the other hand, an in-depth characterization of BSF larvae microbiota and the factors that influence its composition is particularly important. Microbiota composition is known to impact insect health and performance, and has to be considered in the effort to optimize biomass yield (De Smet et al., 2018). In addition, the analysis of the microbiota could allow the identification of bacterial species with peculiar and unique characteristics, such as the capacity to degrade complex substrates, as cellulose, hemicellulose and lignin (Rehman et al., 2017), or xenobiotics. These microorganisms,

or even the enzymes responsible for the degradation, could be isolated and exploited at industrial level for waste recycling and bioremediation. Populations of gut bacteria able to compete with pathogens or to act as probiotics could be boosted for the improvement of BSF larvae performances and bioconversion efficiency or may be used in other animal hosts with similar purposes. Moreover, the study of BSF microbiota has a strong potential in contributing to the global problem of the identification of new antimicrobials. Indeed, BSF larvae feeding activity is able to reduce the bacterial load of substrates and, importantly, this capacity is not accompanied by the accumulation of pathogens in their gut (Erickson et al., 2004; Liu et al., 2008; Lalander et al., 2013; 2015). Such evidence implies the presence of potent antimicrobial effectors produced by BSF larvae and their intestinal microbiota. It should be pointed out that the latter is implicated in turn in the maintenance of gut homeostasis and supports gut immune functions (Broderick 2016; De Smet et al., 2018; Zdybicka-Barabas et al., 2017).

A few studies on microbiota of BSF larvae have already been performed (Jeon et al., 2011; Zheng et al., 2013). Rearing substrate and insect development stage have a significant impact on the overall composition of the microbial community (Jeon et al., 2011; Zheng et al., 2013). A very critical issue that these preliminary microbiological surveys have not taken into account is the high complexity of the gut of fly larvae. In fact, this organ, and in particular the midgut, shows peculiar regional structural and functional features associated with changes of luminal pH (Lemos and Terra 1991; Pimentel et al., 2018; Shanbhag and Tripathi, 2009). The differences in gut morphology and epithelial architecture along different intestinal tracts of some insects are in fact accompanied by remarkable differences in physiological, metabolic and immune features that impact on microbiota composition (Buchon and Osman, 2015; Lehane and Billingsley, 1996; Terra, 1990). These complex relationships have been exhaustively described in the model insect, the fly *Drosophila melanogaster* (Diptera: Drosophilidae) (Broderick et al., 2014; Broderick 2016; Buchon et al., 2013; Capo et al., 2016; Marianes and Spradling, 2013).

In all insect, the digestive tract is divided into three regions with different embryonic origin and peculiar morphological and functional features: a short initial tract, the foregut, a long midgut where digestion and absorption occur and a final hindgut where water, salts, and other molecules are absorbed prior to elimination of the feces. Even though a detailed morphofunctional description of *H. illucens* larval midgut is lacking, it is expected that, as in other non-hematophagous brachycerous Diptera, discrete regions with peculiar pH values can be recognized along the midgut and that each distinct midgut region possesses its own features, at both structural and functional levels, and a peculiar resident microbiota (Broderick et al., 2014; Broderick, 2016; Buchon et al.,

2013; Buchon and Osman, 2015; Capo et al., 2016; Lehane and Billingsley, 1996; Marianes and Spradling, 2013; Terra, 1990).

In the present work we analyzed the effects of different diets and their microbial community on the midgut microbiota of BSF larvae, and the impact of the insect feeding activity on the diet microbiota. Most importantly, we analyzed the different tracts of BSF larval midgut separately, and highlighted the need of having future research on BSF larval midgut considering each midgut domain independently.

RESULTS

Determination of the pH values of the midgut lumen content

Since luminal pH is a good marker for midgut regionalization in flies (Lemos and Terra, 1991; Shanbhag and Tripathi 2009; Pimentel et al., 2018), we evaluated how the pH of the lumen content of BSF larvae changed along the midgut in order to have a clear identification of the regions in which this organ could be subdivided. For this purpose, last instar *H. illucens* larvae were fed with diet containing two pH indicators, bromophenol blue and phenol red. The color of the luminal content of larvae fed with diet containing bromophenol blue was clearly visible through the isolated epithelium (Fig. 1A). The anterior region of the midgut presented a blue color, indicating that its luminal content has a pH $\geq$ 4.6. Then, a marked change was observed, since the middle region turned yellow, revealing that its lumen has a pH $\leq$ 3. Moving towards the posterior midgut, the color gradually turned blue. Bromophenol blue turns at pH values between 3.0 and 4.6, thus differences in the pH values of the anterior and posterior midgut contents could not be evidenced. Figure 1B shows the gut isolated from a larva fed with diet containing phenol red, a dye that turns yellow at pH $\leq$ 6.8 and fuchsia at pH $\geq$ 8.2. Since the anterior and the middle regions of the midgut presented a golden yellow color, whereas the posterior midgut content appeared fuchsia, it is possible to state that the luminal content of the anterior and middle regions have an acidic pH and the posterior has an alkaline pH. The evidence obtained with phenol red supported and completed results obtained with bromophenol blue.

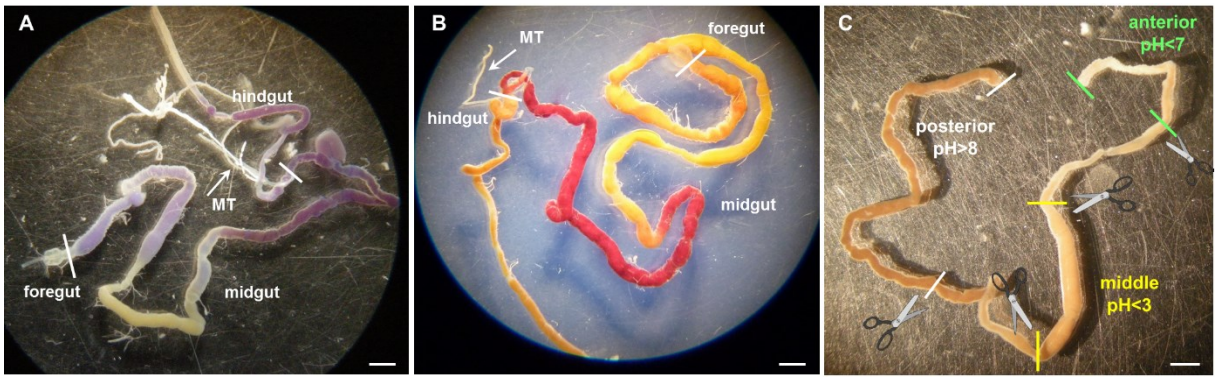

Figure 1. Determination of pH value in BSF larvae midgut lumen (A and B) and definition of the midgut portions for the microbiota analysis (C). In (A) and (B) the anatomy of the larval BSF gut is visible. The short foregut is followed by a very long midgut. The beginning of the hindgut (which extends out of the field of view) is easily recognizable by the insertion of Malpighian tubules (MT), structures involved in excretion in insects and that deliver the primary urine into hindgut lumen. The whole gut isolated from *H. illucens* larvae fed with diet containing bromophenol blue (A) or phenol red (B) pH indicators shows the presence of different pH values along the midgut lumen. (C) Image of the midgut, that is subdivided in a relatively short and thick anterior midgut, a middle midgut characterized by an enlarged highly acidic portion (stomach), and the posterior midgut. Bars of different color highlight the position of the cuts for the isolation of the portions used for microbiota analyses. Bars: 2 mm.

In conclusion, the luminal content of the midgut of *H. illucens* larvae presents different pH values: the anterior region has an acid luminal content, the middle region presents a strongly acid pH (pH $\leq$ 3) and the posterior region has an alkaline luminal content. These three regions are separated by transition zones, in which the pH values gradually change (Fig. 1A and B). Taking into account this evidence, we could easily distinguish three main regions of the larval midgut of *H. illucens*, a fundamental aspect to isolate midgut samples for the analyses reported below (Fig. 1C).

Insect performances on different diets

The microbiota analyses were performed on larvae reared on three different feeding substrates: Standard diet, an optimal diet for fly larvae rearing (Hogsette 1992), Veg Mix diet, containing a mixture of fruits and vegetables, and Fish diet, based on fish meal (see Material and Methods for detailed composition). We thus evaluated the performances of the BSF larvae on these substrates. The maximum weight reached before pupation by BSF larvae reared on Standard diet was significantly higher compared to the other two diets (Table 1) (One Way ANOVA: $F_{(2,12)}$=15.50, *P*=0.0005, df=14). There was also a trend in the increase of larval period duration ($F_{(2,12)}$=12.00, *P*=0.0014, df=14). This was particularly evident for the larvae reared on Fish diet, that showed doubled developmental time and almost halved maximum weight compared to larvae grown on Standard diet (Table 1).

Diet	Larval period (days)	Maximum weight (mg)	Day of sample collection for microbiota analysis
Standard	18 ± 1 (5)[a]	218 ± 8 (5)[a]	16
Veg Mix	24 ± 2 (5)[a]	195 ± 5 (5)[b]	22
Fish	36 ± 3 (5)[b]	173 ± 3 (5)[c]	30

Table 1. Length of BSF larval cycle and maximum weight at pupation* for the different diets used in this study. *Data are expressed as mean ± standard error, number of experiments in parenthesis. For each experiment at least 20 larvae have been monitored for development time and weight. Different letters denote statistical differences (One-Way ANOVA).

Evaluation of relative bacterial counts in the different regions of BSF larval midgut

The bacterial loads in different midgut regions of *H. illucens* larvae (Fig.1C) were determined by qRT-PCR on RNA samples in order to narrow in the analysis on live bacteria. The results demonstrate that the profile of the relative bacterial counts in the different midgut regions was similar for the three diets. In particular, while anterior and middle midgut had comparable bacterial loads, they were higher in the posterior portion (Fig. 2) (One Way ANOVA: Standard $F_{(2,12)}$= 8.869, n=5, P=0.0043, df=14; Veg Mix $F_{(2,12)}$= 295.51, n=5, P<0.0001, df=14; Fish $F_{(2,12)}$= 33.882, n=5, P<0.0001, df=14). We observed a statistically significant interaction between the effects of diet and midgut region on bacterial load ($F_{(4,36)}$=17.601, P<0.0001) which was significantly affected from both the considered independent variables (diet: $F_{(2,36)}$=23.339, P<0.0001; midgut region: $F_{(2,36)}$=137.170, P<0.0001).

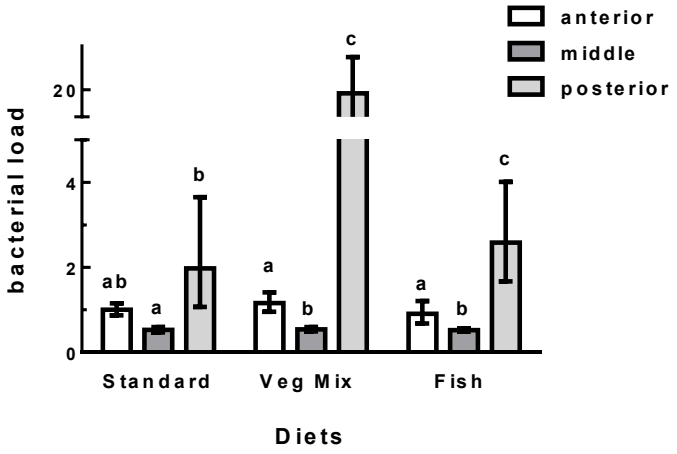

Figure 2. Relative quantification of bacterial load by qRT-PCR in the different tracts of the midgut of BSF larvae reared on different diets. The values reported are the mean ± standard error (n=5 for each sampling point containing pools of 5 midgut portions each) of the relative expression of the *16S rRNA* gene normalized to that of the *Hi RPL5* gene (see "qRT-PCR for relative bacterial load determination" in Materials and Methods). Different letters denote significant differences for each diet (One-Way ANOVA).

Microbiota composition in the different regions of BSF larval midgut and diet substrates

We analyzed the microbiota by *16S rRNA* gene sequencing starting from cDNAobtained from RNA samples in order to consider communities of live bacteria. A total of 2,175,325 high quality reads were analyzed, with an average of 29,000 reads/sample. Our study included also the analysis of the microbiota of the feeding substrates prior to BSF larvae administration (fresh diet) and after BSF larvae feeding (conditioned diet). This is particularly important because BSF larvae feed and develop inside the food substrate, which is not renewed but periodically added with fresh one. The anterior part of the midgut was always characterized by a high microbial diversity (P<0.05), that progressively decreased going from the anterior to the posterior part (Fig. 3), and this trend happened regardless of the diet.

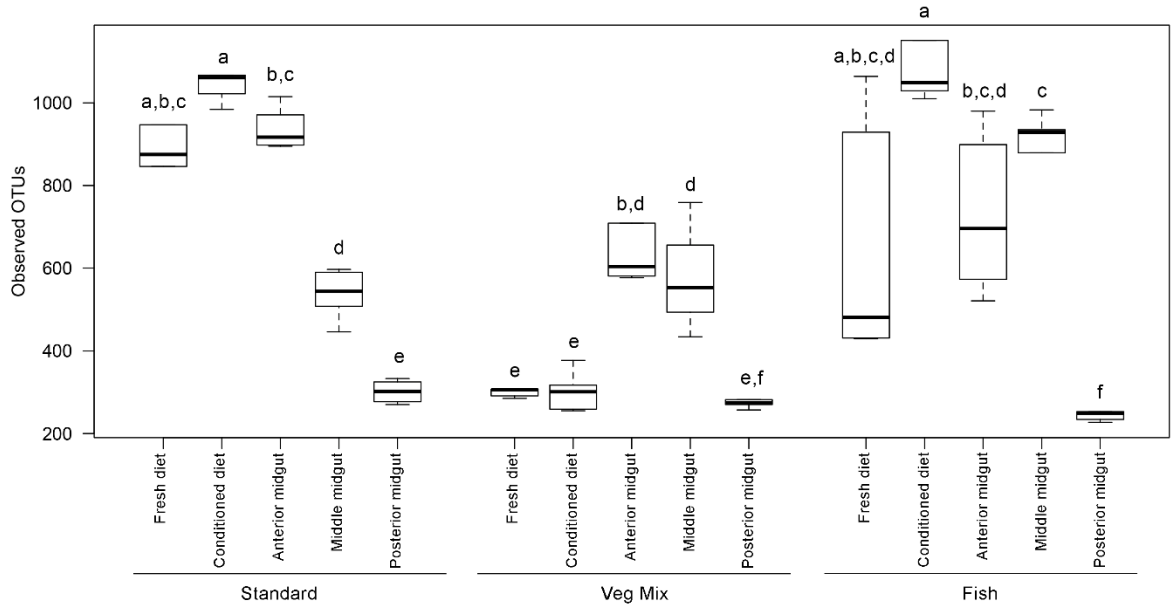

Figure 3. Microbial diversity. Box plot showing the number of Observed OTUs in the different samples, as detected by high-throughput sequencing of the *16S rRNA* gene. Boxes represent the interquartile range (IQR) between the first and third quartiles, and the line inside represents the median (second quartile). Whiskers denote the lowest and the highest values within 1.5×IQR from the first and third quartiles, respectively. Different letters indicate a significant difference (P<0.05) as obtained by pairwise Wilcoxon's tests. "Fresh diet" and "conditioned diet" refer to the analysis of the microbiota of the feeding substrates just after preparation and after larval feeding, respectively.

The microbiota of the feeding substrate showed a strong impact in shaping the midgut microbiota in larvae fed with Standard or Fish diet, at least in the first regions of the midgut (Fig. 4); by contrast, the microbiota of Veg Mix diet was not found in the midgut (Fig. 4).

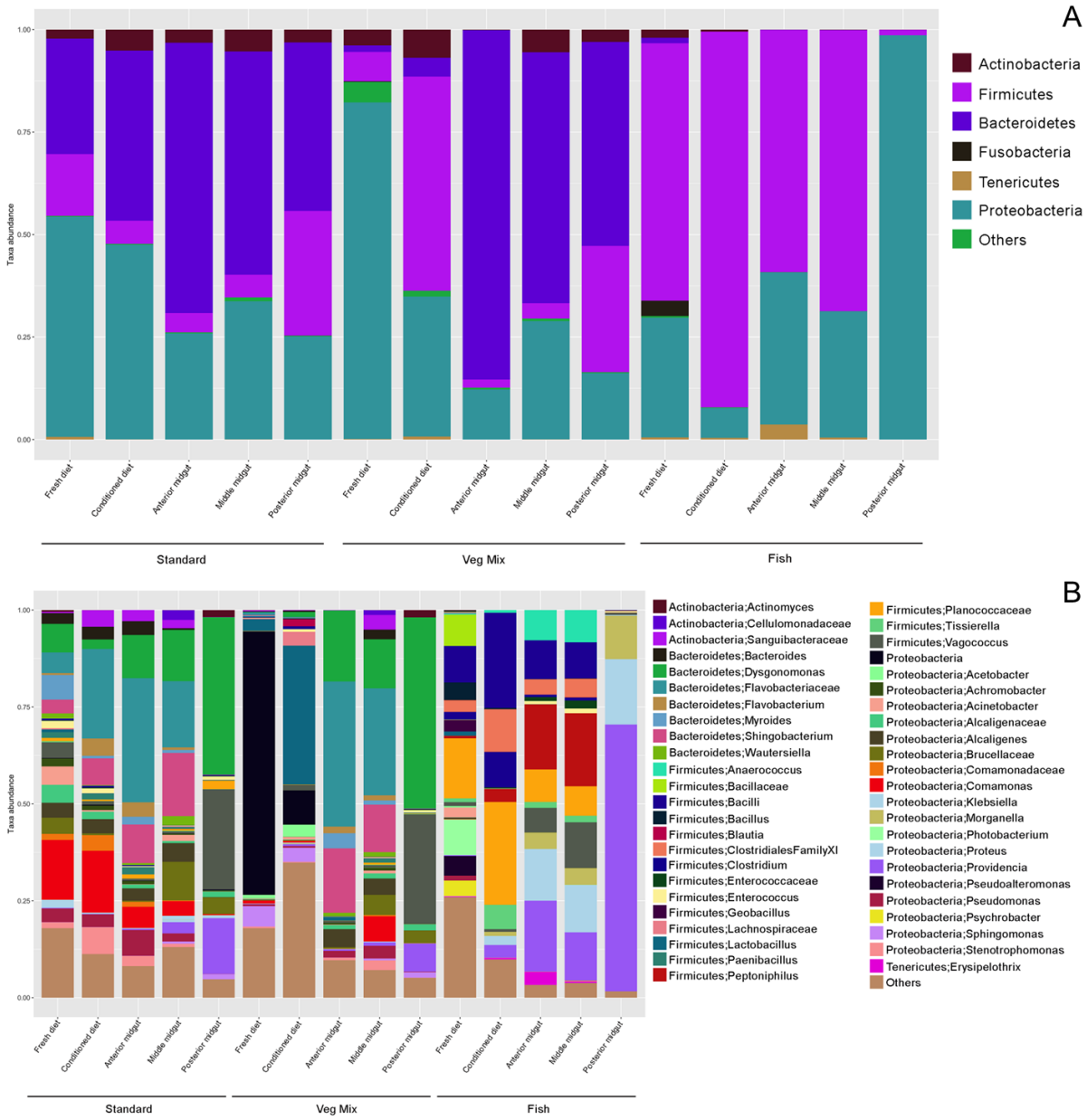

Figure 4. Incidence of the major bacterial taxonomic groups. The stacked bar chart shows the relative abundance of bacterial phyla (A) and genera (B) identified in midgut and diet samples analyzed. Values are the average of 5 replicates. Genera and phyla with abundance < 2% in at least 5 samples are summed up and showed as "others".

The posterior part always showed a significantly different microbiota when compared with middle and anterior part of the midgut, as determined by MANOVA based on Bray Curtis distance (Standard: $F_{(2,12)}= 24.945$, $P<0.001$; Veg Mix: $F_{(2,12)}= 46.287$, $P<0.001$; Fish: $F_{(2,12)}=16.968$, $P<0.001$) and the composition of the microbiota in this region reflected a strong selection of 171 the species that were present in the food substrate, an aspect of particular extent for Fish diet

(Fig. 4 and 5). The composition of the microbiota determined a clear differentiation of the samples according to both midgut portion and diet (Fig. 5)

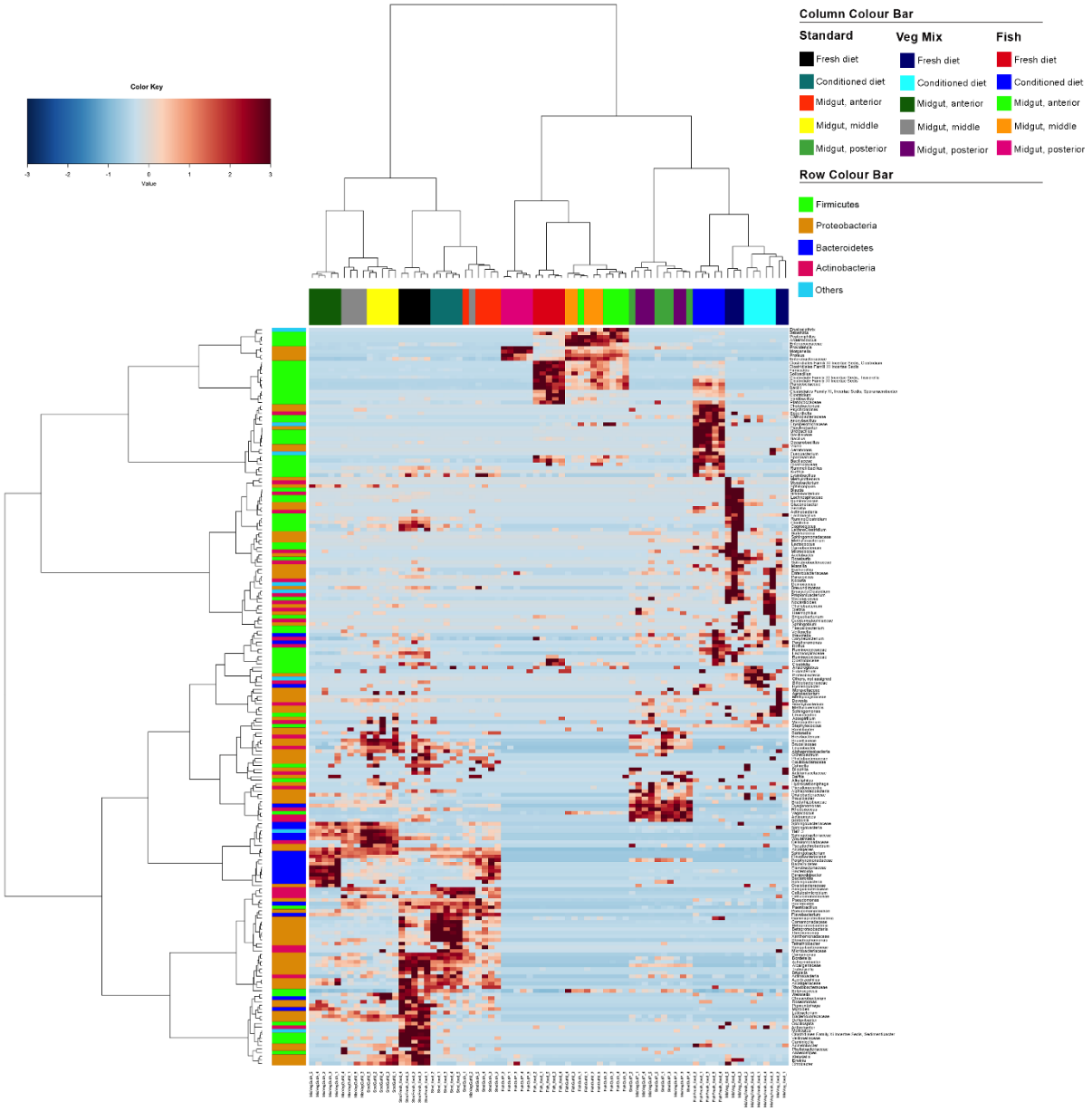

Figure 5. Heatplot based on microbiota composition at genus level. Hierarchical Ward-linkage clustering based on the Spearman's correlation coefficient of the microbial taxa abundance. Column bar is color-coded according to the type of diet and the midgut region. Row bar is colored according to the taxa assignment at phylum level. The color scale represents the scaled abundance of each variable, denoted as Z-score, with red indicating high abundance and blue indicating low abundance.

Indeed, a significant effect of both diet type and midgut region was found by MANOVA, for both the independent variables (diet: $F_{(2,36)}=57.047$, $P<0.001$; midgut region: $F_{(2,36)}=39.256$, $P<0.001$) and for the interaction between them ($F_{(4,36)}=19.540$, $P<0.001$). Fish diet microbiota seemed to have the strongest effect on the gut microbiota, leading to a higher abundance of Proteobacteria taxa in the posterior tract of the midgut, while Firmicutes prevailed in the anterior and middle tract (Fig. 4A). On the contrary, the midgut of BSF larvae fed with Standard and Veg Mix diets were

more similar and characterized by higher levels of Bacteroidetes (Fig. 4). Indeed, the midgut of larvae fed with Fish diet showed significantly higher weighted Unifrac distance from Standard and Veg Mix diets, compared to the distance of between Standard and Veg Mix, in all the three portions (Fig. S1). Although the larvae feed and develop into the diet, the data show that BSF larvae do not significantly alter microbiota composition of the substrate, except for an increase in *Lactobacillus* population in Veg Mix diet (Fig. 4B). A complete list of the taxa identified is reported in Supplementary Tables S1, S2, S3, S4.

DISCUSSION

Despite the great and exponentially increasing interest in BSF larvae for bioconversion (Cicková et al., 2015; Makkar et al., 2014; Müller et al., 2017) and bioremediation (Bulak et al., 2018), several aspects concerning the biology of this insect are still neglected. Surprisingly, there is still paucity of information on its intestinal microbiota (De Smet et al., 2018), an issue that should be instead considered a priority for an organism that can be used for such purposes. A recent review on the microbial community associated to BSF (De Smet et al., 2018) highlights knowledge gaps and provides suggestions on criticisms to unravel, rather than presenting a summary of the available data.

Firstly, none of the few studies on BSF intestinal microbiota has taken into account the correlation between the different regions of the midgut of this insect and the microbiota. In this paper we provide evidence that discrete regions can be recognized along the midgut of BSF larvae as clearly demonstrated by the differences in the luminal pH (Fig. 1). Anterior region ischaracterized by an acid luminal content, followed by a strongly acidic middle region and an alkaline posterior tract. These data are partially in accordance with previous reports on non-hematophagous brachycerous Diptera. Indeed, in the larvae of *Musca domestica* (Diptera: Muscidae) three main segments can be identified: the anterior and the posterior midgut are characterized by a slightly acidic luminal pH, while the middle midgut presents a very low pH in the lumen (Lemos and Terra, 1991) that is generated by the so called “copper cells”, a distinctive cell type present in the acidic segment of the midgut of flies (Terra et al., 1988; McNulty et al., 2001; Dubreuil 2004; Shanbhag and Tripathi 2009). The midgut of *D. melanogaster* larvae presents distinct regions as well (Dubreuil 2004; Shanbhag and Tripathi 2009) with different pH of the luminal content: the anterior segment and the anterior part of the posterior segment is between neutral to mild alkalinity, while the middle segment is highly acidic and the posterior part of the posterior segment is highly alkaline (Shanbhag and Tripathi 2009). The differences of the pH in fly midgut regions are associated to

peculiar physiological, immune and microbiological features (Broderick et al., 2014; Buchon et al., 2013; Marianes and Spradling 2013; Pimentel et al., 2018; Terra, 1990).

Here we demonstrate that in BSF larvae the presence of different midgut regions associates to differences in microbial density and composition. We have observed that each tract is characterized by a different bacterial load, which is higher in the posterior compared to the anterior midgut. Interestingly, microbial diversity has an opposite trend, since it gradually decreases along the midgut, suggesting that a selection of fewer taxa takes place. A simple explanation may be a reduced flow rate of luminal content to the posterior region due to the possible presence of sphincters or epithelium folding. In alternative or in addition, most bacteria are killed in the anterior and middle region and only a selection of the initial microbiota proliferate in the posterior midgut using the available nutrients, thus leading to higher numbers. This process of selection may result by the fine combination of extreme pH values in the middle region of the midgut and the activity of antimicrobial peptides, lysozyme and digestive enzymes produced and secreted by midgut cells into the lumen of anterior and middle midgut (Broderick 2016; Broderick et al., 2014; Lemos and Terra, 1991; Lemos et al., 1993; Vogel et al., 2018).

To understand whether and how food affects the microbial communities that colonize the digestive tract of BSF larvae, we have examined dietary substrates that strongly differ in terms of nutrient composition. In particular, the three diets were characterized by a different protein/carbohydrate ratio, a parameter that has been demonstrated to impact on the gut microbiota (Fan et al., 2014; Rothe and Blaut 2013; Zhao et al., 2018) and insect performances (Behmer 2009; Raubenheimer and Simpson 1997; Ponton et al., 2013). Indeed, we detected differences in BSF larvae development on the different diets. A major novelty introduced by our study is the characterization of the microbiota of the dietary substrates, an aspect that was previously overlooked (De Smet et al., 2018) and that could strongly affect the composition of the bacterial community of the midgut. In addition, we studied the influence of feeding activity of BSF larvae on dietary substrates. A comparative analysis of the results shows that diet composition plays a major role in shaping the diversity of the midgut microbiota. Similarly, the microbiota present in the diet influences the composition of the microbiota resident in the anterior/middle tracts of the midgut and less the one occurring in the posterior that presented a very narrow selection of the species in the food substrate. Interestingly, BSF larvae do not have detrimental effects on the microbiota of the substrates on which they feed and develop. They are not able to significantly change the bacterial community of the Standard and Fish diet substrates, and, although an increase of a specific population (i.e. *Lactobacillus*) occurs in Veg Mix substrate, these bacteria are known as non-pathogenic for their potential probiotic properties for humans (Azad et al., 2018; Gareau et al., 2010; Sri Vinusha et

al., 2018) and some species are involved in detoxification of pesticides and xenobiotics in humans and insects (Chen et al., 2018; Daisley et al., 2018; Trinder et al., 2015; 2016). This evidence is in contrast with previous claims about the capacity of BSF larvae to change the microbiota of substrates and, in particular, to reduce pathogenic bacteria of substrates (Wang and Shelomi 2017; De Smet et al., 2018), but is a valuable trait for an organism that has to be mass- reared for bioconversion and bioremediation on a variety of substrates.

The differences found in the microbiota of larvae fed on different diets could reflect their physiological performances and bioconversion efficiency, and the posterior midgut, where the resident microbiota results from a selection of microbes present in previous midgut tracts, may have a relevant contribution in nutrient conversion and thus in energy harvest and overall fitness. Standard and Veg Mix diets were associated to an overall similar microbiota composition, both leading to increased levels of Bacteroidetes in the midgut, bacteria known as glycan degraders because of the presence of polysaccharide utilization loci in their genome (Gibiino et al., 2018). Genera of *Sphingobacterium* and *Dysgonomonas* were particularly abundant, likely reflecting a remarkable potential for complex polysaccharide degradation, and worthy to be isolated and explored for biotechnological purposes. Bacteroidetes have been identified as core members of the gut microbiome in many *Drosophila* species across the globe and also in other insects, including termites and honeybees (Poff et al. 2017), and several have xylanases directly involved in hemicellulose digestion (Zhou et al., 2009; Arias-Cordero et al., 2012). On the other hand, Fish diet apparently induces a more putrefactive environment, with a microbiota severely dominated by Proteobacteria (Fig. 4A), mainly *Providencia* (Fig. 4B), which are highly transmitted vertically throughout insect life cycle (De Smet et al., 2018) but can also be pathogens of many organisms including humans and insects (Galac and Lazzaro, 2011). On the basis of the above consideration, Fish diet may induce a gut dysbiosis which may contribute to the reduced performance that we detected for BSF larvae reared on Fish diet compared to the other two feeding substrates. These data, along with a previous study performed on the same insect (Cammack and Tomberlin, 2017), suggest that unbalanced diets with a high protein/carbohydrate ratio content are not optimal for BSF larvae rearing.

Despite the great potential of *H. illucens* larvae (see Introduction for details), information on its microbiota is surprisingly very limited. Apart from a recent study on mycobiota (Varotto Boccazzi et al., 2017), only two studies have previously examined the microbiota of *H. illucens* larvae. In the first study (Jeon et al., 2011, Table 2) the microbiota of the entire gut from larvae reared on three different feeding substrates were investigated. In the second one (Zheng et al., 2013, Table 2) the microbiota analysis was performed on whole larvae. The differences in the experimental

samples analyzed make it difficult to compare the results from those studies and, for the same reason, results from previous studies and the present. Moreover, both studies completely overlooked the bacteria communities present in the feeding substrates, that we demonstrated can affect midgut microbiota composition. Nevertheless, as summarized in Table 2, a few considerations can be done. In Zheng et al. (2013), larvae were reared on a diet with a composition very similar to Standard diet used in this study and the major Phyla that characterize the microbiota quite match (both considering each midgut tract separately or the average value of the different tracts). This evidence, along with the differences associated to the microbiota of larvae reared on different substrates, suggests that diet composition had a role in shaping bacterial communities. In particular, when diets were very unbalanced (i.e. cooked rice and Fish diet) the diversity of microbial communities decreased compared to nutritionally more balanced diets. In those unbalanced diets Proteobacteria were the major group identified, whereas in all other cases Bacterioidetes were one of the dominant Phyla (Table 2). Interestingly, our data (Table 2) demonstrate that the overall gut microbiota does not mirror the microbiota composition of each tract, confirming the relevance of working with each tract separately.

Study	Sample	Feeding substrate	Major Phyla	%[c]
Jeol et al., 2011	larval gut	Food waste	Bacterioidetes	67.4
			Proteobacteria	18.9
			Firmicutes	9.4
			Fusobacteria	2.0
			Actinobacteria	1.9
		Cooked rice	Proteobacteria	54.0
			Firmicutes	47.3
			Unclassified	3.5
		Calf forage	Proteobacteria	31.1
			Actinobacteria	24.6
			Firmicutes	23.5
			Bacterioidetes	20.5
Zheng et al., 2013	whole larvae	Gainesville diet[d]	Bacterioidetes	54.4
			Firmicutes	20.0
			Proteobacteria	16.0
			Actinobacteria	9.0
Present study	larval midgut	Standard diet	Bacterioidetes	41.5 (A:65.9, M:54.4, P:41.1)
			Proteobacteria	28.2 (A:25.9, M:33.7, P:25.2)
			Firmicutes	13.6 (A:4.7, M:5.6, P:30.4)
			Actinobacteria	3.9 (A:3.2, M:5.3, P:3.1)
		Veg Mix	Bacterioidetes	65.4 (A:85.2, M:61.2, P:49.8)
			Proteobacteria	19.1 (A:12.2, M:28.9, P:16.2)
			Firmicutes	15.7 (A:2.0, M:28.9, P:16.2)
			Actinobacteria	11.6 (A:0.1, M:3.8, P:30.8)
		Fish diet	Proteobacteria	55.5 (A:37.1, M:30.8,P:98.6)
			Firmicutes	43.0 (A:59.1, M:68.6, P:1.4)

Table 2. Short summary of the data on microbiota composition of *H. illucens* larvae from present work and published studies[a] (Jeol et al., 2011; Zheng et al., 2013[b]).

[a]In all the studies the microbiota composition was obtained by *16S rRNA* gene sequencing.

[b]Estimated on the basis of the histogram presented in the paper.

[c]Only percentages >1% are reported. For the present study the % reported is the average of the % in the three different midgut portions (A: anterior, M: middle, P: posterior) that are specified in parenthesis.

[d]Gainesville diet is composed by 20% corn meal, 30% alfalfa meal, and 50% wheat bran, saturated with water.

Our study focused on the effect of midgut morphofunctional regionalization in shaping the residing microbiota. Future work on microbiota in the hindgut of *H. illucens* larvae is also needed, although the establishment of a stable bacterial community in the hindgut of insect larvae is problematic (due to the molts during the larval period that involve the removal of the cuticle lining the hindgut epithelium) and often requires the presence of special structures that provides a stable environment for bacterial colonization (Engel and Moran, 2013), structures that have never been reported for *H. illucens* larvae.

In conclusion, the presence of different midgut domains, diet composition and diet microbiota have a non-negligible effect on BSF larvae microbial ecology. These factors and their interdependence are going to play a major role for a proper exploitation of the biotechnological uses of insects.

MATERIALS AND METHODS

Insect rearing

BSF eggs were collected from a colony established in 2015 at the University of Insubria (Varese, Italy), and maintained in a humid chamber at 27°C until hatching. The eggs were laid on a Petri dish (9×1.5 cm) with the experimental diet. Three diets were used in the current study: standard diet for Diptera (Standard), a diet containing fruits and vegetables (Veg Mix), and a diet based on fish feed (Fish). Standard diet (Hogsette, 1992), was composed by wheat bran (50%), corn meal (30%) and alfalfa meal (20%) mixed in the ratio 1:1 dry matter/water (approximately 13% protein, protein/carbohydrate ratio 1:1). Veg Mix diet was composed by seven fruits and vegetables (apple, banana, pear, broccoli, zucchini, potato and carrot) in equal quantity and appropriately minced (approximately 1% protein, protein/carbohydrate ratio 1:9). Fish diet was composed by fish meal (FF type, Mazzoleni SpA, Bergamo, Italy), mixed in the ratio 1:1 dry matter/water (approximately 35% protein, no carbohydrates). Percentages are calculated on diet weight, including water. The values in parenthesis concerning protein and carbohydrate content were estimated on data available on the web for Standard and Veg Mix diet, whereas for Fish diet they were reported in the product data sheet. Nipagin (Methyl 4-hydroxybenzoate) was added to the diet administered to larvae the first 4 days after hatching to avoid mold growth (a 18% (w/v) stock solution in absolute ethanol was prepared; each gram of Veg Mix diet was added with 20 µl of this stock solution, whereas each gram of Standard and Fish diet was added with 1 ml of a 1.7% (v/v) dilution in water of the stock solution). Four days after hatching, 300 larvae were placed in a plastic container (16×16×9 cm), and fed *ad libitum* with the three experimental diets described above without nipagin. The larvae were maintained at 27.0 ± 0.5 °C, 70 ± 5% RU, in the dark. Fresh diet was added every two days, until larvae reached the last larval instar. Five independent rearing

groups were set up for each diet. Random samples of 30 individuals were weighed every two days. For each experimental diet, the sampling and the annotation of the larval weight were made in triplicate. Before weighing, the larvae were washed in tap water to remove diet matter from their body and then wipe dried. The weights were recorded until 25% of insects reached the pupal stage. Last instar, actively feeding larvae were used for the measurement of midgut lumen pH and microbiota analyses

Determination of pH in the midgut lumen with colorimetric indicators

The presence of different pH in the midgut lumen of *H. illucens* larvae was assessed using phenol red and bromophenol blue, two pH indicators that assume different coloration at different pH values. Bromophenol blue is yellow at pH values lower than or equal to 3.0, blue at pH higher than or equal to 4.6; phenol red is yellow at pH lower than or equal to 6.8, fuchsia at pH higher than or equal to 8.2, with a gradual color transition for intermediate values. *H. illucens* larvae were fed *ad libitum* with Standard diet until they reached the last instar as described above. Larvae with a weight ranging between 180 and 200 mg were selected and transferred to plastic containers on Standard diet added with 0.2% (w/w) bromophenol blue or phenol red. After 24 h the larvae were removed from the diet, placed in a plastic tube, and anesthetized on ice with CO_2. The guts were isolated and the coloration of the midgut content was evaluated by means of a stereomicroscope.

Collection of midgut and diet samples and RNA extraction

Last instar larvae were washed with 70% ethanol in autoclaved distilled water and then dissected with the help of a stereomicroscope, under a horizontal-flow hood, by using sterile tweezers and scissors, to avoid cross-contaminations of the samples. Each midgut was isolated in autoclaved 1× PBS (Phosphate Buffered Saline: 137 mM NaCl, 2.7 mM KCl, 4.3 mM Na_2HPO_4, 1.4 mM KH_2PO_4, pH 7.4) in a sterile Petri dish (5.5×1.3 cm). Once collected, the midgut was divided into three districts: anterior, middle, and posterior region (see Results and Fig.1). For the dissection of each larva a new Petri dish was used, and tweezers and scissors were washed with 70% ethanol in water. For each diet, pools of five midgut regions samples for each of the five replicates of insect rearing were collected in a cryovial, immediately put into TRIzol reagent (Life Technologies, Carlsbad, CA, USA), and kept at -80°C until total RNA extraction that was performed according to the manufacturer's instructions. Briefly, after homogenization with eppendorf-fitting pestles to lyse samples in TRIzol reagent, total RNA was precipitated with isopropanol, washed with ethanol, and suspended in RNase-free water. Samples of fresh (before administration to larvae) and conditioned diets (on which larvae have fed) were also immediately put into TRIzol reagent and kept at -80°C until total RNA extraction. Ten samples of both fresh and conditioned diets were collected for each of the 5 experimental replicates on the 3 different feeding substrates. RNA

concentration was assessed by measuring the absorbance at 280 nm, with a Varioskan™ Flash Multimode Reader (Thermo Scientific, Waltham, MA, USA), and sample purity was evaluated by assessing 260/280 nm absorbance ratio. Total RNA preparations were then treated with TURBO DNase I (Life Technologies), according to the manufacturer's instructions and RNA quality was checked by electrophoresis on 1% agarose gel.

qRT-PCR for relative bacterial load determination

Total RNA was isolated as described above. The relative bacterial load in the three midgut regions (n=5 for each sampling point containing pools of 5 midgut portions each), was quantified by normalization of the relative expression of the *16S rRNA* gene (accession number SRP064613; *16S rRNA* forward primer: ACTCCTACGGGAGGCAGC, *16S rRNA* reverse primer: ATTACCGCGGCTGCTGGC) to that of the ribosomal protein L5 gene of *H. illucens* (*Hi RPL5*). The primers used for *Hi RPL5* (*Hi RPL5* forward primer: AGTCAGTCTTTCCCTCACGA, *Hi RPL5* reverse primer: GCGTCAACTCGGATGCTA) were designed on conserved regions of *RPL5* in other insect species and their sequence checked by sequencing the PCR product. Changes in relative bacterial loads were measured by one-step qRT-PCR (Caccia et al., 2016; Renoz et al., 2015; Rodgers et al., 2017), using the SYBR Green PCR Kit (Applied Biosystems, Carlsbad, CA, USA), according to the manufacturer's instructions, using the primers reported above. Relative gene expression data were analyzed using the $2^{\Delta\Delta CT}$ method (Livak and Schmittgen 2001; Pfaffl 2001; Pfaffl et al., 2002). Expression data were normalized taking into account the differences in the area of the cross-section of the different intestinal tracts (81,000 ± 7,300 μm^2, 250,000 ± 17,200 μm^2 and 46,000 ± 1,700 μm^2 for the anterior, middle and posterior midgut, respectively, n=10 for each tract) by dividing the Ct values (for both *16S rRNA* and *Hi RPL5* transcripts) by the area of the cross-section of the corresponding midgut tract. The areas were calculated using the diameter of the lumen of each midgut tract obtained by direct measurement on the micrographs of different cross-sections acquired from semithin cross- sections of BSF larval midguts stained with crystal violet and basic fuchsin, prepared for light microscopy analysis (Franzetti et al., 2015). For validation of the ΔΔCt method the difference between the Ct value of *16S rRNA* and the Ct value of *Hi RPL5* transcripts [ΔCt = Ct(*16S rRNA*)-Ct (*Hi RPL5*)] was plotted versus the log of two-fold serial dilutions (200, 100, 50, 25 and 12.5 ng) of the purified RNA samples. The plot of log total RNA input versus ΔCt displayed a slope lower than 0.1 ($Y=1.3895 - 0.0137X$, $R^2=0.0566$), indicating that the efficiencies of the two amplicons were approximately equal

Analysis of the microbiota and bioinformatics of the *16S rRNA* gene sequencing data

After extraction, 400 ng of RNA were reverse-transcribed into cDNA with random primers using RETROscript (Life Technologies), according to the manufacturer's instructions. The midgut

microbiota was assessed by sequencing of the amplified V3-V4 region of the *16S rRNA* gene as recently described (Berni Canani et al., 2017). Demultiplexed, forward and reverse reads were joined by using FLASH (Magoc and Salzberg, 2011). Joined reads were quality trimmed (Phred score < 20) and short reads (< 250 bp) were discarded by using Prinseq (Schmieder and Edwards, 2011). High quality reads were then imported in QIIME1 (Caporaso et al., 2010). Operational Taxonomic Units (OTUs) were picked through *de novo* approach and uclust method and taxonomic assignment was obtained by using the RDP classifier and the Greengenes database (Mc Donald et al., 2012), following a pipeline previously reported (Berni Canani et al., 2017). To avoid biases due to different sequencing depth, OTU tables were rarefied to the lowest number of sequences per sample. Statistical analyses and visualization were carried out in R environment (https://www.r-project.org). Alpha-diversity analysis was carried out in QIIME on rarefied OTU tables. Kruskal-Wallis and pairwise Wilcoxon tests were used to determine significant differences in alpha diversity parameters, weighted Unifrac distance or in OTU abundance. Permutational Multivariate Analysis of Variance (non-parametric MANOVA) based on Bray Curtis distance matrix was carried out to detect significant differences in the overall microbial community composition among the different parts of the midgut or as affected by the type of diet, by using the *adonis* function in R *vegan* package.

The *16S rRNA* gene sequences produced in this study are available at the Sequence Read Archive (SRA) of the National Centre for Biotechnology Information (NCBI), under accession number SRP064613.

Statistical analysis

Data were analyzed using Prism (GraphPad Software Inc. version 6.0b, San Diego, CA, USA) software using One-Way ANOVA with Tukey's multiple comparison test to compare bacterial load and parameters of larval performances within any single diet treatment. Two-Way ANOVA analysis followed by Bonferroni's post-hoc tests, when significant effects were observed (*P* value<0.05), was carried out on bacterial load as affected by different diet treatment and different midgut trait. When necessary transformation of data was carried out, to meet assumptions of normality. Levene's test was carried out to test the homogeneity of variance

ACKNOWLEDGMENTS

This work was supported by Fondazione Cariplo (Insect bioconversion: from vegetable waste to protein production for fish feed, ID 2014-0550).

S.C., M.C., D.E. and G.T. designed the research; M.B., D.B., F.D.F. and I.D.L. performed the experiments; F.D.F. and I.D.L. analyzed data and contributed figures and tables; S.C., M.C., D.E. and G.T. wrote the article.

REFERENCES

Arias-Cordero E, Ping L, Reichwald K, Delb H, Platzer M, Boland W (2012) Comparative evaluation of the gut microbiota associated with the below- and above-ground life stages (Larvae and Beetles) of the Forest Cockchafer, *Melolontha hippocastani.* PLoS ONE. 7: e51557. doi:10.1371/journal.pone.0051557.

Azad AK, Sarker M, Li T, Yin J (2018) Probiotic species in the modulation of gut microbiota: an overview. BioMed Res Int. 2018: ID 9478630.

Behmer ST (2009) Insect herbivore nutrient regulation. Annu Rev Entomol. 54: 165-87.

Berni Canani R, De Filippis F, Nocerino R, Laiola M, Paparo L, Calignano A, De Caro C, Coretti L, Chiariotti L, Gilbert JA, Ercolini D (2017) Specific signatures of the gut microbiota and increased levels of butyrate in children treated with fermented cow's milk containing heat-killed *Lactobacillus paracasei* CBA L74. Appl Environ Microbiol. 83: e01206-17.

Broderick NA (2016) Friend, foe or food? Recognition and the role of antimicrobial peptides in gut immunity and *Drosophila*-microbe interactions. Phil Trans R Soc B. 371: 20150295. doi:10.1098/rstb.2015.0295

Broderick NA, Buchon N, Lemaitre B (2014) Microbiota-induced changes in *Drosophila melanogaster* host gene expression and gut morphology. mBio. 5: e01117-14. doi:10.1128/mBio.01117-14

Buchon N, Osman D, David FPA, Fang HY, Boquete JP, Deplancke B, Lemaitre B (2013) Morphological and molecular characterization of adult midgut compartmentalization in *Drosophila*. Cell Rep. 3: 1725-1738.

Buchon N, Osman D (2015) All for one and one for all: regionalization of the *Drosophila* intestine. Insect Biochem Mol Biol. 67: 2-8. doi: 10.1016/j.ibmb.2015.05.015.

Bulak P, Polakowski C, Nowak K, Waśko A, Wiącek D, Bieganowski A (2018) *Hermetia illucens* as a new and promising species for use in entomoremediation. Sci Total Environ. 633: 912-919.

Caccia S., Di Lelio I, La Storia A, Marinelli A, Varricchio P, Franzetti E, Banyuls N, Tettamanti G, Casartelli M, Giordana B, Ferrè J, Gigliotti S, Ercolini D, Pennacchio F (2016) Midgut microbiota and host immunocompetence underlie *Bacillus thuringiensis* killing mechanism. PNAS USA. 113: 9486-9491.

Cammack JA, Tomberlin JK (2017). The impact of diet protein and carbohydrate on select life-history traits of the black soldier fly *Hermetia illucens* (L.) (Diptera: Stratiomyidae). Insects 8: 56. doi.org/10.3390/insects8020056.

Capo F, Charroux B, Royet J (2016) Bacteria sensing mechanisms in Drosophila gut: Local and systemic consequences. Dev Comp Immunol. 64: 11-21. doi: 10.1016/j.dci.2016.01.001.

Caporaso JG, Kuczynski J, Stombaugh J, Bittinger K, Bushman FD, Costello EK, Fierer N, Peña AG, Goodrich JK, Gordon JI, Huttley GA, Kelley ST, Knights D, Koenig JE, Ley RE, Lozupone CA, McDonald D, Muegge BD, Pirrung M, Reeder J, Sevinsky JR, Turnbaugh PJ, Walters WA, Widmann J, Yatsunenko T, Zaneveld J, Knight R (2010) QIIME allows analysis of high-throughput community sequencing data. Nat Methods. 7: 335-336.

Chen SW, Hsu JT, Chou YA, Wang HT (2018) The application of digestive tract lactic acid bacteria with high esterase activity for zearalenone detoxification. J Sci Food Agric. 98: 3870-3879. doi: 10.1002/jsfa.8904.

Čičková H, Newton GL, Lacy RC, Kozánek M (2015) The use of fly larvae for organic waste treatment. Waste Manag. 35: 68-80.

Daisley BA, Trinder M, McDowell TW, Collins SL, Sumarah MW, Reid G (2018) Microbiota-mediated modulation of organophosphate insecticide toxicity by species-dependent interactions with *Lactobacilli* in a *Drosophila melanogaster* insect model. Appl Environ Microbiol. 84: e02820-17. doi: 10.1128/AEM.02820-17.

De Smet J, Wynants E, Cos P, Van Campenhout L (2018) Microbial community dynamics during rearing of black soldier fly larvae (*Hermetia illucens*) and impact on exploitation potential. Appl Environ Microbiol. 84:e02722-17. doi.org/10.1128/AEM.02722-17.

Dubreuil RR (2004) Copper cells and stomach acid secretion in the *Drosophila* midgut. Int J Biochem Cell Biol. 36: 745-752.

Engel P, Moran NA (2013) The gut microbiota of insects - diversity in structure and function. FEMS Microbiol Rev. 37: 699-735.

Erickson MC, Islam M, Sheppard C, Liao J, Doyle MP (2004) Reduction of *Escherichia coli* O157:H7 and *Salmonella enterica* serovar *Enteritidis* in chicken manure by larvae of the black soldier fly. J Food Prot. 67: 685-690.

Fan W, Tang Y, Qu Y, Cao F, Huo G (2014) Infant formula supplemented with low protein and high carbohydrate alters the intestinal microbiota in neonatal SD rats. BMC Microbiol. 14: 279. doi: 10.1186/s12866-014-0279-2.

Franzetti E, Romanelli D, Caccia S, Cappellozza S, Congiu T, Rajagopalan M, Grimaldi A, de Eguileor M, Casartelli M, Tettamanti G (2015) The midgut of the silkmoth *Bombyx mori* is able to recycle molecules derived from degeneration of the larval midgut epithelium. Cell Tissue Res. 361: 509-528.

Galac MR, Lazzaro BP (2011) Comparative pathology of bacteria in the genus *Providencia* to a natural host, *Drosophila melanogaster*. Microbes Infect. 13: 673-683.

Gareau MG, Sherman PM, Walker WA (2010) Probiotics and the gut microbiota in intestinal health and disease. Nat Rev Gastroenterol Hepatol. 7: 503-514.

Gibiino G, Lopetuso LR, Scaldaferri F, Rizzatti G, Binda C, Gasbarrini A (2018) Exploring Bacteroidetes: Metabolic key points and immunological tricks of our gut commensals. Dig Liver Dis. 50: 635-639. doi: 10.1016/j.dld.2018.03.016.

Harnden LM, Tomberlin JK (2016) Effects of temperature and diet on black soldier fly, *Hermetia illucens* (L.) (Diptera: Stratiomyidae), development. Forensic Sci Int. 266: 109-116. doi: 10.1016/j.forsciint.2016.05.007.

Hogsette JA (1992) New diets for production of house-flies and stable flies (Diptera, Muscidae) in the laboratory. J Econ Entomol. 85: 2291-2294.

Jeon H, Park S, Choi J, Jeong G, Lee S-B, Choi Y, Lee S-J (2011) The intestinal bacterial community in the food waste-reducing larvae of *Hermetia illucens*. Curr Microbiol. 62: 1390-1399. doi.org/10.1007/s00284-011-9874-8.

Jucker C, Erba D, Leonardi MG, Lupi D, Savoldelli S (2017) Assessment of Vegetable and Fruit Substrates as Potential Rearing Media for *Hermetia illucens* (Diptera: Stratiomyidae) Larvae. Environ Entomol. 46: 1415-1423. doi: 10.1093/ee/nvx154.

Lalander C, Diener S, Magri ME, Zurbrügg C, Lindström A, Vinnerås B (2013) Faecal sludge management with the larvae of the black soldier fly (*Hermetia illucens*)-from a hygiene aspect. Sci Total Environ. 458-460: 312-318.

Lalander C, Fidjeland J, Diener S, Eriksson S, Vinnerås B (2015) High waste-to-biomass conversion and efficient Salmonella spp. reduction using black soldier fly for waste recycling. Agron Sustain Dev. 35: 261-271. doi:10.1007/s13593-014-0235-4

Lehane M, Billingsley P (1996) Biology of the insect midgut. Lehane and Billingsley Eds.

Lemos FJA, Terra WR (1991) Digestion of bacteria and the role of midgut lysozyme in some insect larvae. Comp Biochem physiol. 100B: 265-268.

Lemos FJA, Ribeiro AF, Terra WR (1993) A bacteria-digesting midgut-lysozyme from *Musca domestica* (diptera) larvae. Purification, properties and secretory mechanism. Insect Biochem Mol Biol. 23: 533-541.

Livak KJ, Schmittgen TD (2001) Analysis of relative gene expression data using real-time quantitative PCR and the $2^{-\Delta\Delta CT}$ method. Methods. 25: 402-408.

Liu Q, Tomberlin JK, Brady JA, Sanford MR, Yu Z (2008) Black soldier fly (Diptera: Stratiomyidae) larvae reduce *Escherichia coli* in dairy manure. Environ Entomol. 37: 1525-1530.

Lord WD, Goff ML, Adkins TR, Haskell NH (1994) The black soldier fly *Hermetia illucens* (Diptera: Stratiomyidae) as a potential measure of human postmortem interval: observations and case histories. J Forensic Sci. 39: 215-22.

Ma J, Lei Y, Rehman KU, Yu Z, Zhang J, Li W, Li Q, Tomberlin JK, Zheng L (2018) Dynamic Effects of Initial pH of Substrate on Biological Growth and Metamorphosis of Black Soldier Fly (Diptera: Stratiomyidae). Environ Entomol. 47: 159-165. doi: 10.1093/ee/nvx186.

Magoc T, Salzberg SL (2011) FLASH: Fast length adjustment of short reads to improve genome assemblies. Bioinformatics. 27: 2957-2963.

Makkar HPS, Tran G, Heuzé V, Ankers P (2014) State-of-the-art on use of insects as animal feed. Anim Feed Sci Technol. 197:1-33. doi.org/10.1016/j.anifeedsci.2014.07.008.

Marianes A, Spradling AC (2013) Physiological and stem cell compartmentalization within the *Drosophila* midgut. eLife. 2:e00886. DOI: 10.7554/eLife.00886.

McDonald D, Price MN, Goodrich J, Nawrocki EP, DeSantis TZ, Probst A, Andersen GL, Knight R, Hugenholtz P (2012) An improved Greengenes taxonomy with explicit ranks for ecological and evolutionary analyses of bacteria and archea. ISME J. 6: 610-618.

McNulty M, Puljung M, Jefford G, Dubreuil RR (2001) Evidence that a copper-metallothionein complex is responsible for fluorescence in acid-secreting cells of the *Drosophila* stomach. Cell Tissue Res. 304: 383-389. doi:10.1007/s004410100371

Müller A, Wolf D, Gutzeit HO (2017) The black soldier fly, *Hermetia illucens* - a promising source for sustainable production of proteins, lipids and bioactive substances. Z Naturforsch. 72(9-10)c: 351-363. doi:10.1515/znc-2017-0030

Pfaffl MW (2001) A new mathematical model for relative quantification in real-time RT-PCR. Nucleic Acids Res. 29: 2002-2007.

Pfaffl MW, Horgan GW, Dempfle L (2002) Relative expression software tool (REST(C)) for group-wise comparison and statistical analysis of relative expression results in real-time PCR. Nucleic Acids Res. 30:e36.

Pimentel AC, Barroso IG, Ferreira JMJ, Dias RO, Ferreira C, Terra WR (2018) Molecular machinery of starch digestion and glucose absorption along the midgut of *Musca domestica*. J Insect Physiol. 109: 11-20.

Poff KE, Stever H, Reil JB, Seabourn P, Ching AJ, Aoki S, Logan M, Michalski JR, Santamaria J, Adams JW, Eiben JA, Yew JY, Ewing CP, Magnacca KN, Bennett GM (2017) The native Hawaiian insect microbiome initiative: a critical perspective for Hawaiian insect evolution. Insects. 8: 130.

Ponton F, Wilson K, Holmes AJ, Cotter SC, Raubenheimer D, Simpson SJ (2013) Integrating nutrition and immunology: a new frontier. J Insect Physiol. 59: 130-137.

Raubenheimer D, Simpson SJ (1997) Integrative models of nutrient balancing: application to insects and vertebrates. Nutr Res Rev. 10: 151-179.

Rehman KU, Cai M, Xiao X, Zheng L, Wang H, Soomro AA, Zhou Y, Li W, Yu Z, Zhang J (2017) Cellulose decomposition and larval biomass production from the co-digestion of dairy manure and chicken manure by mini-livestock (*Hermetia illucens* L.). J Environ Manage. 196: 458-465.

Renoz F, Noël C, Errachid A, Foray V, Hance T (2015) Infection dynamic of symbiotic bacteria in the pea aphid *Acyrthosiphon pisum* gut and host immune response at the early steps in the infection process. PLoS ONE. 10: e0122099. doi:10.1371/journal.pone.0122099

Rodgers FH, Gendrin M, Wyer CAS, Christophides GK (2017) Microbiota-induced peritrophic matrix regulates midgut homeostasis and prevents systemic infection of malaria vector mosquitoes. PLoS Pathog. 13(5): e1006391.

Rothe M, Blaut M (2013) Evolution of the gut microbiota and the influence of diet. Benef Microbes. 4: 31-37. doi: 10.3920/BM2012.0029

Schmieder R, Edwards R (2011) Quality control and preprocessing of metagenomic datasets. Bioinformatics. 27: 863-864.

Shanbhag S, Tripathi S (2009) Epithelial ultrastructure and cellular mechanisms of acid and base transport in the *Drosophila* midgut. J Exp Biol. 212: 1731-1744.

Sri Vinusha K, Deepika K, Sudhakar Johnson T, Agrawal GK, Rakwal R (2018) Proteomic studies on lactic acid bacteria: a review. Biochem Biophys Rep. 14: 140-148.

Terra W (1990) Evolution of digestive systems in insects. Annual Rev Entomol. 35: 181-200.

Terra WR, Espinoza-Fuentesa FP, Ribeiro F, Ferreira C (1998) The larval midgut of the housefly (*Musca domestica*): ultrastructure, fluid fluxes and ion secretion in relation to the organization of digestion. J Insect Physiol. 34: 463-472.

Trinder M, Bisanz JE, Burton JP, Reid G (2015) Probiotic *lactobacilli*: a potential prophylactic treatment for reducing pesticide absorption in humans and wildlife. Benef Microbes. 6: 841-847. doi: 10.3920/BM2015.0022.

Trinder M, McDowell TW, Daisley BA, Ali SN, Leong HS, Sumarah MW, Reid G (2016) Probiotic *Lactobacillus rhamnosus* reduces organophosphate pesticide absorption and toxicity to *Drosophila melanogaster*. Appl Environ Microbiol. 82:6204-6213.

Turchetto M, Lafisca S, Costantini G (2001) Postmortem interval (PMI) determined by study sarcophagous biocenoses: three cases from the province of Venice (Italy). Forensic Sci Int. 120: 28-31.

Varotto Boccazzi I, Ottoboni M, Martin E, Comandatore F, Vallone L, Spranghers T, Eeckhout M, Mereghetti V, Pinotti L, Epis S (2017) A survey of the mycobiota associated with larvae of the black soldier fly (*Hermetia illucens*) reared for feed production. PLoS ONE 12(8):e0182533. https://doi.org/10.1371/journal.pone.0182533

Vogel H, Müller A, Heckel DG, Gutzeit H, Vilcinskas A (2018) Nutritional immunology: diversification and diet-dependent expression of antimicrobial peptides in the black soldier fly *Hermetia illucens*. Dev Comp Immunol. 78: 141-148.

Wang YS, Shelomi M (2017) Review of Black Soldier Fly (*Hermetia illucens*) as animal feed and human food. Foods. 6: 91. doi:10.3390/foods6100091.

Zdybicka-Barabas A, Bulak P, Polakowski C, Bieganowski A, Waśko A, Cytryńska M (2017) Immune response in the larvae of the black soldier fly *Hermetia illucens*. ISJ 14: 9-17.

Zhao J, Zhang X, Liu H, Brown MA, Qiao S (2018) Dietary protein and gut microbiome composition and function. Curr Protein Pept Sci. doi:10.2174/1389203719666180514145437.

Zheng L, Crippen TL, Singh B, Tarone AM, Dowd S, Yu Z, Wood TK, Tomberlin JK (2013) A survey of bacterial diversity from successive life stages of black soldier fly (Diptera: Stratiomyidae) by using 16S rDNA pyrosequencing. J Med Entomol. 50: 647- 658. doi.org/10.1603/ME12199.

Zhou J, Huang H, Meng K, Shi P, Wang Y, Luo H, Yang P, Bai Y, Zhou Z, Yao B (2009) Molecular and biochemical characterization of a novel xylanase from the symbiotic *Sphingobacterium* sp TN19. Appl Microbiol Biotechnol. 85: 323-333.

SUPPLEMENTARY MATERIAL

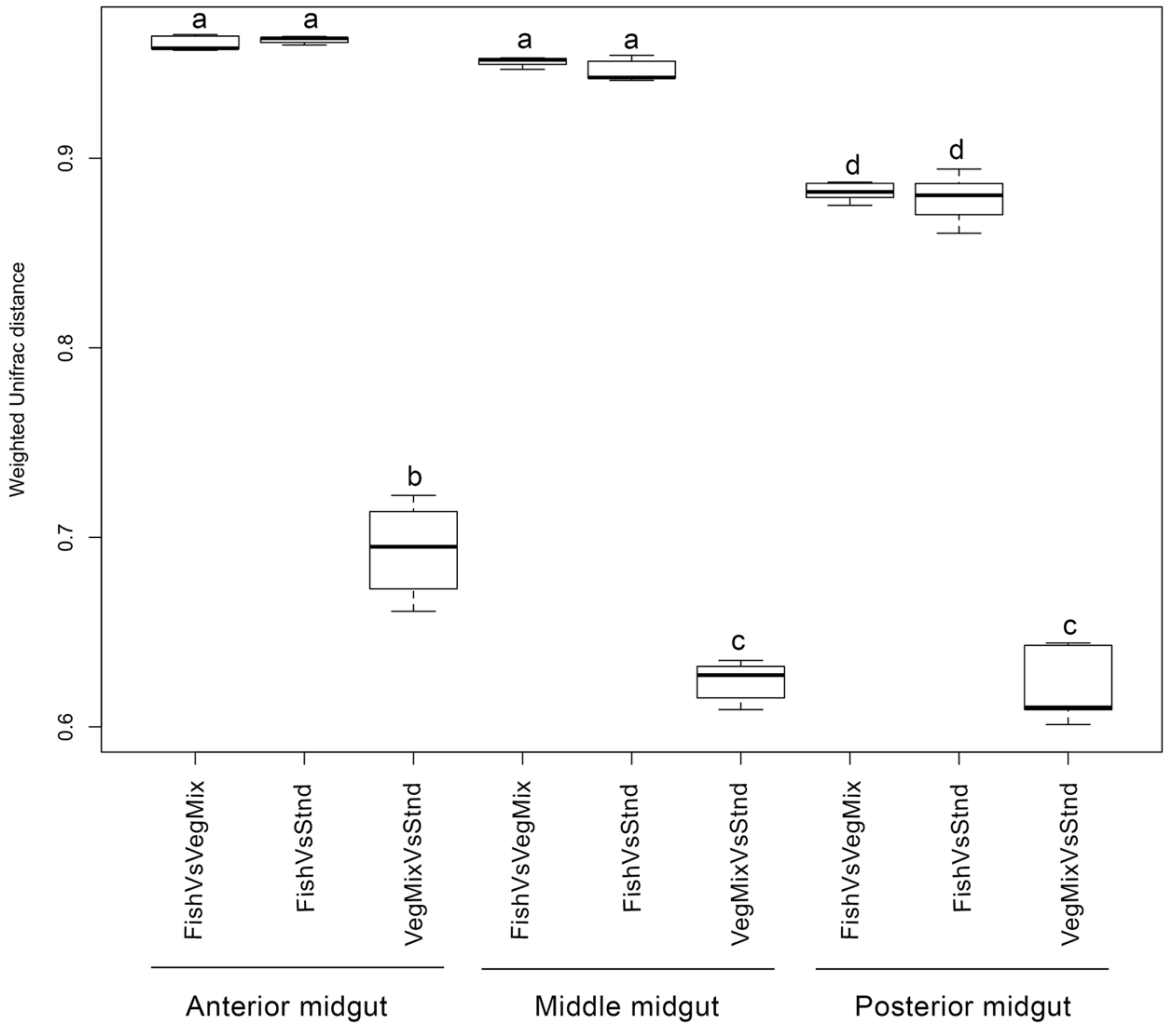

Figure S1. Boxplots showing Weighted Unifrac distance between anterior, middle and posterior midgut samples of BSF larvae fed with different diets. Each point represents the average distance between one sample and all the samples from the other group.

Taxa	Fish_FreshDiet	Fish_ConditionedDiet	Fish_AnteriorMidgut	Fish_MiddleMidgut	Fish_PosteriorMidgut	VegMix_FreshDiet	VegMix_ConditionedDiet	VegMix_AnteriorMidgut	VegMix_MiddleMidgut	VegMix_PosteriorMidgut	Standard_FreshDiet	Standard_ConditionedDiet	Standard_AnteriorMidgut	Standard_MiddleMidgut	Standard_PosteriorMidgut
Others	0.00046	0.00154	0.00096	0.00058	0.00000	0.04321	0.00496	0.00079	0.00017	0.00017	0.00154	0.00242	0.00104	0.00038	0.00104
Acidobacteria	0.01996	0.00492	0.00067	0.00096	0.00033	0.03908	0.06946	0.00121	0.05521	0.03029	0.02196	0.05137	0.03208	0.05375	0.03158
Armatimonadetes	0.00004	0.00000	0.00000	0.00000	0.00000	0.00004	0.00000	0.00000	0.00000	0.00000	0.00000	0.00000	0.00000	0.00000	0.00000
Bacteroidetes	0.01804	0.00017	0.00017	0.00037	0.00012	0.01904	0.06283	1.03908	0.76463	0.99162	0.38467	0.47283	0.80883	0.68217	0.81850
Chlamydiae	0.00042	0.00000	0.00000	0.00000	0.00000	0.00000	0.00033	0.00000	0.00000	0.00067	0.00000	0.00000	0.00000	0.00004	0.00000
Chloroflexi	0.00025	0.00000	0.00000	0.00000	0.00000	0.00025	0.00029	0.00000	0.00000	0.00021	0.00000	0.00000	0.00000	0.00004	0.00000
Firmicutes	0.62821	0.91650	0.59104	0.68554	0.01350	0.07171	0.52200	0.01975	0.03754	0.30817	0.15079	0.05646	0.04742	0.05558	0.30417
Fusobacteria	0.03746	0.00000	0.00000	0.00000	0.00000	0.00150	0.00004	0.00000	0.00008	0.00004	0.00000	0.00000	0.00000	0.00000	0.00025
Gemmatimonadetes	0.00004	0.00000	0.00000	0.00000	0.00000	0.00021	0.00033	0.00000	0.00000	0.00021	0.00000	0.00004	0.00000	0.00000	0.00000
Nitrospirae	0.00004	0.00000	0.00000	0.00000	0.00000	0.00000	0.00000	0.00000	0.00000	0.00000	0.00000	0.00000	0.00000	0.00000	0.00000
Planctomycetes	0.00042	0.00000	0.00004	0.00008	0.00004	0.00004	0.00279	0.00000	0.00000	0.00017	0.00004	0.00000	0.00000	0.00004	0.00000
Proteobacteria	0.29208	0.07271	0.37062	0.30758	0.98604	0.82096	0.34133	0.12117	0.28862	0.16150	0.53596	0.47204	0.25608	0.33662	0.25154
Spirochaetes	0.00012	0.00000	0.00000	0.00000	0.00000	0.00004	0.00008	0.00000	0.00000	0.00025	0.00000	0.00000	0.00004	0.00000	0.00000
Synergistetes	0.00033	0.00000	0.00004	0.00000	0.00000	0.00004	0.00000	0.00004	0.00000	0.00008	0.00008	0.00000	0.00000	0.00000	0.00004
TM6	0.00000	0.00000	0.00000	0.00000	0.00000	0.00000	0.00067	0.00000	0.00000	0.00000	0.00000	0.00000	0.00000	0.00000	0.00000
TM7	0.00000	0.00000	0.00000	0.00000	0.00000	0.00000	0.00000	0.00383	0.00563	0.00025	0.00012	0.00000	0.00121	0.00838	0.00021
Tenericutes	0.00513	0.00417	0.03654	0.00500	0.00000	0.00125	0.00737	0.00004	0.00025	0.00017	0.00646	0.00038	0.00000	0.00050	0.00004
Thermi	0.00079	0.00000	0.00000	0.00000	0.00000	0.00567	0.00354	0.00000	0.00004	0.00033	0.00000	0.00000	0.00000	0.00008	0.00021
Thermotogae	0.00088	0.00000	0.00000	0.00000	0.00000	0.00000	0.00000	0.00000	0.00000	0.00000	0.00000	0.00000	0.00000	0.00000	0.00000
Verrucomicrobia	0.00000	0.00004	0.00000	0.00000	0.00000	0.00025	0.00071	0.00000	0.00000	0.00004	0.00000	0.00000	0.00000	0.00000	0.00004
WPS-2	0.00000	0.00000	0.00000	0.00000	0.00000	0.00013	0.00013	0.00000	0.00000	0.00000	0.00004	0.00000	0.00000	0.00004	0.00008

Table S1. Microbiota composition in the samples of diet and midgut analysed. Phylum-level taxonomy was reported when available. The average value of 5 replicates is reported.

	Fish					VegMix					Standard				
Taxa	Fish_FreshDiet	Fish_ConditionedDiet	Fish_AnteriorMidgut	Fish_MiddleMidgut	Fish_PosteriorMidgut	VegMix_FreshDiet	VegMix_ConditionedDiet	VegMix_AnteriorMidgut	VegMix_MiddleMidgut	VegMix_PosteriorMidgut	Standard_FreshDiet	Standard_ConditionedDiet	Standard_AnteriorMidgut	Standard_MiddleMidgut	Standard_PosteriorMidgut
Others	0.00046	0.00154	0.00096	0.00058	0.00000	0.04321	0.00496	0.00079	0.00017	0.00017	0.00154	0.00242	0.00104	0.00038	0.00104
Acidobacteria;c__Acidobacteria	0.00000	0.00000	0.00000	0.00000	0.00000	0.00017	0.00058	0.00000	0.00000	0.00000	0.00000	0.00004	0.00000	0.00017	0.00004
Acidobacteria;c__Chloracidobacteria	0.00000	0.00000	0.00000	0.00000	0.00000	0.00008	0.00025	0.00000	0.00000	0.00004	0.00000	0.00000	0.00000	0.00021	0.00000
Acidobacteria;c__Solibacteres	0.00004	0.00000	0.00000	0.00000	0.00000	0.00000	0.00000	0.00000	0.00004	0.00000	0.00000	0.00000	0.00000	0.00000	0.00000
Actinobacteria;c__Actinobacteria	0.01992	0.00492	0.00067	0.00096	0.00033	0.03883	0.06862	0.00121	0.05517	0.03025	0.02196	0.05133	0.03208	0.05337	0.03154
Armatimonadetes;c__Armatimonadia	0.00004	0.00000	0.00000	0.00000	0.00000	0.00000	0.00000	0.00000	0.00000	0.00000	0.00000	0.00000	0.00000	0.00000	0.00000
Armatimonadetes;c__CH21	0.00000	0.00000	0.00000	0.00000	0.00000	0.00004	0.00000	0.00000	0.00000	0.00000	0.00000	0.00000	0.00000	0.00000	0.00000
Bacteroidetes	0.00000	0.00000	0.00000	0.00000	0.00000	0.00000	0.01183	0.00158	0.00029	0.00000	0.00025	0.00063	0.00150	0.00038	0.00000
Bacteroidetes;c__Bacteroidia	0.00533	0.00004	0.00008	0.00008	0.00004	0.00350	0.01698	0.19958	0.15408	0.49454	0.10356	0.05852	0.15665	0.13912	0.40794
Bacteroidetes;c__Flavobacteria	0.01121	0.00008	0.00008	0.00021	0.00008	0.01108	0.02002	0.63875	0.46650	0.49533	0.24277	0.34319	0.54077	0.35108	0.40865
Bacteroidetes;c__Sphingobacteria	0.00150	0.00004	0.00000	0.00008	0.00000	0.00446	0.01400	0.19917	0.14375	0.00175	0.03808	0.07050	0.10992	0.19158	0.00192
Chlamydiae;c__Chlamydiae	0.00042	0.00000	0.00000	0.00000	0.00000	0.00000	0.00033	0.00000	0.00000	0.00067	0.00000	0.00000	0.00000	0.00004	0.00000
Chloroflexi;c__Anaerolineae	0.00000	0.00000	0.00000	0.00000	0.00000	0.00025	0.00025	0.00000	0.00000	0.00000	0.00000	0.00000	0.00000	0.00000	0.00000
Chloroflexi;c__Bljii12	0.00000	0.00000	0.00000	0.00000	0.00000	0.00000	0.00000	0.00000	0.00000	0.00000	0.00000	0.00000	0.00000	0.00004	0.00000
Chloroflexi;c__Chloroflexi	0.00000	0.00000	0.00000	0.00000	0.00000	0.00000	0.00000	0.00000	0.00000	0.00017	0.00000	0.00000	0.00000	0.00000	0.00000
Chloroflexi;c__Thermomicrobia	0.00025	0.00000	0.00000	0.00000	0.00000	0.00000	0.00004	0.00000	0.00000	0.00004	0.00000	0.00000	0.00000	0.00000	0.00000
Firmicutes	0.00042	0.02542	0.00563	0.00796	0.00000	0.00004	0.00000	0.00004	0.00008	0.00000	0.00029	0.00046	0.00008	0.00000	0.00000
Firmicutes;c__Bacilli	0.50250	0.54283	0.27396	0.32737	0.01150	0.05679	0.40996	0.01700	0.02829	0.30392	0.10383	0.05012	0.04475	0.04175	0.30175
Firmicutes;c__Clostridia	0.12529	0.34825	0.31146	0.35021	0.00200	0.01487	0.11204	0.00271	0.00917	0.00425	0.04667	0.00587	0.00258	0.01383	0.00242
Fusobacteria;c__Fusobacteria	0.03746	0.00000	0.00000	0.00000	0.00000	0.00150	0.00004	0.00000	0.00008	0.00004	0.00000	0.00000	0.00000	0.00000	0.00025
Gemmatimonadetes;c__Gemmatimonadetes	0.00004	0.00000	0.00000	0.00000	0.00000	0.00021	0.00033	0.00000	0.00000	0.00021	0.00000	0.00004	0.00000	0.00000	0.00000
Nitrospirae;c__Nitrospira	0.00004	0.00000	0.00000	0.00000	0.00000	0.00000	0.00000	0.00000	0.00000	0.00000	0.00000	0.00000	0.00000	0.00000	0.00000
Planctomycetes;c__PW285	0.00004	0.00000	0.00000	0.00000	0.00000	0.00000	0.00000	0.00000	0.00000	0.00000	0.00000	0.00000	0.00000	0.00000	0.00000
Planctomycetes;c__Planctomycea	0.00038	0.00000	0.00004	0.00008	0.00004	0.00004	0.00279	0.00000	0.00000	0.00017	0.00004	0.00000	0.00000	0.00004	0.00000
Proteobacteria	0.00021	0.00013	0.00000	0.00000	0.00000	0.67883	0.08850	0.00029	0.00021	0.00050	0.00108	0.00233	0.00096	0.00013	0.00271
Proteobacteria;c__Alphaproteobacteria	0.00946	0.00017	0.00029	0.00021	0.00025	0.09317	0.18829	0.00967	0.06842	0.05562	0.06925	0.01283	0.00983	0.12283	0.06654
Proteobacteria;c__Betaproteobacteria	0.00750	0.00008	0.00008	0.00012	0.00000	0.02283	0.02000	0.07500	0.13633	0.02529	0.29925	0.29663	0.12892	0.10096	0.02500
Proteobacteria;c__Deltaproteobacteria	0.00046	0.00000	0.00000	0.00000	0.00000	0.00021	0.00021	0.00133	0.00125	0.00029	0.00304	0.00004	0.00037	0.00225	0.00042

Proteobacteria;c__Epsilonproteobacteria	0.00142	0.00000	0.00000	0.00000	0.00000	0.00000	0.00004	0.00000	0.00000	0.00000	0.00000	0.00000	0.00000	0.00000	0.00000
Proteobacteria;c__Gammaproteobacteria	0.27304	0.07233	0.37025	0.30725	0.98579	0.02592	0.04429	0.03487	0.08242	0.07979	0.16333	0.16021	0.11600	0.11046	0.15687
Spirochaetes	0.00004	0.00000	0.00000	0.00000	0.00000	0.00000	0.00000	0.00000	0.00000	0.00000	0.00000	0.00000	0.00000	0.00000	0.00000
Spirochaetes;c__Spirochaetes	0.00008	0.00000	0.00000	0.00000	0.00000	0.00004	0.00008	0.00000	0.00000	0.00025	0.00000	0.00000	0.00004	0.00000	0.00000
Synergistetes;c__Synergistia	0.00033	0.00000	0.00004	0.00000	0.00000	0.00004	0.00000	0.00004	0.00000	0.00008	0.00008	0.00000	0.00000	0.00000	0.00004
TM6;c__SJA-4	0.00000	0.00000	0.00000	0.00000	0.00000	0.00000	0.00067	0.00000	0.00000	0.00000	0.00000	0.00000	0.00000	0.00000	0.00000
TM7;c__TM7-3	0.00000	0.00000	0.00000	0.00000	0.00000	0.00000	0.00000	0.00383	0.00563	0.00025	0.00012	0.00000	0.00121	0.00838	0.00021
Tenericutes	0.00000	0.00000	0.00004	0.00000	0.00000	0.00000	0.00000	0.00000	0.00000	0.00000	0.00008	0.00000	0.00000	0.00000	0.00000
Tenericutes;c__Erysipelotrichi	0.00504	0.00417	0.03650	0.00500	0.00000	0.00125	0.00737	0.00000	0.00000	0.00000	0.00063	0.00000	0.00000	0.00008	0.00004
Tenericutes;c__ML615J-28	0.00000	0.00000	0.00000	0.00000	0.00000	0.00000	0.00000	0.00000	0.00000	0.00000	0.00150	0.00000	0.00000	0.00004	0.00000
Tenericutes;c__Mollicutes	0.00008	0.00000	0.00000	0.00000	0.00000	0.00000	0.00000	0.00004	0.00025	0.00017	0.00425	0.00038	0.00000	0.00037	0.00000
Thermi;c__Deinococci	0.00079	0.00000	0.00000	0.00000	0.00000	0.00567	0.00354	0.00000	0.00004	0.00033	0.00000	0.00000	0.00000	0.00008	0.00021
Thermotogae;c__Thermotogae	0.00088	0.00000	0.00000	0.00000	0.00000	0.00000	0.00000	0.00000	0.00000	0.00000	0.00000	0.00000	0.00000	0.00000	0.00000
Verrucomicrobia;c__Spartobacteria	0.00000	0.00004	0.00000	0.00000	0.00000	0.00004	0.00000	0.00000	0.00000	0.00004	0.00000	0.00000	0.00000	0.00000	0.00000
Verrucomicrobia;c__Verrucomicrobiae	0.00000	0.00000	0.00000	0.00000	0.00000	0.00021	0.00071	0.00000	0.00000	0.00000	0.00000	0.00000	0.00000	0.00000	0.00004
WPS-2	0.00000	0.00000	0.00000	0.00000	0.00000	0.00013	0.00013	0.00000	0.00000	0.00000	0.00004	0.00000	0.00000	0.00004	0.00008

Table S2. Microbiota composition in the samples of diet and midgut analysed. Class-level taxonomy was reported when available. The average value of 5 replicates is reported.

	Fish					VegMix					Standard				
Taxa	Fish_FreshDiet	Fish_ConditionedDiet	Fish_AnteriorMidgut	Fish_MiddleMidgut	Fish_PosteriorMidgut	VegMix_FreshDiet	VegMix_ConditionedDiet	VegMix_AnteriorMidgut	VegMix_MiddleMidgut	VegMix_PosteriorMidgut	Standard_FreshDiet	Standard_ConditionedDiet	Standard_AnteriorMidgut	Standard_MiddleMidgut	Standard_PosteriorMidgut
Others	0.00046	0.00154	0.00096	0.00058	0.00000	0.04321	0.00496	0.00079	0.00017	0.00017	0.00154	0.00242	0.00104	0.00038	0.00104
Acidobacteria;c__Acidobacteria	0.00000	0.00000	0.00000	0.00000	0.00000	0.00017	0.00058	0.00000	0.00000	0.00000	0.00000	0.00004	0.00000	0.00017	0.00004
Acidobacteria;c__Chloracidobacteria	0.00000	0.00000	0.00000	0.00000	0.00000	0.00008	0.00025	0.00000	0.00000	0.00004	0.00000	0.00000	0.00000	0.00021	0.00000
Acidobacteria;c__Solibacteres;f__Solibacteraceae	0.00004	0.00000	0.00000	0.00000	0.00000	0.00000	0.00000	0.00000	0.00004	0.00000	0.00000	0.00000	0.00000	0.00000	0.00000
Actinobacteria;c__Actinobacteria	0.00038	0.00000	0.00000	0.00000	0.00004	0.00017	0.00125	0.00000	0.00088	0.00104	0.00229	0.00271	0.00117	0.00062	0.00079
Actinobacteria;c__Actinobacteria;f__AKIW874	0.00000	0.00000	0.00000	0.00000	0.00000	0.00017	0.00004	0.00000	0.00000	0.00000	0.00000	0.00000	0.00000	0.00000	0.00000
Actinobacteria;c__Actinobacteria;f__Actinomycetaceae	0.00067	0.00000	0.00000	0.00000	0.00004	0.00079	0.00125	0.00008	0.00042	0.01950	0.00596	0.00037	0.00004	0.00058	0.02083
Actinobacteria;c__Actinobacteria;f__Beutenbergiaceae	0.00000	0.00000	0.00000	0.00000	0.00000	0.00000	0.00000	0.00000	0.00000	0.00000	0.00000	0.00004	0.00000	0.00000	0.00017
Actinobacteria;c__Actinobacteria;f__Bifidobacteriaceae	0.00017	0.00000	0.00000	0.00000	0.00000	0.00388	0.01479	0.00000	0.00004	0.00012	0.00196	0.00017	0.00000	0.00017	0.00033
Actinobacteria;c__Actinobacteria;f__Bogoriellaceae	0.00000	0.00000	0.00000	0.00000	0.00000	0.00000	0.00004	0.00000	0.00000	0.00000	0.00000	0.00000	0.00000	0.00000	0.00000
Actinobacteria;c__Actinobacteria;f__Brevibacteriaceae	0.00000	0.00000	0.00000	0.00000	0.00000	0.00000	0.00000	0.00000	0.00004	0.00013	0.00004	0.00000	0.00000	0.00008	0.00012
Actinobacteria;c__Actinobacteria;f__CL500-29	0.00000	0.00000	0.00000	0.00000	0.00000	0.00000	0.00113	0.00000	0.00000	0.00000	0.00000	0.00000	0.00000	0.00000	0.00000
Actinobacteria;c__Actinobacteria;f__Cellulomonadaceae	0.00004	0.00000	0.00000	0.00000	0.00000	0.00000	0.00004	0.00004	0.01263	0.00013	0.00008	0.00029	0.00025	0.02521	0.00000
Actinobacteria;c__Actinobacteria;f__Coriobacteriaceae	0.00950	0.00000	0.00000	0.00000	0.00000	0.00017	0.00200	0.00000	0.00000	0.00000	0.00004	0.00000	0.00000	0.00000	0.00000
Actinobacteria;c__Actinobacteria;f__Corynebacteriaceae	0.00383	0.00467	0.00067	0.00083	0.00008	0.00579	0.00392	0.00013	0.00083	0.00304	0.00312	0.00046	0.00008	0.00183	0.00288
Actinobacteria;c__Actinobacteria;f__Dermabacteraceae	0.00017	0.00000	0.00000	0.00000	0.00000	0.00004	0.00067	0.00000	0.00004	0.00021	0.00004	0.00000	0.00000	0.00004	0.00004
Actinobacteria;c__Actinobacteria;f__Dietziaceae	0.00004	0.00000	0.00000	0.00000	0.00000	0.00071	0.00000	0.00000	0.00000	0.00046	0.00000	0.00000	0.00004	0.00000	0.00008
Actinobacteria;c__Actinobacteria;f__EB1017	0.00000	0.00000	0.00000	0.00000	0.00000	0.00000	0.00000	0.00000	0.00008	0.00000	0.00000	0.00000	0.00000	0.00000	0.00000
Actinobacteria;c__Actinobacteria;f__Frankiaceae	0.00013	0.00000	0.00000	0.00000	0.00000	0.00000	0.00075	0.00000	0.00000	0.00000	0.00000	0.00000	0.00000	0.00000	0.00000
Actinobacteria;c__Actinobacteria;f__Geodermatophilaceae	0.00029	0.00000	0.00000	0.00000	0.00004	0.00163	0.00104	0.00000	0.00000	0.00013	0.00008	0.00004	0.00004	0.00000	0.00000
Actinobacteria;c__Actinobacteria;f__Gordoniaceae	0.00013	0.00000	0.00000	0.00000	0.00000	0.00000	0.00000	0.00004	0.00013	0.00113	0.00075	0.00008	0.00000	0.00000	0.00146
Actinobacteria;c__Actinobacteria;f__Intrasporangiaceae	0.00000	0.00000	0.00000	0.00000	0.00000	0.00004	0.00017	0.00000	0.00000	0.00000	0.00000	0.00000	0.00000	0.00000	0.00000
Actinobacteria;c__Actinobacteria;f__Jonesiaceae	0.00004	0.00000	0.00000	0.00000	0.00000	0.00000	0.00008	0.00000	0.00000	0.00000	0.00000	0.00000	0.00000	0.00000	0.00000
Actinobacteria;c__Actinobacteria;f__Kineosporiaceae	0.00013	0.00000	0.00000	0.00000	0.00000	0.00008	0.00000	0.00000	0.00000	0.00000	0.00000	0.00000	0.00000	0.00000	0.00000
Actinobacteria;c__Actinobacteria;f__Microbacteriaceae	0.00029	0.00008	0.00000	0.00004	0.00004	0.00033	0.00808	0.00017	0.00058	0.00088	0.00104	0.00096	0.00013	0.00146	0.00142
Actinobacteria;c__Actinobacteria;f__Micrococcaceae	0.00287	0.00013	0.00000	0.00000	0.00000	0.01817	0.01921	0.00008	0.00017	0.00054	0.00113	0.00008	0.00017	0.00029	0.00054
Actinobacteria;c__Actinobacteria;f__Mycobacteriaceae	0.00021	0.00000	0.00000	0.00004	0.00000	0.00013	0.00688	0.00000	0.00000	0.00004	0.00000	0.00004	0.00000	0.00013	0.00021
Actinobacteria;c__Actinobacteria;f__Nakamurellaceae	0.00008	0.00000	0.00000	0.00000	0.00000	0.00000	0.00000	0.00000	0.00000	0.00000	0.00000	0.00000	0.00000	0.00000	0.00000

Actinobacteria;c__Actinobacteria;f__Nocardiaceae	0.00004	0.00000	0.00000	0.00000	0.00000	0.00017	0.00000	0.00000	0.00013	0.00129	0.00054	0.00046	0.00008	0.00000	0.00129
Actinobacteria;c__Actinobacteria;f__Nocardioidaceae	0.00029	0.00000	0.00000	0.00000	0.00008	0.00108	0.00146	0.00000	0.00000	0.00008	0.00000	0.00000	0.00000	0.00004	0.00004
Actinobacteria;c__Actinobacteria;f__Promicromonosporaceae	0.00000	0.00000	0.00000	0.00000	0.00000	0.00004	0.00000	0.00004	0.00133	0.00000	0.00104	0.00225	0.00117	0.00063	0.00004
Actinobacteria;c__Actinobacteria;f__Propionibacteriaceae	0.00021	0.00000	0.00000	0.00000	0.00000	0.00246	0.00346	0.00004	0.00004	0.00038	0.00008	0.00000	0.00000	0.00012	0.00033
Actinobacteria;c__Actinobacteria;f__Pseudonocardiaceae	0.00025	0.00000	0.00000	0.00004	0.00000	0.00029	0.00079	0.00000	0.00000	0.00108	0.00000	0.00000	0.00000	0.00042	0.00071
Actinobacteria;c__Actinobacteria;f__Rarobacteraceae	0.00000	0.00000	0.00000	0.00000	0.00000	0.00000	0.00000	0.00000	0.00004	0.00000	0.00008	0.00012	0.00000	0.00000	0.00000
Actinobacteria;c__Actinobacteria;f__Rubrobacteraceae	0.00000	0.00000	0.00000	0.00000	0.00000	0.00000	0.00000	0.00000	0.00000	0.00000	0.00004	0.00000	0.00000	0.00000	0.00000
Actinobacteria;c__Actinobacteria;f__Sanguibacteraceae	0.00000	0.00000	0.00000	0.00000	0.00000	0.00254	0.00104	0.00054	0.03775	0.00004	0.00350	0.04325	0.02892	0.02158	0.00017
Actinobacteria;c__Actinobacteria;f__Solirubrobacteraceae	0.00000	0.00000	0.00000	0.00000	0.00000	0.00013	0.00050	0.00000	0.00000	0.00004	0.00004	0.00000	0.00000	0.00000	0.00004
Actinobacteria;c__Actinobacteria;f__Streptomycetaceae	0.00004	0.00000	0.00000	0.00000	0.00000	0.00004	0.00000	0.00000	0.00000	0.00000	0.00004	0.00000	0.00000	0.00000	0.00000
Actinobacteria;c__Actinobacteria;f__Williamsiaceae	0.00008	0.00000	0.00000	0.00000	0.00000	0.00000	0.00004	0.00004	0.00004	0.00000	0.00004	0.00000	0.00000	0.00017	0.00004
Actinobacteria;c__Actinobacteria;f__Yaniellaceae	0.00004	0.00004	0.00000	0.00000	0.00000	0.00000	0.00000	0.00000	0.00000	0.00000	0.00000	0.00000	0.00000	0.00000	0.00000
Armatimonadetes;c__Armatimonadia;f__Armatimonadaceae	0.00004	0.00000	0.00000	0.00000	0.00000	0.00000	0.00000	0.00000	0.00000	0.00000	0.00000	0.00000	0.00000	0.00000	0.00000
Armatimonadetes;c__CH21	0.00000	0.00000	0.00000	0.00000	0.00000	0.00004	0.00000	0.00000	0.00000	0.00000	0.00000	0.00000	0.00000	0.00000	0.00000
Bacteroidetes	0.00000	0.00000	0.00000	0.00000	0.00000	0.00000	0.01183	0.00158	0.00029	0.00000	0.00025	0.00063	0.00150	0.00038	0.00000
Bacteroidetes;c__Bacteroidia	0.00058	0.00000	0.00000	0.00000	0.00000	0.00000	0.00015	0.01292	0.00171	0.00037	0.00073	0.00056	0.00702	0.00137	0.00023
Bacteroidetes;c__Bacteroidia;f__Bacteroidaceae	0.00283	0.00004	0.00008	0.00000	0.00000	0.00150	0.00383	0.00012	0.02496	0.00000	0.02796	0.03304	0.03542	0.00450	0.00033
Bacteroidetes;c__Bacteroidia;f__Porphyromonadaceae	0.00104	0.00000	0.00000	0.00008	0.00004	0.00125	0.01287	0.18654	0.12725	0.49392	0.07479	0.02488	0.11421	0.13317	0.40725
Bacteroidetes;c__Bacteroidia;f__Prevotellaceae	0.00075	0.00000	0.00000	0.00000	0.00000	0.00067	0.00013	0.00000	0.00017	0.00025	0.00008	0.00004	0.00000	0.00008	0.00013
Bacteroidetes;c__Bacteroidia;f__Rikenellaceae	0.00013	0.00000	0.00000	0.00000	0.00000	0.00008	0.00000	0.00000	0.00000	0.00000	0.00000	0.00000	0.00000	0.00000	0.00000
Bacteroidetes;c__Flavobacteria	0.00000	0.00000	0.00000	0.00000	0.00000	0.00000	0.00033	0.00004	0.00000	0.00000	0.00000	0.00000	0.00008	0.00000	0.00000
Bacteroidetes;c__Flavobacteria;f__Flavobacteriaceae	0.00587	0.00004	0.00000	0.00013	0.00004	0.00758	0.00271	0.43913	0.31242	0.00079	0.13921	0.28467	0.38404	0.21196	0.00071
Bacteroidetes;c__Sphingobacteria	0.00004	0.00004	0.00000	0.00000	0.00000	0.00071	0.01188	0.01117	0.00967	0.00117	0.00017	0.00000	0.00271	0.01379	0.00125
Bacteroidetes;c__Sphingobacteria;f__Flammeovirgaceae	0.00000	0.00000	0.00000	0.00004	0.00000	0.00000	0.00000	0.00000	0.00004	0.00000	0.00004	0.00000	0.00000	0.00004	0.00000
Bacteroidetes;c__Sphingobacteria;f__Flexibacteraceae	0.00079	0.00000	0.00000	0.00000	0.00000	0.00100	0.00004	0.00017	0.00000	0.00000	0.00008	0.00000	0.00000	0.00008	0.00000
Bacteroidetes;c__Sphingobacteria;f__Sphingobacteriaceae	0.00067	0.00000	0.00000	0.00004	0.00000	0.00275	0.00208	0.18783	0.13404	0.00058	0.03779	0.07050	0.10721	0.17767	0.00067
Chlamydiae;c__Chlamydiae;f__Parachlamydiaceae	0.00042	0.00000	0.00000	0.00000	0.00000	0.00000	0.00033	0.00000	0.00000	0.00021	0.00000	0.00000	0.00000	0.00004	0.00000
Chlamydiae;c__Chlamydiae;f__Rhabdochlamydiaceae	0.00000	0.00000	0.00000	0.00000	0.00000	0.00000	0.00000	0.00000	0.00000	0.00042	0.00000	0.00000	0.00000	0.00000	0.00000
Chlamydiae;c__Chlamydiae;f__Simkaniaceae	0.00000	0.00000	0.00000	0.00000	0.00000	0.00000	0.00000	0.00000	0.00000	0.00004	0.00000	0.00000	0.00000	0.00000	0.00000
Chloroflexi;c__Anaerolineae	0.00000	0.00000	0.00000	0.00000	0.00000	0.00025	0.00025	0.00000	0.00000	0.00000	0.00000	0.00000	0.00000	0.00000	0.00000
Chloroflexi;c__Blji12;f__Dolo_23	0.00000	0.00000	0.00000	0.00000	0.00000	0.00000	0.00000	0.00000	0.00000	0.00000	0.00000	0.00000	0.00000	0.00004	0.00000

Chloroflexi;c__Chloroflexi;f__Roseiflexaceae	0.00000	0.00000	0.00000	0.00000	0.00000	0.00000	0.00000	0.00000	0.00000	0.00017	0.00000	0.00000	0.00000	0.00000	0.00000
Chloroflexi;c__Thermomicrobia	0.00025	0.00000	0.00000	0.00000	0.00000	0.00000	0.00004	0.00000	0.00000	0.00004	0.00000	0.00000	0.00000	0.00000	0.00000
Firmicutes	0.00042	0.02542	0.00563	0.00796	0.00000	0.00004	0.00000	0.00004	0.00008	0.00000	0.00029	0.00046	0.00008	0.00000	0.00000
Firmicutes;c__Bacilli	0.09450	0.24517	0.09963	0.09287	0.00058	0.00150	0.00025	0.00025	0.00025	0.00079	0.00246	0.00379	0.00167	0.00013	0.00150
Firmicutes;c__Bacilli;f__Aerococcaceae	0.00008	0.00000	0.00000	0.00004	0.00000	0.00000	0.00004	0.00000	0.00000	0.00000	0.00000	0.00000	0.00000	0.00000	0.00000
Firmicutes;c__Bacilli;f__Alicyclobacillaceae	0.00004	0.00000	0.00000	0.00000	0.00000	0.00000	0.00000	0.00000	0.00000	0.00000	0.00000	0.00000	0.00000	0.00000	0.00000
Firmicutes;c__Bacilli;f__Bacillaceae	0.17138	0.01037	0.00263	0.00329	0.00033	0.00137	0.00187	0.00008	0.00096	0.00092	0.00213	0.00137	0.00121	0.00046	0.00067
Firmicutes;c__Bacilli;f__Carnobacteriaceae	0.00492	0.00171	0.00192	0.00171	0.00000	0.00071	0.00162	0.00000	0.00012	0.00042	0.00004	0.00000	0.00000	0.00017	0.00046
Firmicutes;c__Bacilli;f__Enterococcaceae	0.01096	0.01021	0.08200	0.15075	0.01013	0.00287	0.02104	0.00596	0.00763	0.28963	0.06113	0.02346	0.00783	0.00788	0.26879
Firmicutes;c__Bacilli;f__Exiguobacteraceae	0.00025	0.00042	0.00008	0.00000	0.00004	0.00046	0.00163	0.00000	0.00004	0.00004	0.00000	0.00000	0.00000	0.00000	0.00000
Firmicutes;c__Bacilli;f__Gemellaceae	0.00004	0.00000	0.00000	0.00000	0.00000	0.00000	0.00000	0.00004	0.00000	0.00008	0.00000	0.00000	0.00000	0.00004	0.00004
Firmicutes;c__Bacilli;f__Haloplasmataceae	0.00004	0.00004	0.00000	0.00000	0.00000	0.00000	0.00000	0.00000	0.00000	0.00000	0.00004	0.00000	0.00000	0.00000	0.00000
Firmicutes;c__Bacilli;f__Lactobacillaceae	0.01079	0.00038	0.00013	0.00008	0.00000	0.02979	0.35854	0.00867	0.00067	0.00121	0.00733	0.00100	0.00104	0.00067	0.00046
Firmicutes;c__Bacilli;f__Leuconostocaceae	0.00033	0.00000	0.00000	0.00000	0.00000	0.00087	0.00063	0.00017	0.00050	0.00029	0.00200	0.00025	0.00017	0.00263	0.00004
Firmicutes;c__Bacilli;f__Listeriaceae	0.00000	0.00000	0.00000	0.00000	0.00000	0.00000	0.00021	0.00000	0.00000	0.00004	0.00000	0.00000	0.00000	0.00000	0.00004
Firmicutes;c__Bacilli;f__Paenibacillaceae	0.00158	0.00004	0.00000	0.00000	0.00000	0.00038	0.00017	0.00083	0.01038	0.00092	0.01492	0.01492	0.01762	0.00438	0.00142
Firmicutes;c__Bacilli;f__Planococcaceae	0.19404	0.27417	0.08721	0.07829	0.00017	0.00050	0.00088	0.00054	0.00621	0.00117	0.01267	0.00529	0.01492	0.00558	0.02237
Firmicutes;c__Bacilli;f__Staphylococcaceae	0.01225	0.00029	0.00025	0.00029	0.00021	0.00921	0.00796	0.00025	0.00117	0.00363	0.00079	0.00004	0.00021	0.01863	0.00442
Firmicutes;c__Bacilli;f__Streptococcaceae	0.00129	0.00004	0.00012	0.00004	0.00004	0.00912	0.01512	0.00021	0.00038	0.00479	0.00033	0.00000	0.00008	0.00121	0.00154
Firmicutes;c__Clostridia	0.00171	0.00371	0.00125	0.00063	0.00000	0.00008	0.01125	0.00162	0.00087	0.00000	0.00937	0.00008	0.00017	0.00088	0.00000
Firmicutes;c__Clostridia;f__Catabacteriaceae	0.00000	0.00000	0.00000	0.00000	0.00000	0.00000	0.00000	0.00000	0.00000	0.00008	0.00000	0.00000	0.00000	0.00000	0.00000
Firmicutes;c__Clostridia;f__Clostridiaceae	0.02054	0.09225	0.00600	0.00792	0.00021	0.00025	0.00767	0.00008	0.00033	0.00025	0.00304	0.00042	0.00017	0.00062	0.00025
Firmicutes;c__Clostridia;f__ClostridialesFamilyXI,IncertaeSedis	0.07029	0.25188	0.30408	0.34117	0.00158	0.00204	0.00083	0.00004	0.00158	0.00154	0.00567	0.00063	0.00008	0.00204	0.00067
Firmicutes;c__Clostridia;f__Eubacteriaceae	0.00008	0.00004	0.00000	0.00004	0.00004	0.00017	0.00004	0.00004	0.00004	0.00000	0.00000	0.00000	0.00000	0.00013	0.00000
Firmicutes;c__Clostridia;f__Lachnospiraceae	0.02083	0.00013	0.00000	0.00025	0.00004	0.01087	0.07796	0.00062	0.00550	0.00200	0.02350	0.00417	0.00183	0.00904	0.00146
Firmicutes;c__Clostridia;f__ML1228J-1	0.00000	0.00000	0.00000	0.00000	0.00000	0.00000	0.00008	0.00000	0.00000	0.00000	0.00000	0.00000	0.00000	0.00000	0.00000
Firmicutes;c__Clostridia;f__Peptococcaceae	0.00000	0.00000	0.00000	0.00000	0.00000	0.00000	0.00000	0.00000	0.00000	0.00000	0.00004	0.00000	0.00000	0.00000	0.00000
Firmicutes;c__Clostridia;f__Peptostreptococcaceae	0.00279	0.00000	0.00000	0.00000	0.00000	0.00000	0.00021	0.00004	0.00000	0.00000	0.00000	0.00000	0.00000	0.00000	0.00000
Firmicutes;c__Clostridia;f__Ruminococcaceae	0.00563	0.00021	0.00004	0.00013	0.00000	0.00046	0.01325	0.00017	0.00054	0.00021	0.00379	0.00046	0.00017	0.00079	0.00004
Firmicutes;c__Clostridia;f__Thermoanaerobacteraceae	0.00129	0.00000	0.00000	0.00000	0.00000	0.00000	0.00000	0.00000	0.00000	0.00000	0.00000	0.00000	0.00000	0.00000	0.00000
Firmicutes;c__Clostridia;f__Thermodesulfobiaceae	0.00013	0.00000	0.00000	0.00000	0.00000	0.00000	0.00000	0.00000	0.00000	0.00000	0.00000	0.00000	0.00000	0.00000	0.00000

Firmicutes;c__Clostridia;f__Veillonellaceae	0.00200	0.00004	0.00008	0.00008	0.00013	0.00100	0.00075	0.00008	0.00029	0.00017	0.00125	0.00013	0.00017	0.00033	0.00000
Fusobacteria;c__Fusobacteria;f__Fusobacteriaceae	0.03746	0.00000	0.00000	0.00000	0.00000	0.00150	0.00004	0.00000	0.00008	0.00004	0.00000	0.00000	0.00000	0.00000	0.00025
Gemmatimonadetes;c__Gemmatimonadetes	0.00004	0.00000	0.00000	0.00000	0.00000	0.00021	0.00033	0.00000	0.00000	0.00004	0.00000	0.00004	0.00000	0.00000	0.00000
Gemmatimonadetes;c__Gemmatimonadetes;f__Gemmatimonadaceae	0.00000	0.00000	0.00000	0.00000	0.00000	0.00000	0.00000	0.00000	0.00000	0.00017	0.00000	0.00000	0.00000	0.00000	0.00000
Nitrospirae;c__Nitrospira;f__Nitrospiraceae	0.00004	0.00000	0.00000	0.00000	0.00000	0.00000	0.00000	0.00000	0.00000	0.00000	0.00000	0.00000	0.00000	0.00000	0.00000
Planctomycetes;c__PW285	0.00004	0.00000	0.00000	0.00000	0.00000	0.00000	0.00000	0.00000	0.00000	0.00000	0.00000	0.00000	0.00000	0.00000	0.00000
Planctomycetes;c__Planctomycea	0.00025	0.00000	0.00004	0.00000	0.00004	0.00004	0.00050	0.00000	0.00000	0.00000	0.00000	0.00000	0.00000	0.00000	0.00000
Planctomycetes;c__Planctomycea;f__Gemmataceae	0.00013	0.00000	0.00000	0.00000	0.00000	0.00000	0.00129	0.00000	0.00000	0.00000	0.00004	0.00000	0.00000	0.00004	0.00000
Planctomycetes;c__Planctomycea;f__Isosphaeraceae	0.00000	0.00000	0.00000	0.00008	0.00000	0.00000	0.00050	0.00000	0.00000	0.00004	0.00000	0.00000	0.00000	0.00000	0.00000
Planctomycetes;c__Planctomycea;f__Pirellulaceae	0.00000	0.00000	0.00000	0.00000	0.00000	0.00000	0.00050	0.00000	0.00000	0.00013	0.00000	0.00000	0.00000	0.00000	0.00000
Proteobacteria	0.00021	0.00013	0.00000	0.00000	0.00000	0.67883	0.08850	0.00029	0.00021	0.00050	0.00108	0.00233	0.00096	0.00013	0.00271
Proteobacteria;c__Alphaproteobacteria	0.00004	0.00000	0.00000	0.00000	0.00000	0.00012	0.00075	0.00058	0.00113	0.00096	0.00217	0.00188	0.00050	0.00238	0.00125
Proteobacteria;c__Alphaproteobacteria;f__Acetobacteraceae	0.00504	0.00004	0.00004	0.00004	0.00000	0.01017	0.03513	0.00042	0.00046	0.00067	0.00046	0.00012	0.00008	0.00033	0.00050
Proteobacteria;c__Alphaproteobacteria;f__Aurantimonadaceae	0.00000	0.00000	0.00000	0.00000	0.00000	0.00379	0.00000	0.00000	0.00000	0.00000	0.00000	0.00000	0.00000	0.00000	0.00000
Proteobacteria;c__Alphaproteobacteria;f__Bartonellaceae	0.00000	0.00000	0.00000	0.00000	0.00000	0.00000	0.00000	0.00004	0.00013	0.00021	0.00004	0.00008	0.00021	0.00046	0.00033
Proteobacteria;c__Alphaproteobacteria;f__Beijerinckiaceae	0.00000	0.00000	0.00000	0.00000	0.00000	0.00000	0.00017	0.00004	0.00000	0.00000	0.00000	0.00000	0.00000	0.00000	0.00000
Proteobacteria;c__Alphaproteobacteria;f__Bradyrhizobiaceae	0.00013	0.00000	0.00000	0.00000	0.00000	0.00088	0.00050	0.00013	0.00050	0.00183	0.00025	0.00012	0.00000	0.00063	0.00204
Proteobacteria;c__Alphaproteobacteria;f__Brucellaceae	0.00025	0.00000	0.00004	0.00004	0.00000	0.00112	0.00133	0.00375	0.05467	0.03342	0.04558	0.00654	0.00379	0.10504	0.04542
Proteobacteria;c__Alphaproteobacteria;f__Caulobacteraceae	0.00058	0.00000	0.00004	0.00000	0.00004	0.00142	0.00192	0.00033	0.00104	0.00008	0.00133	0.00025	0.00158	0.00050	0.00008
Proteobacteria;c__Alphaproteobacteria;f__Erythrobacteraceae	0.00000	0.00000	0.00000	0.00000	0.00000	0.00000	0.00000	0.00021	0.00029	0.00000	0.00096	0.00025	0.00004	0.00021	0.00000
Proteobacteria;c__Alphaproteobacteria;f__Hyphomicrobiaceae	0.00008	0.00000	0.00000	0.00000	0.00000	0.00000	0.00496	0.00067	0.00179	0.00213	0.00146	0.00033	0.00029	0.00233	0.00104
Proteobacteria;c__Alphaproteobacteria;f__Methylobacteriaceae	0.00021	0.00000	0.00000	0.00000	0.00000	0.00029	0.00454	0.00000	0.00008	0.00058	0.00008	0.00000	0.00000	0.00012	0.00054
Proteobacteria;c__Alphaproteobacteria;f__Methylocystaceae	0.00000	0.00000	0.00000	0.00000	0.00000	0.00067	0.08042	0.00004	0.00008	0.00000	0.00013	0.00000	0.00000	0.00000	0.00008
Proteobacteria;c__Alphaproteobacteria;f__Phyllobacteriaceae	0.00021	0.00000	0.00000	0.00000	0.00000	0.00104	0.00004	0.00125	0.00196	0.00025	0.00767	0.00100	0.00083	0.00346	0.00079
Proteobacteria;c__Alphaproteobacteria;f__Rhizobiaceae	0.00008	0.00004	0.00008	0.00000	0.00000	0.00021	0.00008	0.00008	0.00013	0.00008	0.00025	0.00012	0.00000	0.00021	0.00017
Proteobacteria;c__Alphaproteobacteria;f__Rhodobacteraceae	0.00154	0.00000	0.00000	0.00000	0.00017	0.01850	0.01321	0.00104	0.00088	0.00067	0.00846	0.00196	0.00208	0.00021	0.00054
Proteobacteria;c__Alphaproteobacteria;f__Rhodobiaceae	0.00004	0.00000	0.00000	0.00000	0.00000	0.00000	0.00000	0.00000	0.00000	0.00000	0.00000	0.00000	0.00000	0.00000	0.00000
Proteobacteria;c__Alphaproteobacteria;f__Rhodospirillaceae	0.00017	0.00004	0.00000	0.00004	0.00000	0.00008	0.00042	0.00000	0.00000	0.00012	0.00004	0.00008	0.00008	0.00042	0.00017
Proteobacteria;c__Alphaproteobacteria;f__Rickettsiaceae	0.00000	0.00000	0.00000	0.00000	0.00000	0.00000	0.00000	0.00000	0.00000	0.00000	0.00000	0.00000	0.00000	0.00038	0.00000
Proteobacteria;c__Alphaproteobacteria;f__Sphingomonadaceae	0.00104	0.00004	0.00008	0.00008	0.00004	0.05483	0.04483	0.00108	0.00529	0.01462	0.00037	0.00008	0.00033	0.00617	0.01358
Proteobacteria;c__Alphaproteobacteria;f__Xanthobacteraceae	0.00004	0.00000	0.00000	0.00000	0.00000	0.00004	0.00000	0.00000	0.00000	0.00000	0.00000	0.00000	0.00000	0.00000	0.00000

Proteobacteria;c__Betaproteobacteria	0.00021	0.00000	0.00000	0.00000	0.00000	0.00300	0.00017	0.00029	0.00088	0.00217	0.01033	0.01633	0.00300	0.00071	0.00083
Proteobacteria;c__Betaproteobacteria;f__Alcaligenaceae	0.00437	0.00004	0.00004	0.00004	0.00000	0.00250	0.00254	0.07029	0.06550	0.01767	0.11804	0.07975	0.05783	0.05792	0.01763
Proteobacteria;c__Betaproteobacteria;f__Burkholderiaceae	0.00017	0.00000	0.00000	0.00000	0.00000	0.00008	0.00067	0.00000	0.00004	0.00017	0.00000	0.00000	0.00000	0.00000	0.00008
Proteobacteria;c__Betaproteobacteria;f__Comamonadaceae	0.00100	0.00000	0.00004	0.00008	0.00000	0.01138	0.00483	0.00121	0.06821	0.00079	0.17012	0.19996	0.06758	0.03975	0.00342
Proteobacteria;c__Betaproteobacteria;f__Hydrogenophilaceae	0.00012	0.00000	0.00000	0.00000	0.00000	0.00004	0.00008	0.00000	0.00013	0.00000	0.00000	0.00000	0.00000	0.00008	0.00000
Proteobacteria;c__Betaproteobacteria;f__Methylophilaceae	0.00083	0.00000	0.00000	0.00000	0.00000	0.00000	0.00321	0.00000	0.00004	0.00004	0.00000	0.00000	0.00000	0.00013	0.00021
Proteobacteria;c__Betaproteobacteria;f__Neisseriaceae	0.00008	0.00000	0.00000	0.00000	0.00000	0.00029	0.00029	0.00000	0.00000	0.00000	0.00000	0.00000	0.00000	0.00008	0.00004
Proteobacteria;c__Betaproteobacteria;f__Oxalobacteraceae	0.00054	0.00004	0.00000	0.00000	0.00000	0.00413	0.00238	0.00321	0.00142	0.00408	0.00071	0.00058	0.00050	0.00183	0.00196
Proteobacteria;c__Betaproteobacteria;f__Rhodocyclaceae	0.00017	0.00000	0.00000	0.00000	0.00000	0.00142	0.00583	0.00000	0.00013	0.00038	0.00004	0.00000	0.00000	0.00046	0.00083
Proteobacteria;c__Deltaproteobacteria	0.00013	0.00000	0.00000	0.00000	0.00000	0.00017	0.00004	0.00000	0.00000	0.00013	0.00004	0.00000	0.00000	0.00000	0.00008
Proteobacteria;c__Deltaproteobacteria;f__Bacteriovoracaceae	0.00000	0.00000	0.00000	0.00000	0.00000	0.00000	0.00000	0.00133	0.00121	0.00008	0.00292	0.00004	0.00033	0.00208	0.00029
Proteobacteria;c__Deltaproteobacteria;f__Bdellovibrionaceae	0.00013	0.00000	0.00000	0.00000	0.00000	0.00000	0.00008	0.00000	0.00000	0.00004	0.00000	0.00000	0.00000	0.00000	0.00000
Proteobacteria;c__Deltaproteobacteria;f__Desulfobulbaceae	0.00008	0.00000	0.00000	0.00000	0.00000	0.00000	0.00000	0.00000	0.00000	0.00000	0.00000	0.00000	0.00000	0.00000	0.00000
Proteobacteria;c__Deltaproteobacteria;f__Desulfovibrionaceae	0.00000	0.00000	0.00000	0.00000	0.00000	0.00004	0.00004	0.00000	0.00004	0.00004	0.00008	0.00000	0.00004	0.00000	0.00004
Proteobacteria;c__Deltaproteobacteria;f__Haliangiaceae	0.00000	0.00000	0.00000	0.00000	0.00000	0.00000	0.00000	0.00000	0.00000	0.00000	0.00000	0.00000	0.00000	0.00013	0.00000
Proteobacteria;c__Deltaproteobacteria;f__JTB38	0.00008	0.00000	0.00000	0.00000	0.00000	0.00000	0.00000	0.00000	0.00000	0.00000	0.00000	0.00000	0.00000	0.00000	0.00000
Proteobacteria;c__Deltaproteobacteria;f__Nannocystaceae	0.00004	0.00000	0.00000	0.00000	0.00000	0.00000	0.00000	0.00000	0.00000	0.00000	0.00000	0.00000	0.00000	0.00000	0.00000
Proteobacteria;c__Deltaproteobacteria;f__Syntrophobacteraceae	0.00000	0.00000	0.00000	0.00000	0.00000	0.00000	0.00004	0.00000	0.00000	0.00000	0.00000	0.00000	0.00000	0.00004	0.00000
Proteobacteria;c__Epsilonproteobacteria;f__Campylobacteraceae	0.00142	0.00000	0.00000	0.00000	0.00000	0.00000	0.00004	0.00000	0.00000	0.00000	0.00000	0.00000	0.00000	0.00000	0.00000
Proteobacteria;c__Gammaproteobacteria	0.00167	0.00029	0.00012	0.00033	0.00000	0.00000	0.00000	0.00000	0.00017	0.00000	0.00163	0.00342	0.00188	0.00008	0.00000
Proteobacteria;c__Gammaproteobacteria;f__Aeromonadaceae	0.00313	0.00000	0.00004	0.00000	0.00000	0.00183	0.00025	0.00000	0.00000	0.00000	0.00000	0.00000	0.00000	0.00000	0.00000
Proteobacteria;c__Gammaproteobacteria;f__Alcanivoracaceae	0.00004	0.00000	0.00000	0.00000	0.00000	0.00004	0.00000	0.00000	0.00000	0.00000	0.00000	0.00000	0.00000	0.00000	0.00004
Proteobacteria;c__Gammaproteobacteria;f__Alteromonadaceae	0.00050	0.00000	0.00000	0.00000	0.00000	0.00000	0.00000	0.00000	0.00000	0.00000	0.00000	0.00000	0.00000	0.00000	0.00000
Proteobacteria;c__Gammaproteobacteria;f__Cardiobacteriaceae	0.00004	0.00000	0.00000	0.00000	0.00000	0.00000	0.00000	0.00000	0.00000	0.00000	0.00000	0.00000	0.00000	0.00000	0.00000
Proteobacteria;c__Gammaproteobacteria;f__Chromatiaceae	0.00192	0.00000	0.00000	0.00000	0.00000	0.00021	0.00000	0.00000	0.00000	0.00000	0.00000	0.00000	0.00000	0.00000	0.00000
Proteobacteria;c__Gammaproteobacteria;f__Enterobacteriaceae	0.00887	0.07142	0.36975	0.30542	0.98571	0.01108	0.02867	0.00521	0.01454	0.07621	0.05100	0.00992	0.00712	0.06171	0.15383
Proteobacteria;c__Gammaproteobacteria;f__Halomonadaceae	0.00946	0.00000	0.00000	0.00000	0.00000	0.00000	0.00033	0.00000	0.00000	0.00000	0.00000	0.00000	0.00000	0.00000	0.00000
Proteobacteria;c__Gammaproteobacteria;f__Idiomarinaceae	0.00046	0.00000	0.00000	0.00000	0.00000	0.00000	0.00000	0.00000	0.00000	0.00000	0.00000	0.00000	0.00000	0.00000	0.00000
Proteobacteria;c__Gammaproteobacteria;f__Moraxellaceae	0.06537	0.00054	0.00029	0.00121	0.00000	0.00204	0.00704	0.00117	0.00754	0.00033	0.04771	0.00433	0.00104	0.01625	0.00067
Proteobacteria;c__Gammaproteobacteria;f__Moritellaceae	0.00246	0.00000	0.00000	0.00000	0.00000	0.00000	0.00000	0.00000	0.00000	0.00000	0.00000	0.00000	0.00000	0.00000	0.00000
Proteobacteria;c__Gammaproteobacteria;f__Oceanospirillaceae	0.00096	0.00000	0.00000	0.00000	0.00000	0.00000	0.00033	0.00004	0.00000	0.00000	0.00000	0.00008	0.00025	0.00000	0.00000

Proteobacteria;c__Gammaproteobacteria;f__Pasteurellaceae	0.00000	0.00000	0.00000	0.00000	0.00000	0.00092	0.00083	0.00000	0.00004	0.00046	0.00000	0.00000	0.00000	0.00008	0.00004
Proteobacteria;c__Gammaproteobacteria;f__Pseudoalteromonadaceae	0.05075	0.00000	0.00000	0.00000	0.00000	0.00000	0.00000	0.00000	0.00000	0.00000	0.00000	0.00000	0.00000	0.00000	0.00000
Proteobacteria;c__Gammaproteobacteria;f__Pseudomonadaceae	0.01358	0.00000	0.00000	0.00012	0.00008	0.00454	0.00400	0.02008	0.03321	0.00088	0.04142	0.03746	0.06946	0.02121	0.00037
Proteobacteria;c__Gammaproteobacteria;f__Shewanellaceae	0.01154	0.00000	0.00000	0.00000	0.00000	0.00000	0.00000	0.00000	0.00000	0.00000	0.00000	0.00000	0.00000	0.00000	0.00000
Proteobacteria;c__Gammaproteobacteria;f__Sinobacteraceae	0.00050	0.00000	0.00000	0.00000	0.00000	0.00046	0.00021	0.00000	0.00008	0.00150	0.00021	0.00000	0.00004	0.00192	0.00179
Proteobacteria;c__Gammaproteobacteria;f__Vibrionaceae	0.10033	0.00004	0.00004	0.00008	0.00000	0.00004	0.00033	0.00000	0.00008	0.00017	0.00000	0.00000	0.00000	0.00004	0.00000
Proteobacteria;c__Gammaproteobacteria;f__Xanthomonadaceae	0.00146	0.00004	0.00000	0.00008	0.00000	0.00475	0.00229	0.00837	0.02675	0.00025	0.02138	0.10500	0.03621	0.00917	0.00012
Spirochaetes	0.00004	0.00000	0.00000	0.00000	0.00000	0.00000	0.00000	0.00000	0.00000	0.00000	0.00000	0.00000	0.00000	0.00000	0.00000
Spirochaetes;c__Spirochaetes;f__Spirochaetaceae	0.00008	0.00000	0.00000	0.00000	0.00000	0.00004	0.00008	0.00000	0.00000	0.00025	0.00000	0.00000	0.00004	0.00000	0.00000
Synergistetes;c__Synergistia;f__Aminiphilaceae	0.00000	0.00000	0.00000	0.00000	0.00000	0.00000	0.00000	0.00000	0.00000	0.00004	0.00000	0.00000	0.00000	0.00000	0.00000
Synergistetes;c__Synergistia;f__Dethiosulfovibrionaceae	0.00033	0.00000	0.00000	0.00000	0.00000	0.00000	0.00000	0.00000	0.00000	0.00000	0.00000	0.00000	0.00000	0.00000	0.00000
Synergistetes;c__Synergistia;f__Synergistaceae	0.00000	0.00000	0.00004	0.00000	0.00000	0.00004	0.00000	0.00004	0.00000	0.00004	0.00008	0.00000	0.00000	0.00000	0.00004
TM6;c__SJA-4	0.00000	0.00000	0.00000	0.00000	0.00000	0.00000	0.00067	0.00000	0.00000	0.00000	0.00000	0.00000	0.00000	0.00000	0.00000
TM7;c__TM7-3	0.00000	0.00000	0.00000	0.00000	0.00000	0.00000	0.00000	0.00371	0.00563	0.00025	0.00012	0.00000	0.00121	0.00838	0.00021
TM7;c__TM7-3;f__A29	0.00000	0.00000	0.00000	0.00000	0.00000	0.00000	0.00000	0.00012	0.00000	0.00000	0.00000	0.00000	0.00000	0.00000	0.00000
Tenericutes	0.00000	0.00000	0.00004	0.00000	0.00000	0.00000	0.00000	0.00000	0.00000	0.00000	0.00008	0.00000	0.00000	0.00000	0.00000
Tenericutes;c__Erysipelotrichi;f__Erysipelotrichaceae	0.00500	0.00417	0.03650	0.00500	0.00000	0.00125	0.00737	0.00000	0.00000	0.00000	0.00063	0.00000	0.00000	0.00008	0.00004
Tenericutes;c__Erysipelotrichi;f__vadinHA31;g__RFN20	0.00004	0.00000	0.00000	0.00000	0.00000	0.00000	0.00000	0.00000	0.00000	0.00000	0.00000	0.00000	0.00000	0.00000	0.00000
Tenericutes;c__ML615J-28	0.00000	0.00000	0.00000	0.00000	0.00000	0.00000	0.00000	0.00000	0.00000	0.00000	0.00150	0.00000	0.00000	0.00004	0.00000
Tenericutes;c__Mollicutes	0.00000	0.00000	0.00000	0.00000	0.00000	0.00000	0.00000	0.00004	0.00025	0.00017	0.00400	0.00025	0.00000	0.00037	0.00000
Tenericutes;c__Mollicutes;f__Acholeplasmataceae	0.00008	0.00000	0.00000	0.00000	0.00000	0.00000	0.00000	0.00000	0.00000	0.00000	0.00025	0.00008	0.00000	0.00000	0.00000
Tenericutes;c__Mollicutes;f__Anaeroplasmataceae	0.00000	0.00000	0.00000	0.00000	0.00000	0.00000	0.00000	0.00000	0.00000	0.00000	0.00000	0.00004	0.00000	0.00000	0.00000
Thermi;c__Deinococci;f__Deinococcaceae	0.00050	0.00000	0.00000	0.00000	0.00000	0.00550	0.00354	0.00000	0.00000	0.00033	0.00000	0.00000	0.00000	0.00008	0.00021
Thermi;c__Deinococci;f__Thermaceae	0.00029	0.00000	0.00000	0.00000	0.00000	0.00017	0.00000	0.00000	0.00004	0.00000	0.00000	0.00000	0.00000	0.00000	0.00000
Thermotogae;c__Thermotogae;f__Thermotogaceae	0.00088	0.00000	0.00000	0.00000	0.00000	0.00000	0.00000	0.00000	0.00000	0.00000	0.00000	0.00000	0.00000	0.00000	0.00000
Verrucomicrobia;c__Spartobacteria;f__Spartobacteriaceae	0.00000	0.00004	0.00000	0.00000	0.00000	0.00004	0.00000	0.00000	0.00000	0.00004	0.00000	0.00000	0.00000	0.00000	0.00000
Verrucomicrobia;c__Verrucomicrobiae;f__Verrucomicrobiaceae	0.00000	0.00000	0.00000	0.00000	0.00000	0.00021	0.00071	0.00000	0.00000	0.00000	0.00000	0.00000	0.00000	0.00000	0.00004
WPS-2	0.00000	0.00000	0.00000	0.00000	0.00000	0.00013	0.00013	0.00000	0.00000	0.00000	0.00004	0.00000	0.00000	0.00004	0.00008

Table S3. Microbiota composition in the samples of diet and midgut analysed. Family-level taxonomy was reported when available. The average value of 5 replicates is reported.

Table S4 is available at the following link: https://aem.asm.org/highwire/filestream/208371/field_highwire_adjunct_files/1/AEM.01864-18-sd002.xlsx

Table S4. Microbiota composition in the samples of diet and midgut analysed. Genus-level taxonomy was reported when available. The average value of 5 replicates is reported.

CHAPTER 4

The digestive system of the adult *Hermetia illucens* (Diptera: Stratiomyidae) morphological features and functional properties

The digestive system of the adult *Hermetia illucens* (Diptera: Stratiomyidae): morphological features and functional properties

Daniele Bruno[a,*], Marco Bonelli[b,*], Agustin G. Cadamuro[a], Marcella Reguzzoni[c], Annalisa Grimaldi[a], Morena Casartelli[b], Gianluca Tettamanti[a]

[a]Department of Biotechnology and Life Sciences, University of Insubria, Varese, Italy

[b]Department of Biosciences, University of Milan, Milano, Italy

[c]Department of Medicine and Surgery, University of Insubria, Varese, Italy

*These authors contributed equally.

Corresponding authors:

Morena Casartelli, morena.casartelli@unimi.it

Gianluca Tettamanti, gianluca.tettamanti@uninsubria.it

submitted to *Cell and Tissue Research* in January 2019

ABSTRACT

The larvae of black soldier fly (BSF), *Hermetia illucens* (Linnaeus, 1758) (Diptera: Stratiomyidae), are considered an efficient system for the bioconversion of organic waste into usable products, such as insect protein for animal feed and bioactive molecules. Despite the great interest towards *H. illucens* and its biotechnological applications, information on the biology of this insect is still scarce. In particular, no data on the structural and functional properties of the digestive system of the adult insect are available and it is a common belief that the fly does not eat. In the present work, we therefore investigated the remodeling process of BSF larval midgut during metamorphosis, analyzed the morphofunctional properties of the adult midgut, evaluated if the fly is able to ingest and digest food, and assessed whether the feeding supply influences the adult performances.
Our results show that the larval midgut of *H. illucens* is removed during metamorphosis and a new pupal-adult epithelium, characterized by peculiar features compared to the larval organ, is formed by proliferation and differentiation of intestinal stem cells. Moreover, our experiments indicate that the adult insect possesses a functional digestive system and that food administration affects the longevity of the fly. These data not only demonstrate that the adult BSF is able to eat, but also open up the possibility to manipulate the feeding substrate of the fly to improve its performances in mass rearing procedures.

INTRODUCTION

The larvae of the black soldier fly (BSF), *Hermetia illucens* (Linnaeus, 1758) (Diptera: Stratiomyidae), can convert low-quality biomass, such as food waste, organic residues, and byproducts of the agri-food transformation chain, into nutritionally valuable proteins and bioactive molecules (Cickova et al. 2015; Meneguz et al. 2018; Muller et al. 2017; Nguyen et al. 2015; Vogel et al. 2018). In particular, the high nutritional value of the larvae renders this insect useful for producing feedstuffs (Makkar et al. 2014; Wang and Shelomi 2017). Recently, the European Commission Regulation N°2017/893 partially lifted the feed ban rules regarding the use of processed animal proteins from BSF and six other insect species for aquaculture (European Commission 2017). This change in the European legislative landscape will surely contribute to promoting the development of the insect industry for the feed sector, as demonstrated by the increasing number of insect companies in Europe (Ilkka Taponen's entomology database, https://ilkkataponen.com/entomology-company-database/). However, despite the great interest in BSF, data on the biology of this species remain scarce. In particular, a deep characterization of the morphology, physiology, and development of the alimentary canal, and especially of the midgut, which is responsible for food digestion and nutrient absorption, would not only increase the

information on the biology of this insect, but also provide data that could be exploited to improve the performances of the fly during mass rearing. Another aspect that has been neglected so far concerns the feeding habits of the adult insect. This lack of knowledge could represent a major obstacle to using BSF, since such information is correlated with the safety of the procedures for rearing this insect. In fact, it must be considered that the mouthparts of adult Diptera (Gullan and Cranston 2014), as well as some structures associated to the digestive system (Stoffolano and Haselton 2013), have been implicated in the transmission of pathogens, thus representing a potential risk factor in the use of BSF as feed (EFSA Scientific Committee 2015). The urgent need to investigate the feeding habits of the fly can be further appreciated if we consider that, according to the current literature, but without any supporting experimental data, *H. illucens* does not need to eat or is even considered unable to eat in the adult stage, and therefore it depends exclusively on reserves accumulated during the larval stage (Gobbi et al. 2013; Sheppard et al. 1994; Sheppard et al. 2002; Tomberlin et al. 2009; Tomberlin and Sheppard 2002; Tomberlin et al. 2002). Consequently, only the quality and quantity of food administered to the larvae are considered able to affect the growth, survival, and biological traits of adult flies (Gobbi et al. 2013). For this reason, attention in past years has been focused on how the food ingested by the larva (Gobbi et al. 2013; Nguyen et al. 2013; Tomberlin et al. 2002), rearing temperature (Tomberlin et al. 2009), relative humidity (Holmes et al. 2012), and pupation substrate (Holmes et al. 2013) determine both the morphological and physiological development of the adults, while the alimentary behavior of the fly has been ignored so far. It is noteworthy that in most of these studies no food, or only water, was offered to the flies and, according to the results collected, this did not seem to be a limiting factor for successful reproduction (Sheppard et al. 2002; Tomberlin and Sheppard 2002; Tomberlin et al. 2002). Considering this evidence, the adult stage did not attract the attention of researchers and an accurate study of this developmental stage has never been performed. To our knowledge, only one study has evaluated the longevity of adult BSF fed on sugar, but the functional properties of the digestive system were not considered (Nakamura et al. 2016).

The alimentary canal of insects is organized in three main regions. In addition to the foregut and the hindgut that are involved in food ingestion, storage and grinding, and water and ion absorption, respectively, the midgut represents the central part of the gut and is involved in food digestion and nutrient absorption (Dow 1986). Notwithstanding its apparent simplicity (the insect midgut consists of only a single-layered epithelium surrounded by a basal lamina and striated muscle fibers), it is characterized by a marked regionalization and cellular diversity. This organization is necessary to optimize digestion by enabling sequential functions ranging from enzyme secretion to nutrient absorption and from endocrine signaling to regulation of midgut homeostasis (Dow

1986; Sehnal and Zitnan 1996; Terra 1990; Terra and Ferreira 1994; Terra et al. 1996a; Terra et al. 1996b). In particular, in the nonhematophagous brachycerous Diptera examined so far, the larval midgut presents three regions with differing luminal content pH and morphofunctional properties (Dubreuil 2004; Lemos and Terra 1991; Pimentel et al. 2018; Shanbhag and Tripathi 2009; Terra et al. 1988b). Holometabolous insects undergo significant remodeling of the larval midgut during metamorphosis to fulfill changes in dietary requirements between the larval and the adult stage. The adult midgut of the common fruit fly, *Drosophila melanogaster* (Diptera: Drosophilidae), a model species among Diptera, is generated *de novo* during larva-adult transition. In fact, the larval midgut degenerates completely during metamorphosis and the adult midgut epithelium is formed by proliferation and differentiation of adult midgut precursors, i.e., stem cells, that lie in the basal region of the larval epithelium (Lemaitre and Miguel-Aliaga 2013; Micchelli and Perrimon 2006; Ohlstein and Spradling 2006; Ohlstein and Spradling 2007). The midgut of the adult *D. melanogaster* is characterized by regional variation: although it maintains a tripartite organization that roughly resembles that of the larval midgut, it presents a complex organization and different subregions have been identified according to gene expression patterns and anatomical and histological features (Buchon et al. 2013; Marianes and Spradling 2013). Another peculiar feature of the alimentary canal of the fly is the crop, a bag-like organ that is connected to the gut just before the midgut, where food is mixed, detoxified, and stored (Stoffolano and Haselton 2013).
In the present study we structurally and functionally characterized the midgut of *H. illucens* during the larva-pupa and pupa-adult transition, to investigate the remodeling process of this organ during metamorphosis. To this aim, we analyzed the morphology of the midgut epithelium, the ability of stem cells to proliferate and differentiate into mature cells, and the mobilization of long-term storage molecules. Moreover, we investigated the morphofunctional features of the midgut of the adult insect and its ability to ingest and digest food by means of vital stains and fluorescent molecules, and measuring digestive enzyme activity.
Our results demonstrate that the larval midgut of *H. illucens* is completely removed during metamorphosis and a new pupal-adult epithelium, characterized by peculiar features, is progressively formed by the proliferation and differentiation of stem cells. Moreover, the feeding habits of the adult insect and the morphofunctional features of its digestive system demonstrate that *H. illucens* fly, at variance with information reported in literature, can ingest and digest food and that this has an impact on its lifespan.

MATERIALS AND METHODS

Experimental animals

H. illucens larvae, pupae, and adults used in this study were obtained from a colony established in 2015 at the University of Insubria (Varese, Italy) starting from larvae purchased from a local dealer (Redbug, Italy). Table 1 reports definition and description of the developmental stages of *Hermetia illucens*.

The larvae were reared on standard diet for Diptera (Hogsette 1992) as previously reported (Pimentel et al. 2017). After eclosion, the flies were maintained at 27.0 ± 0.5°C and 70 ± 5% relative humidity. A 36W/765 FLUO lamp (Osram, Munich, Germany) guaranteed a 12:12-h light:dark photoperiod. The insects were anesthetized on ice prior to dissection. As preliminary investigation did not show any significant differences between the sexes, the midguts from both males and females were used for all the analyses on the flies.

Stage	Larva	Prepupa	Pupa
Cuticle	Light brown color	Brown color	Dark brown color
Motility	High	High	Decreases along the stage
Lifespan	17 days	24-48 h	12 days
Feeding habits	Active feeding	No feeding	No feeding

Table 1. Definition and description of the developmental stages of *Hermetia illucens*. Rearing conditions are reported in Materials and Methods.

Scanning electron microscopy (SEM)

For three-dimensional SEM imaging, head samples were fixed with 4% glutaraldehyde in 0.1 M Na-cacodylate buffer (pH 7.4) for 1 h at room temperature. After washes in Na-cacodylate buffer, specimens were postfixed in a solution of 1% osmium tetroxide and 1.25% potassium ferrocyanide for 1 h. Samples were then dehydrated in an increasing series of ethanol and washed twice (8 min each) with hexamethyldisilazane. Dried samples were mounted on stubs, gold-coated with a Sputter K250 coater, and then observed with a SEM-FEG XL-30 microscope (Philips, Amsterdam, The Netherlands).

Light microscopy and transmission electron microscopy (TEM)

The midgut was isolated from last instar larvae, pupae (day 4, 8, and 10), and flies (day 1) and immediately fixed in 4% glutaraldehyde (in 0.1 M Na-cacodylate buffer, pH 7.4) overnight at 4°C. After postfixation in 2% osmium tetroxide for 1 h, samples were dehydrated in an ethanol series and embedded in resin (Epon/Araldite 812 mixture). Semi-thin sections were stained with crystal violet and basic fuchsin and observed by using a Nikon Eclipse Ni-U microscope (Nikon, Tokyo, Japan) equipped with a TrueChrome II S digital camera system (Tucsen Photonics, Fuzhou, China). Thin sections were stained with uranyl acetate and lead citrate and observed by using a Jeol JEM-

1010 electron microscope (Jeol, Tokyo, Japan) equipped with an Olympus Morada digital camera (Olympus, Tokyo, Japan).

Analysis of stem cell proliferation

Midguts were isolated from pupae (day 4, 8, and 10) and flies (day 1) and homogenized with a T10 basic ULTRA-TURRAX (IKA, Staufen im Breisgau, Germany) in 1 ml/0.14 g tissue of RIPA buffer (150 mM NaCl, 1% NP-40, 0.5% sodium deoxycholate, 0.1% SDS, 50 mM Tris, pH 8.0), to which 1× protease inhibitor cocktail (Sigma-Aldrich, Saint Louis, Missouri, USA) was added. Homogenates were clarified by centrifugation at 15,000 × *g* for 15 min at 4°C and supernatants were denatured by boiling the samples in 4× gel loading buffer for 5 min. SDS-PAGE was performed on a 12% acrylamide gel by loading 60 µg protein per lane. After electrophoretic separation, proteins were transferred onto nitrocellulose membranes (Merck-Millipore, Burlington, Massachusetts, USA). Membranes were saturated with a solution of 5% milk in Tris-buffered saline (TBS) (50 mM Tris-HCl, 150 mM NaCl, pH 7.5) for 2 h at room temperature and subsequently incubated for 1 h at room temperature with anti-phospho-histone H3 (H3P) antibody (dilution 1:1,000 in 2% milk in TBS; Merck-Millipore) and anti-GAPDH antibody (dilution 1:2,500 in 5% milk in TBS; Proteintech, Rosemont, Illinois, USA) to ensure equal gel loading. Antigens were revealed with an anti-rabbit HRP-conjugated secondary antibody (diluted 1:7,500; Jackson ImmunoResearch Laboratories, West Grove, Pennsylvania, USA) and immunoreactivity was detected with SuperSignal chemiluminescence substrates (Thermo Fisher Scientific, Waltham, Massachusetts, USA).

Histochemistry

Midgut samples were isolated from last instar larvae and pupae (day 4 and 8), embedded in polyfreeze cryostat embedding medium after dissection, and stored in liquid nitrogen until use. Subsequently, 7-□m-thick cryosections were obtained with a Leica CM 1850 cryostat and slides were immediately used or stored at -20°C. Sections were processed with Bio-Optica Histopatological kit (Bio-Optica, Milano, Italy) to reveal lipid droplets (Oil red O staining) and glycogen (Periodic acid-Schiff, PAS, staining) in the midgut tissue. PAS reaction was also performed in combination with diastase (PAS-D), which breaks down glycogen, to confirm the presence of this polysaccharide. Stainings were performed according to the manufacturer's instructions.

DNA fragmentation analysis

Midguts were dissected from pupae (day 4, 8, and 10) and immediately frozen in liquid nitrogen. Genomic DNA was extracted from 15 mg of midgut tissue using the PureLink Genomic DNA kit (Life Technologies, Carlsbad, California, USA) according to the manufacturer's instructions. After

spectrophotometric quantification, 200 ng of genomic DNA were loaded on 1% agarose gel to which EuroSafe (Euroclone, Pero, Italy) was added for DNA staining. Electrophoresis was performed at 100 V for about 45 min and the gel was then observed with a UV transilluminator.

Enzyme assays

Midguts with the enclosed luminal content were dissected from adults (day 4) fed *ad libitum* with banana pulp and immediately frozen in liquid nitrogen.

The total proteolytic activity was assayed with azocasein (Sigma-Aldrich) (Caccia et al. 2014; Charney and Tomarelli 1947; Vinokurov et al. 2006). Frozen samples of midgut were thawed at 4°C and homogenized in 1 ml/100 mg tissue of Universal Buffer (UB) at pH 8.5 (Coch Frugoni 1957). Samples were then centrifuged at 15,000 × g for 10 min at 4°C and supernatant was collected. Protein concentration was determined by Bradford method (Bradford 1976). Different volumes of homogenate were diluted to 100 µl with UB at pH 8.5, 200 µl of 1% (w/v) azocasein solution dissolved in the same buffer were added to the samples and the mixtures were incubated for 30 min at 45°C. The reaction was stopped by adding 300 µl of 12% (w/v) trichloroacetic acid at 4°C. The samples were maintained for 30 min on ice and then centrifugated at 15,000 × g for 10 min at 4°C. An equal volume of 500 mM NaOH was added to the supernatant, and the absorbance was measured at 440 nm. One unit (U) of total proteolytic activity with azocasein was defined as the amount of enzyme that causes an increase in absorbance by 0.1 unit per min per mg of proteins.

α-amylase activity was assayed using starch as substrate (Bernfeld 1955). A standard curve was determined through linear regression of the maltose absorbance at 540 nm. Frozen samples of midgut were thawed at 4°C and homogenized in 1 ml/100 mg tissue of amylase buffer (AB) (20 mM NaH_2PO_4, 6.7 mM NaCl, pH 6.9). Samples were then centrifuged at 15,000 × g for 10 min at 4°C and supernatant was collected. Protein concentration was determined and different volumes of homogenate were diluted to 595 µl with AB. Then, 90 µl of 1% (w/v) soluble starch solution in AB were added to the samples. Controls without homogenate and controls without substrate were performed for each experiment. All samples were incubated for 30 min at 45°C, and, after adding 115 µl of Color Reagent Solution (1 M sodium potassium tartrate, 48 mM 3,5-dinitrosalicylic acid, 0.4 M NaOH), were heated at 100°C for 15 min, then cooled in ice to 25 °C, and their absorbance was measured at 540 nm. One unit of α-amylase activity (U) was defined as the amount of enzyme necessary to produce 1 mg of maltose per min per mg of proteins.

The activity of aminopeptidase N (APN) was assayed using L-leucine p-nitroanilide (Sigma-Aldrich) as substrate (Franzetti et al. 2015) and measuring its degradation by release of p-nitroaniline (pNA). Frozen samples of midgut were thawed at 4°C and homogenized in 1 ml/100

mg tissue of Tris-HCl 50 mM, pH 7.5. Samples were then centrifuged at 15,000 × g for 10 min at 4°C and supernatant was collected. Protein concentration was determined and different volumes of homogenate were diluted to 800 µl with the same buffer; then, 200 µl of 20 mM L-leucine p-nitroanilide were added. Samples were subjected to continuous absorbance reading at 410 nm at 45°C. One unit/mg protein (U/mg) of APN activity was defined as the amount of enzyme that releases 1 µmol of pNA per min per mg of proteins.

Sucrose hydrolysis in midgut samples was measured using the Invertase Activity Colorimetric Assay Kit (BioVision, Milpitas, California, USA). Frozen samples of midgut were thawed at 4°C and homogenized in Invertase Hydrolysis buffer provided with the kit (40 µl buffer/1 mg of midgut sample). The homogenate was centrifuged at 15,000 × g for 10 min at 4°C, and the supernatant was collected and processed according to the manufacturer's instructions.

RT-PCR

Midguts were collected from flies just after eclosion. Insects were dissected on ice and immediately frozen in liquid nitrogen until use. Total RNA was isolated from 15 mg of frozen tissue using TRIzol reagent (Life Technologies) according to the manufacturer's instructions. RNA was treated with a TURBO DNA-free Kit (Life Technologies) to remove possible genomic DNA contamination, and its integrity was assessed by electrophoresis. RNA was retrotranscribed to cDNA using M-MLV reverse transcriptase (Life Technologies) (Montali et al. 2017). PCR was performed using GoTaq DNA Polimerase (Promega, Madison, Wisconsin, USA) (95°C for 30 s, Tm - 2°C for 30 s, 72°C for 30 s, 35 cycles) and a MyCycler Thermal Cycler System (Bio-Rad, Hercules, California, USA). The primers used for PCR are listed in Table 2. The primers for *Hiα-glucosidase* were designed on conserved regions of this gene in other insect species and the sequence was checked by sequencing the PCR product.

Gene name	Accession number	Primer sequences	T melting	Length of amplificate
HiTrypsin	HQ424575	F: ATCAAGGTCTCCCAGGTC	56 °C	126 bp
		R: GGCAAGAGCAATAAGTTGGAT		
HiChymotrypsin	HQ424574	F: AGAATGGAGGAAAGTTGGAGA	57 °C	109 bp
		R: CAATCGGTGTAAGCAGAGACA		
Hiα-glucosidase		F: GGCTTTCAGTTGCTCCGTTA	58 °C	127 bp
		R: AGGCTCGTTATTGATGTCGC		

Table 2. Sequence of primers used in this study.

Analyses of food transit along the alimentary canal

To demonstrate the food transit along the alimentary canal of the adult insect, flies were collected just after eclosion, divided into separate groups (10 flies/group), and kept in a 165 x 30 mm Petri dish. A filter paper (214 cm^2) was put on bottom of the Petri dish. The experimental groups were subjected to the following treatments: 1) no feeding (control) and 2) feeding *ad libitum* with banana + 2% (w/w) purple food coloring. The groups were monitored daily and the color and number of spots observed on the filter paper were recorded until the flies died. Each condition was performed in triplicate. Flies fed with banana and food coloring (treatment 2) for 4 days were also video recorded to evaluate the release of fecal spots. Video recordings were performed with a camera with a macro lens (Canon EOS 550D equipped with Canon EF-S 60 mm f/2.8 Macro USM, Canon Inc., Tokyo, Japan) fixed onto a tripod placed under a Petri dish containing six BSF adults. The bottom of the Petri dish was covered with a white sheet.

The following treatments were performed to directly visualize the food transit in the midgut of the adult insect: 1) no feeding or feeding *ad libitum* with banana (controls); 2) feeding *ad libitum* with banana + 1.25% (w/w) FITC (Sigma-Aldrich); and 3) feeding *ad libitum* with banana + 3.75% (w/w) 25 nm gold-conjugated protein A (Electron Microscopy Sciences, Hatfield, Pennsylvania, USA). For all treatments, flies were dissected every 24 hours from 1 to 6 days after beginning of the experiment. For the first and second treatments the alimentary canal was mounted with Citifluor (Electron Microscopy Sciences) on a glass slide and observed under a fluorescent microscope (filter 488 nm). Presence of green fluorescence was also analyzed on the labella, dorsal and ventral translucent windows on the abdomen, and on the spots released on the filter paper. For the third treatment the alimentary canal was processed for TEM analysis as described in the section "Light microscopy and transmission electron microscopy".

Fly longevity

Forty newly emerged flies (<15 h after eclosion) were placed in 30 x 30 x 30-cm cages and maintained under the environmental conditions reported in the section "Experimental animals". The flies were reared in different conditions: 1) no food or water (starved); 2) only water (water); and 3) water and sugar cube (sugar). Water was provided to the animals in a 50-ml plastic tube containing cotton. Each experimental condition was performed in triplicate. The survival of the flies under different conditions was recorded every day.

Statistical analyses were performed with R-statistical software (ver. 3.3.2). One-way analysis of variance (ANOVA) with longevity as the dependent variable followed by Tukey's test was performed. Statistical differences between groups were considered significant at p-value ≤ 0.05.

RESULTS

Morphological analysis of the fly mouthparts

The adult Diptera, depending on dietary habits, exhibit a great variety of modifications of the mouthparts, but in all of them the food canal is formed between the apposed labrum and labium and the salivary canal runs through the hypopharynx. BSF showed typical sponging mouthparts. As common in nonhematophagous Diptera, the mandibles and maxillae were lacking and the distal part of the labium was expanded to form the labella (Fig. 1a) which were traversed by a series of grooves known as pseudotracheae (Fig. 1b). These structures were maintained open by cuticular ribs (Fig. 1c), giving them a superficial similarity to tracheae, and converged centrally on the distal end of the food canal. Prestomal tooth-like structures (Fig. 1b) could be used to scrape semi-solid feeding substrates. Similar teeth are present in other Brachycera, including the housefly, *Musca domestica* Linnaeus, 1758 (Diptera: Muscidae) (Broce and Elzinga 1984; Giangaspero and Broce 1993; Kovacs et al. 1990). The mouthparts presented many sensilla (Fig. 1b) protruding from the cuticle, which are probably involved in chemo- and mechano-reception.

The morphological features of BSF mouthparts indicated that the adult insect can ingest food and prompted us to investigate the digestive apparatus of the fly.

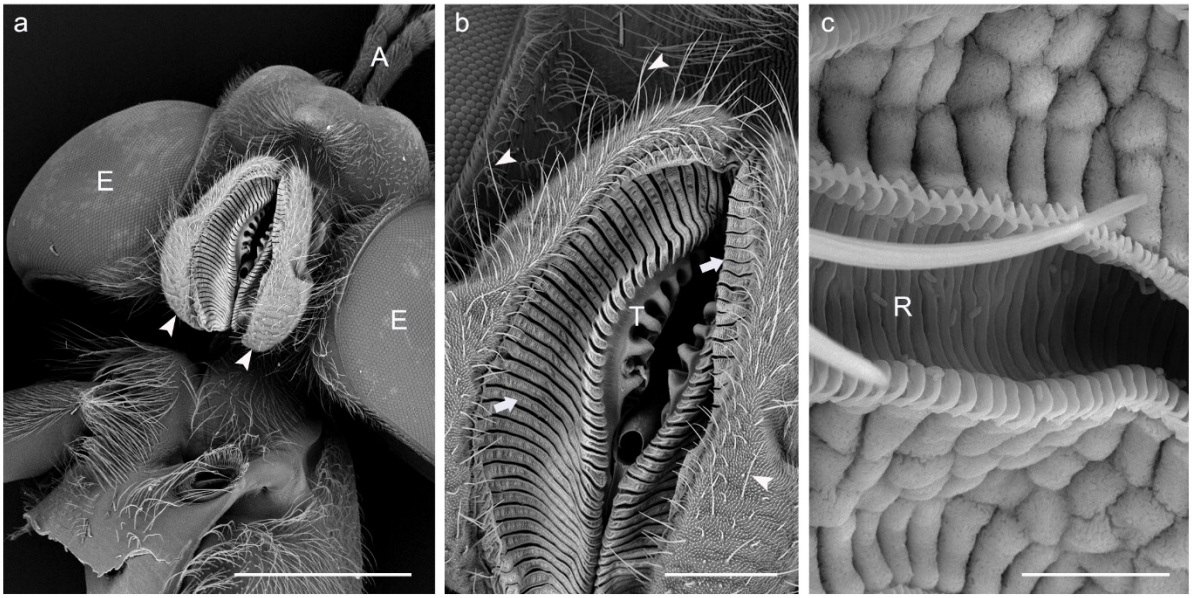

Figure 1. SEM analysis of BSF adult mouthparts. (a) Ventral view of BSF head in which everted labella (arrowheads) are visible. (b) View of the sponging mouthparts where tooth-like structures (T), pseudotracheae (arrows), and sensilla on the labella (arrowheads) can be observed. (c) Detail of pseudotracheae characterized by cuticular ribs (R). A: antennae; E: compound eye. Bars: 1 mm (a), 200 µm (b), 10 µm (c).

Modification of the alimentary canal during metamorphosis: degeneration of the larval midgut epithelium and differentiation of the pupal-adult midgut

In holometabolous insects the remodeling of the larval midgut is a key process that occurs during metamorphosis (Hakim et al. 2010); therefore, we first investigated the morphology of the alimentary canal during the larva-pupa molt.

Although regional differentiation was observed along the anteroposterior axis of the larval midgut of *H. illucens* (Bonelli et al. unpublished data), this organ consisted of a monolayered epithelium, mainly formed by columnar cells, organized over a thin basal lamina and encircled by an extraepithelial layer composed of muscle fibers (Fig. 2a). Sparse stem cells were localized in the basal region of the epithelium (Fig. 2a). During the early pupal stage (up to day 4), the general morphology of the midgut epithelium was maintained and columnar cells could still be identified (Figs. 2b, e), while at pupa day 8 the presence of a large number of stem cells could be observed in the basal part of the epithelium (Figs. 2c, f). At late pupal stage (day 10), a newly forming epithelial layer was visible, while the larval cells were pushed in the lumen (Figs. 2d, g). The proliferation of stem cells at pupa day 8 was confirmed by western blot analysis of H3P, showing a high expression of this mitotic marker (Fig. 2h). The mitotic activity was also maintained at later stages (pupa day 10), close to the pupa-adult molt, but no signal was detected in the adult midgut (Fig. 2h).

During the pupal stage (day 8-10) the newly forming midgut was characterized by features that are typical of a secretory/absorptive epithelium (Figs 2i-l). In fact, the apical membrane formed microvilli (Fig. 2i), abundant rough endoplasmic reticulum and mitochondria could be observed in the cytoplasm (Fig. 2j), and the cells were linked by septate junctions (Fig. 2k). Moreover, glycogen granules and lipid droplets were present in the cytoplasm (Figs. 2i, l). On the other hand, the old larval epithelium underwent a consistent remodeling during the pupal stage. In fact, the cells gave rise to a compact mass (called “yellow body”) that later detached from the newly forming epithelium (Figs. 2d, g, m). Although during the removal of the larval midgut epithelium clear signs of degeneration could be detected in some cells, i.e., vacuolization of the cytoplasm (Figs. 2m, n) and unusual organization of the nuclear chromatin (Fig. 2o), the large part of the cells showed an intact morphology (Fig. 2o) during pupal stage.

Given the presence of condensed chromatin in some yellow body cells, we investigated the occurrence of apoptosis in the midgut undergoing remodeling. Quite surprisingly, DNA ladder analysis did not show any DNA fragmentation in the degenerating larval tissue (Fig. 2p).

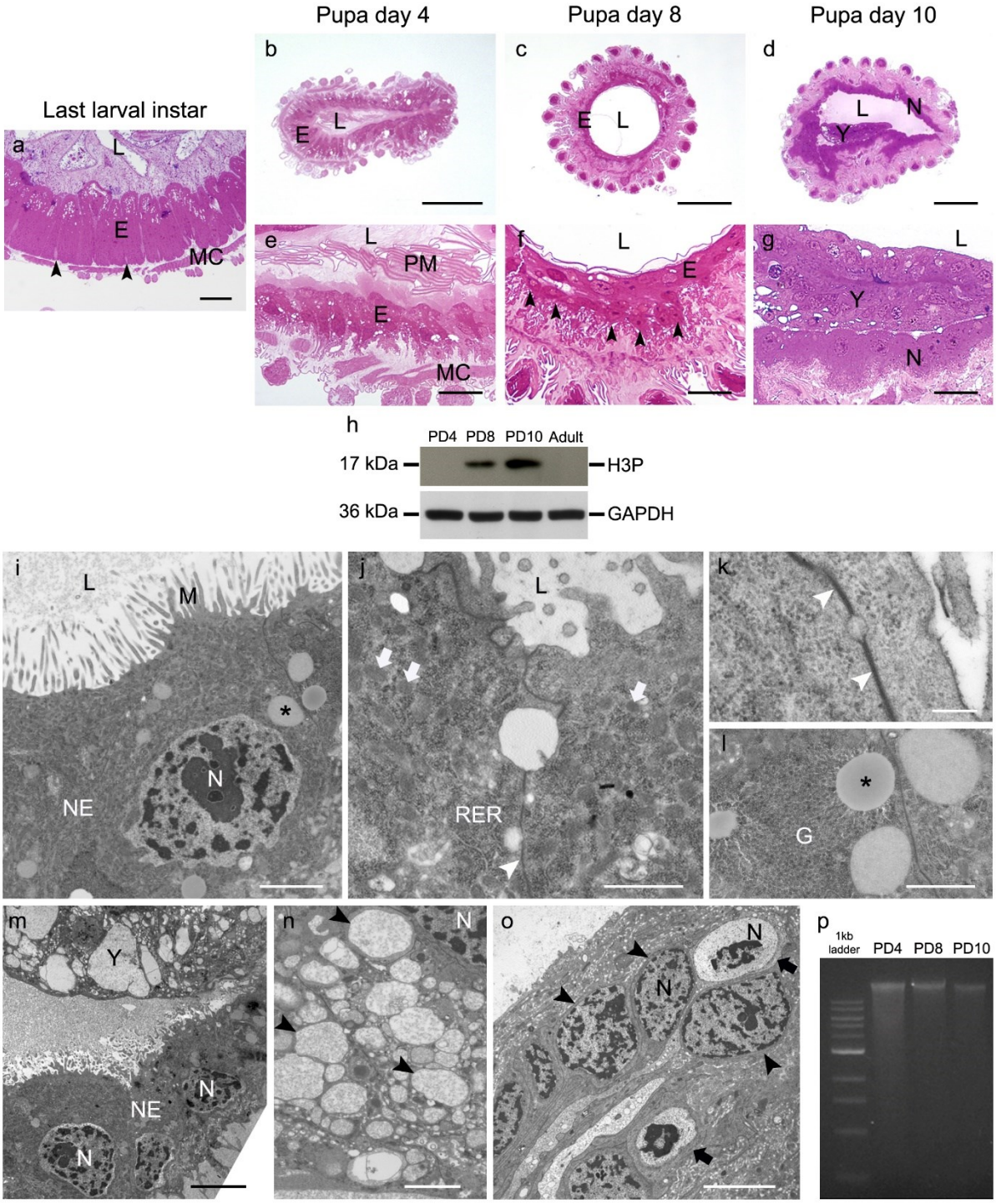

Figure 2. Modification of the larval midgut during metamorphosis and ultrastructural analysis of pupal midgut. (a) Cross-section of the midgut epithelium of last instar larvae. Stem cells (arrowheads) are visible at the base of the epithelium. (b, e) Cross-sections of the midgut epithelium of day 4 pupae. (c, f) Cross-sections of the midgut epithelium of day 8 pupae. A high number of stem cells (arrowheads) are recognizable at the base of the epithelium. (d, g) Cross-sections of the midgut epithelium of day 10 pupae. The larval midgut detaches from the newly forming epithelium (N) and is pushed toward the lumen, forming the yellow body (Y). (h) Western blot analysis of phospho-histone H3 (H3P). (i-l) The newly forming midgut epithelium (NE) displays microvilli (M) in the apical membrane (i), abundant rough endoplasmic reticulum (RER), and mitochondria (arrows) in the cytoplasm (j). Septate junctions (arrowheads) are present among columnar cells (j, k). Glycogen (G) and lipid droplets (asterisks) can be observed in the cytoplasm (i, l). (m) The newly forming midgut epithelium (NE) progressively detaches from the larval midgut, which forms the yellow body (Y). (n) Vacuoles (arrowheads) in the cytoplasm of yellow body cells

(o) Yellow body that contains a high number of cells with an intact nucleus (arrowheads) and some cells with pyknotic nuclei (arrows). (p) Ladder analysis of genomic DNA from midgut cells at pupa day 4, 8, and 10. (e, f, g) are details at higher magnification of (b, c, d), respectively. E: epithelium; L: lumen; MC: muscle cells; N: nucleus; PM: peritrophic matrix. Bars: 25 µm (a, e-g), 100 µm (b-d), 2 µm (i, n), 1 µm (j, l), 500 nm (k), 5 µm (m, o).

The histochemical analysis gave evidence that long-term storage molecules were mobilized during larva-pupa transition: in particular, a reduction of glycogen (Figs. 3a-c) and lipid (Figs. 3g-i) reservoirs was detected in the larval midgut epithelium at early pupal stage (Figs. 3a, b, g, h) and no reactivity was present inside the yellow body (Figs. 3c, i). Specificity of the PAS reaction towards glycogen was confirmed by treatment with diastase (Figs. 3d-f).

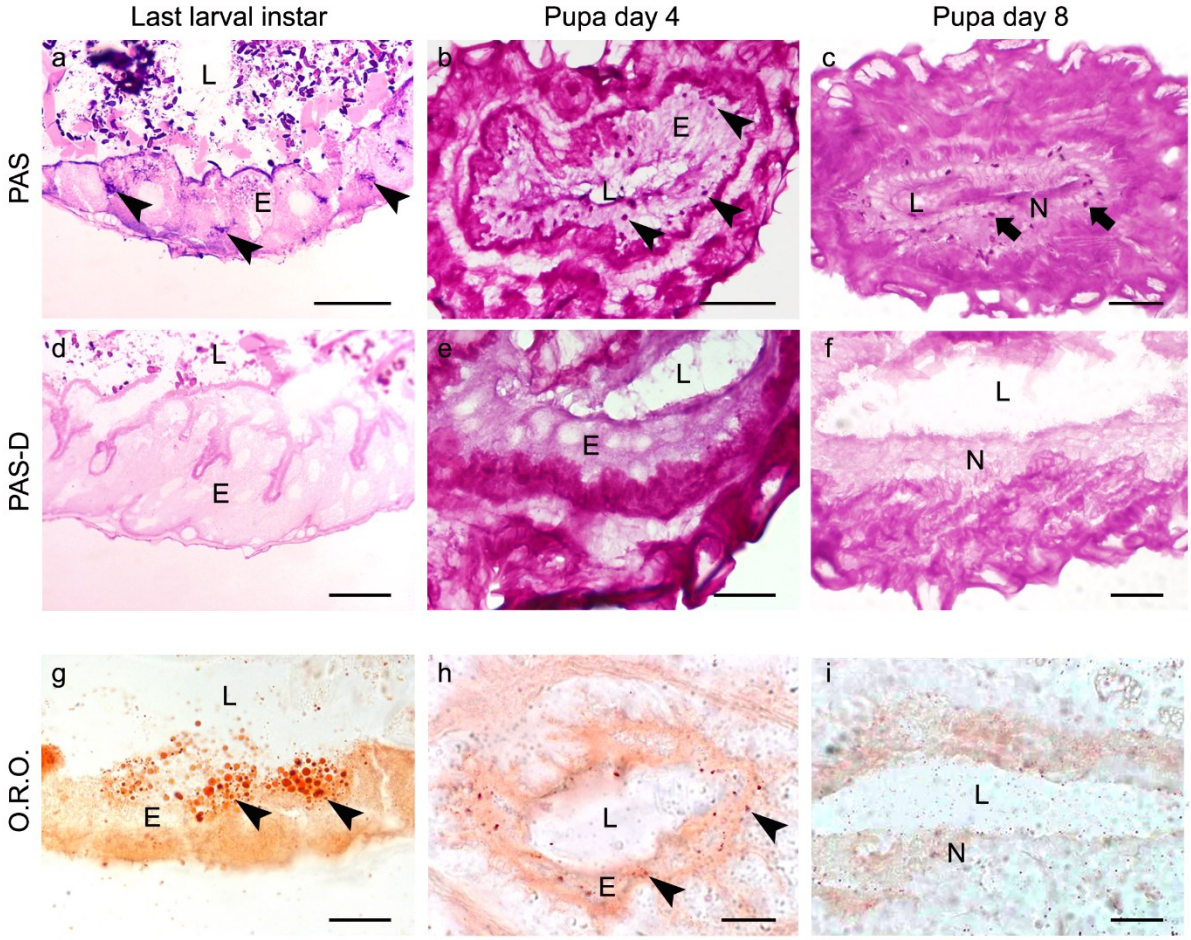

Figure 3. Histochemical analysis of the midgut epithelium. (a-c) PAS. Staining for PAS reveals that glycogen deposits (purple, arrowheads) disappear in the larval midgut epithelium at pupal stage. A signal is visible only in the newly forming midgut epithelium (arrows). (d-f) Glycogen deposits disappear after the treatment with diastase (PAS-D). (g-i) O.R.O. Staining for O.R.O. shows that lipid droplets (red, arrowheads) disappear in the larval midgut epithelium at pupal stage. E: larval epithelium, L: lumen; N: newly forming epithelium. Bars: 50 µm (a, b), 20 µm (c-e, g, h), 10 µm (f, i).

Morphological analysis of the adult midgut

The new midgut epithelium observed in late pupae (day 10), just before the adult emerged, was retained in the fly, where it further differentiated. The midgut of the adult insect was subdivided

into three morphologically distinct regions: while the anterior and posterior districts were thin and tubular structures, the middle region appeared as an enlarged compartment (Fig. 4a). A large crop was associated to the foregut (Fig. 4b). The regional organization of the central part of the alimentary canal of the fly was supported by the histological analysis showing a different organization of the epithelium along the midgut (Figs. 4c-h). While the anterior (Figs. 4c, f) and posterior (Figs. 4e, h) midgut were lined by a thick and infolded epithelium, a wide lumen was surrounded by a thin and unfolded cell monolayer in the middle region (Figs. 4d, g).

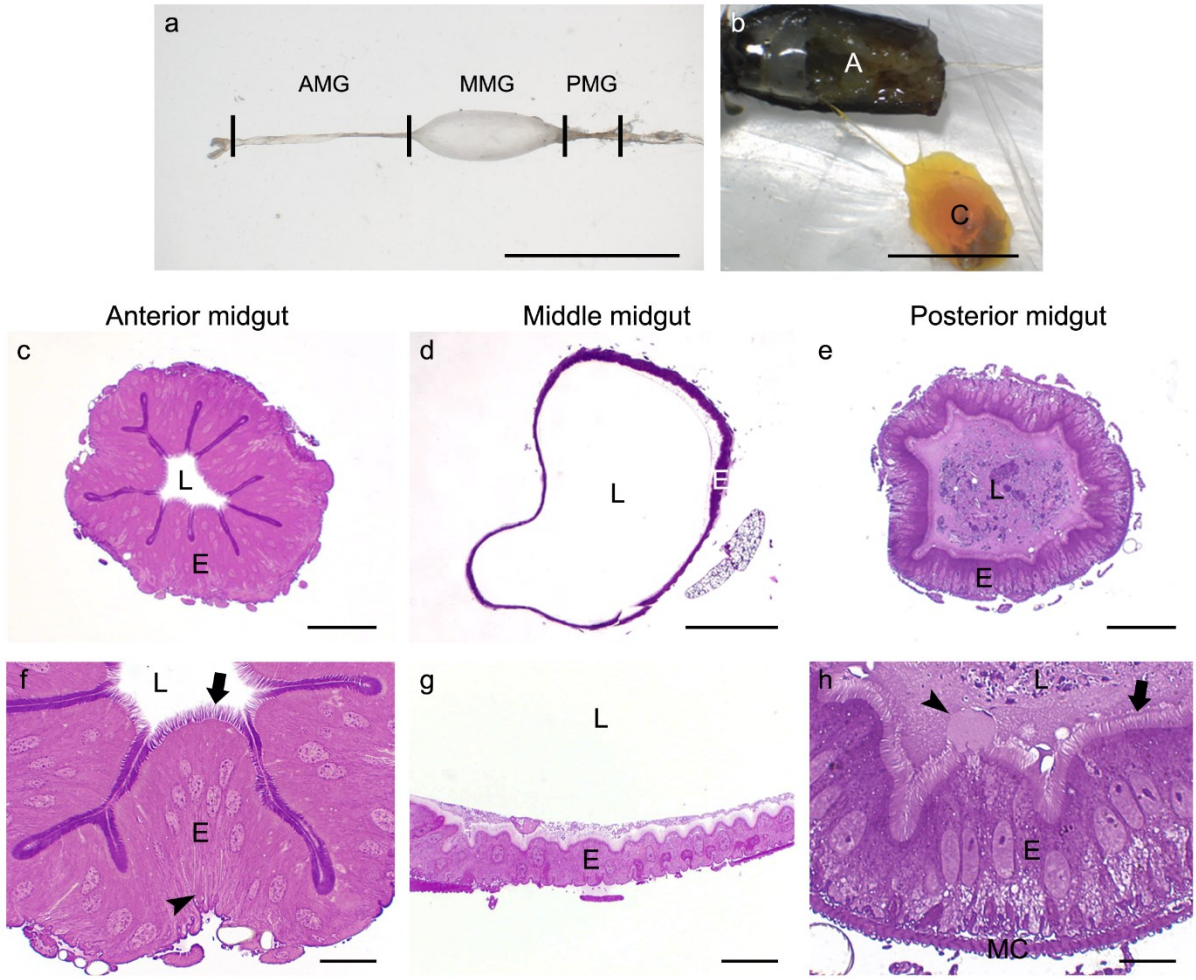

Figure 4. Morphological analysis of the adult midgut. (a) General view of the adult midgut subdivided in anterior (AMG), middle (MMG), and posterior (PMG) midgut. (b) General view of the crop (C) associated to the gut. (c, f) Cross-section of the anterior midgut characterized by a thick epithelium with apical brush border (arrow) and developed basal infolding (arrowhead). (d, g) Cross-section of the middle midgut that shows a very thin epithelium. (e, h) Cross-section of the posterior midgut characterized by a thick epithelium with developed brush border (arrow) and apocrine secretion (arrowhead) in the apical membrane. (f, g, h) are details at higher magnification of (c, d, e), respectively. A: abdomen of the fly; E: epithelium; L: lumen; MC: muscle cells. Bars: 5 mm (a), 3 mm (b), 50 µm (c, e), 200 µm (d), 10 µm (f-h).

Columnar cells represented the main cell type found in all the three midgut districts. These cells, although characterized by a different thickness in the various districts, always showed a wide basal infolding (Fig. 5a) and apical brush border (Fig. 5b), and were linked by septate junctions (Fig. 5c). A great number of mitochondria was present in the apical region of the cells (Figs. 5b, d). Glycogen granules and abundant rough endoplasmic reticulum were visible in the cytoplasm (Fig. 5d). This evidence correlated well with a consistent secretory activity. In fact, we observed microvilli with an enlarged tip (Fig. 5e), a feature typical of microapocrine secretion, and the release of secretory vesicles along the apical surface of the epithelium (apocrine secretion) (Terra and Ferreira 2005) (Fig. 5f). Interestingly, the peritrophic matrix was not present and the lumen content was in direct contact with the brush border (Figs. 5g, h). The midgut epithelium was supported by a thick basal lamina (Fig. 5i) and muscle (Fig. 5a). In all three midgut regions, endocrine cells localized in the basal region of the epithelium (Fig. 5j), containing electron-dense granules in the cytoplasm (encircled by a membrane) (Fig. 5k), were visible. Sparse, small round cells were localized in the basal region of the epithelium (Fig. 5l): due to their undifferentiated morphology and high nucleus-to-cytoplasm ratio, they could be classified as stem cells. Neither morphological analysis nor feeding assay with cupric chloride and pH lumen measurement indicated the presence of copper cells in the epithelium (Supplementary 1).

Some yellow body cells could be observed in the midgut lumen: similarly to the yellow body cells observed at pupal stage (Fig. 2g), these cells showed a vacuolated cytoplasm, but the nucleus appeared intact (Fig. 5m).

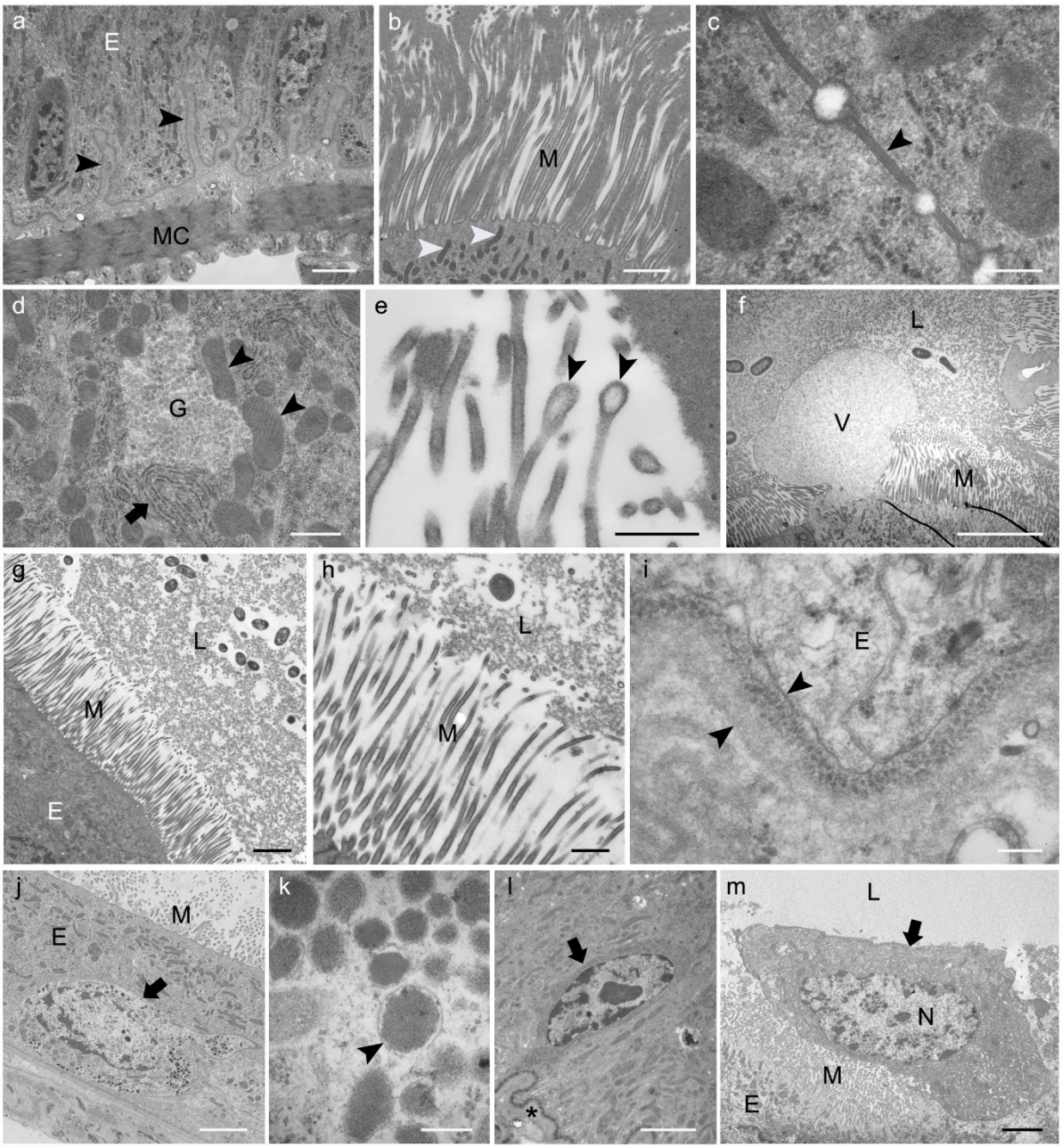

Figure 5. Ultrastructural analysis of the adult midgut - TEM. (a) A thick muscle layer (MC) surrounds the epithelium, characterized by developed basal infolding (arrowheads). (b) A high number of mitochondria (arrowheads) are present in the apical region of the cells, under the brush border (M). (c) Detail of septate junctions (arrowhead) between two columnar cells. (d) Glycogen granules (G), abundant rough endoplasmic reticulum (arrow) and mitochondria (arrowheads) are visible in the cytoplasm. (e) Apical microvilli show enlarged tips (arrowheads). (f) Secretion vesicles (V) can be observed in the apical membrane of the cells. (g, h) The lumen content (L) is in direct contact with the brush border (M) due to the absence of a peritrophic matrix. (i) A thick basal lamina (arrowheads) supports the midgut epithelium. (j, k) Endocrine cells (arrow) are located at the base of the epithelium (j). Their cytoplasm is filled with a high number of electron-dense granules encircled by a membrane (arrowhead) (k). (l) Detail of a stem cell (arrow) located at the base of the epithelium. Asterisk indicates the basal lamina. (m) Yellow body cell (arrow), localized in the midgut lumen close to the newly forming epithelium, characterized by an intact nucleus (N). E: epithelium; L: lumen; M: microvilli. Bars: 2 µm (a, g, h, j, l, m), 1 µm (b), 500 nm (d, e), 200 nm (c, i, k), 5 µm (f).

Analysis of the ingested food transit in the adult midgut and its digestive capability

We first performed feeding experiments to evaluate the function of the alimentary canal in the fly (i.e., the ability of the adult insect to ingest food and move the bolus along the organ). Flies were fed *ad libitum* with banana and FITC, and the midgut isolated from the insects was observed under a fluorescent microscope. Four days after the food substrate was administered, the whole midgut was characterized by a green fluorescence that could not be detected in the midgut of flies subjected to starvation or fed only with banana (controls) (Figs. 6a, a'). In addition, the analysis of the labella (Figs. 6b, b'), of the dorsal and ventral translucent windows on the abdomen (Figs. 6c-d'), and of the fecal spots (Figs. 6e, e') revealed green fluorescence only in animals fed with banana and FITC. These results confirmed that the fluorescent dye, after being ingested, passed through the midgut and was released by the anus.

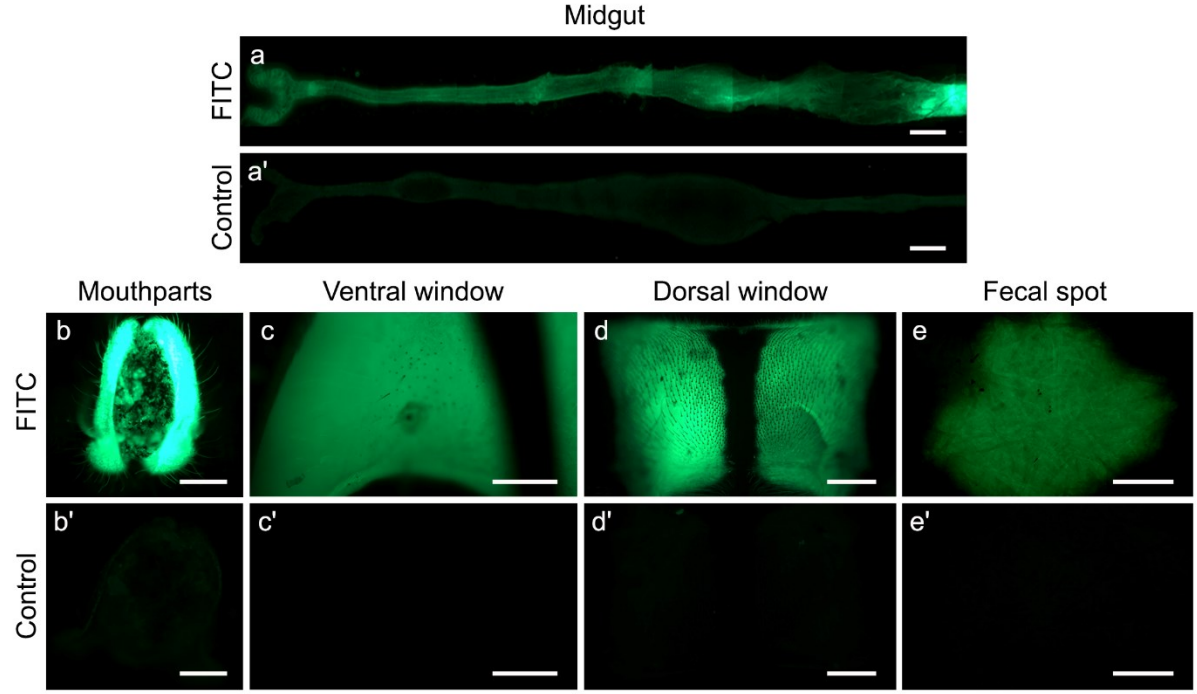

Figure 6. Analysis of the transit of ingested food - FITC. (a-d) Midgut, mouthparts, and ventral and dorsal translucent windows of flies fed with banana and FITC. (e) Fecal spot produced by flies fed with banana and FITC. (a'-e') Midgut, mouthparts, and ventral and dorsal translucent windows, and fecal spot of unfed flies or fed with banana (control). Bars: 500 μm (a, a', e, e'), 250 μm (b-d, b'-d').

To better analyze the food transit along the digestive system, flies were fed with banana and purple food coloring, and the fecal spots released by the insects on the filter paper on the bottom of the Petri dish were analyzed and counted. As shown in Figures 7a-c, while in control insects (no food substrate administered) some spots were observed from day 1 to day 6, the number of fecal spots rapidly increased from day 1 up to day 12 in animal fed with food coloring. It is noteworthy that, while in control flies the color of the spot was light brown, the spots were dark purple in fed animals (Figs. 7d, e), thus demonstrating the transit of the stain throughout the alimentary canal.

Production of fecal spots could be clearly observed in the video (Figs. 7f-h' and Supplementary 2).

To confirm that the adult insect was able to ingest food and the bolus transited along the alimentary canal, the midgut of flies fed with gold-conjugated protein A was isolated six days after administering the food substrate and analyzed at the ultrastructural level. TEM analysis demonstrated the presence of gold particles in the midgut lumen (Figs. 7i, j).

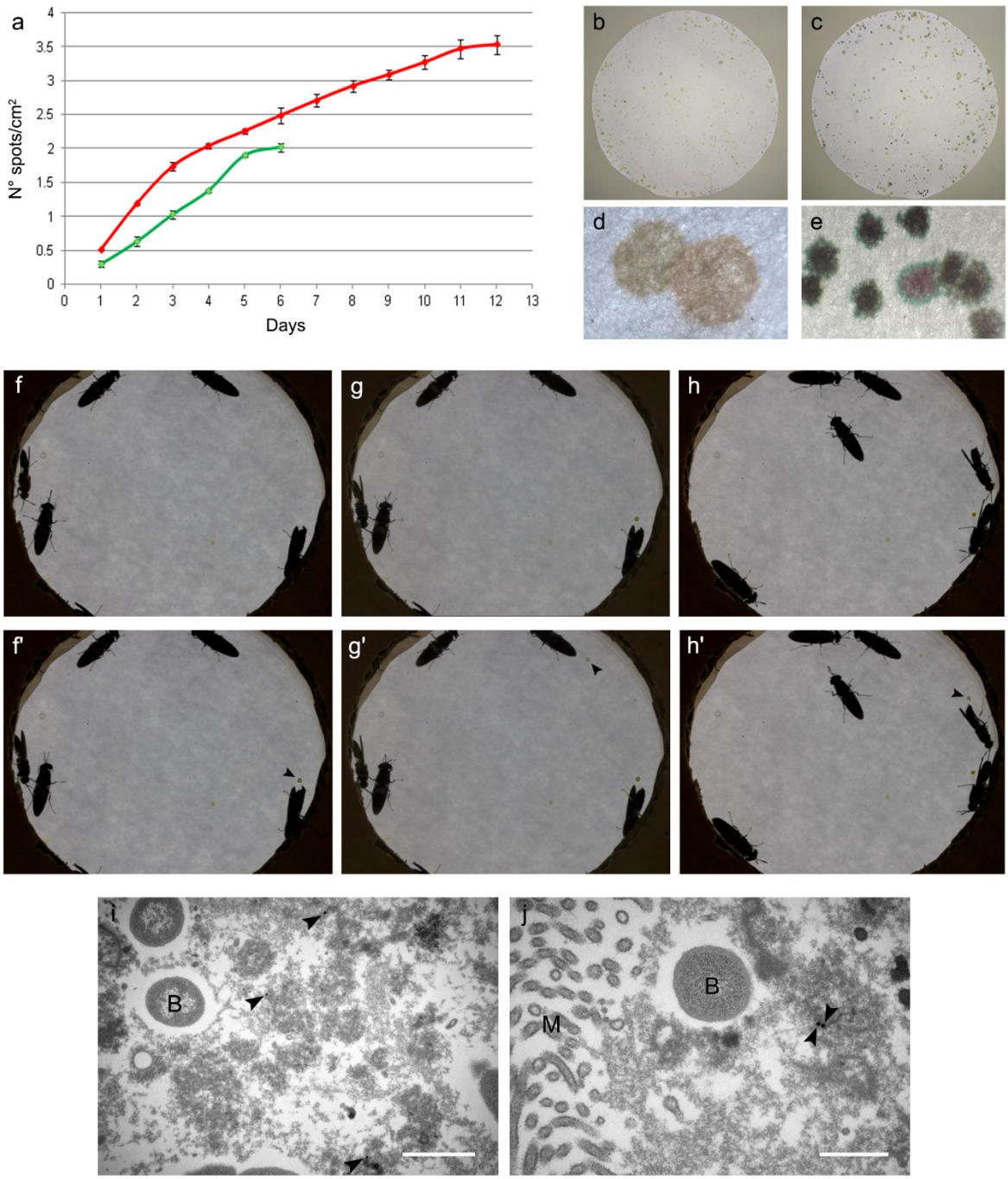

Figure 7. Evaluation of the transit of ingested food - Food coloring and gold-conjugated protein A. (a) Spot counting. Flies fed with banana to which purple food coloring was added are indicated in red; starved flies are indicated in green. (b, d) Filter paper showing spots produced by starved flies. (c, e) Filter paper showing spots produced by flies fed with banana added with purple food coloring. (f-h') Video frames showing flies immediately before (f-h) and after (f'-h') the production of the spots (arrows). (i-j) The

presence of gold particles (arrowheads) inside the midgut lumen of flies fed with gold-conjugated protein A can be appreciated in TEM micrographs. (d, e) are details at higher magnification of (b, c), respectively. B: bacteria; M: microvilli. Bars: 1 μm (i), 500 nm (j).

To better examine alimentary canal function, we investigated the digestive capabilities of the fly midgut by measuring the activity of enzymes that are involved in the initial phase of carbohydrate and protein digestion. As shown in Table 3, a significant, total proteolytic activity was recorded, while no α-amylase activity was measured. We also evaluated the activity of enzymes involved in the final phase of sugar and protein digestion, i.e., sucrase and aminopeptidase N, two hydrolytic enzymes present in the apical membranes of insect absorptive epithelia (Terra and Ferreira 1994). The activity of both enzymes could be measured in the homogenate of the adult midgut (Table 3).

Total proteolytic activity (U)	**α-amylase activity (U)**	**APN activity (U/mg)**	**Sucrase activity (U/ml)**
64±0.46 (4)	Non-detectable	0.27±0.05 (4)	30.45±1.33 (3)

Table 3. Activity of digestive enzymes. Mean ± SEM, with number of replicates in parentheses, expressed in units as described in Materials and Methods.

Finally, we analyzed the expression of chymotrypsin- and trypsin-like proteases, the two most common endopeptidases involved in insect digestion, and of α-glucosidase, which hydrolyzes terminal, non-reducing (1→4)-linked alpha-glucose residues to release glucose molecules, by RT-PCR. The amplification of a DNA band of the expected length for all the genes tested was obtained, thus demonstrating their expression in the adult midgut (Fig. 8).

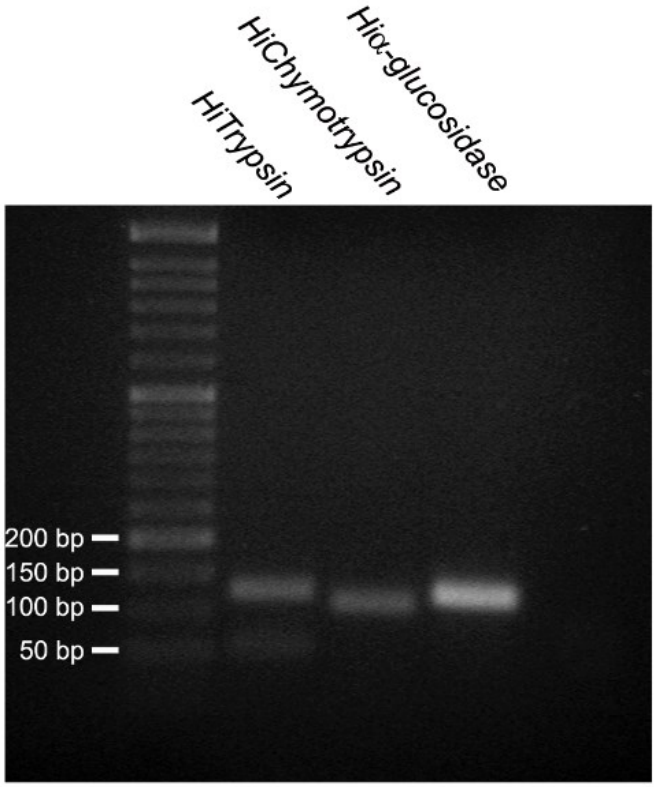

Figure 8. Gene expression of digestive enzymes. PCR analysis of the expression of *HiTrypsin*, *HiChymotrypsin*, and *Hiα-glucosidase* in the midgut of adult BSF

Fly longevity under different nutrient conditions

To evaluate whether and how nutrient administration affected the lifespan of *H. illucens* adults, flies were reared in the absence or in the presence of a food source. A remarkable mortality was recorded in starved flies five days after beginning the experiments, and all the insects died about one week after eclosion (Fig. 9a). On the contrary, a higher survival rate was observed when water or water and sugar cube were provided to flies (Fig. 9a). A significant difference in fly longevity was observed under the three different conditions, with the best performance obtained when water and sugar cube were provided to insects (Fig. 9b).

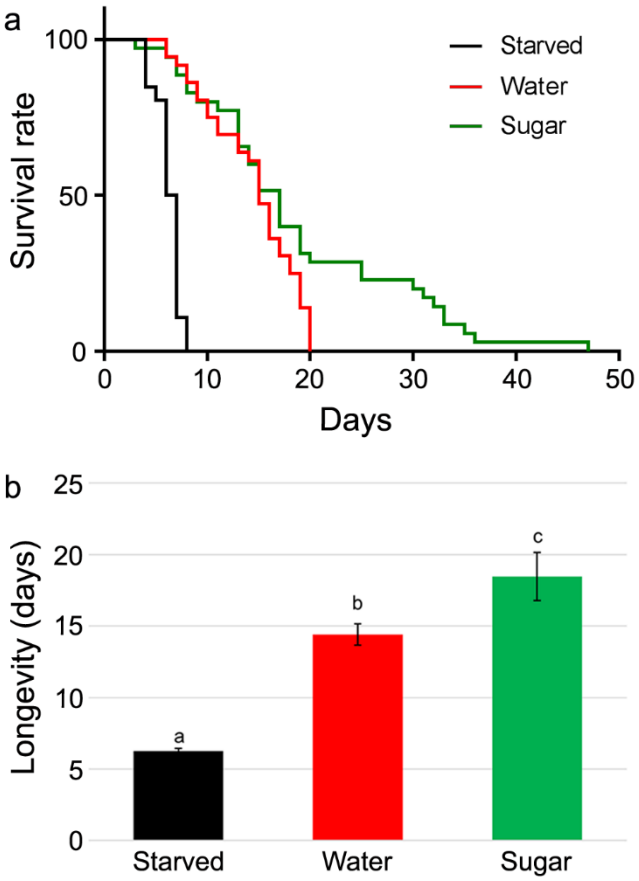

Figure 9. Longevity of adult *H. illucens*. (**a**) Survival curves of flies under different dietary conditions. (**b**) Fly longevity under different nutrient conditions. The values are reported as mean ± s.e.m. of at least 40 individuals. Different letters denote significant differences (ANOVA test followed by Tukey's test. ANOVA p-value < 0.001, Tukey's test p-values: Water *vs* Starved $p < 0.001$, Sugar *vs* Starved $p < 0.001$, Sugar *vs* Water $p < 0.05$).

DISCUSSION

The larvae of BSF represent a relevant option in the search for sustainable and alternative protein sources as they can convert low-quality biomass into nutritionally valuable proteins (Wang and Shelomi 2017). However, to support the growth of the emerging industrial sector of edible insects and their use in the feed market, important issues must be addressed, e.g., the safety of the production process, the production of high-quality insect meal, and the exploitation of insects and their products for applications other than feed. In this scenario, a deep knowledge of the biology of the adult insect, and in particular of its feeding habits, is necessary as this information could not only improve mass rearing of BSF, but also provide insights into the safety of using this insect for feed purposes. To fill in this gap of knowledge we undertook the present work and investigated three specific aspects: i) the remodeling process of the larval midgut during metamorphosis with particular attention on stem cells; ii) the morphology and function of the adult midgut; and iii) the feeding habits of the fly.

Histolysis of larval organs is one of the key events that occurs in holometabolous insects and is necessary to remove larval cells that the adult insect no longer needs. Concomitantly, the growth and differentiation of adult tissues and organs takes place (Franzetti et al. 2012; Hakim et al. 2010; Romanelli et al. 2016). Our results demonstrate that, in *H. illucens*, the larval midgut is completely replaced during metamorphosis by a new functional epithelium that is maintained up to the adult stage. During pupal stage, midgut stem cells actively proliferate, as confirmed by the expression of H3P, a marker of cells undergoing mitosis. Western blot analysis showed that proliferation activity continues until pupa day 10 when the differentiation of these cells leads to the formation a well-organized epithelium that will become the midgut of the fly. The larval cells are pushed toward the lumen, form the yellow body, and then degenerate. This coordinated series of events, which is responsible for the remodeling of BSF larval midgut, is generally conserved among Diptera (Lee et al. 2002; Takashima et al. 2011), Coleoptera (Parthasarathy and Palli 2008), and Lepidoptera (Franzetti et al. 2012; Li et al. 2018; Tettamanti et al. 2011; Tettamanti et al. 2007; Tettamanti et al. 2008)). In *Bombyx mori* it has been previously demonstrated that the complete digestion of larval midgut cells by autophagy, followed by their death, and the release of their content in the lumen of the newly forming epithelium can contribute to trophically substain the adult insect, which is unable to feed (Franzetti et al. 2015; Romanelli et al. 2016). Our results show that intact/viable yellow body cells apparently persist until late pupal stage in *H. illucens*, and some of them are still observable in the lumen of the midgut of the adult insect. This peculiar characteristic could be related to the fact that the fly is able to feed and process food, as demonstrated by our data. Thus, although long-term storage molecules, i.e., glycogen and lipids, are progressively reduced in the larval midgut epithelium during the early phase of metamorphosis, a trophic supply from degenerating larval cells might not be mandatory for the adult insect. Conversely, the reserves accumulated in the larval fat body could be sufficient to trophically sustain the insect during metamorphosis: this could explain why an early and complete degeneration of the yellow body in the pupa is not needed in *H. illucens* and the timing of the degeneration of the larval midgut is different from that in those holometabolous species whose adult insect does not feed (Franzetti et al. 2015; Romanelli et al. 2016).

The midgut epithelium of the adult BSF is mainly formed by columnar cells that are responsible for the digestive processes. The activity of this organ is supported by endocrine and stem cells. Only closed-type endocrine cells, which remain close to the basal lamina, and do not extend through the whole epithelium thickness (Fujita and Kobayashi 1977), with the presence of a large number of electron-dense granules in the cytoplasm (Endo and Nishiitsutsuju-Uwo 1981; Nishiitsutsuju-Uwo and Endo 1981), were observed. The number of stem cells, identified on the

basis of their morphology (Franzetti et al. 2015), was limited, which is in accordance with the lack of expression of H3P in adult samples. The absence of intestinal damage or pathogenic bacteria in our rearing conditions, two strong inducers of intestinal stem cell proliferation in adult *D. melanogaster* (Amcheslavsky et al. 2009; Buchon et al. 2013), could maintain these cells in a quiescent state.

Morphological analysis highlighted two peculiar aspects that characterize the midgut epithelium of the adult insect: the lack of copper cells and the absence of peritrophic matrix (PM). Copper cells are a peculiar cell type that in Diptera are able to acidify the middle midgut lumen thanks to the secretion of protons (Shanbhag and Tripathi 2009). In *D. melanogaster* larvae, the administration of copper in the diet causes copper cells to acquire an orange fluorescence signal due to the formation of a complex between copper and metallothioneins (McNulty et al. 2001). The absence of a fluorescent signal in our feeding experiments with cupric chloride, as well as the absence of a midgut region with a very acidic pH in the lumen, confirm the morphological evidence. In contrast, copper cells in the midgut epithelium of BSF larvae contribute to the establishment of a strongly acidic pH (about pH 2) in the middle midgut (Bonelli et al. unpublished data). This feature, differing between the two developmental stages of BSF, could be due to their feeding habits: at variance with the adults, the larvae grow on substrates that can be highly contaminated by microorganisms and the very acidic pH of the middle midgut lumen helps kill them (Bruno et al. 2019; Padilha et al. 2009). Our morphological investigation was not able to detect the presence of PM in all the midgut districts analyzed: this result did not appear to be an artifact, nor was the acellular sheath lost during dissection of the organ, as the lumen content was clearly visible and in close contact with the microvilli. The absence of PM could be explained by considering different aspects related to the feeding habits of the insect: i) it has been suggested that fluid-feeding species might not need PM for the mechanical protection of the midgut epithelium (Lehane 1997); ii) according to Billingsley and Lehane (Billingsley and Lehane 1996), the degree of microbial contamination of the liquid diet may be a more important factor determining presence or absence of the PM, so that insects feeding on a less infected liquid diet tend to lack PM; and iii) Villanon and collaborators (Villalon et al. 2003) demonstrated that the absence of PM increases the rate of protein hydrolysis; thus, despite the protective action, this acellular layer could partially restrict hydrolytic enzyme movement from the midgut cells to the lumen.

The midgut of the adult BSF is endowed with features typical of a functional epithelium. In addition to the presence of well-developed microvilli, abundant mitochondria under the brush border, rough endoplasmic reticulum, and secretory vesicles, all features that indicate a secretory and absorbing activity of these cells, the evaluation of enzymatic activity revealed that this organ

is able to digest macromolecules. A significant enzymatic activity involved in both protein and sugar digestion was measured in the midgut homogenate. Total proteolytic activity and APN activity are responsible for digesting proteins, from the initial to the final phase of this process (Terra and Ferreira 1994).

Surprisingly, differently from other brachyceran flies such as *D. melanogaster* (Chng et al. 2014) and *M. domestica* (Shina 1975; Terra et al. 1988a), and from *H. illucens* larvae (Bonelli et al. unpublished data; Pimentel et al. 2018), we did not record α-amylase activity in the midgut of adult BSF. However, it was demonstrated that the expression of amylase is repressed in *D. melanogaster* flies fed on high sugar diets (Benkel and Hickey 1986; Chng et al. 2014; Hickey and Benkel 1982). Since we fed flies with fully ripe banana pulp, which contains a high percentage of reducing sugars (33.6-33.8%) and sucrose (52.0-53.2%), and a very low percentage of starch (2.6-3.3%) (Lii et al. 1982), monosaccharides are already available to be absorbed and they can also be produced by the hydrolysis of sucrose thanks to sucrase activity. Thus, it is possible that the expression of amylase was repressed in our experimental conditions.

The results on midgut morphology and physiology, together with the presence of a typical sponging mouthpart, led us to investigate the function of the alimentary canal in terms of food ingestion and transit of the bolus. All our evidence supports data indicating that *H. illucens* flies possess a fully functional alimentary canal: feeding experiments with food coloring and gold-conjugated protein A, video recording, and evaluation of fecal spots clearly demonstrate that the alimentary canal of the fly is endowed with motility and that bolus transit in the lumen occurs. As shown by the movie, fecal spots are produced by fed flies. However, we cannot exclude that some of the spots observed on filter paper derive from regurgitation, i.e., the expulsion of material from any location within the foregut out of the oral cavity (Rivers and Geiman 2017). This process, which can be associated with different functions in flies, such food processing or elimination of excess water, involves the crop, a foregut organ present in Diptera (Stoffolano et al. 2008; Stoffolano and Haselton 2013). Although spots deriving from secretion and excretion processes that occur in the alimentary canal of flies are not easy to identify on the basis of their morphology (Rivers and Geiman 2017), the presence of a large crop associated to the gut of adult *H. illucens*, as well as the spots observed both in fed and unfed insects, suggest that BSF might regurgitate. It must be highlighted that fecal spots visible in unfed flies are produced in smaller numbers than in fed flies. Moreover, it cannot be excluded that these spots may be due not only to regurgitation but also to the elimination of meconium after eclosion (Rivers and Geiman 2017).

There is general agreement that *H. illucens* adults emerge relatively free of pathogens and, due to their relatively short lifespan compared to other flies, they do not eat. This common belief not only

contradicts the few previous studies that used sugar solutions to rear BSF (Furman et al. 1959; Nakamura et al. 2016), but is definitely contradicted by our evidence that the adult BSF is able to ingest and process food, produce frass, and may even regurgitate. In addition, our feeding experiments clearly show that food administration affects the longevity of the fly, confirming Nakamura's results (Nakamura et al. 2016). This evidence suggests that the energy requirements of the fly do not depend exclusively on reserves accumulated during the larval stage as reported in the literature (Sheppard et al. 2002; Tomberlin and Sheppard 2002; Tomberlin et al. 2002). In contrast, the ability of the fly to ingest and process food could be exploited to increase its performance in terms of lifespan and oviposition. In this scenario, our study paves the way for a deeper understanding of the nutrient requirements of the adult and a better exploitation of this insect in mass rearing processes. Moreover, the feeding behavior of adult *H. illucens* should be carefully considered in view of the recommendations reported in EFSA opinion (EFSA Scientific Committee 2015) concerning the safety of insects used for feed production and the lack of pathogenic effects, as also required by the European Commission Regulation N°2017/893 (European Commission 2017). In fact, regurgitation, defecation, and transtadial transmission have been described as potential routes of pathogen transmission in nonbiting flies (Graczyk et al. 2001; Graczyk et al. 2005).

CONCLUSIONS

Thanks to a multidisciplinary approach, our study clearly demonstrates for the first time that *H. illucens* adults can feed and provides an in-depth description of the morphofunctional features of the fly midgut. This information not only directs attention to the safety of this species as feedstuff, but could also represent a useful platform of knowledge to improve the performance of BSF in mass rearing procedures.

ACKNOWLEDGEMENTS

This work was supported by Fondazione Cariplo (grant n° 2014-0550). DB is a PhD student of the "Biotechnology, Biosciences and Surgical Technology" course at Università degli Studi dell'Insubria. MB is a PhD student of the "Environmental Sciences" course at Università degli Studi di Milano. We thank Prof. Pietro Brandmayr for the identification of mouthparts and Sherryl Sundell for English editing

REFERENCES

Amcheslavsky A, Jiang J, Ip YT (2009) Tissue damage-induced intestinal stem cell division in *Drosophila*. Cell Stem Cell 4:49-61

Benkel BF, Hickey DA (1986) Glucose repression of amylase gene expression in *Drosophila melanogaster*. Genetics 114:137-144

Bernfeld P (1955) Amylases, α and β. Methods Enzymol 1:149-158

Billingsley PF, Lehane MJ (1996) Structure and ultrastructure of the insect midgut. In: Lehane MJ, Billingsley PF (eds) Biology of the insect midgut. Springer, Dordrecht, pp 3-30

Bradford MM (1976) A rapid and sensitive method for the quantification of microgram quantities of protein utilizing the principle of protein-dye binding. Anal Biochem 72:248-254

Broce AB, Elzinga RJ (1984) Comparison of prestomal teeth in the face fly (*Musca autumnalis*) and the house fly (*Musca domestica*) (Diptera: Muscidae). J Med Entomol 21:82-85

Bruno D, Bonelli M, De Filippis F, Di Lelio I, Tettamanti G, Casartelli M, Ercolini D, Caccia S (2019) The intestinal microbiota of *Hermetia illucens* larvae is affected by diet and shows a diverse composition in the different midgut regions. Appl Environ Microbiol 85: e01864-18

Buchon N, Osman D, David FP, Fang HY, Boquete JP, Deplancke B, Lemaitre B (2013) Morphological and molecular characterization of adult midgut compartmentalization in *Drosophila*. Cell Rep 3:1725-1738

Caccia S, Chakroun M, Vinokurov K, Ferre J (2014) Proteolytic processing of *Bacillus thuringiensis* Vip3A proteins by two *Spodoptera* species. J Insect Physiol 67:76-84

Charney J, Tomarelli RM (1947) A colorimetric method for the determination of the proteolytic activity of duodenal juice. J Biol Chem 171:501-505

Chng WA, Sleiman MSB, Schupfer F, Lemaitre B (2014) Transforming growth factor beta/activin signaling functions as a sugar-sensing feedback loop to regulate digestive enzyme expression. Cell Rep 9:336-348

Cickova H, Newton GL, Lacy RC, Kozanek M (2015) The use of fly larvae for organic waste treatment. Waste Manage 35:68-80

Coch Frugoni JA (1957) Tampone universale di Britton e Robinson a forza ionica costante. Gazz Chim Ital 84:403-407

Dow JAT (1986) Insect midgut function. Adv Insect Physiol 19:187-328

Dubreuil RR (2004) Copper cells and stomach acid secretion in the *Drosophila* midgut. Int J Biochem Cell Biol 36:745-752

EFSA Scientific Committee (2015) Scientific Opinion on a risk profile related to production and consumption of insects as food and feed. EFSA Journal 13:4257-4317

Endo Y, Nishiitsutsuju-Uwo J (1981) Gut endocrine cells in insects: the ultrastructure of the gut endocrine cells of the lepidopterous species. Biomed Res 2:270-280

European Commission (2017) Commission regulation (EU) 2017/893 of 24 May 2017 amending Annexes I and IV to regulation (EC) No 999/2001 of the European Parliament and of the Council and Annexes X, XIV and XV to commission regulation (EU) No 142/2011 as regards the provisions on processed animal protein. Official Journal of the European Union L138:92-116

Franzetti E, Huang ZJ, Shi YX, Xie K, Deng XJ, Li JP, Li QR, Yang WY, Zeng WN, Casartelli M, Deng HM, Cappellozza S, Grimaldi A, Xia Q, Feng Q, Cao Y, Tettamanti G (2012) Autophagy precedes apoptosis during the remodeling of silkworm larval midgut. Apoptosis 17:305-324

Franzetti E, Romanelli D, Caccia S, Cappellozza S, Congiu T, Rajagopalan M, Grimaldi A, de Eguileor M, Casartelli M, Tettamanti G (2015) The midgut of the silkmoth *Bombyx mori* is able to recycle molecules derived from degeneration of the larval midgut epithelium. Cell Tissue Res 361:509-528

Fujita T, Kobayashi S (1977) Structure and function of gut endocrine cells. Int Rev Cytol Suppl 187-233

Furman DP, Young RD, Catts EP (1959) *Hermetia illucens* (Linnaeus) as a factor in the natural control of *Musca domestica* Linnaeus. J Econ Entomol 52:917-921

Giangaspero A, Broce AB (1993) Micromorphology of the prestomal teeth and feeding-behavior of *Musca autumnalis*, *M. larvipara* and *M. osiris* (Diptera, Muscidae). Med Vet Entomol 7:398-400

Gobbi P, Martinez-Sanchez A, Rojo S (2013) The effects of larval diet on adult life-history traits of the black soldier fly, *Hermetia illucens* (Diptera: Stratiomyidae). Eur J Entomol 110:461-468

Graczyk TK, Knight R, Gilman RH, Cranfield MR (2001) The role of non-biting flies in the epidemiology of human infectious diseases. Microbes Infect 3:231-235

Graczyk TK, Knight R, Tamang L (2005) Mechanical transmission of human protozoan parasites by insects. Clin Microbiol Rev 18:128-132

Gullan PJ, Cranston PS (2014) The insects: an outline of entomology. Wiley-Blackwell, Chichester, pp 156-189

Hakim RS, Baldwin K, Smagghe G (2010) Regulation of midgut growth, development, and metamorphosis. Annu Rev Entomol 55:593-608

Hickey DA, Benkel B (1982) Regulation of amylase activity in *Drosophila melanogaster*: effects of dietary carbohydrate. Biochem Genet 20:1117-1129

Hogsette JA (1992) New diets for production of house flies and stable flies (Diptera, Muscidae) in the laboratory. J Econ Entomol 85:2291-2294

Holmes LA, Vanlaerhoven SL, Tomberlin JK (2012) Relative humidity effects on the life history of *Hermetia illucens* (Diptera: Stratiomyidae). Environ Entomol 41:971-978

Holmes LA, Vanlaerhoven SL, Tomberlin JK (2013) Substrate effects on pupation and adult emergence of *Hermetia illucens* (Diptera: Stratiomyidae). Environ Entomol 42:370-374

Kovacs F, Medveczky I, Papp L, Gondar E (1990) Role of prestomal teeth in feeding of the house fly, *Musca domestica* (Diptera, Muscidae). Med Vet Entomol 4:331-335

Lee CY, Cooksey BA, Baehrecke EH (2002) Steroid regulation of midgut cell death during *Drosophila* development. Dev Biol 250:101-111

Lehane MJ (1997) Peritrophic matrix structure and function. Annu Rev Entomol 42:525-550

Lemaitre B, Miguel-Aliaga I (2013) The digestive tract of *Drosophila melanogaster*. Annu Rev Genet 47:377-404

Lemos FJA, Terra WR (1991) Digestion of bacteria and the role of midgut lysozyme in some insect larvae. Comp Biochem Physiol 100:265-268

Li YB, Yang T, Wang JX, Zhao XF (2018) The steroid hormone 20-hydroxyecdysone regulates the conjugation of autophagy-related proteins 12 and 5 in a concentration and time-dependent manner to promote insect midgut programmed cell death. Front Endocrinol (Lausanne) 9:28

Lii CY, Chang SM, Young YL (1982) Investigation of the physical and chemical properties of banana starches. J Food Sci 47:1493-1497

Makkar HPS, Tran G, Henze V, Ankers P (2014) State-of-the-art on use of insects as animal feed. Anim Feed Sci Tech 197:1-33

Marianes A, Spradling AC (2013) Physiological and stem cell compartmentalization within the *Drosophila* midgut. Elife 2:e00886

McNulty M, Puljung M, Jefford G, Dubreuil RR (2001) Evidence that a copper-metallothionein complex is responsible for fluorescence in acid-secreting cells of the *Drosophila* stomach. Cell Tissue Res 304:383-389

Meneguz M, Schiavone A, Gai F, Dama A, Lussiana C, Renna M, Gasco L (2018) Effect of rearing substrate on growth performance, waste reduction efficiency and chemical composition of black soldier fly (*Hermetia illucens*) larvae. J Sci Food Agric

Micchelli CA, Perrimon N (2006) Evidence that stem cells reside in the adult *Drosophila* midgut epithelium. Nature 439:475-479

Montali A, Romanelli D, Cappellozza S, Grimaldi A, de Eguileor M, Tettamanti G (2017) Timing of autophagy and apoptosis during posterior silk gland degeneration in *Bombyx mori*. Arthropod Struct Dev 46:518-528

Muller A, Wolf D, Gutzeit HO (2017) The black soldier fly, *Hermetia illucens* - a promising source for sustainable production of proteins, lipids and bioactive substances. Z Naturforsch C 72:351-363

Nakamura S, Ichiki RT, Shimoda M, Morioka S (2016) Small-scale rearing of the black soldier fly, *Hermetia illucens* (Diptera: Stratiomyidae), in the laboratory: low-cost and year-round rearing. Appl Entomol Zool 51:161-166

Nguyen TTX, Tomberlin JK, Vanlaerhoven S (2013) Influence of resources on *Hermetia illucens* (Diptera: Stratiomyidae) larval development. J Med Entomol 50:898-906

Nguyen TTX, Tomberlin JK, Vanlaerhoven S (2015) Ability of black soldier fly (Diptera: Stratiomyidae) larvae to recycle food waste. Environ Entomol 44:406-410

Nishiitsutsuju-Uwo J, Endo Y (1981) Gut endocrine cells in insects: the ultrastructure of the gut endocrine cells of the cockroach midgut. Biomed Res 2:30-44

Ohlstein B, Spradling A (2006) The adult *Drosophila* posterior midgut is maintained by pluripotent stem cells. Nature 439:470-474

Ohlstein B, Spradling A (2007) Multipotent *Drosophila* intestinal stem cells specify daughter cell fates by differential notch signaling. Science 315:988-992

Padilha MH, Pimentel AC, Ribeiro AF, Terra WR (2009) Sequence and function of lysosomal and digestive cathepsin D-like proteinases of *Musca domestica* midgut. Insect Biochem Mol Biol 39:782-791

Parthasarathy R, Palli SR (2008) Proliferation and differentiation of intestinal stem cells during metamorphosis of the red flour beetle, *Tribolium castaneum*. Dev Dyn 237:893-908

Pimentel AC, Barroso IG, Ferreira JMJ, Dias RO, Ferreira C, Terra WR (2018) Molecular machinery of starch digestion and glucose absorption along the midgut of *Musca domestica*. J Insect Physiol 109:11-20

Pimentel AC, Montali A, Bruno D, Tettamanti G (2017) Metabolic adjustment of the larval fat body in *Hermetia illucens* to dietary conditions. J Asia-Pac Entomol 20:1307-1313

Rivers D, Geiman T (2017) Insect artifacts are more than just altered bloodstains. Insects 8

Romanelli D, Casartelli M, Cappellozza S, de Eguileor M, Tettamanti G (2016) Roles and regulation of autophagy and apoptosis in the remodelling of the lepidopteran midgut epithelium during metamorphosis. Sci Rep 6:32939

Sehnal F, Zitnan D (1996) Midgut endocrine cells. In: Lehane MJ, Billingsley PF (eds) Biology of the insect midgut. Springer, Dordrecht, pp 55-85

Shanbhag S, Tripathi S (2009) Epithelial ultrastructure and cellular mechanisms of acid and base transport in the *Drosophila* midgut. J Exp Biol 212:1731-1744

Sheppard DC, Newton GL, Thompson SA, Savage S (1994) A value-added manure management-system using the black soldier fly. Bioresource Technol 50:275-279

Sheppard DC, Tomberlin JK, Joyce JA, Kiser BC, Sumner SM (2002) Rearing methods for the black soldier fly (Diptera: Stratiomyidae). J Med Entomol 39:695-698

Shina M (1975) Amylase activity in the midgut of *Sarcophaga ruficornis* and *Musca domestica*. Entomol Exp Appl 18:290-296

Stoffolano JG, Acaron A, Conway M (2008) "Bubbling" or droplet regurgitation in both sexes of adult *Phormia regina* (Diptera: Calliphoridae) fed various concentrations of sugar and protein solutions. Ann Entomol Soc Am 101:964-970

Stoffolano JG, Jr., Haselton AT (2013) The adult Dipteran crop: a unique and overlooked organ. Annu Rev Entomol 58:205-225

Takashima S, Younossi-Hartenstein A, Ortiz PA, Hartenstein V (2011) A novel tissue in an established model system: the *Drosophila* pupal midgut. Dev Genes Evol 221:69-81

Terra WR (1990) Evolution of digestive systems of insects. Annu Rev Entomol 35:181-200

Terra WR, Espinoza-Fuentes FP, Ferreira C (1988a) Midgut amylase, lysozyme, aminopeptidase, and trehalase from larvae and adults of *Musca domestica*. Arch Insect Biochem 9:283-297

Terra WR, Espinoza-Fuentes FP, Ribeiro BM, Ferreira C (1988b) The larval midgut of the housefly (*Musca domestica*): ultrastructure, fluid fluxes and ion secretion in relation to the organization of digestion. J Insect Physiol 34:463-472

Terra WR, Ferreira C (1994) Insect digestive enzymes: properties, compartmentalization and function. Comp Biochem Phys B 109:1-62

Terra WR, Ferreira C (2005) Biochemistry of digestion. In: Gilbert LI, Iatrou K, Gill SS (eds) Comprehensive molecular insect science, vol 4. Elsevier Pergamon Press, Oxford, pp 171-224

Terra WR, Ferreira C, Baker JE (1996a) Compartmentalization of digestion. In: Lehane MJ, Billingsley PF (eds) Biology of the insect midgut. Springer, Dordrecht, pp 206-235

Terra WR, Ferreira C, Jordão BP, Dillon RJ (1996b) Digestive enzymes. In: Lehane MJ, Billingsley PF (eds) Biology of the insect midgut. Springer, Dordrecht, pp 153-194

Tettamanti G, Cao Y, Feng Q, Grimaldi A, de Eguileor M (2011) Autophagy in Lepidoptera: more than old wine in new bottle. Invert Sur J 8:5-14

Tettamanti G, Grimaldi A, Casartelli M, Ambrosetti E, Ponti B, Congiu T, Ferrarese R, Rivas-Pena ML, Pennacchio F, Eguileor M (2007) Programmed cell death and stem cell differentiation are responsible for midgut replacement in *Heliothis virescens* during prepupal instar. Cell Tissue Res 330:345-359

Tettamanti G, Salo E, Gonzalez-Estevez C, Felix DA, Grimaldi A, de Eguileor M (2008) Autophagy in invertebrates: insights into development, regeneration and body remodeling. Curr Pharm Des 14:116-125

Tomberlin JK, Adler PH, Myers HM (2009) Development of the black soldier fly (Diptera: Stratiomyidae) in relation to temperature. Environ Entomol 38:930-934

Tomberlin JK, Sheppard DC (2002) Factors influencing mating and oviposition of black soldier flies (Diptera: stratiomyidae) in a colony. J Entomol Sci 37:345-352

Tomberlin JK, Sheppard DC, Joyce JA (2002) Selected life-history traits of black soldier flies (Diptera: Stratiomyidae) reared on three artificial diets. Ann Entomol Soc Am 95:379-386

Villalon JM, Ghosh A, Jacobs-Lorena M (2003) The peritrophic matrix limits the rate of digestion in adult *Anopheles stephensi* and *Aedes aegypti* mosquitoes. J Insect Physiol 49:891-895

Vinokurov KS, Elpidina EN, Oppert B, Prabhakar S, Zhuzhikov DP, Dunaevsky YE, Belozersky MA (2006) Diversity of digestive proteinases in *Tenebrio molitor* (Coleoptera: Tenebrionidae) larvae. Comp Biochem Physiol B Biochem Mol Biol 145:126-137

Vogel H, Muller A, Heckel DG, Gutzeit H, Vilcinskas A (2018) Nutritional immunology: Diversification and diet-dependent expression of antimicrobial peptides in the black soldier fly *Hermetia illucens*. Dev Comp Immunol 78:141-148

Wang YS, Shelomi M (2017) Review of black soldier fly (*Hermetia illucens*) as animal feed and human food. Foods 6

SUPPLEMENTARY MATERIAL

SUPPLEMENTARY 1 - Evaluation of the presence of copper cells in the midgut of adult *H. illucens*

Materials and Methods

A) Evaluation of midgut juice pH

H. illucens flies were fed *ad libitum* with banana, renewing the food substrate every day. Flies were dissected at day four: the lumen content was recovered from the midgut and spotted on pH indicator strips.

B) Copper feeding trials

H. illucens flies were fed *ad libitum* on standard diet prepared with a water solution containing 4 mM $CuCl_2$, renewing the diet every day. Flies were dissected at day four: the midgut was isolated and analyzed under fluorescence microscope at 365 nm excitation wavelength.

Results

Copper cells are able to acidify the lumen of BSF larval midgut through the extrusion of H^+, leading to a very acidic pH (pH = 2.1 ± 0.1) in the middle midgut region (Bonelli et al., unpublished data). In addition, in copper-fed fly larvae, the accumulation of this metal in copper cells determines the emission of an orange fluorescence (Bonelli et al., unpublished data; McNulty et al., 2001), probably due to the formation of a metallothionein-copper complex (McNulty et al., 2001). In *H. illucens* flies, the anterior-middle region of the midgut showed a slightly acidic pH (Fig. S1a), while the posterior midgut presented a basic pH (Fig. S1b). Therefore, the absence of a midgut region with a very acidic pH in the lumen strongly suggests that the epithelium does not contain copper cells. The analysis of the midgut from flies subjected to copper feeding trials did not reveal any orange fluorescence due to the metal intake (Fig. S1c), thus confirming the lack of copper cells in the midgut of adult BSF.

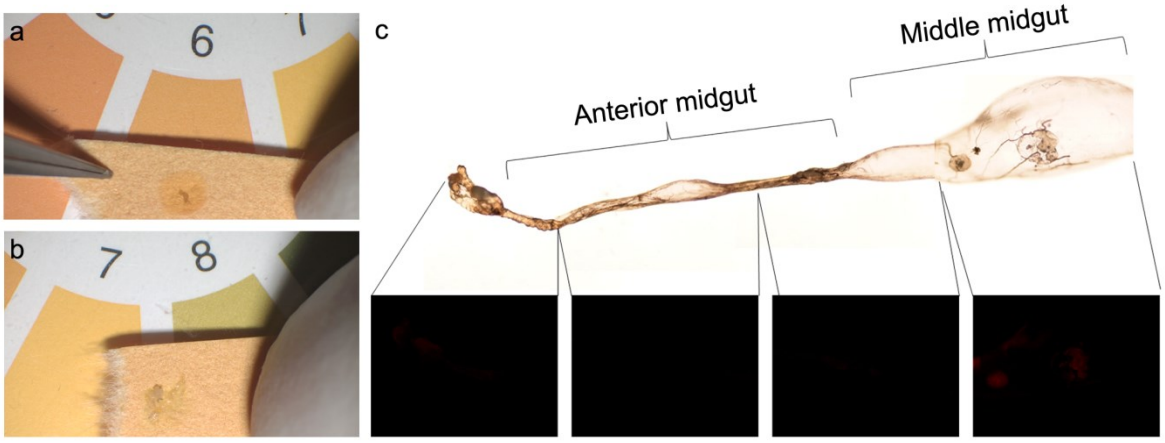

Figure S1. (a-b) pH value in the anterior-middle (a) and posterior (b) midgut lumen as shown by pH indicator strips. (c) Evaluation of fluorescence generated by the metallothionein-copper complex in fed-copper flies

SUPPLEMENTARY 2 - Analysis of the transit of ingested food by video recording

The supplementary video is available at the following link: https://www.dropbox.com/s/9y2ms6aywpfjgp5/Hermetia%20video1.mp4?dl=0

CONCLUSIONS AND PERSPECTIVES

This PhD project provides new insights on different aspects of *H. illucens* biology, focusing the attention on the physiology of midgut, the organ responsible for digestion and nutrient absorption.

The main results obtained are:

i. Structural and functional characterization of *H. illuces* larval midgut

It was established that this organ is characterized by a strong regionalization since districts with peculiar morphofunctional features can be recognized. In particular, the presence of epithelial cells with peculiar morphological and functional properties, pH of the midgut lumen, and enzymes production, secretion and activity are strictly related to midgut regions. Thanks to our results we propose a functional model of the larval midgut of *H. illucens*. In the anterior region the digestion of polysaccharides begins; the first part of the middle midgut is characterized by the presence of copper cells, responsible for the acidification of middle midgut lumen. In this region high lysozyme activity is present, a functional feature that, together with the strong acidic luminal pH, suggests a main role of the middle midgut in killing pathogens ingested with the feeding substrate. Finally, the posterior midgut plays a fundamental role in protein digestion, from the initial to the final phase of this process, and in nutrient absorption.

Despite the great interest towards *H. illucens* larvae for their ability to bioconvert low quality organic matter into valuable biomass for feed production and for their use as a source of bioactive molecules (e.g., antimicrobial peptides, enzyme able to digest complex substrates), little information on the biology of this insect has been obtained so far. Our findings contribute to fill this gap of knowledge and can be fundamental to promote the exploitation of *H. illucens*, in particular, to develop strategies to optimize the bioconversion ability of this insect and its biotechnological applications.

ii. The feeding substrate affects morphological and functional features of the *H. illucens* larval midgut

Morphofunctional modifications were observed in the midgut of *H. illucens* larvae in response to feeding substrates with different nutritional composition: differences in the morphology, activity of digestive enzymes, and accumulation of long-term storage molecules were observed. These data demonstrated the existence of a diet-dependent adaptation process of the midgut. This plasticity may be responsible for the ability of *H. illucens* larvae to grow and develop on very different organic substrates. Further studies are needed in order to evaluate how the metabolic cost of the midgut plasticity impacts on the insect performances, both on larvae and adults, since it has to be considered that the food ingested by the larvae can influence adult features. Moreover, an

evaluation of the impact of feeding substrates on larvae and prepupae nutritional profile is fundamental for feed purposes.

iii. The intestinal microbiota of *H. illucens* larvae is affected by diet and shows a diverse composition in the different midgut regions

A detailed analysis of *H. illucens* larval midgut microbiota was performed. Using three feeding substrates with different protein/carbohydrates (P/C) ratio, we established that the diet impacts on the midgut microbiota, in particular a diet with very high P/C ratio do not seem to be optimal for *H. illucens* rearing, since it induces a dysbiosis. Moreover, the regionalization of this organ influences the microbiota: the bacterial community of the anterior midgut always shows higher diversity than the posterior, whereas bacterial load has an opposite trend, being maximal in the posterior region. The middle midgut could be involved in the reduction of microbial diversity thanks to the activity of lysozyme and the strong acidic pH of the lumen in this region, while in the posterior midgut a proliferation of some genera could occur, leading to an increase in bacterial load in this region. Finally, *H. illucens* does not affect the microbiota composition of the feeding substrate in our experimental conditions. Our data overcome the current limited information on the larval midgut microbiota of *H. illucens*, representing a platform of knowledge for further investigation on this topic and for evaluations of possible microbiological hazards in mass rearing conditions. Moreover, our work represents a good starting point for the identification and isolation of bacterial strains with biotechnological interest.

iv. The digestive system of the adult Hermetia illucens (Diptera: Stratiomyidae): morphological features and functional properties

Our results demonstrate that the larval midgut of *H. illucens* is removed during metamorphosis and a pupal-adult epithelium is formed *de novo* by proliferation and differentiation of intestinal stem cells. At variance with majority of current literature, we demonstrated that the adult insect possesses a functional digestive system: mouthpart allows food ingestion, the bolus can transit along the gut, and the midgut epithelium is endowed with digestive capability. This new scenario not only opens up the possibility to feed the adult insect to improve its performances in mass rearing procedures, but could also provide insights into the safety on the use of this insect for feed purposes, considering that the mouthparts of adult Diptera have implications for the transmission of pathogens, representing a potential risk factor in *H. illucens* rearing and in its use as feed. Our findings on this topic represent a basis for further research that are mandatory for application purposes.

In conclusion, our data represent a platform of knowledge useful for further scientific investigation on brachyceran Diptera midgut biology and, in particular, on *H. illucens*. Moreover, they have a strong applicative interest since our results set the stage for the best exploitation of the biotechnological potential of *H. illucens* and its use as a model to develop industrial bioconversion processes.

CONFERENCE PAPERS

Bonelli, M., Bruno, D., Tettamanti, G., Casartelli, M. (2018). Characterization of *Hermetia illucens* (Diptera: Stratiomyidae) larval midgut. Book of Abstract European PhD Network "Insect Science", Firenze (IT) 14-16 November 2018

Bruno, D., Bonelli, M., Lupi, D., Casartelli, M., Tettamanti, G. (2018). Morphofunctional characterization of *Hermetia illucens* larval midgut. Riassunti UZI 2018 79° Congresso Nazionale Unione Zoologica Italiana, Lecce (IT) 25-27 September 2018

Bonelli, M., Bruno, D., Cagnola, A., Gianfranceschi, N., Jucker, C., Leonardi, M.G., Tettamanti, G., Casartelli, M. (2018). Comparison of the morphofunctional properties of the larval midgut of *Hermetia illucens* (Diptera: Stratiomyidae) reared on different diets. Book of Abstracts ECE 2018 XI European Congress of Entomology, Napoli (IT) 02-06 July 2018

Bruno, D., Bonelli, M., Jucker, C., Lupi, D., Casartelli, M., Tettamanti, G. (2018). Replacement of *Hermetia illucens* larval midgut during metamorphosis. Book of Abstracts ECE 2018 XI European Congress of Entomology, Napoli (IT) 02-06 July 2018

Casartelli, M., Bonelli, M., Bruno, D., Cappellozza, S., Lupi, D., Tettamanti, G. (2018). Morphological and functional characterization of the larval midgut of Hermetia illucens (Diptera: Stratiomyidae), a promising insect for bioconversion and feed production. Book of Abstracts ECE 2018 XI European Congress of Entomology, Napoli (IT) 02-06 July 2018

Bonelli, M., Bruno, D., Gianfranceschi, N., Jucker, C., Leonardi, M.G., Tettamanti, G., Casartelli, M. (2018). The influence of diet on the morphofunctional properties of *Hermetia illucens* (Diptera: Stratiomyidae) larval midgut. Journal of Insects as Food and Feed: 4 (Supplement 1), The 2nd International Conference 'Insects to Feed the World' (IFW 2018), Wuhan (CN) 15-18 May 2018. doi:10.3920/JIFF2018.S1

Bruno, D., Bonelli, M., Jucker, C., Lupi, D., Casartelli, M., Tettamanti, G. (2018). Metamorphic remodelling of the larval midgut in *Hermetia illucens*. Journal of Insects as Food and Feed: 4 (Supplement 1), The 2nd International Conference 'Insects to Feed the World' (IFW 2018), Wuhan (CN) 15-18 May 2018. doi:10.3920/JIFF2018.S1

Bruno, D., Bonelli, M., Savoldelli, S., Cappellozza, S., Casartelli, M., Tettamanti, G. (2018). The bioconversion capability of *Hermetia illucens* larvae: a morphofunctional study of the larval midgut. Journal of Insects as Food and Feed: 4 (Supplement 1), The 2nd International Conference 'Insects to Feed the World' (IFW 2018), Wuhan (CN) 15-18 May 2018. doi:10.3920/JIFF2018.S1

Bruno, D., Bonelli, M., Casartelli, M., Tettamanti, G. (2017). The larval midgut of *Hermetia illucens* is characterized by a highly complex structural organization. Book of Abstract European PhD Network "Insect Science", Napoli (IT) 15-16 November 2017

Bonelli, M., Bruno, D., Tettamanti, G. & Casartelli, M. (2017). Molecular and functional characterization of *Hermetia illucens* larval midgut. Book of Abstract European PhD Network "Insect Science", Napoli (IT) 15-16 November 2017

Bonelli, M., Bruno, D., Montali, A., Jucker, C., Lupi, D., Casartelli, M., Tettamanti, G. (2017). Structural and functional characterization of the larval midgut of *Hermetia illucens* for the best exploitation of its bioconversion ability. Book of Abstract INSECTA 2017, Berlin (DE) 07-08 September 2017. ISSN 0947-7314

Leonardi, M.G., Jucker, C., Savoldelli, S., Palamara Mesiano, M., Lupi, D., Casartelli, M., Bonelli, M., Cappellozza, S., Bruno, D., Romanelli, D., Tettamanti, G. (2016). Utilizzo di *Hermetia illucens* per la produzione di proteine da substrati vegetali. Atti del XXV Congresso Nazionale Italiano di Entomologia (a cura di Faccoli, M., Mazzon, L., Petrucco-Toffolo, E.), Padova (IT) 20-24 June 2016

OTHER JOURNAL ARTICLES AND CONFERENCE PAPERS

eco.mont – Volume 9, Number 2, July 2017
ISSN 2073-106X print version – ISSN 2073-1558 online version: http://epub.oeaw.ac.at/eco.mont
https://dx.doi.org/10.1553/eco.mont-9-2s23

Mountain protected areas as refuges for threatened freshwater species: the detrimental effect of the direct introduction of alien species.

Marco Bonelli, Raoul Manenti, Davide Scaccini

Abstract

One of the main threats to native European crayfish species is presented by the spread of invasive ones, which are vectors of the crayfish plague *Aphanomyces astaci*. In particular, the *Austropotamobius pallipes* complex is suffering extensive decline in its whole distribution range. In this paper, we describe a case of extinction of a native population of the *A. pallipes* complex driven by the direct human introduction of the alien species *Orconectes limosus*, in a mountain protected area in northern Italy. The local extinction event of the native crayfish population is reported, and the factors that drove it are reconstructed. Our results help to better understand the threats to native crayfish species occurring even in protected areas, as well as to establish proper prevention and management actions.

Ferrante, L., Bonelli, M., Scaccini, D., Manenti, R., Normando, S., Florio, D., De Mori, B. (2018). The extinction risk for threatened species in protected areas: the case of the freshwater crayfish (*Austropotamobius pallipes*) in Italy. Abstract accepted in 5th European Congress of Conservation Biology, Jyväskylä (FIN), 12-15 June 2018. doi:10.17011/conference/eccb2018/107432

Bonelli, M., Scaccini, D. (2016). Realizzazione e gestione di siti di nidificazione per i pronubi selvatici del Parco Monte Barro: il Progetto BarroBugBox. Atti del XXV Congresso Nazionale Italiano di Entomologia (a cura di Faccoli, M., Mazzon, L., Petrucco-Toffolo, E.), Padova (IT) 20-24 June 2016